Impact des conditions nutritionnelles sur la dissolution de la silice biogénique des diatomées à travers l'étude de la variabilité de la structure biphasique du frustule

Julia Boutorh

▶ **To cite this version:**

Julia Boutorh. Impact des conditions nutritionnelles sur la dissolution de la silice biogénique des diatomées à travers l'étude de la variabilité de la structure biphasique du frustule. Autre. Université de Bretagne occidentale - Brest, 2014. Français. NNT : 2014BRES0009 . tel-01679338

HAL Id: tel-01679338
https://theses.hal.science/tel-01679338

Submitted on 9 Jan 2018

HAL is a multi-disciplinary open access archive for the deposit and dissemination of scientific research documents, whether they are published or not. The documents may come from teaching and research institutions in France or abroad, or from public or private research centers.

L'archive ouverte pluridisciplinaire **HAL**, est destinée au dépôt et à la diffusion de documents scientifiques de niveau recherche, publiés ou non, émanant des établissements d'enseignement et de recherche français ou étrangers, des laboratoires publics ou privés.

THÈSE / UNIVERSITÉ DE BRETAGNE OCCIDENTALE

sous le sceau de l'Université européenne de Bretagne

pour obtenir le titre de

DOCTEUR DE L'UNIVERSITÉ DE BRETAGNE OCCIDENTALE

Mention : Chimie Marine

École Doctorale des Sciences de la Mer

présentée par

Julia Boutorh

Préparée à l'Institut Universitaire Européen de la Mer (IUEM), au Laboratoire des Sciences de de l'Environnement Marin (LEMAR)

Impact des conditions nutritionnelles sur la dissolution de la silice biogénique des diatomées à travers l'étude de la variabilité de la structure biphasique du frustule

Thèse soutenue le 14 février 2014

devant le jury composé de :

Daniel CONLEY
Professeur, Lund University, Dept. of Geology / *Rapporteur*

Marion GEHLEN
Directrice de Recherche, Laboratoire des Sciences du Climat et de L'Environnement, UMR 8212 / *Rapportrice*

Pascal CLAQUIN
Professeur, Université de Caen Basse-Normandie, FRE 3484 CNRS BioMEA / *Examinateur*

Pascal Jean LOPEZ
Chargé de Recherche, Muséum National d'Histoire Naturelle, UMR-BOREA / *Examinateur*

Eva BUCCIARELLI
Maître de conférences, UBO, UMR 6539 / *Invitée*

Brivaëla MORICEAU
Chargée de Recherche, IUEM, UMR 6539 / *Directrice scientifique*

Olivier RAGUENEAU
Directeur de Recherche, IUEM, UMR 6539 / *Directeur de thèse*

Ce travail a bénéficié d'un financement de **l'Université de Bretagne Occidentale (UBO)**.

Cette thèse s'inscrit dans l'axe de recherche 2 du **LabexMer**, « La complexité et l'efficacité de la "pompe biologique" de carbone », qui a également financé une partie de ce travail.

La **région Bretagne** a soutenu la présentation de ces travaux au congrès international ASLO 2013 Aquatic Sciences Meeting.

Cette thèse a été réalisée dans le cadre des programmes suivants :

Projet Lefe:

Understanding silica **T**o carbon **I**nteractions and **L**inkage during production and their impact for diatom degradation (**UTIL**)

Chef de projet: Brivaëla Moriceau

Projet ANR, programme jeunes chercheuses et jeune chercheurs :

Iron, **C**opper and **O**ceanic **P**hytoplankton (**ICOP**)

Chef de projet: Eva Bucciarelli

Remerciements

Ce travail a pu être réalisé grâce à l'aide et au soutien de très nombreuses personnes. Aussi, je voudrais ici dire un grand merci à:

Olivier, pour avoir accepté d'être mon directeur de thèse. Merci également de m'avoir donné l'opportunité de partir sur la campagne océanographique WACS.

Laurent, pour m'avoir accepté au LEMAR lorsqu'il était directeur et pour les discussions que nous avons pu avoir.

Briva, merci de m'avoir encadré et guidé durant ces trois années, d'avoir cru en moi et m'avoir fait confiance. Et merci de m'avoir permis d'aller aux 4 coins du monde !

Aux membres du jury, Marion, Daniel, Pascal, Eva et Pascal Jean, merci d'avoir accepté d'évaluer mon travail un jour de grande tempête! J'ai eu la chance de rencontrer Daniel et Pascal avant ce jour de soutenance, merci pour les discussions enrichissantes que nous avons pu avoir. Eva, un grand merci pour ta disponibilité et tes conseils lors de la rédaction des papiers métaux traces.

Merci à tous les gens rencontrés au LEMAR ou ailleurs, pour avoir participé à cette aventure:

A Morgane, tu m'as été d'une grande aide, merci pour ta bonne humeur ! Ce fut un vrai plaisir de partir avec toi et Géraldine à la Nouvelle Orléans. Merci encore les filles pour le collier!

A Claire Labry pour avoir accepté de faire partie de mon comité externe et pour avoir participé aux manips de dissolution.

A Daniel Delmas pour nos discussions enrichissantes sur les bactéries et pour son aide sur les expériences de dissolution.

A Aicha, Kada et Emmanuel pour leur aide précieuse sur le traitement des données IRTF.

A Alain Marhic, pour toutes ces autoclaves et pour toujours avoir le matériel dont on a besoin.

A Alain Le Mercier, pour toujours régler les problèmes informatiques, et ceci avec énergie!

A Elisabeth, pour ces discussions et pour les petites bouteilles d'eau quand c'était nécessaire.

A Sébastien pour ces belles figures ! Et pour ce temps passé à comprendre la structure du frustule…

A Annick, pour les analyses POC/PON, pour avoir toujours répondu à mes questions. Ce fut un plaisir de partager avec toi l'expérience mésocosme.

A Emilie pour les sessions récupération d'eau de mer à SOMLIT.

A Gene et Anne-So, les wonderwomen du secrétariat, pour avoir toujours été là pour tous les problèmes administratifs (même au dernier moment) et pour votre bonne humeur!

A Fred, Hélène et Philippe pour votre gentillesse et pour ces RU sympathiques.

A Olivier Gauthier, pour avoir pris le temps de répondre à mes questions sur les stats!

A Vianney, pour m'avoir donné l'opportunité d'encadrer des TP. Merci également à Marie Anne, Claire et Stella pour m'avoir aiguillé lors de cette expérience.

A Christophe Lambert pour son aide lors de l'utilisation du cytomètre et pour le traitement des données.

A Philippe Elies, pour les heures passées devant le microscope à tenter de comprendre les mystères du frustule!

A Maud et à Fanny, pour les pique-niques au soleil.

A Cécile, merci pour tous tes conseils depuis mon stage de Master 2.

A Aurélie Godrant, pour les sessions papotage.

A Aurélie Lelong, pour ses conseils, son aide pour l'utilisation du cytomètre et pour les cultures de diatomées.

Un grand merci également à tous les gens rencontrés lors de mes diverses expatriations:

A Pascal Claquin et à Caroline Amiel pour leur accueil à Caen, ainsi qu'à Nicolas et aux étudiants du Master AquaCaen pour m'avoir fait passer un bon séjour à la station de Luc- sur-Mer.

Aux participants de la campagne océanographique BaRFlux3, au large des Bermudes. Thank you Cindy for offering me the opportunity to join this cruise, and thank you Carolina for the great time we had and for your help in TEP measurements!

A l'équipe de la campagne océanographique WACS, en particulier à Nadia, Rudolph et Livio, pour avoir été si gentils avec une jeune thésarde lors de sa première campagne !

A l'équipe du projet EURO-BASIN, pour ces bons moments autour des mésocosmes en Norvège, et pour m'avoir fait découvrir l'Aquavit. Thank you Marja for your patience teaching me how to recognize and catch zooplankton!

Maxime, merci à toi d'avoir partagé non seulement les expériences de dissolution, mais également les expériences à Ouessant et aux Bermudes. Je te suis également extrêmement reconnaissante d'avoir partagé tes Mercalm avec moi!

Un immense merci également à tous les copains qui m'ont supporté, dans tous les sens du terme, pendant cette aventure:

Un grand grand merci à Marie, Nathalie, Violette, Morgane, Fabien et Thomas, le destin a fait que nous soyons « co-bureau » et c'est tant mieux (Et oui Thomas, en fait il fallait juste que l'on passe des heures dans la même pièce pour qu'on se rappelle l'un de l'autre, c'est tout)! Merci pour cette bonne ambiance, et merci d'avoir partagé ces années avec moi. Merci à Thomas de m'avoir fait marquer à jamais mon empreinte dans un buisson quelque part rive droite et pour ces bons repas à 23h. Fabien, on se supporte depuis 5 ans maintenant (je vais d'ailleurs devoir prendre rdv chez l'ORL je pense…) merci pour ton soutien et pour tes goûts culinaires douteux. Marie, la matrice a fait que nos chemins se sont croisés (pour mon plus grand bien !) lorsque j'étais en licence. Merci d'avoir accueilli la jeune doctorante un peu perdue que j'étais dans le bureau A159. Merci pour tous ces conseils, pour ces discussions, pour m'avoir fait découvrir le yoga... On la fera cette BD !

Merci à Gaspard, pour les pauses clopes qui font du bien, pour avoir volé à mon secours quand une Bordelaise en Porsche Cayenne a décidé de tester la résistance de ma voiture, pour toutes ces bonnes bières en bas de siam et ailleurs, pour la découverte du 1900... Et aussi, merci d'aimer ABBA mais de ne pas l'imposer en société.

Merci à Marie Czam pour les séances de yoga et pour les bons moments autour d'un verre de vin et d'une planche au Barado.

Manon, je t'ai réellement découverte lorsque j'ai placé ma vie entre tes mains lors de quelques tentatives d'ascension du mur de Strasbourg, et j'ai bien fait! Merci d'avoir été là pour tous les bons et moins bons moments de cette aventure. J'espère devoir te supporter encore longtemps !

Merci à Thomas, Thibaut, Jk, Carole, Loic, Gwen, Ju, Pierre, Laurence, Olivier, Arnaud… pour tous ces bons moments, ces fiestas, ces discussions philosophiques à 2 heures du matin! Vous m'avez chacun été d'un grand soutien pendant cette aventure qu'est la thèse, merci beaucoup! Une spéciale dédicace pour notre animologue (j'attends toujours le cri qui tue), ca fait un bout de temps maintenant que l'on se suit, merci d'être toujours là quand ca va pas (et quand ça va aussi d'ailleurs !).

Une énorme merci à mon expatrié préféré, merci Guillaume d'avoir su être présent et de m'avoir soutenu depuis chez les Vikings. Merci pour toutes ces corrections, pour avoir supporté mes humeurs sans broncher, pour me dire quand « c'est pas très grave » et pour m'apprendre que le bonheur, c'est un peu comme une partie de Jenga.

Un immense merci à mon père, ma mère et ma sœur, mon pilier durant ces trois années (et pas que…). Merci d'être là, merci pour votre soutien inébranlable, et pour avoir rendu ces dernières semaines de thèse quasiment agréables!

Enfin un grand merci à ceux et celles qui ont participé de près ou de loin à cette aventure et que j'oublie ici aujourd'hui, mais je suis sûr que vous saurez vous reconnaitre !

SOMMAIRE

Chapitre I.

Introduction

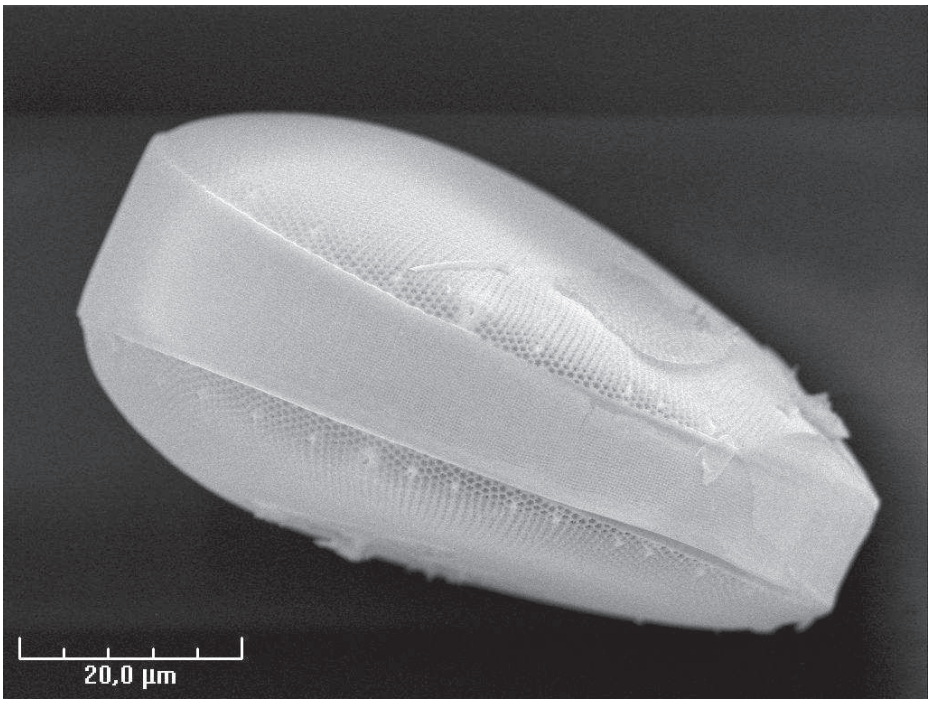

I. Chapitre I : Introduction

1. Contexte sociétal et scientifique

Depuis le milieu du XVIII siècle et le commencement de l'ère industrielle, l'utilisation des combustibles fossiles, les changements d'affectation des terres et l'intensification de l'agriculture ont entrainé une augmentation des concentrations atmosphériques en dioxyde de carbone (CO_2) , en méthane et en oxyde nitreux (GIEC 2007). Ces modifications de la teneur de l'atmosphère en gaz à effet de serre et en aérosols ont entrainé un réchauffement du système climatique (GIEC 2007). En particulier, le CO_2 représente la composante majoritaire du forçage radiatif[1] d'origine anthropique (GIEC 2007).

Afin de mieux comprendre les conséquences de ces modifications sur le climat de la planète, les scientifiques se sont attachés à la conception de modèles climatiques, dont l'amélioration nécessite une meilleure compréhension du cycle du carbone. Le CO_2 atmosphérique est absorbé par deux puits : la biosphère terrestre et l'océan. De 2000 à 2006, l'émission annuelle moyenne de CO_2 anthropique a été estimée à 9.1 giga tonnes (GT) de carbone par an, dont 4.1 GT restent dans l'atmosphère, 2.7 GT sont absorbées par la biosphère terrestre et 2.2 GT sont absorbées par l'océan (Canadell et al. 2007). Ainsi, chaque année, un quart de la production de CO_2 anthropique est absorbé par l'océan, au moyen de la pompe physique (pompe de solubilité) et de la pompe biologique. La solubilité du CO_2 dans l'océan, régie par des processus chimiques et physiques, est plus importante dans les zones où la température est faible. Aux hautes latitudes, et plus particulièrement dans l'Atlantique Nord, la circulation thermohaline grande échelle transfère les eaux de surface froides, donc riches en CO_2, vers le fond de l'océan: c'est ce que l'on appelle la pompe physique (Broecker 1991). Durant la circulation profonde, le CO_2 est ainsi soustrait de tout contact avec l'atmosphère, pour une durée de l'ordre du millier d'années (Broecker et al. 1982). Dans la couche de surface de l'océan, les organismes phytoplanctoniques vont fixer le carbone inorganique dissous via le processus de photosynthèse, et produire de la matière organique (MO) : il s'agit de la production primaire. Celle-ci va ensuite transiter au sein des réseaux trophiques. Une partie de la production primaire va être reminéralisée par les processus de respiration et l'activité bactérienne (Figure I-1). Une autre partie va être exportée vers le fond de l'océan, par des migrations verticales du zooplancton ou par la sédimentation de particules détritiques: c'est ce que l'on appelle la pompe biologique (Figure I-1) (Volk et Hoffert 1985).

[1] Le *forçage radiatif* est une mesure de l'influence d'un facteur dans la modification de l'équilibre entre l'énergie qui entre dans l'atmosphère terrestre et celle qui en sort, et constitue un indice de l'importance de ce facteur en tant que mécanisme potentiel du changement climatique. Un forçage positif tend à réchauffer la surface et un forçage négatif à la refroidir. Selon le rapport du GIEC 2007.

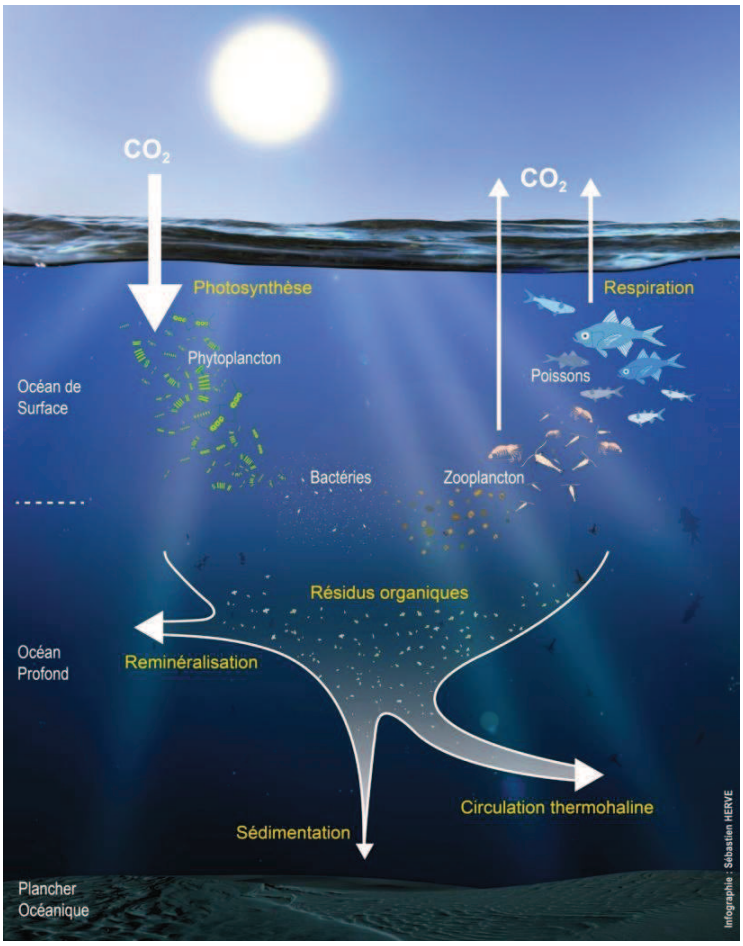

Figure I-1: Schéma conceptuel représentant les différents processus impliqués dans la pompe biologique océanique de carbone. Réalisation Sébastien Hervé.

Moins de 10 % de la production primaire quitte l'océan de surface, et seulement 1 % de cette MO exportée va être stockée dans les sédiments (Memery 2011). Sans cette faible proportion de MO exportée de l'océan de surface, la teneur en CO_2 de l'atmosphère serait le double de la concentration actuelle (Sarmiento et Toggweiler 1982, Memery 2011). La pompe biologique océanique joue donc un rôle clé dans le fonctionnement du cycle du carbone à l'échelle de la planète. L'étude de son fonctionnement et des facteurs contrôlant son efficacité est donc nécessaire pour mieux appréhender sa réaction face à l'augmentation des teneurs en CO_2 atmosphériques.

Les diatomées sont des éléments clés dans le cycle du carbone océanique (Smetacek 1999). Elles participent à hauteur de 35% à la production primaire dans les océans oligotrophes et jusqu'à 75% dans les eaux riches telles que les zones côtières ou l'océan Austral (Nelson et al. 1995; Treguer et al. 1995).

Elles ont la particularité d'être entourées d'une coquille en silice biogénique ($bSiO_2$), le frustule, constituant un ballast leur permettant de sédimenter plus efficacement (Armstrong 2009). Ces micro-algues ont également la capacité d'intégrer de plus grosses particules telles que les agrégats (Thornton 2002) et les pelotes fécales de zooplancton (Schrader 1971), particules représentant la part majoritaire du flux sédimentant dans la colonne d'eau (Fowler et Knauer 1986). Il a été estimé que les diatomées représentent à elles seules 40 % du flux d'export de carbone organique particulaire (COP) (Jin et al. 2006). Si des différences existent dans les rapports $bSiO_2$: C durant la production phytoplanctonique suivant les régions océaniques, ce rapport augmente de façon similaire avec la profondeur quel que soit le bassin océanique (Ragueneau et al. 2002). Compte tenu de l'importance des diatomées dans la production primaire et l'export de carbone, et du lien entre les flux de Si et de C organique, les cycles biogéochimiques de ces deux éléments apparaissent étroitement liés. Une meilleure compréhension de la dynamique de la silice provenant des diatomées est essentielle pour améliorer les modèles globaux des cycles biogéochimiques du C mais aussi du Si dans l'océan.

2. Les diatomées

2.1. Généralités

Les diatomées sont des micro-organismes photosynthétiques unicellulaires eucaryotes, appartenant à la super-classe des Bacillariophycées. Entre 10 000 et 12 000 espèces ont été reconnues, et leur nombre total pourrait s'avérer bien supérieur (Martin-Jezequel et al. 2000 et références incluses). Ces micro-organismes sont abondants dans presque tous les systèmes aquatiques, et sont trouvés sous la forme de cellules solitaires ou de chaînes de cellules, dans les milieux pélagiques ou benthiques (Round et al. 1990). On distingue deux types de structure : les diatomées centriques possèdent une symétrie centrale, tandis que les diatomées pennées ont une symétrie axiale (Hildebrand 2008). Ces micro-algues ont la particularité d'utiliser de l'acide silicique $Si(OH)_4$ (dSi) pour construire leur enveloppe externe : le frustule. Cette enveloppe a une structure complexe, percée de pores plus ou moins larges (Figure I-2). Sa morphologie est spécifique à chaque espèce de diatomées et est donc la base de la classification taxonomique des diatomées (Round et al. 1990). Le frustule est, entre autre, composé de silice amorphe hydratée, de formule générale $[Si_nO_{2n-(nx/2)}(OH)_{nx}]$, $x \leq 4$ (Martin-Jezequel et al. 2000).

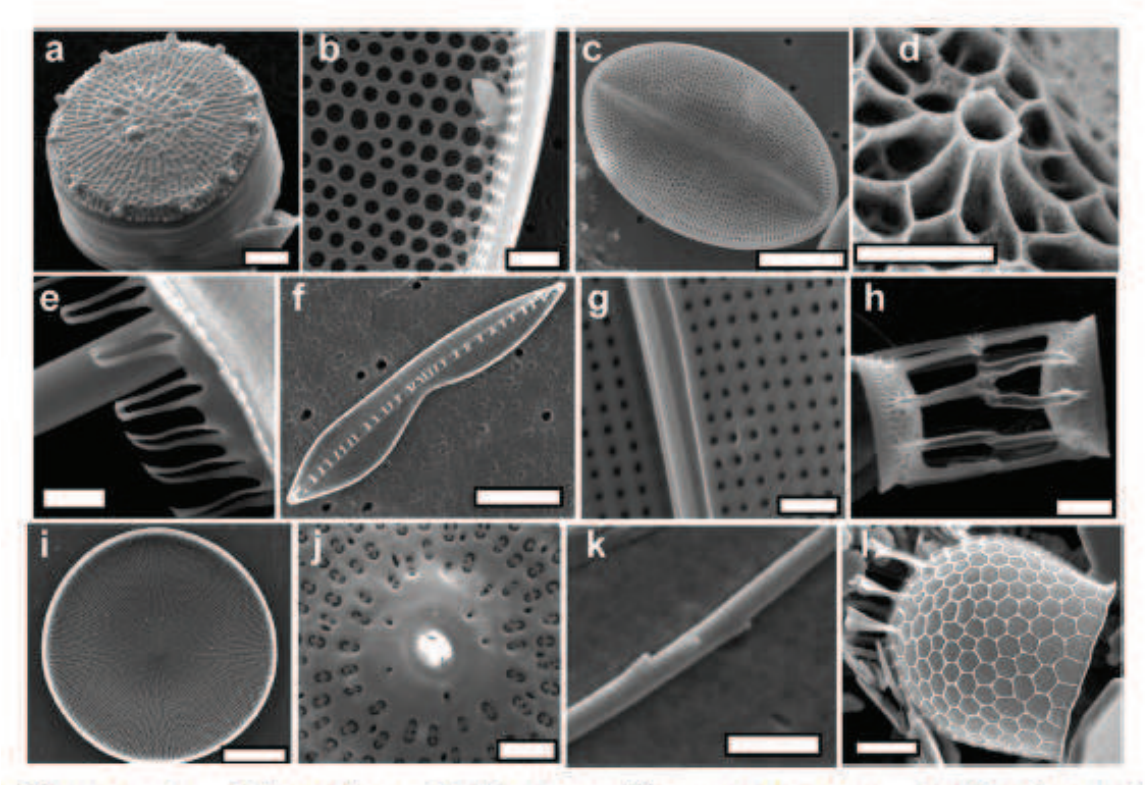

Figure I-2: Diversité de la structure du frustule des diatomées. Les diatomées présentées ici ont été préalablement nettoyées à l'acide. (a) *Thalassiosira pseudonana* (échelle = 1 µm) (b) détail du frustule de *Coscinodiscus wailesii* (échelle = 5 µm) (c) *Cocconeis* sp. (échelle = 10 µm) (d) rimoportula de *Thalassiosira weissflogii* (échelle = 500 nm) (e) structure en couronne de *Ditylum brighwellii* (échelle = 2 µm) (f) *Bacilaria paxillifer* (échelle = 10 µm) (g) détail des pores de *Gyrosigma balticum* (échelle = 2 µm) (h) *Skeletonema costatum* (échelle = 2 µm) (i) valve de Coscinodiscus wailesii (échelle = 50 µm) (j) détail des pores de *Ditylum brighwellii* (échelle = 2 µm), seta de *Chaetoceros gracilis* (échelle = 1 µm) (l) *Stephanopyxis turris* (échelle = 10 µm). D'après Hildebrand (2008).

2.2. Le frustule

2.2.1. Rôle

Le succès écologique des diatomées peut être expliqué en partie par leur particularité architecturale : la présence d'un frustule de silice biogénique, $bSiO_2$ (Martin-Jezequel et al. 2000). Si l'origine de ce squelette siliceux reste inconnue, sa présence semble apporter différents bénéfices aux diatomées.

Il semble, tout d'abord, que le frustule constitue un avantage chimique pour les diatomées. Les organismes photosynthétiques ont besoin de concentrer le CO_2 afin que l'enzyme clé de la fixation du CO_2, appelée la RubisCO (ribulose-1,5-diphosphate carboxylase/oxygénase), soit saturée en CO_2, et pour

ainsi diminuer la photorespiration[2], consommatrice d'énergie. Beaucoup de ces organismes ont développé un mécanisme de concentration du carbone (CCM) afin de concentrer le CO_2 autour de la RubisCO (Aizawa et Miyachi 1986). Le CCM requiert la présence d'anhydrase carbonique (CA), une enzyme qui catalyse la réaction entre le bicarbonate (HCO_3^-) et le CO_2 (Nimer et al. 1999), à la surface des diatomées. Un tampon pH est nécessaire pour accepter ou donner le proton impliqué dans cette réaction: il a été suggéré que, chez les diatomées, la $bSiO_2$ puisse jouer ce rôle (Milligan et Morel 2002).
En 2003, une étude s'est intéressée au rôle de protection du frustule face aux prédateurs (Hamm et al. 2003). Ces scientifiques ont testé la résistance du frustule en appliquant différentes forces à sa surface, jusqu'à sa rupture. Ils ont montré que cette carapace siliceuse est extrêmement résistante, grâce à son architecture et sa composition, et ont suggéré que la grande variété de formes des frustules (Figure I-2) soit le résultat de l'évolution des diatomées en fonction de prédateurs spécifiques.

Le frustule des diatomées pourrait également lui être favorable pour capter la lumière nécessaire à la photosynthèse. Une étude des propriétés optiques du frustule de la diatomée *Coscinodiscus wailesii* a montré que le frustule pourrait concentrer la lumière grâce à la superposition des ondes diffusées par les pores présents à la surface des valves (De Stefano et al. 2005). De plus, le frustule pourrait protéger la cellule des rayonnements ultraviolets (UV). En effet, une récente étude a montré la présence de composés absorbant les UV, appelés acides aminés « *mycosporyne-like* », associés à la structure siliceuse (Ingalls et al. 2010). D'après l'hypothèse de Raven et Waite (2004), le rôle principal du frustule des premières diatomées silicifiées serait son action sur leurs vitesses de sédimentation. Celles-ci pourraient être augmentées en cas de conditions non-optimales pour la croissance des diatomées, via un changement de la densité des cellules planctoniques (augmentation de la quantité de silice et diminution de la flottabilité par diminution de la densité du protoplaste). Cela permettrait aux cellules d'accéder à un habitat un peu plus profond, ayant des ressources plus abondantes. L'augmentation de la densité cellulaire, et donc de la vitesse de sédimentation, pourrait également être un moyen d'éliminer des cellules infectées par un parasite d'une population en bonne santé (Raven et Waite 2004).

[2] La carboxylation correspond à la fixation de CO_2 sur le ribulose-1,5-diphosphate, tandis que la photorespiration correspond à la fixation de dioxygène O_2 sur le ribulose-1,5-diphosphate. Ces deux réactions sont catalysées par la RuBisCO.

2.2.2. Biogénèse et composition

La formation du frustule est un processus complexe très étudié par la communauté scientifique. Le frustule des diatomées est constitué de « couvercles » s'emboitant l'un dans l'autre, appelés thèques (Figure I-3). L'épithèque est la thèque la plus large, englobant la seconde, appelée hypothèque. Ces thèques sont divisées en deux parties: une valve (épivalve et hypovalve) entourée d'une ceinture connective qualifiée de cingulum (épicingulum et hypocingulum). Ce cingulum peut lui-même être divisé en plusieurs bandes, appelée bandes cingulaires (girdle bands), la bande se trouvant à l'endroit où les deux thèques se chevauchent étant appelée plus particulièrement bande pleurale (Loir 2004). L'épithèque et l'hypothèque d'une cellule mère constitueront chacune l'épithèque des deux cellules filles.

Les valves de chaque thèque du frustule sont formées durant la division cellulaire tandis que les bandes cingulaires sont formées durant l'interphase[3] du cycle cellulaire (Figure I-3). La biogénèse de la silice a lieu dans les vésicules de dépôt de la silice (SDV), et il semble y avoir différentes SDV, impliquées respectivement dans la biogénèse des valves et des bandes cingulaires. La concentration en dSi est bien supérieure dans les SDV comparée au milieu naturel, résultat d'un transport actif de dSi du milieu extérieur vers la SDV au moyen de protéines transporteuses d'acide silicique, les SITs (Hildebrand 2008 et références incluses). Plusieurs études se sont intéressées à comprendre les mécanismes de polycondensation de la silice chez les diatomées (Coradin et Lopez 2003 et références incluses, Helmecke et al. 2007 et références incluses). A l'intérieur de la SDV, des composés organiques sont supposés être impliqués dans la biogénèse de la silice, en influençant les cinétiques de polycondensation de la dSi et/ou en fournissant un « patron » pour l'organisation des nanoparticules de silice. Une fois formés, les éléments siliceux vont être déposés à la surface de la cellule par exocytose[4] de la SDV.

[3] Période du cycle de multiplication d'une lignée de cellules pendant laquelle la cellule double la masse et le volume de chacune de ses structures par assimilation.
(http://www.larousse.fr/dictionnaires/francais/interphase/43797?q=interphase#43719)
[4] Processus par lequel une cellule libère une substance (sécrétion, déchets) dans le milieu extracellulaire (http://www.larousse.fr/encyclopedie/medical/exocytose/13000)

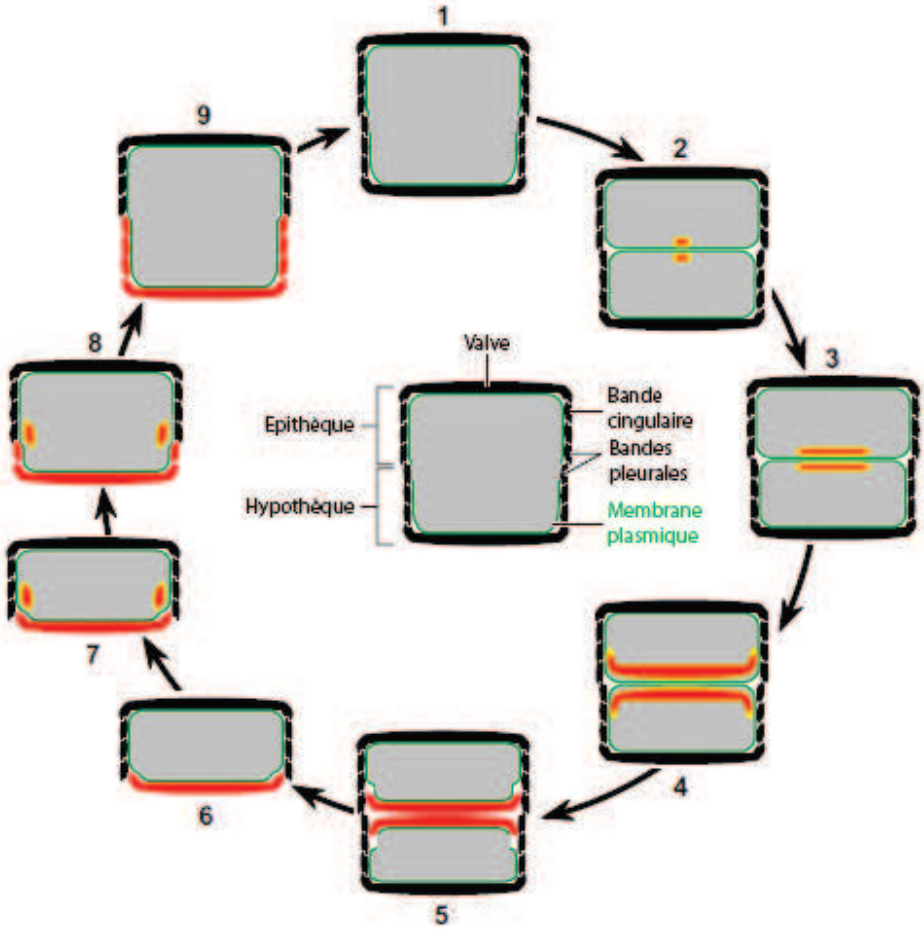

Figure I-3: Au centre, schéma de la structure du frustule des diatomées, en coupe. Autour, cycle cellulaire des diatomées. Les zones grisées représentent le protoplaste, les lignes vertes les membranes plasmiques. Les organites intracellulaires autres que les vésicules de dépôt de la silice (SDV). Les cellules du cercle montrent les différents stades du cycle cellulaire : (1) juste avant la division la cellule contient le maximum de bandes cingulaires ; (2) immédiatement après la cytocinèse[5], de la nouvelle silice biogénique (en rouge) est formée dans chaque cellule fille à l'intérieur de la SDV des valves (en jaune) (3) expansion des SDVs des valves, de plus en plus de silice est déposée (4) au stade final du développement de la SDV, chaque SDV contient une valve pleinement développée (5) les valves nouvellement formées sont déposées à la surface de chaque protoplaste par exocytose[2] de la SDV (6) les cellules filles se sont séparées (7+8) l'expansion du protoplaste durant l'interphase nécessite la synthèse de silice (en rouge) à l'intérieur des SDVs des bandes cingulaires (en jaune); chaque bande est synthétisée dans une SDV qui lui est propre, et après exocytose, est ajoutée à la valve nouvellement formée (hypovalve) (9) après la synthèse de la bande cingulaire finale (la bande pleurale) l'expansion cellulaire s'arrête et la réplication de l'ADN est initiée. D'après Kröger et Poulsen (2008).

[5] Réarrangement du cytoplasme autour de chaque noyau par division (Atlas de Biologie)

Certains pools organiques qui seraient impliquées dans la polymérisation de la silice et dans la structure du frustule se retrouveraient associés au réseau siliceux, en particulier certaines protéines ou certains acides aminés ont été identifiés dans des frustules plus ou moins dégradés. Les silaffines, des phosphoprotéines, et les polyamines à longue chaine (« Long-chain Polyamines » ou LCPA), semblent être étroitement associées à la structure du frustule, car ces molécules ne sont solubilisées que lorsque la silice est totalement dissoute (Kröger et Poulsen 2008 et références incluses). Les interactions silaffines-LCPA pourraient jouer le rôle de « patron » lors de la formation de la silice biogénique (Kröger et Poulsen 2008 et références incluses). Les pleuralines sont, quant à elles, des protéines qui ont été retrouvées uniquement dans les bandes pleurales de l'épithèque et joueraient un rôle dans la formation des cellules filles (Kröger et Poulsen 2008 et références incluses). Un autre type de protéines, les silacidines, sont supposées jouer un rôle dans l'organisation de la matrice et l'initialisation de la minéralisation (Sumper et Brunner 2008). Enfin, une famille de protéines nommées cingulines a été récemment trouvée dans une matrice organique extraite du frustule de *Thalassiosira pseudonana,* dont l'apparence est calquée sur celle des bandes cingulaires de la diatomée et qui, en présence de polyamines, peut polymériser la dSi in vitro (Scheffel et al. 2011).

Les polysaccarides ont longtemps été considérés comme faiblement attachés au frustule (Hoagland et al. 1993). Cependant, il a été récemment montré que des polysaccharides, composés principalement de mannose ainsi que de polymères de glucose, pourraient être étroitement liés au réseau siliceux et pourraient donc avoir un rôle dans sa morphogénèse (Chiovitti et al. 2005, Tesson et Hildebrand 2013).

Concernant le pool organique lipidique, peu d'études ont été réalisées jusqu'à présent sur sa présence dans le frustule. Il semble néanmoins que des lipides, comme les protéines ou les polysaccharides, soient liés au frustule des diatomées, puisque l'analyse par Résonance Magnétique Nucléaire (RMN) du frustule de *Thalassiosira pseudonana* nettoyé avec de l'eau oxygénée indique leur présence (Tesson et al. 2008). Les travaux récents de Suroy (2013) confirment la présence d'une fraction lipidique liée au frustule des diatomées qui ne se solubiliserait qu'une fois le frustule dissous.

Si pendant longtemps certains des pools organiques mentionnés ci-dessus ont même été considérés comme intégrés à la structure du frustule, une très récente étude, combinant analyses d'images et analyses biochimiques sur 5 espèces de diatomées, semble indiquer que cette matrice organique n'est pas encapsulée dans le réseau siliceux mais semble être plutôt très proche de la surface des structures siliceuse (Tesson et Hildebrand 2013). Il n'en reste pas moins que certains de ces pools (i) ne peuvent être solubilisés qu'après dissolution totale de la silice et (ii) sont considérés comme contrôlant la

biogénèse de la silice. Ceci indique clairement des interactions chimiques entre ces pools de MO et la silice, comme mentionné par Abramson et al. (2009).

En plus de ces composants organiques intimement liés au frustule, celui-ci possède un fin revêtement organique, dénommé « *organic coating* », composé principalement de polysaccharides (Round et al. 1990). Sa présence a été suggérée par Lewin (1961) puis a été confirmée par des études microscopiques sur C*ylindrotheca fusiformis* et *Navicula pelliculosa* (Reimann, Lewin et Volcani, 1965 et 1966). Hecky et ses collaborateurs (1973) ont suggéré que cette enveloppe organique soit également composée de lipides (Kates et Volcani 1968, Tesson et al. 2009) et de protéines (Kröger et Poulsen 2008 et références incluses). Plus particulièrement, une famille de protéines, appelée frustuline, est localisée à la surface des diatomées (Kröger et Poulsen 2008 et références incluses).

2.3. Les diatomées dans le cycle du silicium : de la production à l'export

2.3.1. La production des diatomées dans l'océan de surface

Comme mentionné précédemment les diatomées ont besoin d'acide silicique pour se développer et construire leur frustule. De plus, comme tout organisme photosynthétique, le métabolisme de ces micro-algues nécessite de l'énergie lumineuse. Pour pouvoir synthétiser les macro-molécules qui les composent (c'est-à-dire les polysaccharides, les acides nucléiques, les protéines et les lipides) ces organismes ont également besoin d'éléments essentiels (C, H, N, O, P et S) qu'ils vont puiser dans leur environnement extérieur. Outre ces macronutriments, les diatomées ont besoin d'ions inorganiques (calcium, potassium et sodium) (Moore et al. 2013) ainsi que des éléments traces comme le fer (Fe), le cuivre (Cu) et le zinc (Zn) qui sont présents dans des métalloprotéines impliquées dans des processus biochimiques essentiels à leur croissance (Twining et Baines 2013).

L'atténuation rapide de la lumière avec la profondeur restreint la croissance phytoplanctonique à la couche de surface de l'océan, appelée zone euphotique. La concentration des organismes phytoplanctoniques dans cette zone va engendrer une consommation des sels nutritifs. Cela peut, *in fine*, conduire à un appauvrissement de certains éléments nutritifs dans la couche de surface, à des concentrations suffisamment faibles pour limiter la croissance et l'abondance phytoplanctonique. Dans un très récent papier, Moore et collaborateurs (2013) ont synthétisé les différents concepts qui ont été évoqués pour parler des limitations en nutriments :

- Les limitations de Blackman et Liebig

La limitation de Blackman indique que de faibles concentrations d'éléments nutritifs peuvent limiter le taux de croissance des cellules individuelles, tandis que la limitation de Liebig énonce que la quantité totale disponible d'un nutriment définit la limite supérieure de la quantité de biomasse qui peut être produite, appelée le rendement.

- Stress et déficience

Un stress est la réponse physiologique d'une cellule face au manque d'un nutriment. La déficience nutritive correspond quant à elle au manque d'un nutriment par rapport à un autre nutriment. En 1934, Albert Redfield a montré que les rapports stœchiométriques molaires moyens des organismes planctoniques étaient relativement constants et valaient C : N : P = 106 : 16 : 1. En ce qui concerne la dSi, en conditions non limitantes, les diatomées l'absorbent dans les proportions Si : N = 1 mol mol^{-1} et Si : C = 0.09 - 0.13 mol mol^{-1} (en fonction de leur taille) (Brzezinski 1985). Ainsi, si la mesure des sels nutritifs de l'eau de mer indique des concentrations ayant un rapport Si : N > 1, alors les cellules seront plus déficitaires en N qu'en Si.

- La co-limitation nutritive

Il arrive que dans les systèmes océaniques la faible disponibilité de deux nutriments, ou plus, limite la croissance phytoplanctonique. La co-limitation nutritive est attribuée aux conditions où au moins deux nutriments ont été simultanément épuisés, l'addition des deux nutriments étant alors nécessaire pour stimuler la croissance.

En utilisant un modèle global d'écosystème marin, Moore et collaborateurs (2002) ont réalisé des cartographies des limitations nutritives auxquelles sont soumis différents organismes phytoplanctoniques, dont les diatomées, durant les mois d'été (Figure I-4). Cette carte indique qu'en période estivale, la croissance des diatomées est limitée par de faibles concentrations en N dans la moitié de l'océan global, le second macronutriment limitant étant la dSi. Ce modèle indique que le Fe, un des éléments traces, limite la production des diatomées en été pour 39 % de l'océan global. En effet, de nombreuses expériences d'incubation en bouteilles et in-situ ont montré que l'addition de fer dans certaines régions, appelée « High Nutrient Low Chlorophyll » (HNLC), zones comprenant l'Océan Austral, engendre des efflorescences phytoplanctoniques, souvent dominées par les diatomées (Martin 1990; de Baar et al. 2005; Boyd and Ellwood 2010). Deux expériences d'enrichissement de communautés

phytoplanctoniques naturelles ont également montré que l'ajout de Cu favorise la croissance phytoplanctonique (Coale 1991; Peers et al. 2005).

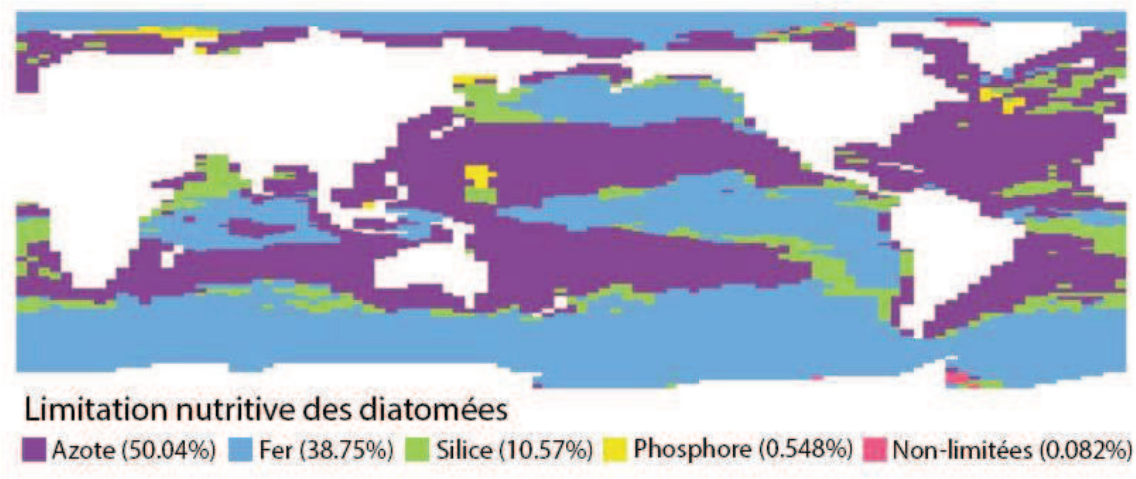

Figure I-4 : Répartition des limitations en sels nutritifs et éléments traces subies par les diatomées en période estivale d'après Moore et collaborateurs (2002). Le pourcentage de la surface totale de l'Océan où chaque élément nutritif limite la croissance des diatomées est indiqué.

Ces limitations en sels nutritifs ne sont pas sans conséquence sur le métabolisme des diatomées. La diminution de la disponibilité des nutriments va diminuer les taux de croissance des cellules et entraîner un découplage dans l'utilisation des nutriments (Geider et La Roche 2002). Il a par exemple été montré que des limitations en N et P (Claquin et al. 2002) ou en Fe (Marchetti et Cassar 2009) vont augmenter les rapports Si : C et Si : N. **Pour le moment, aucune étude n'a été réalisée sur l'effet de faibles concentrations en Cu sur les rapports élémentaires des diatomées.**

En ce qui concerne plus précisément le métabolisme de la silice, des études ont indiqué que la quantité de $bSiO_2$ du frustule des diatomées serait fonction du taux de croissance des diatomées et de la quantité de dSi dans le milieu (Martin-Jezequel et al. 2000). Il a été montré que le contenu en $bSiO_2$ des diatomées est augmenté en cas de limitation en N, P et en lumière (Claquin et al. 2002) et dans certains cas lors de limitation en Fe (Marchetti et Cassar 2009 et références incluses), et que le degré d'augmentation serait plutôt lié à l'intensité de la limitation plutôt qu'à la limitation en elle-même (Claquin et al. 2002). Bucciarelli et collaborateurs (2010) ont cependant indiqué qu'**il n'existe pas de tendance générale significative quant au contenu en $bSiO_2$ des diatomées face à la limitation en Fe**. Etant donné que les diatomées utilisent la dSi pour synthétiser leur frustule siliceux, la diminution du taux de croissance des diatomées en cas de conditions limitantes en dSi induit une diminution de la $bSiO_2$ cellulaire. D'autres

paramètres, comme la présence de brouteurs (Pondaven et al. 2007), ou bien la disponibilité en aluminium (Gensemer 1990), peuvent également affecter le degré de silicification des diatomées.
Si de nombreuses études se sont attachées à comprendre l'effet des conditions nutritives limitantes sur la composition élémentaire des diatomées, notamment sur le degré de silicification du frustule, seules deux études se sont intéressées aux effets de conditions nutritives limitantes sur la composition même du frustule (Soler 2010, Suroy 2013), qui comme nous l'avons vu plus haut est extrêmement complexe. Ces études, réalisées sur la diatomée *Thalasiossira weissflogii* exposée à des conditions de carences strictes en N, Si et P, indiquent que la composition du frustule évolue en fonction des conditions nutritionnelles auxquelles la diatomée est soumise. Par ailleurs, il a été montré que les conditions environnementales, comme des changements de salinité ou l'ajout d'aluminium (Al) sous la forme $AlCl_3$, affectent l'architecture du frustule, comme la taille des pores et leur distribution (Vrieling et al. 1999, 2000). **Une étude approfondie de l'effet des conditions nutritives limitantes sur la structure fine du frustule permettra de mieux comprendre le devenir de la $bSiO_2$ dans la colonne d'eau.**

2.3.2. Facteur influençant la dissolution des diatomées dans la colonne d'eau

- Les processus biotiques

Comme expliqué précédemment, le frustule des diatomées est entouré d'une enveloppe organique. Lewin (1961) a suggéré que la dissolution de la $bSiO_2$ du frustule puisse être retardée par l'existence de cette barrière organique, qui limiterait les contacts entre l'eau de mer environnante et le réseau siliceux. Cette hypothèse a par la suite été confirmée, puisque la vitesse de dissolution de diatomées vivantes, et donc capables de maintenir cette enveloppe, est proche de zéro (Nelson et al. 1976). Lorsque les diatomées ne peuvent plus maintenir cette barrière, sa suppression va être fonction de la composition de la communauté bactérienne et de son activité, ainsi que les conditions environnementales qui vont affecter cette communauté (Patrick et Holding 1985, Bidle et Azam 1999, 2001, Bidle et al. 2002). Une fois le frustule mis à nu, sa dépolymérisation, c'est-à-dire sa dissolution, a lieu.

Le recyclage de la silice biogénique dépend également de deux autres processus biotiques.
Les diatomées peuvent sécréter des substances polymériques, majoritairement constituées de polysaccharides, appelées EPS (Extracellular Polymeric Substances). On distingue les EPS attachées à la cellule, les EPS solubles et les particules exo-polymériques transparentes (TEP). Ces dernières ont été montrées comme favorisant l'agrégation des diatomées (Passow et al. 2001). L'excrétion des EPS (et donc des TEP) par les diatomées est favorisée lorsque les cultures sont limitées en nutriments (Thornton

2002). Les agrégats jouent un rôle important dans le recyclage et l'export de la silice, d'une part parce que ce sont des acteurs clés du flux de sédimentation (Turner 2002), et d'autre part parce que ces particules protègent les frustules du milieu environnant, retardant leur dissolution (Moriceau et al. 2007).

Les diatomées peuvent également être ingérées par le maillon trophique supérieur, le zooplancton. Tandis que le carbone est digéré, on peut retrouver 85% de la $bSiO_2$ initialement ingérée dans les pelotes fécales (Cowie et Hedges 1996, Tande et Slagstad 1985). Comme les agrégats, les pelotes fécales sont des acteurs majeurs du flux de sédimentation (Turner 2002) et semblent offrir une protection contre la dissolution. Par contre, certains organismes sont capables de casser le frustule, ce qui augmentent la surface de contact avec l'eau environnante et tendrait à favoriser la dissolution (Schultes et al. 2010).

- Les processus abiotiques

Il est généralement admis que la dissolution de la silice consiste en une hydrolyse de la surface minérale via des attaques nucléophiles des dipôles de l'eau sur les ponts siloxane Si-O-Si du réseau siliceux, formant alors des groupements silanol, SiOH (Loucaides et al. 2012). Sverjensky et Sahai (1996) ont montré que le pH auquel la silice existe à un potentiel électrique neutre, autrement appelé pH de charge de surface nulle (zero surface charge, pH_{ZSC}) est autour de 2 – 3,5. A ce pH, les groupements silanol sont sous la forme SiOH tandis qu'au dessus et en dessous de ce pH les groupements silanol perdent ou acquièrent un proton suivant les équations suivantes:

$$SiOH + H^+ \Leftrightarrow SiOH_2^+ \qquad (1)$$

$$SiOH \Leftrightarrow SiO^- + H^+ \qquad (2)$$

Puisque le pH_{ZSC} est acide, au pH de l'eau de mer la réaction (2) va prédominer, induisant la forte abondance de groupements silanol déprotonés, SiO^-. Cette charge négative va accroître la dissociation des molécules d'eau et va donc augmenter son caractère nucléophile, ce qui va faciliter l'hydrolyse des liaisons siloxanes (Dove 1994), conduisant finalement à la libération de $Si(OH)_4$ dans l'eau de mer (Figure I-5).

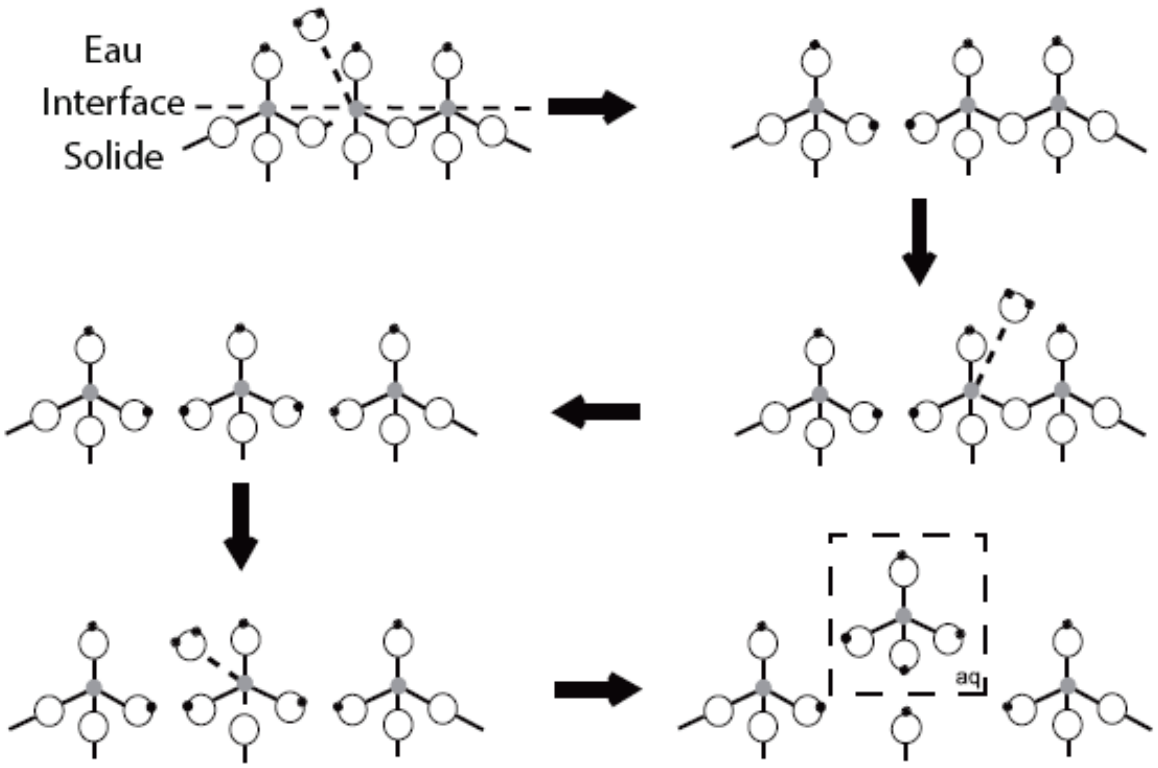

Figure I-5: Réaction d'hydrolyse de la silice dans l'eau, sous un pH quasi-neutre. Les sphères blanches représentent les atomes d'oxygènes O, les sphères grises les atomes de silice Si et les sphères noires les atomes d'hydrogène H. D'après Loucaides (2009).

Une compréhension mécanistique de la dissolution de la $bSiO_2$ est nécessaire pour pouvoir quantifier son devenir de la surface jusqu'au fond des océans.

Les propriétés physico-chimiques de l'eau de mer environnante vont influencer la dissolution du frustule des diatomées. La vitesse de dissolution de la silice biogénique est fonction de la température, et augmenterait d'un facteur de 2,27 lorsque la température augmente de 10 °C (Kamatani 1982). La concentration en dSi de l'eau de mer environnante affecte également la vitesse de dissolution de la $bSiO_2$ (Rickert et al. 2002). Les études de Tamburini et al. (2006) et de Loucaides et al. (2012) sont les seules à s'être, pour le moment, intéressées à la cinétique de dissolution et à la solubilité de la $bSiO_2$ en cas d'augmentation de pression. Comme précédemment présenté, le pH va également affecter la dissolution de la silice, une augmentation du pH par rapport au pH_{ZSC} favorisant la dissolution. La teneur en électrolytes du milieu aqueux affecte la vitesse de dissolution de la $bSiO_2$, la dissolution étant favorisée en présence de cations alcalins (Loucaides et al. 2008).

Les propriétés intrinsèques du frustule vont également influencer sa dissolution. Lorsque de l'aluminium est présent dans le milieu, les diatomées vont l'associer à la silice au sein de la silice biogénique (Van Beusekom et Weber 1992, Gehlen et al. 2002) ce qui va diminuer sa solubilité et sa vitesse de dissolution (Van Bennekom et al. 1991). S'il a été suggéré que cette association se fasse durant la biogénèse (Gehlen et al. 2002), Koning et al. (2007) ont montré que les ratios Al : Si de diatomées mortes et nettoyées de la matière organique augmentent au cours du temps lorsqu'elles sont placées dans un milieu riche en Al, et ont suggéré que l'incorporation d'Al se fasse lorsque les diatomées sont mortes, entrainant la formation d'une couche d'aluminosilicates à la surface du frustule. Les concentrations en Al dans l'eau de mer étant généralement assez faibles (< 0.1 µmol L^{-1}), les rapports Al : Si des diatomées dans l'océan sont le plus souvent peu élevés (Van Bennekom et al. 1991). L'incorporation d'aluminium se fait majoritairement dans les sédiments où les concentrations en Al sont plus élevées (Loucaides et al. 2012). La vitesse de dissolution du frustule va être également affectée par sa surface spécifique. Les espèces ayant des frustules comportant de nombreuses ornementations auront une surface spécifique importante (une interface solide-eau de mer élevée) ce qui va favoriser leur dissolution (Dixit et Van Cappellen 2002 ; Loucaides et al. 2012). Les vitesses de dissolution sont également affectées par la quantité de sites actifs de la surface de silice exposée à l'eau de mer (Van Cappellen et al. 2002). Van Cappellen (1996) a d'abord suggéré que la réactivité de la $bSiO_2$ diminue avec la profondeur dans les sédiments, ce qu'il a appelé « le vieillissement » (aging). Puisque, plus la quantité de groupements silanol est élevée, plus la dissolution est facilitée, la quantité de groupements silanol permet donc une estimation de la réactivité du frustule. En utilisant la spectroscopie infrarouge à transformée de Fourier (IRTF), Schmidt et al. (2001) ont estimé la quantité relative de groupements siloxane (Si-O-Si) par rapport aux groupements silanol (SiOH). Ils ont montré que ce ratio augmente avec l'âge de l'échantillon (et donc que la quantité relative de groupements silanol diminue), ce rapport étant plus élevé dans le frustule des diatomées de surface que dans celui des diatomées provenant des trappes à sédiments. Ainsi, la diminution de la quantité de sites réactifs à la surface du frustule des diatomées a lieu dès sa sédimentation dans la colonne d'eau.

2.3.3. Modélisation de la cinétique chimique de dissolution de la $bSiO_2$

Les expériences en laboratoire s'attachant à l'étude de la cinétique chimique de la dissolution de la silice biogénique sont importantes dans l'étude du cycle de la Si et donc du C. L'objectif final est de pouvoir réaliser des équations mathématiques dans lesquelles les effets des processus biotiques et abiotiques seraient inclus.

Les premières études sur la cinétique de la dissolution de la silice biogénique ont considéré une simple exponentielle (équation 3) pour modéliser la dissolution de la $bSiO_2$ (ou l'augmentation de la dSi) dans des expériences en milieu fermé, appelé batch, et dans des conditions sous-saturées par rapport à la solubilité de la silice (Truesdale et al. 2005 et références incluses)

$$\hat{C}_{(t)} = C_0 . e^{-k.t} \qquad (3)$$

Où $\hat{C}_{(t)}$ est la concentration en $bSiO_2$ (µmol L^{-1}) calculée au temps t (jours), C_0 est la concentration initiale en $bSiO_2$ (µmol L^{-1}), et k est la constante de dissolution spécifique (d^{-1}). Le terme « constante de dissolution spécifique » se réfère à la vitesse de dissolution normalisée par la concentration en $bSiO_2$ (Passow et al. 2011).

Cette approche considère que toutes les molécules du solide sont disponibles pour la dissolution à tout moment. Toutefois, dans un solide comme le frustule, les molécules sont réparties sur une épaisseur et ne sont donc pas forcement toutes accessibles en même temps (Truesdale et al. 2005). De ce fait, une grande majorité des expériences de dissolution en batch est mieux modélisée par des sommes d'exponentielles (Truesdale et al. 2005). Parmi elles, l'expérience de Kamatani et Riley (1979) indique une dissolution en deux temps du frustule des diatomées *Thalassiosira decipiens* et *Rhizosolenia hebetata*. Cette dissolution serait le reflet d'une composition fractionnée du frustule de ces diatomées, chaque fraction ayant une vitesse de dissolution qui lui est propre (Kamatani et Riley, 1979). En étudiant le matériel provenant de trappes à sédiments de l'Atlantique Nord, Gallinari et al. (2002) ont suggéré l'existence de deux phases de $bSiO_2$ ayant des propriétés de dissolution et des solubilités différentes. Ils ont mesuré des solubilités de 500 à 700 µmol L^{-1}, soit 30 à 50 % plus faibles que les solubilités estimées à 2°C (1000 µmol L^{-1}, Dixit et al. 2001), et ont donc suggéré qu'une phase du frustule, la plus réactive, se soit dissoute avant d'avoir été collectée. Cette structure du frustule en deux phases de $bSiO_2$ semble être renforcée par le papier récent de Tesson et al. (2009) qui, en étudiant le frustule de deux diatomées, *Phaeodactylum tricornutum et Thalassiosira pseudonana*, ont montré que la surface du frustule est composée de deux types de silice, de la silice condensée (SiO_2) et de la silice faiblement polymérisée. **La structure en deux phases du frustule nécessite d'utiliser des équations mathématiques de plus grande complexité que celle de l'équation (3) pour modéliser la cinétique chimique de dissolution de la $bSiO_2$, et pour ainsi pouvoir mieux estimer le recyclage de la silice dans la colonne d'eau et son export au fond de l'océan.**

2.3.4. Export de $bSiO_2$

L'export de la silice biogénique va dépendre de la vitesse de dissolution du frustule des diatomées et de leur vitesse de sédimentation. En effet, la quantité de $bSiO_2$ pouvant atteindre le fond de l'océan va être affectée par l'intensité de la dissolution dans la colonne d'eau. Une bonne compréhension des processus régissant la dissolution des frustules des diatomées est donc importante pour mieux estimer l'export de $bSiO_2$. La quantité de matériel exportée au fond des océans va également être affectée par la vitesse de sédimentation des diatomées. La silice biogénique du frustule constitue un ballast qui, par sa densité supérieure à celle de la matière organique, va augmenter la vitesse de sédimentation des diatomées par rapport à d'autres cellules phytoplanctoniques non ballastées (Armstrong 2009). De plus, l'export de ces micro-algues est favorisé lorsqu'elles sont intégrées aux agrégats et aux pelotes fécales de zooplancton, particules jouant un rôle clé dans les flux de sédimentation (Turner 2002). Lorsque la faible disponibilité les éléments nutritifs limite la croissance phytoplanctonique, la formation d'agrégats augmente (Turner 2002) : ainsi, l'export de $bSiO_2$ des diatomées semble être favorisé lorsque celles-ci ont été limitées en nutriments en fin d'efflorescence phytoplanctonique.

Le flux d'export moyen de la $bSiO_2$ produite dans la zone euphotique a été estimé à ~ 44 % (Tréguer et De La Rocha 2013). Cependant, l'intensité de la dissolution de la $bSiO_2$ par rapport à la production de silice (D : P) est variable suivant les régions de l'océan mondial, avec des valeurs allant de 0.46 dans le Pacifique Nord à 0.82 dans l'Atlantique Nord (Tréguer et de la Rocha 2013). Ces différences de préservation sont attribuées à la diversité des conditions physiques, chimiques et biologiques des différents bassins océaniques. Notamment, les différentes conditions environnementales entrainent une variabilité des communautés phytoplanctoniques présentes dans les eaux de surface qui peut, en partie, expliquer les différences de préservation de la $bSiO_2$ dans l'océan mondial. Par exemple, l'efficacité d'export important dans le Pacifique Nord pourrait être liée à la présence de diatomées de grande taille dans cette région de l'océan mondial (Brzezinki et al. 2011, Tréguer et De La Rocha 2013). L'effet des conditions de croissance sur la structure du frustule et sur la capacité d'export de la $bSiO_2$ n'a pour le moment que peu été étudié, mais pourrait permettre de mieux comprendre les différences de préservation entre les bassins océaniques.

3. Les objectifs de cette thèse

Comme nous l'avons vu précédemment, la structure même du frustule est susceptible d'influencer sa vitesse de dissolution. Or s'il a été montré que des conditions nutritives limitantes peuvent changer le degré de silicification du frustule, peu d'études ont étudié l'impact de ces limitations sur la structure même du frustule et encore moins sur la dissolution. Cette étape est pourtant indispensable à l'estimation de l'export. Dans cette thèse nous nous proposons donc de mieux comprendre l'impact de l'environnement nutritionnel des diatomées sur la structure du frustule, et par la suite sur le recyclage et l'export de la silice biogénique dans la colonne d'eau. Comme le montre la carte de Moore et al. (2002) (Figure I-4), les principales limitations de la croissance des diatomées, identifiées dans l'océan global en période estivale, sont la limitation en fer (39 % de l'océan global) et les limitations en nitrate et acide silicique (50 et 11 % de l'océan global). Nous avons choisi d'estimer l'impact de ces limitations sur la structure du frustule des diatomées et sur sa dissolution. Nous nous sommes également intéressés aux effets de la limitation en cuivre, dont l'impact sur la composition élémentaire et la dissolution des diatomées n'a été que très peu étudié. Pour cela, ce travail tentera de répondre aux questions suivantes :

(i) Quel est l'effet de l'environnement nutritif sur la structure du frustule des diatomées?

(ii) L'environnement nutritif des diatomées affecte-il la dissolution post-mortem des frustules?

(iii) Quel est l'effet des l'environnement nutritif des diatomées sur l'export de $bSiO_2$?

Pour répondre à ces questions, ce manuscrit s'articule autour de plusieurs chapitres (Figure I-6).
Les chapitres II et III sont centrés sur l'effet de limitation en micronutriments sur la production et l'export de la silice des diatomées.
Plus particulièrement, dans le chapitre II, les effets d'une limitation en fer et d'une carence stricte en cuivre sur le taux de croissance, la composition élémentaire et les caractéristiques morphologiques de la diatomée pennée *Pseudo-nitzschia delicatissima* ont été étudiés. La structure fine et la composition du frustule des diatomées soumises aux deux conditions de croissance limitantes ont été étudiées au moyen de la spectroscopie InfraRouge à Transformée de Fourier (IRTF). Ce travail fait l'objet d'un article « Copper and iron availability affects differently the elemental composition and the export ability of the diatom *Pseudo-nitzschia delicatissima*. Part I – Elemental composition and frustule structure» qui sera prochainement soumis à la revue *Limnology and Oceanography*.

Le chapitre III est centré sur le devenir dans la colonne d'eau des cellules de *Pseudo-nitzschia delicatissima* précédemment limitées en micronutriments Fe et Cu. La cinétique de dissolution du frustule des diatomées a été suivie et modélisée, afin de mieux comprendre la variabilité de la dissolution dans la colonne d'eau, et d'estimer l'impact de l'environnement nutritionnel sur l'export de silice biogénique. Ce travail fait l'objet d'un article compagnon de l'article précédent, « Copper and iron availability affects differently the elemental composition and the export ability of the diatom *Pseudo-nitzschia delicatissima*. Part II – Diatom dissolution », qui sera prochainement soumis à la revue *Limnology and Oceanography*.

Le chapitre IV est centré sur l'effet de limitation en macronutriments, acide silicique (dSi) et nitrates (NO_3^-) sur l'export de la silice des diatomées. A la suite d'une expérience, durant laquelle la diatomée *Thalassiosira weissfloggi* a été soumise à des conditions de croissance déficitaires en dSi ou en NO_3^-, le devenir de son frustule a été étudié au cours d'expériences de dissolution, puis modélisé. La structure fine et la composition du frustule des diatomées ont été suivies tout au long de leur dissolution, par IRTF, afin de déterminer si les différences dans les cinétiques de dissolution et dans l'export de la $bSiO_2$, en fonction des conditions de croissance, peuvent être expliquées par des modifications dans la structure fine du frustule. Cette étude est développée sous la forme d'un article, « Effect of Si and N deficiencies on *Thalassiosira weissflogii* frustule structure and consequences on biogenic silica dissolution », qui sera soumis à Global Biogeochemical Cycles.

Enfin, le chapitre V constitue une synthèse des travaux effectués et présente les perspectives suggérées par les résultats obtenus.

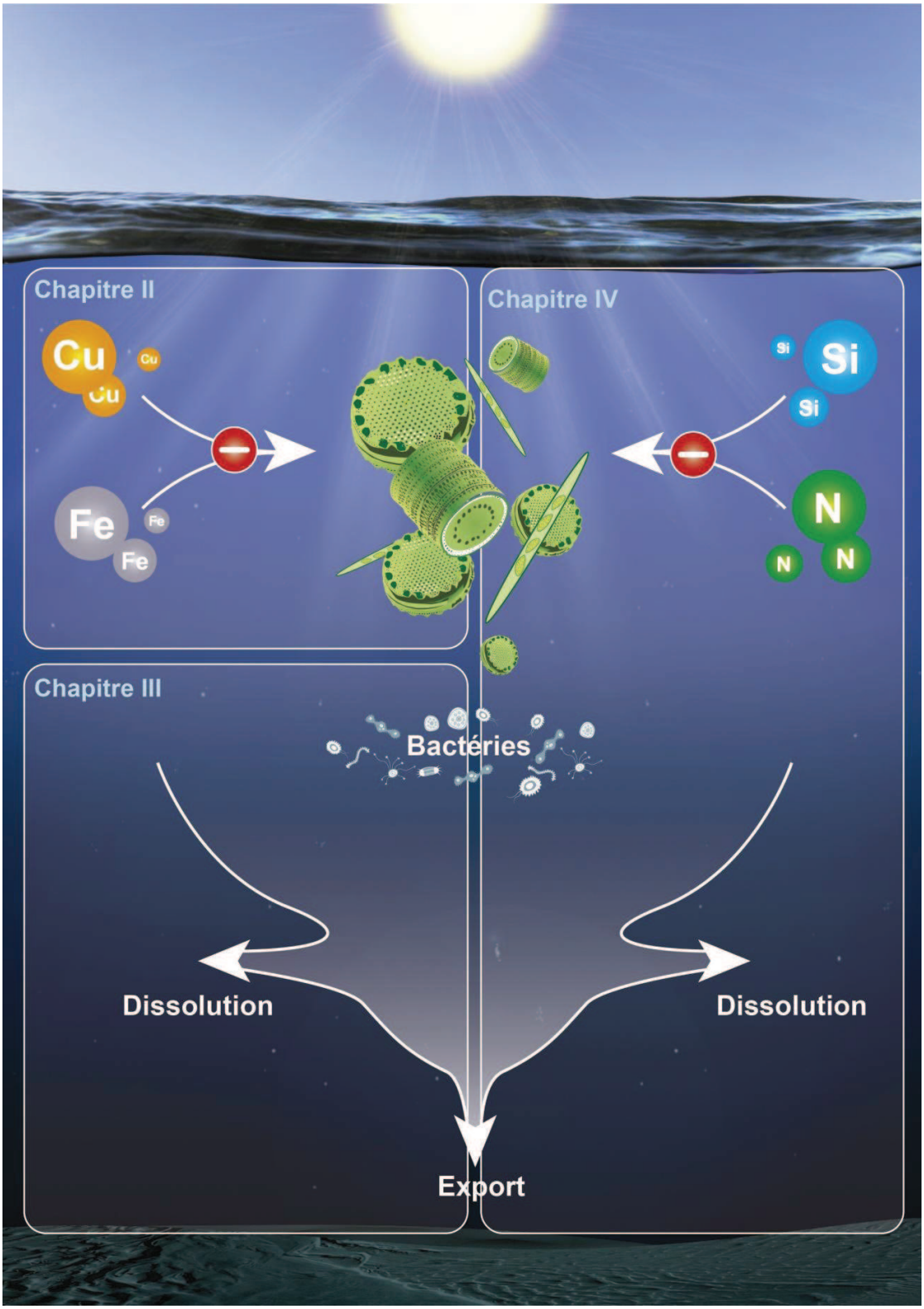

Figure I-6 : Schéma de la stratégie scientifique adoptée dans le cadre de cette thèse. Réalisation Sébastien Hervé.

Chapitre II.

Effet d'une carence stricte en Cu et d'une limitation en Fe sur la structure du frustule et la composition élémentaire de *Pseudo-nitzschia delicatissima*

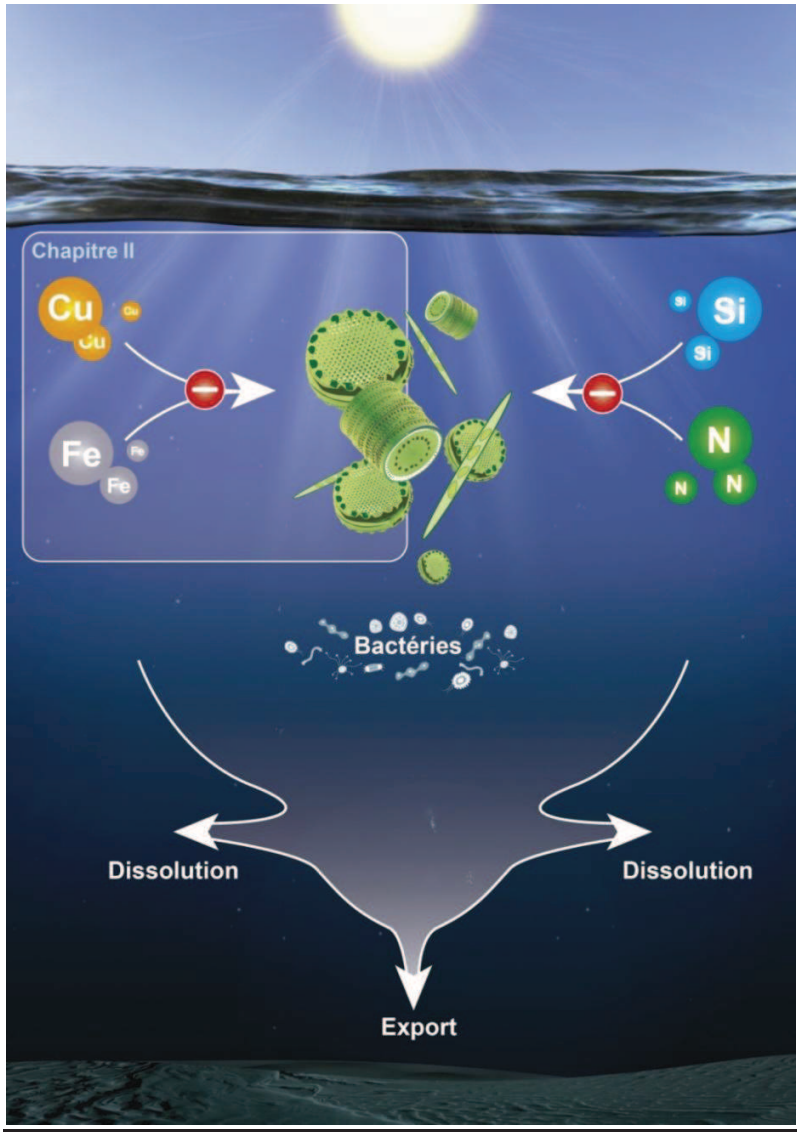

II. Chapitre II : Effet d'une carence stricte en Cu et d'une limitation en Fe sur la structure du frustule et la composition élémentaire de la diatomée *Pseudo-nitzschia delicatissima*

1. Préambule

1.1. La structure biphasique du frustule

Comme nous l'avons souligné dans l'introduction, le frustule des diatomées possède une structure complexe dont les processus de formation sont de mieux en mieux décrits, mais dont la composition reste encore peu déterminée. En 1973, Hecky et collaborateurs ont proposé un schéma hypothétique du frustule siliceux et de la couche de matière organique de surface lui étant associée, qui a par la suite été complété par l'étude de Lobel et al. (1996). Si le schéma d'Hecky et collaborateurs est classiquement utilisé pour représenter la structure du frustule, de nombreuses études, réalisées sur la cinétique chimique de dissolution de la silice biogénique et sur la solubilité du matériel provenant de trappes à sédiments, indiquent que la matrice siliceuse serait en fait composée de deux phases de silice biogénique, chaque phase possédant des propriétés de dissolution et de solubilité qui lui sont propres (Kamatani and Riley 1979; Gallinari et al. 2002; Truesdale et al. 2005; Moriceau et al. 2009). De plus, certaines molécules organiques, qu'elles jouent un rôle identifié ou non dans les processus de silicification des diatomées, sont clairement associées à la matrice siliceuse (Kröger et Poulsen 2008 et références incluses, Suroy et al. en révision) certaines ne pouvant être solubilisées qu'après dissolution de la silice biogénique.

Pendant ma thèse, j'ai entamé un travail d'identification visuelle des phases de $bSiO_2$ en utilisant des outils de microscopie (microscopie à force atomique, AFM, ou microscopie électronique à balayage, MEB) sur une diatomée centrique de grande taille, *Coscinodiscus granii*. Pendant cette étude, détaillée en annexe I et dont les résultats sont en cours de traitement, nous avons suivi l'évolution de l'architecture du frustule en fonction de sa dissolution par de nombreuses mesures de la taille des pores et des ornements. Nous sommes partis de l'idée qu'en fin de dissolution, seule la phase la moins soluble serait visible, et que si celle ci correspondait à une structure physique particulière du frustule, nous pourrions l'identifier. Les images et premières mesures réalisées permettent, à première vue, de déduire que pour la diatomée *Coscinodiscus granii* les phases de $bSiO_2$ ne correspondent à aucune structure physique clairement identifiable. Contrairement à ce que Schrader (1971) a montré pour la diatomée

Thalassiosira baltica, il semble que lorsque la $bSiO_2$ se dissout c'est le frustule entier qui devient poreux et qu'on ne puisse pas suivre, dans ce cas précis, la dissolution par l'agrandissement des pores.

1.2. Les limitations et la structure du frustule

Une diminution du taux de croissance des diatomées, induite par une faible disponibilité en nutriment, va affecter le degré de silicification des frustules des diatomées, i.e. la quantité de silice biogénique rapportée à la surface cellulaire (Martin-Jezequel et al. 2000; Claquin et al. 2002). Si l'effet de ces limitations sur le contenu en $bSiO_2$ du frustule des diatomées a été quantifié, son effet sur la structure fine du frustule a quant à lui été peu étudié. Pendant ma thèse je me suis donc intéressée aux effets de certaines limitations nutritives sur la structure du réseau siliceux composant le frustule de la diatomée *P. delicatissima*, au moyen de la spectroscopie InfraRouge à Transformée de Fourier (IRTF).

1.3. La spectroscopie infrarouge à transformée de Fourier

La spectroscopie infrarouge est une technique analytique basée sur les échanges d'énergie entre la matière et une onde électromagnétique appartenant au domaine de l'infrarouge. Les molécules constituant la matière sont formées d'atomes liés entre eux par des liaisons pouvant être animées de mouvements complexes, autrement appelés modes de vibration. On distingue par exemple les modes de vibration de déformation et les modes de déformations d'élongation (ou encore appelés mode de vibration de valence) (Figure II-1). Les fréquences de vibration de ces liaisons sont du même ordre de grandeur que celles du rayonnement infrarouge (les spectres infrarouge couvrant généralement les longueurs d'onde allant de 2.5 µm à 50 µm)(Fröhlich and Gendron-Badou 2002). Le rayonnement infrarouge va être absorbé lorsque sa fréquence coïncide avec la différence d'énergie de deux niveaux de vibrationnelles de la liaison. La diminution subséquente de l'intensité du rayonnement va dépendre du nombre de molécules irradiées comportant la liaison associée à cette fréquence.

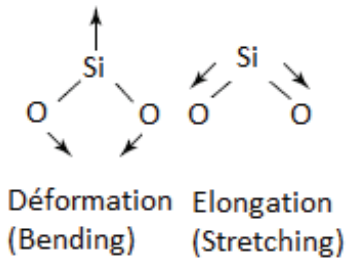

Figure II-1 : Exemple de modes de vibration de déformation et d'élongation (adapté à partir de Stuart 2004)

En particulier, la spectroscopie IRTF exploite le phénomène d'interférences de deux ondes, par l'utilisation d'un interféromètre de Michelson. La source de rayonnement infrarouge fournit un rayonnement continu dirigé vers un interféromètre. Celui-ci est constitué d'un séparateur de rayon, qui va diriger la moitié du rayonnement vers un miroir fixe et l'autre moitié vers un miroir mobile. Ce dernier se déplace de façon continue, ce qui va générer une différence de chemin optique entre les deux faisceaux. Quand ils se recombinent, ils vont interférer. Le tracé de l'intensité d'interférence en fonction du trajet du miroir mobile donne une courbe complexe : l'interférogramme. Celui-ci va ensuite être traité au moyen d'une équation mathématique: la transformation de Fourier. On obtient ainsi le spectre de la matière analysée. Le signal d'un laser hélium-néon est enregistré simultanément, et va servir de référence. Les mesures peuvent se faire par transmission du signal dans l'échantillon (le faisceau traverse l'échantillon), par réflexion du signal, ou par réflexion totale atténuée (ATR). Dans le cadre de cette thèse, les mesures ont été faites par transmission, après dépôt d'échantillons sur microplaque. La confrontation des spectres IRTF à des tables associant nombres d'ondes et liaison atomique permet de déterminer les liaisons présentes dans les échantillons analysés.

1.4. Pourquoi étudier l'effet des limitations en fer et en cuivre sur la structure du frustule?

Les concentrations subnanomolaires en Fe limitent la croissance phytoplanctonique dans 50 % de l'Océan mondial (Boyd and Ellwood 2010), et plus particulièrement dans les zones appelées « High Nutrient Low Chlorophyll » (HNLC). Depuis 1998, et les expériences d'Hutchins et Bruland et de Takeda, il est généralement admis qu'une limitation en Fe induit une augmentation du degré de silicifiation des diatomées. Cette augmentation est d'ailleurs la base de l'hypothèse de Boyle (1998), qui suggère que les diatomées plus silicifiées en cas de limitation en Fe auraient une vitesse de sédimentation plus élevée que les cellules non limitées, et qu'elles exporteraient donc plus de Si que de N et de C au fond de

l'océan. Deux récentes revues ont cependant montré qu'il n'existe pas de tendance générale entre le degré de limitation en Fe et le degré de silicification des diatomées (Marchetti et Cassar 2009, Bucciarelli et al. 2010). L'impact d'une limitation en Fe sur le degré de silicification, et donc sur l'export de $bSiO_2$ vers le fond de l'océan, reste donc à préciser.

Le cuivre (Cu), comme le Fe, est un métal essentiel à la croissance phytoplanctonique. Deux expériences d'enrichissement sur des communautés phytoplanctoniques naturelles ont montré qu'un ajout de Cu entraîne une augmentation de la croissance du phytoplancton (Coale 1991; Peers et al. 2005). Si l'effet de concentrations limitantes en Cu sur les paramètres photosynthétique du phytoplancton a été étudié (e.g. Peers et Price 2006, Lelong et al. 2013), son effet sur le contenu cellulaire en C des diatomées n'a été examiné que dans une seule étude (Annett et al. 2008), et aucune ne s'est intéressée à son effet sur le contenu en N en et $bSiO_2$. De plus, il a été suggéré que le Cu entraine une limitation en Fe chez les diatomées (Maldonado et al. 2006). Dans ce cas, la limitation en Cu entrainerait un découplage dans l'utilisation des macronutriments, ce qui pourrait affecter les cycles biogéochimiques des éléments majeurs. Nous avons donc soumis la diatomée *Pseudo-nitzschia delicatissima* à une carence stricte en Cu et à une forte limitation en Fe, afin d'étudier l'effet de ces limitations sur la composition élémentaire et le degré de silicification de cette diatomée, et pour déterminer si les modifications induites par la carence en Cu sont comparables à celles engendrées par une limitation en Fe.

2. Copper and iron availability affects differently the elemental composition and the export ability of the diatom *Pseudo-nitzschia delicatissima*. Part I – Elemental composition and frustule structure

Boutorh Julia[1], Bucciarelli Eva[1], Boukerma Kada[2], Rinnert Emmanuel[2], Ragueneau Olivier[1], Moriceau Brivaëla[1].

[1] Université de Brest, Institut Universitaire Européen de la Mer (IUEM), CNRS, Laboratoire des Sciences de l'Environnement Marin, UMR 6539 CNRS/UBO/IFREMER/IRD, 29280 Plouzané, France.

[2] Laboratoire Détection, Capteurs et Mesures, Département Recherches et Développements technologiques, Institut Carnot Ifremer-Edrome, IFREMER / Centre de Bretagne, 29280 Plouzané France.

To be submitted to Limnology and Oceanography

2.1. Résumé

Nous avons examiné l'effet de la carence stricte en cuivre (Cu) et de la limitation en fer (Fe) sur le contenu cellulaire en chlorophylle a (Chl a), carbone (C), azote (N) et en silice biogénique ($bSiO_2$) ainsi que les dimensions cellulaires de la diatomée pennée marine *Pseudo-nitzschia delicatissima.* La spectroscopie InfraRouge à Transformée de Fourier (IRTF) a été utilisée pour explorer la structure chimique des frustules limités en micronutriments, à une échelle plus fine. Nous avons observé une augmentation significative des quotas en N, et pas de modifications des quotas en Chl a, C en $bSiO_2$ avec la carence stricte en Cu. La limitation en Fe a, quant à elle, diminué tous les quotas cellulaires. Les analyses par IRTF indiquent une plasticité du frustule à l'échelle moléculaire, en fonction des conditions de croissance. Nous avons compilé les données disponibles dans la littérature, y compris les résultats de cette présente étude, sur l'effet de la limitation en Fe sur le genre *Pseudo-nitzschia*. Cette compilation montre une tendance significative entre le degré de limitation en Fe et la concentration en Chl a, la morphologie des cellules, le contenu en N et C par volume cellulaire et le contenu en $bSiO_2$ par surface cellulaire. Pour un taux de croissance similaire, la limitation en Fe et la carence stricte en Cu n'ont pas les mêmes effets sur le contenu en Chl a, la morphologie de la cellules et les quotas en N, suggérant que la carence stricte en Cu n'induit pas de limitation en Fe. La tendance significative dans la composition élémentaire de *Pseudo-nitzschia* limitée en Fe, pour les souches côtières et océaniques, souligne que des tendances significatives peuvent exister au niveau du genre. En particulier, le degré de silicification diminue aux plus hauts degrés de limitation Fe. Cette tendance s'oppose à l'hypothèse selon laquelle la limitation en Fe conduit à une élévation du degré de silicification, ce qui pourrait avoir d'importants effets sur l'export de $bSiO_2$ des diatomées *Pseudo-nitzschia*.

2.2. Abstract

We examined the effect of copper (Cu) starvation and severe iron (Fe) limitation on the cellular chlorophyll a (Chl *a*), carbon (C), nitrogen (N) and biogenic silica ($bSiO_2$) and on the cell dimensions of the marine pennate diatom *Pseudo-nitzschia delicatissima.* Fourier Transform InfraRed spectroscopy (FTIR) was used to explore the chemical structure of the micronutrient-limited frustule at a finer scale. We observed a significant increase of N quotas and no change in Chl *a,* C and $bSiO_2$ quotas with Cu starvation. By contrast, Fe limitation significantly decreased all the cellular quotas. FTIR analysis indicated a plasticity of diatom frustule at the molecular scale depending on growth conditions. We compiled the data available in the literature, including the results of the present study, about the effect of Fe limitation on the genus *Pseudo-nitzschia*. This compilation showed significant trends between the degree of Fe limitation and Chl a concentration, cell morphology, N and C content per cell volume and $bSiO_2$ content per cell surface. At similar growth rate, Cu starvation and Fe limitation have different effects on Chl a content, cell morphology and N quotas, suggesting that Cu starvation does not induce Fe limitation. The significant trend observed in the elemental composition of Fe-limited *Pseudo-nitzschia,* for both coastal and oceanic strains, highlights that significant trends may exist at the genus level. In particular, the degree of silicification tends to decrease at the highest degrees of Fe limitation. This trend is opposing the assumption that Fe limitation leads to a higher degree of silicification, and may have significant effects on $bSiO_2$ export from *Pseudo-nitzschia* diatoms.

2.3. Introduction

Iron (Fe) is an essential micronutrient for phytoplankton growth. It is part of metalloproteins involved in many biochemical processes, such as electron transport during photosynthesis, nitrogen fixation and detoxification of reactive oxygen species (Twining and Baines 2013). Phytoplankton growth in High Nutrient Low Chlorophyll (HNLC) regions is limited by low Fe availability (Martin 1990; Boyd and Ellwood 2010). In these regions, mesoscale Fe fertilizations and Fe-enriched incubations trigger phytoplankton blooms, mostly dominated by diatoms (e.g. Boyd 2000). In 1998, two publications reported that Fe limitation induces a decoupling in Redfield ratios, increasing Si:N and Si:C ratios in Fe-limited natural planktonic community (Hutchins and Bruland 1998; Takeda 1998) and in two Fe-limited Antarctic diatoms (Takeda 1998). In his study, Takeda (1998) also showed that biogenic silica ($bSiO_2$) content of these Fe-limited diatoms increased per cell volume.

Since then, it is generally assumed that (i) more silicified, Fe-limited diatoms would sink faster than replete cells and (ii) would export more Si than C and N to the bottom of the ocean (Boyle 1998). However, the compilation of about 15 years of data on the effect of Fe limitation on the elemental composition of diatoms show that there is no general trend in $bSiO_2$ per cell or per cell volume (see review from Marchetti and Cassar 2009; Bucciarelli et al. 2010). Fe limitation generally increases Si : N and Si : C ratios, but the magnitude of these increases is strongly dependent on the degree of limitation, i.e., the variations in specific growth rates. In some cases, Si : N and Si : C ratios of severely Fe-limited diatoms are even close to their Fe-replete values (Bucciarelli et al. 2010).

Copper (Cu), like Fe, may also limit phytoplankton growth in the open ocean. Cu is part of many cellular metalloproteins involved in photosynthesis (plastocyanin), respiration (cytochrome oxidase) and detoxification of reactive oxygen species (ascorbate oxidase and superoxide dismutase)(Twining and Baines 2013). Two Cu enrichment experiments on natural phytoplankton assemblages indicate that Cu addition enhances phytoplankton growth in seawater from the Bering Sea (Peers et al. 2005) and from the surbarctic Pacific (Coale 1991). Although the increase in phytoplankton growth of the subarctic Pacific has been attributed to a decrease in microzooplankton grazing due to Cu toxicity (Coale 1991), in the Bering Sea it was demonstrated that Cu addition directly benefited to phytoplankton without affecting zooplankton grazing rate (Peers et al. 2005). Since then, however, few studies have investigated the effects of Cu limitation on phytoplankton. The majority of laboratory experiments have focused on the consequences of Cu-deficiency on photosynthetic parameters of phytoplankton, including diatoms (Peers and Price 2006; Lelong et al. 2013). To date only one publication has reported the cellular C

quotas of Cu-limited diatoms (Annett et al. 2008) and none has investigated how Cu limitation could affect N or $bSiO_2$ quotas. Such data may be all the more important as it has been hypothesized that Cu limitation may be linked to Fe limitation, because of the replacement in the photosynthetic apparatus of Fe-rich cytochrome *c6* by Cu-containing plastocyanin (Peers and Price 2006), and of the use of a multi-copper oxidase in some phytoplankton Fe transport system (Peers et al. 2005; Maldonado et al. 2006). Cu limitation could thus lead to a decoupling between Si, N and C either because of a direct effect of this trace metal on the elemental composition of diatoms, or because Cu limitation may induce Fe limitation (Maldonado et al. 2006). To better understand what controls the (de)coupling between Si, C and N is crucial, as it has important consequences on particles export and the cycling of the major nutrients.

In the present study we compared the cell dimensions, chlorophyll-a content and elemental composition in C, N and $bSiO_2$ of the marine pennate diatom *Pseudo-nitzschia delicatissima* under severe Fe limitation, Cu starvation and replete conditions. We also analyzed the frustules of Fe-limited and Cu-starved cells by Fourier Transform InfraRed spectroscopy (FTIR), in order to investigate the composition of the frustules at a finer scale. *Pseudo-nitzschia* species are often abundant during Fe-fertilized bloom in HNLC region (Trick et al. 2010), and *P. delicatissima* is an ubiquitous species that can dominate Fe-limited open ocean waters (Gómez et al. 2007). Compiling our data with other data from the literature on *Pseudo-nitzschia*, we re-visit for this environmentally important genus the first assumption of Boyle's hypothesis (1998), which assumes an increased degree of silicification of diatoms under low Fe availability. The second assumption of Boyle's hypothesis (1998), that Fe-limited diatoms export more Si than C and N to the bottom of the ocean due to increased Si : N and Si : C ratios, is explored in a companion paper (Boutorh et al. this issue).

2.4. Materials and methods

Pseudo-nitzschia delicatissima is a small *(ca.* 100µm^3), solitary diatom species, which was isolated in 2008 in the Bay of Brest, France (strain Pd08RB) by Beatriz Beker (Laboratoire des Sciences de l'Environnement Marin), and determined at the species level by Aurélie Lelong (Laboratoire des Sciences de l'Environnement Marin). The same clone has been previously studied by Lelong et al. (2013), who investigated how Fe and Cu (co)-limitations affect the physiology of this species.

Although *P. delicatissima* was not axenic, all manipulations were conducted within a sterile laminar flow hood equipped with a Teflon® bench using sterile and trace-metal clean techniques. All bottles and labware were cleaned with suprapure HCl and ultrapure water (MilliQ, > 18.2 MΩ).

2.4.1. Cultures conditions

Pseudo-nitzschia delicatissima was cultured semi-continuously in Fe-EDTA (ethylenediaminetetraacetic acid) buffered batch cultures (Sunda et al. 2005). Cultures were grown in duplicates in 10 L polycarbonate carboys, at 18 °C and under fluorescent light (Vita Lite Plus, Durotest, irradiance of 212 µmol photons m^{-2} s^{-1}, 12 h : 12 h light : dark cycle).

Diatoms were pre-acclimated to Fe limitation, Cu starvation and replete conditions (see below for culture media) until their growth rate remained stable over several days. When the analyses on the cultures were conducted, at least 10 generations have been grown in the same conditions and at an equivalent growth rate. After sampling for analysis of cell concentrations, cell volume, pH, cellular carbon, nitrogen, chlorophyll a (Chl a) and biogenic silica ($bSiO_2$), the remaining culture was filtered onto 1 µm polycarbonate filters, re-suspended in ~ 30 mL of artificial sea water and freezed at -20°C. These filters were later re-suspended in natural filtered seawater for the Fourier Transform InfraRed analysis (FTIR) of the frustules (see Analytical methods below). Only Cu-starved and Fe-limited samples could be analyzed by FTIR. Indeed, a problem with the filter of the replete cells prevented the FTIR analysis. Consequently, FTIR is used in the present study to compare the frustules of cells grown in two different limited conditions only.

2.4.2. Culture media

The complete media consisted of artificial Aquil seawater, enriched with macronutrients, vitamins and trace metals, as described in Price et al. (1988-1989). Because the 10 L polycarbonate carboys could not be sterilized by microwave, the artificial seawater enriched with the macronutrients was filtered in a clean room onto 0.2 µm filter cartridges (SARTOBRAN® 300, Sartorius), and collected into trace metal cleaned polycarbonate carboys. Vitamins and trace metals were filtered onto 0.2 µm filters (Millex) before addition to the artificial seawater. Before use, all filters were cleaned by suprapurHCl and milliQ. The trace metal buffer system consisted of 100 µmol L^{-1} ethylene diamine tetra acetic acid (EDTA), 500 nmol L^{-1} Fe, 19.6 nmol L^{-1} Cu, 50.3 nmol L^{-1} Co, 79.7 nmol L^{-1} Zn and 121 nmol L^{-1} Mn. The buffer system generated free ion concentrations of Fe, Cu, Co, Zn, and Mn of $10^{-19.2}$, $10^{-13.9}$, 10^{-11}, $10^{-10.7}$ and $10^{-8.14}$ mol L^{-1}, respectively, for non-illuminated medium at pH 8.1 and 18 °C according to the chemical equilibrium program MINEQL+ (version 4.62.3). In the Fe-limited medium 5 nmol L^{-1} of Fe ([Fe3+] = $10^{-21.2}$mol L^{-1}) were added instead of 500 nmol L^{-1}. There was no copper addition for the Cu-starved condition. Although we cannot rule out a possible Fe or Cu contamination in our media, we are

confident that these potential contaminations remained low, as we could significantly decrease the specific growth rate of *P. delicatissima*. Besides, our reduction in growth rate under Cu starvation were very similar to those observed by Lelong et al. (2013) on the same clone, and for which Fe starvation completely inhibited growth, indicating very low contamination, if any, of the culture media.

2.4.3. Analytical methods

2.4.3.1. Specific growth rate, surface and volume per cell

Cell concentrations were measured with a flow cytometer FACSCalibur (BD Sciences) with an argon blue laser (488nm). Specific growth rate (μ. d^{-1}) was determined by linear regression of the natural logarithm of the cell concentration versus time.

For each culture condition the cell volume was calculated by measuring maximal width and length of 50 randomly selected cells using software image analysis (Visilog 5) after digitization with an analogic Leica camera. The average cell volume and surface were calculated as an ellipsoid after determination of the semi-width (a, µm) and the semi-length (L, µm):

$$\text{Volume} = 4/3\pi La^2 \quad (1)$$

$$\text{Surface} = 2\pi a^2 + 2\pi a L \arcsin(e)/e \quad (2)$$

$$\text{with the eccentricity } e = (1 - a^2/L^2)^{1/2} \quad (3)$$

2.4.3.2. Cellular chlorophyll a (Chl a), carbon (C) and nitrogen (N)

Cells from culture samples were filtered onto glass fiber filters (GF/F) and rinsed with artificial seawater that had been previously sterilized by microwave. Filters for Chla were immediately stored in glass tubes at -80 °C. Chl a was measured by fluorometry after extraction into 90 % acetone (Lorenzen 1966).

To determine the cellular C and N, culture samples were filtered on a precombusted Whatman GF/F filter (450 °C for 4 hours) and rinsed with sterile artificial seawater containing no nutrient. The filters were dessicated at 60 °C overnight in pre-combusted glassware and stored until analysis using an elemental analyzer Thermo Fisher NA 2100 CN.

Samples for Chla, cellular C and N were collected in duplicate in each carboy.

2.4.3.3. Biogenic silica ($bSiO_2$)

Cellular $bSiO_2$ was determined using a variation of the method by Ragueneau and Tréguer (1994) adapted to culture samples (Moriceau et al. 2007). Samples were filtered on 0.6 µm polycarbonate filters and rinsed with sterile artificial seawater containing no nutrient. The filters were desiccated during one night at 60 °C and stored in polystyrene Petri dishes until analysis. Filters were digested in 20 mL, 0.2 mol L^{-1} NaOH for 3 hours at 95 °C and stirred regularly to ensure the dissolution of all $bSiO_2$. The solution was further acidified with 5 mL of 1 mol L^{-1} HCl, centrifuged to remove solids and analyzed for silicic acid concentrations by the molybdate blue spectrophotometric method of Mullin and Riley (1965), as adapted by Tréguer and Le Corre (1975) and modified by Gordon et al. (1993) for use in segmented flow colorimetry with a Luebbe Technicon Autoanalyser (<1 % precision).

2.4.3.4. Fourier Transform Infra Red (FTIR) spectroscopy

The two batches containing micronutrient-stressed cells were sampled so as to harvest ~2 x 10^7 diatoms in each batch (corresponding to ~2.5 and ~1 µmol of $bSiO_2$ in Cu-starved and Fe-limited batches, respectively). Sampling was done on 0.6 µm polycarbonate filters, which were then rinsed with milli-Q water. Cells were re-suspended in glass Petri dishes using milli-Q water and were frozen at - 20 °C. Samples were freeze-dried and the intracellular and exposed organic matter of the diatoms was removed by 10 hours of low-temperature ashing (LTA) (Koning et al. 2007), using a Plasma – ACE_5 plasma oven (Gala Instrument) equipped with an oxygen gas bottle to obtain oxygen plasma. The efficiency of the organic matter removing was previously assessed by measuring the cellular carbon content vs time exposure for 14 hours. After 9 hours of LTA, a plateau was reached with only 3.4 ± 0.3 % (n = 3, CI = 95 %) of the initial carbon concentration remaining.

The organic matter (OM)-cleaned samples were re-suspended in milli-Q water and centrifuged at 100 rpm during 60 s. Twenty µL were sampled in the pellet, deposited on a 96-well silicon microplate and desiccated in an oven at 40 °C during 5 hours. The plate was then placed in a HTS-XT high-throughput microplate extension (Bruker) and spectra were collected on a FTIR spectrometer (Tensor 27 Bruker). The spectra were collected between 4000 and 700 cm^{-1} at a spectral resolution of 8 cm^{-1} with 64 scans added and averaged. The baseline was corrected in order to reduce the contribution of scattering phenomena. The correction was made using the Origin 8.5 software. This software was also used to decompose the spectra in the 1300-700 cm^{-1} range with Gauss curves in order to integrate some bands. Table II-1 shows the assignment of major peaks based on previous studies.

Table II-1 : Band assignment for FTIR spectroscopy used in this study. ν= stretching δ= bending

Wavenumber range (cm^{-1})	Assignement	References
3800-3000	ν O-H	Naumann et al. 1991
3000-2800	ν C-H of satured C-H	Coates et al. 2006
~ 1630	δ O-H	Naumann et al. 1991
~1515	ν C=C	Socrates 2001
~ 1455	δ_{as} CH_3 and δ_{as} CH_2	Zeroual et al. 1994
~1230	ν_{as} P=O	Giordano et al. 2001
~1180	ν C-O	Giordano et al. 2001
~1075	ν Si-O	Gendron Badou et al. 2003
955-830	γ Si-OH	Socrates 2001
~860	ν Si-C	Socrates 2001
800	δ Si-O	Gendron Badou et al. 2003

2.5. Results

The elemental composition in Table II-2 is expressed per cell and per cell volume for C, N and Chl a, and per cell and per cell surface for $bSiO_2$ since biogenic silica is localized in the frustule. For clarity, only the results per cell volume or cell surface are presented in the Results section.

2.5.1. Specific growth rate, volume per cell (V_{cell}), surface to volume (S:V) ratios

The specific growth rate of *P. delicatissima* decreased by 1.7-fold under Cu starvation and by almost 4-fold under Fe limitation when compared to replete conditions (Table II-2).

The volume and S:V ratio of the replete and Cu-starved cells were not significantly different (Table II-2). On the contrary, due to a significant decrease in cell length, the volume of Fe-limited cells decreased significantly by 1.8-fold and their S : V ratio increased by 1.3-fold compared to replete cells (Table II-2).

Table II-2 : Growth-rate, cell size, elemental composition and elemental ratio of the replete, iron-limited and copper-starved cells. The chlorophyll a (Chl a), carbon and nitrogen quotas are normalized per cell and per cell volume. The biogenic silica quotas are per cell and per cell surface. Results are presented as the means ± confidence interval (CI = 95 %).

	Replete	Cu starvation	Fe limitation
Specific growth rate	1.24±0.05 (n=2)	0.73±0.02 (n=2)	0.32±0.01 (n=2)
Length (µm)	17.9±0.4 (n=50)	20.0±0.5 (n=51)	20.1±0.3 (n=100)
Width (µm)	3.4±0.1 (n=50)	3.3±0.1 n (51)	2.4±0.1 (n=100)
Volume (μm^3)	109±8 (n=50)	115±9 (n=51)	62.1±3.0 (n=100)
Surface area to volume ratio (μm^{-1})	1.4±0.1 (n=50)	1.5±0.1 (n=51)	2.0±0.0 (n=100)
Chl a (mmol L_{cell}^{-1})	2.81±0.18 (n=4)	2.85±0.12 (n=4)	0.74±0.10 (n=4)
Carbon (pmol $cell^{-1}$)	1.19±0.02 (n=4)	1.28±0.06 (n=4)	0.21±0.05 (n=4)
Carbon (mol L_{cell}^{-1})	10.97±0.19 (n=4)	11.12±0.54 (n=4)	3.40±0.89 (n=4)
Nitrogen (pmol $cell^{-1}$)	0.20±0.01 (n=4)	0.25±0.02 (n=4)	0.05±0.01 (n=4)
Nitrogen (mol L_{cell}^{-1})	1.79±0.07 (n=4)	2.20±0.20 (n=4)	0.84±0.12 (n=4)
Biogenic silica (pmol $cell^{-1}$)	0.12±0.01 (n=3)	0.13±0.01 (n=4)	0.06±0.02 (n=4)
Biogenic silica (fmol μm^{-2})	0.81±0.07 (n=3)	0.76±0.03 (n=4)	0.52±0.14 (n=4)
C:N ratio	6.12±0.27 (n=4)	5.08±0.23 (n=4)	4.18±1.39 (n=4)
Si:N ratio	0.63±0.08 (n=3)	0.50±0.04 (n=4)	1.21±0.37 (n=4)
Si:C ratio	0.10±0.01 (n=3)	0.10±0.01 (n=4)	0.33±0.18 (n=4)

2.5.2. Chl a and elemental composition

There was no significant difference in Chl*a,* cellular C or $bSiO_2$ quotas between replete and Cu-starved cells. By contrast, N quotas of Cu-starved cells increased significantly by ~ 20 % compared to replete cells (Table II-2). Fe limitation strongly affected cellular elemental composition compared to replete cells: Chl a, cellular N and cellular C decreased by 3.8-fold, 2.1-fold and 3.2-fold respectively, while cellular $bSiO_2$ decreased by 1.6-fold.

2.5.3. Elemental ratios C : N, Si : C and Si : N

Cu starvation and Fe limitation both decreased the molar ratio C:N relative to the replete cells by 1.2-fold and 1.5-fold, respectively (Table II-2). The elemental ratio Si:C was not different between the replete and Cu-starved cells, while Si:N was 1.3-fold lower under Cu starvation (Table II-2). Fe limitation increased Si:C and Si:N by 3-fold and 2-fold, respectively, compared to replete conditions (Table II-2).

To compare the effects of the different growth conditions, we will use in the Discussion section the R ratio, defined as the relative variation of a given parameter between a limiting condition and a nutrient-replete condition (e.g., at a specific growth rate μ, $R(C:N)_{\mu} = (C:N)_{\mu} : (C:N)_{\mu max}$). The degree of limitation will be defined by its effect on the growth rate using $\mu : \mu_{max}$ (i.e. R(μ)), with the value of maximum growth rate measured in the nutrient-replete conditions (μmax = 1.24 ± 0.05 d^{-1}, n = 2, CI = 95 %).

2.5.4. Fourier Transform InfraRed Analysis

Figure II-2 presents the spectra obtained for the frustules of Fe-limited and Cu-starved cells. Both spectra were dominated by an intense peak at 1074 cm^{-1}, characteristic of SiO_4 (Gendron-Badou et al. 2003). The peak at 800 cm^{-1} is assigned to Si-O-Si binding vibration mode and the band around 945 cm^{-1} to Si-OH (Socrates 2001; Gendron-Badou et al. 2003). The decomposition of the spectra allows calculating the relative abundance of silanol groups (SiOH) within the silica network. It was estimated as the ratio between the integrated band at 945 cm^{-1} relative to the band at 800 cm^{-1} was higher for the Fe-limited frustules than for the Cu-starved frustules ($I_{945cm-1} / I_{800cm-1}$ = 10.2 and $I_{945cm-1} / I_{800cm-1}$ =2.0, respectively). For both samples, the IR absorption in the 3700-3000 cm^{-1} range and near 1635 cm^{-1} is attributed to H_2O molecules stretching and bending modes, respectively. The spectral contribution of water is more intense in Fe-limited frustules than in Cu-starved ones. The higher quantity of silanol and water in Fe-limited frustules suggests that Fe-limited frustules were more hygroscopic than Cu-starved frustules.

These spectra were also different in terms of pools of organic matter associated to the frustules. For the Fe-limited frustules, the presence of ν_{CH} at 2845 cm^{-1} and 2930 cm^{-1} and also the bending bands in the 1550 - 1350 cm^{-1} region indeed clearly indicate the presence of organic matter within the frustule (Socrates 2001). The peak at 860 cm^{-1}, which is characteristic of a Si-C bond (Socrates 2001), also confirms that a large amount of organic matter was directly associated to silica. On the contrary, no silica-linked organic matter was present in the Cu-starved frustules (no organic compound band in the 1550 - 1350 cm^{-1} range).

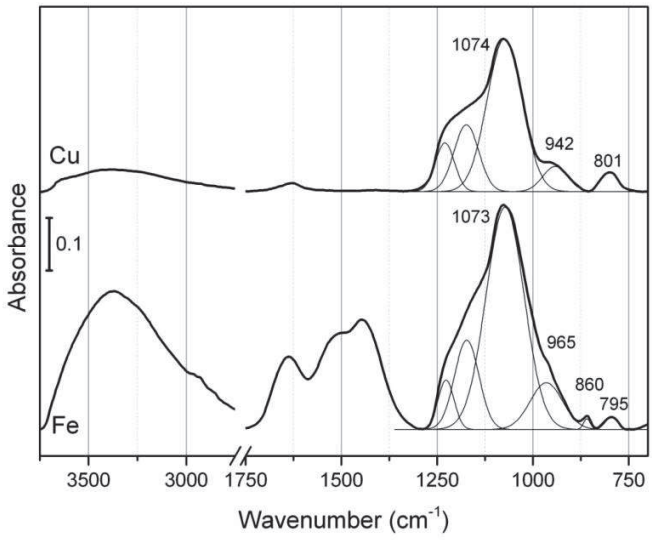

Figure II-2 : Fourier Transform Infra Red (FTIR) absorption spectra of copper-starved frustule and iron-limited frustule. The intern and exposed organic matter was removed by low temperature ashing. The peaks below the curves represent the spectra decomposition into Gauss curves between 1300-700 cm^{-1}.

2.6. Discussion

2.6.1. Effect of copper starvation on the elemental composition of *Pseudo-nitzschia delicatissima.*

In the present study Cu starvation induced a mild decrease of 60% of *P. delicatissima* growth rate, which is similar to the ~ 66% decrease measured under Cu starvation by Lelong et al. (2013) in slightly different conditions (T = 16°C, light : dark of 12 h : 12 h, irradiance of 130 µmol photons m^{-2} s^{-1}). To our knowledge, this experiment is the first to study the effect of Cu starvation on the N and $bSiO_2$ content of a phytoplanktonic species. Cu starvation significantly increased N quotas compared to diatoms grown in replete medium, while maintaining cellular C, Chl *a* and $bSiO_2$ (Table II-2).

Known Cu-containing metalloproteins are not directly involved in N metabolism (Twining and Baines 2013). The increase in cellular N may be linked to increased oxidative stress due to growth-limiting conditions. Increased oxidative stress is due to increased production of reactive oxygen species (ROS, e.g., superoxide radicals), which are generated by reactions of reduced components of the photosynthetic or respiratory electron transport chains with molecular oxygen (Foyer et al. 1994).

Copper-containing cytochrome oxidase is part of the mitochondrial electron transport, and in the oceanic diatom *Thalassiosira oceanica*, the photosynthetic apparatus includes the Cu-containing plastocyanin. As a result, Cu starvation should disrupt photosynthesis and respiration and increase the production of ROS. Besides, a Cu-Zn-superoxide dismutase (SOD) isoform is produced in some phytoplankton species as an antioxidant (Chadd et al. 1996, for *Synechococcus* sp., and Merchant et al. 2006, for *Chlamydomonas*). Increased production of ROS and suppressed production of Cu-Zn-SODs in Cu-starved *P. delicatissima* should increase the need for non-containing Cu-antioxidants. One possible explanation for the ~ 20 % increase of N quotas of Cu-starved *P. delicatissima* may thus be an increased production of N-rich antioxidant molecules (e.g. tripeptide glutathione and phytochelatin).

Maintenance of cellular C under Cu starvation is in agreement with the results from Annett et al. (2008) who measured C quotas of eight centric diatoms. To better compare our results with theirs, we considered the relative variation of C per cell volume (noted R(C)), as defined in Results section) versus the relative variation of specific growth rate (noted R(μ)) of our species and their four coastal and four oceanic species (using cell volume as kindly communicated by Dr A.L. Annett) (Figure II-3).

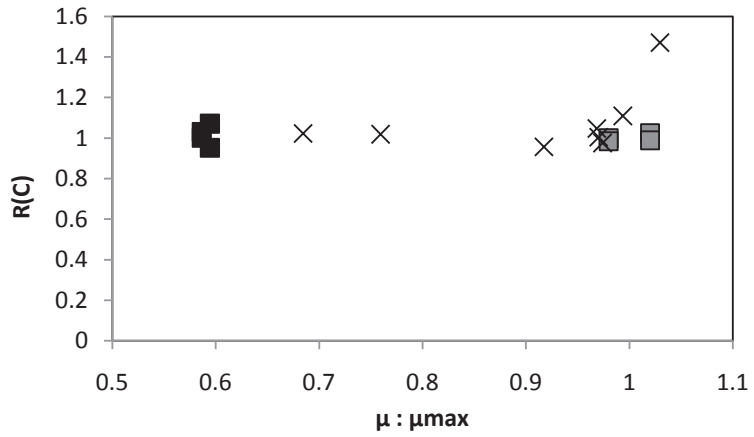

Figure II-3 : Relative variation in cellular C per cell volume (R(C)) versus the relative growth rate (μ:μmax) for copper-limited diatom (kindly communicated by Dr A.L. Annett, black cross) and in the present study (replete condition: grey square; copper starvation: black square).

The cellular C of all these species seems to remain constant under Cu limitation and unrelated to the decrease in specific growth rate (Kendall correlation: $p = 0.59$, $\tau = 0.10$, $n = 16$). However, even if the bulk C does not change between Cu starvation and replete conditions (this study), the lipid content of Cu-starved *P. delicatissima* increases sharply (Lelong et al. 2013), implying a redistribution between the pools of carbon within the cell and indicating that Cu starvation does affect carbon metabolism. This

alteration of carbon metabolism, however, may be linked more to impaired respiration than to impaired photosynthesis. For the same clone, Lelong et al. (2013) indeed showed that photosynthesis efficiency (as estimated by quantum yield measurements), and chlorophyll content (as estimated from cell autofluorescence) were not affected by Cu starvation. In their study, however, cell autofluorescence values could have been biased by a less efficient electron transport into the photosystem II and non-photochemical quenching. Our direct measurement of Chl a content confirms their estimates and previous conclusions. Finally, our study reports no change in $bSiO_2$ in Cu-starved *P. delicatissima*.

2.6.2. General trends for Fe-limited *Pseudo-nitzschia* species and comparison with Cu starvation

Because Cu is at the core of multicopper oxidase (MCO), an enzyme involved in the high-affinity Fe transport system of certain phytoplankton species, Maldonado et al. (2006) suggested that Cu limitation may result in Fe limitation. In that case, Cu limitation should induce similar changes in the elemental composition of the cells as Fe. At the physiological level, *P. delicatissima* does not display the same changes under Cu starvation and Fe limitation, suggesting that for this species Cu starvation does not induce Fe limitation and that most of the cellular Cu is probably used for other physiological mechanisms than Fe transport (Lelong et al. 2013). However, the effects of Fe and Cu limitation on the bulk cellular elemental composition have never been compared. In our study, Fe limitation and Cu starvation did not induce the same reduction in growth rate. To properly compare their effects, i.e., at a similar growth rate, we compiled the available data on elemental composition of Fe-limited *Pseudo-nitzschia* in the literature, including ours, to draw general trends, and compared our data of Cu-starved cells with those of Fe-limited cells at ~ 60 % µmax.

Two recent papers have studied the effect of Fe limitation on the elemental composition of seven species of *Pseudo-nitzschia*: *P. mutliseries; P*. cf. *calliantha*; *P. heimii* type 1; *P.* cf.*heimii* type 2*; P. dolorosa ; P.* cf.*turgidula* (Marchetti and Harrison, 2007), *P. pseudodelicatissima* (Sugie and Yoshimura, 2013). Marchetti and Harrison (2007) and Sugie and Yoshimura (2013) calculated the volume and surface of their cells using measurements of transapical widths, apical lengths and pervalvar widths. To properly compare our results with these two studies, we calculated the cellular volume and surface as ellipsoid using transapical widths and apical lengths (from Marchetti and Harrison 2007, and using values kindly communicated by Dr K. Sugie). We normalized Chl a, C and N quotas on a cell volume basis, and $bSiO_2$ quotas on a cell surface basis for all species.

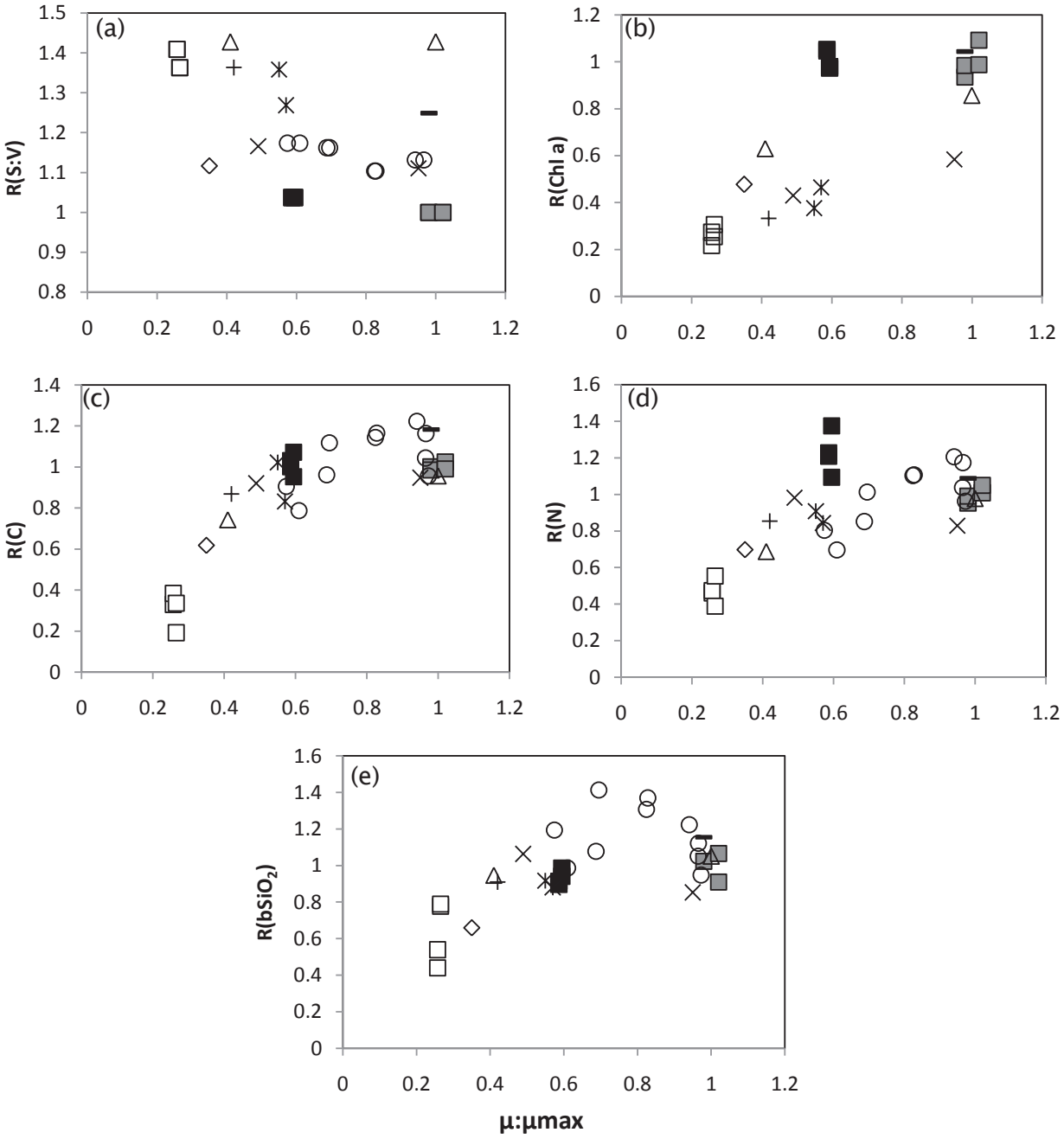

Figure II-4 : Relative variation of (a) the surface:volume ratio (R(S:V)), (b) the Chl a content per cell volume (R(Chl a)), (c) the C content per cell volume (R(C)), (d) the N content per cell volume (R(N)) and (e) the $bSiO_2$ content per cell surface ($R(bSiO_2)$) versus the relative variation of the specific growth rate (µ:µmax) for *P. delicatissima* (this study, replete condition: grey square; copper starvation: black square; iron limitation: open square), *P. heimii* type 1 (×, Marchetti and Harrison, 2007), *P.* cf. *heimii* type 2 (*, Marchetti and Harrison, 2007), *P. dolorosa* (−, Marchetti and Harrison, 2007), *P.* cf. *turgidula* (+, Marchetti and Harrison, 2007), *P. multiseries* (◊, Marchetti and Harrison, 2007), *P.* cf. *calliantha* (Δ, Marchetti and Harrison, 2007) and *P. pseudodelicatissima* (○, Sugie et al. 2013). Values for *P. pseudodelicatissima* were re-calculated from C, N and $bSiO_2$ per cell (Sugie et al. 2013) and corresponding data of cell volume and surface (kindly communicated by Dr K. Sugie)

Figures II-4.a and 4.b. display a significant increase in surface to volume ratio (Kendall correlation: $p = 0.005$, $\tau = -0.45$, $n = 21$) and a significant decrease in chlorophyll a concentration (Kendall correlation: $p < 0.0001$, $\tau = 0.76$, $n = 17$) with decreasing growth rate, some well-known effects of Fe limitation (Sunda and Huntsman 1995; Marchetti and Cassar 2009).

The relative variations of C and N per cell volume and $bSiO_2$ per cell surface (R(C), R(N), and $R(bSiO_2)$, respectively) significantly decreased with decreasing R(μ) (Figures II-4c, 4d, 4e) (Kendall correlation: $p < 0.0001$, $\tau = 0.55$, $n = 27$ for R(C), $p < 0.0001$, $\tau = 0.54$, $n = 27$ for R(N) and $p = 0.006$, $\tau = 0.38$, $n = 26$ for $R(bSiO_2)$). These trends are particularly obvious for our species, our data of Fe-limited *P. delicatissima* being the first, to our knowledge, for a diatom of this genus under severe Fe limitation (i.e., < 25% μmax).

Compiling data from 7 studies on 18 diatoms species from 7 genii (including *Pseudo-nitzschia*), Bucciarelli et al. (2010) have evidenced that under Fe limitation the relative variation of cellular C and N per cell decrease with decreasing relative growth rate. However these trends no longer exist when quotas are corrected from cellular volume (Bucciarelli et al. 2010). Besides, no significant trend exists between $R(bSiO_2)$ and R(μ), whether looking to per cell or per cell surface quotas (Bucciarelli et al. 2010). Our study however shows significant trends in the cellular elemental composition of Fe-limited *Pseudo-nitzschia*, even when taking into account the variations in cell volume or cell surface, whatever the culture conditions and the species' habitat (coastal or oceanic strain). Significant trends may thus exist at the genus level.

Cu-starved *P. delicatissima* cells have similar C and $bSiO_2$ contents as nutrient-replete cells (Table II-2), and as Fe-limited *Pseudo-nitzschia* whose growth rate equals ~ 60% of μmax (Figures II-4c, 4e). However Cu starvation and Fe limitation seem to have different effects on cell morphology, Chl a content, and N quota (Figures II-4a, 4b, 4d). This suggests that, similar to what was observed at the physiological level (Lelong et al. 2013), Cu starvation does not induce Fe limitation and that both micronutrients have different effects on the elemental composition of *Pseudo-nitzschia*.

2.6.3. Effect of micronutrient limitations on the silicification degree and on the frustule structure

The significant trend in R($bSiO_2$) versus R(μ) obtained for the genus *Pseudo-nitzschia* suggests a genus specific response to Fe limitation (Figure II-4e). A few hypotheses, based on the silicification process, can be proposed to explain the link between Fe availability and diatom silicification degree.

(i) The most characterized genes involved in frustule formations are the ones encoding silicic acid transporters (SITs) (e.g. Alverson 2007; Thamatrakoln and Hildebrand 2007; Mock et al. 2008). A recent study pointed out that Fe limitation, inducing an 80 % decrease of μmax, increased the transcript abundance of a SIT gene in *P. multiseries* (Durkin et al. 2012). This result suggests an increase in the dSi transport inside the cells, which could increase the silicification degree of this species. However, at 35 % μmax, Fe limitation leads to a decrease in the silicification degree of *P. multiseries* (Figure II-4e) (Marchetti and Harrison 2007). Considering this trend to desilicification at the highest decrease in growth rate, the increase in the transcription of the SIT gene under the severe Fe limitation might not had resulted in a higher silicification degree. As diatoms could regulate dSi efflux depending on their growth conditions (Milligan et al.2004), the possible increase in the dSi influx in *P. multiseries*, when growing at 20-35 % of μmax, could have been compensated by an increase in dSi efflux. (ii) As Fe is part of numerous metalloproteins involved in phytoplankton respiration (Twining and Baines 2013), process providing the energy needed for silicification (Martin Jezequel 2000), its low availability may impaired respiration and may consequently disrupt silicification, as suggested by Bucciarelli et al. (2010). (iii) In their work on light and nutrient limitations (N and P) on *T. pseudonana*, Claquin et al. (2002) pointed out an elongation of the G2 + M phase of the cell cycle (during which the major uptake of dSi occurs) at low growth rate, which could explain the increase in the silicification degree of this diatom under these limitations. However, it is not certain that this is a general rule for all diatoms species under all limitations. Bucciarelli et al. (2010) suggest that for some diatom species, the G2 + M phase duration might decrease under Fe limitation, thus decreasing the silicification degree of diatoms. This could explain the trend between Fe limitation and the silicification degree of the *Pseudo-nitzschia* genus. Further experiments on the effect of Fe limitation on diatom cell cycle are obviously needed.

The FTIR results show that diatoms possess not only the ability to change their biogenic silica content, but can also alter their frustule structure in response to nutrient stress. The frustule fine structure and its composition were indeed different in Cu-starved and Fe-limited cells with (i) more

silanol groups (Si-OH) relative to Si-O-Si bonds in Fe-limited frustules compared to Cu-starved frustules and (ii) more organic matter associated to the silica lattice of Fe-limited frustules compared to Cu-starved frustules. Some hypothesis may be proposed to explain such modifications at the molecular scale of diatom frustule.

Many of the photosynthetic organisms have developed a Carbon Concentration Mechanism (CCM) in order to concentrate the carbon dioxide (CO_2) close to the ribulose-1,5-diphosphate carboxylase/oxygenase (RubisCO), the main carboxylating enzyme (Aizawa and Miyachi 1986). The CCM requires the presence of an enzyme named Carbonic Anhydrase (CA), catalyzing the reaction between bicarbonate (HCO_3^-) and CO_2 (Nimer et al. 1999). Some forms of this CA need a pH buffer (Tripp et al. 2001). It has been suggested that, for diatom, biogenic silica could play this role (Milligan and Morel, 2002). According to FTIR results, *P .delicatissima* frustule could be more or less hydrolysable depending on growth conditions, as seen by changes in the relative amount of Si-OH within frustules, which could illustrate changes in its buffering capacity.

The frustule structure of diatoms is complex, and involves associations between the silica lattice and organic matter pools (Abramson et al. 2009; Suroy et al. in revision). Some of the latter are supposed to be needed in diatom cell wall biogenesis (Kröger and Poulsen 2008; Tesson and Hildebrand 2013). Mock et al. (2008) showed an up-regulation of genes encoding cell wall proteins in the diatom *Thalassiosira pseudonana* under Fe or Si limitation. If this up-regulation under Fe limitation is a general rule, and if it leads to an increase in the amount of organic pool associated with the frustule, it could explain the higher quantity of organic matter associated with the frustule of Fe-limited *P. delicatissima* compared to Cu-starved cells.

2.6.4. Effect of Fe limitation and Cu starvation on *P. delicatissima* elemental ratios, and consequences on diatom export

Our study on *P. delicatissima* shows a decoupling between Si and C under Fe limitation, and between Si and N under both Fe limitation and Cu starvation. Increases in Si : N and Si : C molar ratios under Fe limitation is well documented and has been evidenced for both laboratories and field studies (Marchetti and Cassar 2009). There are discrepancies in the causal elements leading to these increases, attributed to an increase of the silica content (e.g. Takeda, 1998, Timmermans et al. 2004) or to a decrease in N and C quotas (e.g Takeda, 1998, Hoffmann et al. 2007). Marchetti and Harrison (2007) suggest that the increase in Si : N ratio under Fe limitation may be more related to an alteration of cell morphology (e.g. an increase in surface to volume ratio) than to changes in their nutritional requirement.

Opposite to the Fe limitation, Cu starvation led to a decrease in the Si : N ratio of *P. delicatissima* cells. As this decrease was not concomitant to changes in their surface to volume ratio (Table II-2), it may be a result of changes in the diatoms nutritional requirement under Cu starvation.

The "silicate pump", defined by Dugdale et al. (1995), is the preferential export of Si from the euphotic zone compared to N. Cu starvation led to a decrease in the Si : N ratio of *P. delicatissima*, which would suggest that Cu starvation induces a decrease in the silicate pump efficiency. The increase in the silicification degree and in Si : N ratios of diatoms under Fe limitation is the base of Boyle's hypothesis (1998), who suggests that Fe-limited diatom would sink faster due to their higher density, leading to a more effective export of Si compared to N, thus increasing the silicate pump efficiency. Our present study shows a decrease in both the silicification degree of Fe-limited *P. delicatissima*, opposite to Boyle's assumption, and an increase in its Si : N ratio, in line with Boyle's assumption. These contrasting results question the fate of the genus *Pseudo-nitzschia* through the water column. Indeed, its trend to desilicification under Fe limitation may induce an enhanced dissolution of their frustule. To better investigate the effect of Cu starvation and Fe limitation on particles export, and the consequences of the frustule plasticity on its fate, an additional experiment was performed. We have examined the dissolution of $bSiO_2$ from replete, Cu-starved and Fe-limited *P. delicatissima*, as well as the evolution of their Si : N ratio during diatom dissolution (Boutorh et al., this issue).

Chapitre III.

Effet d'une carence stricte en Cu et d'une limitation en Fe sur la dissolution de la diatomée *Pseudo-nitzschia delicatissima*

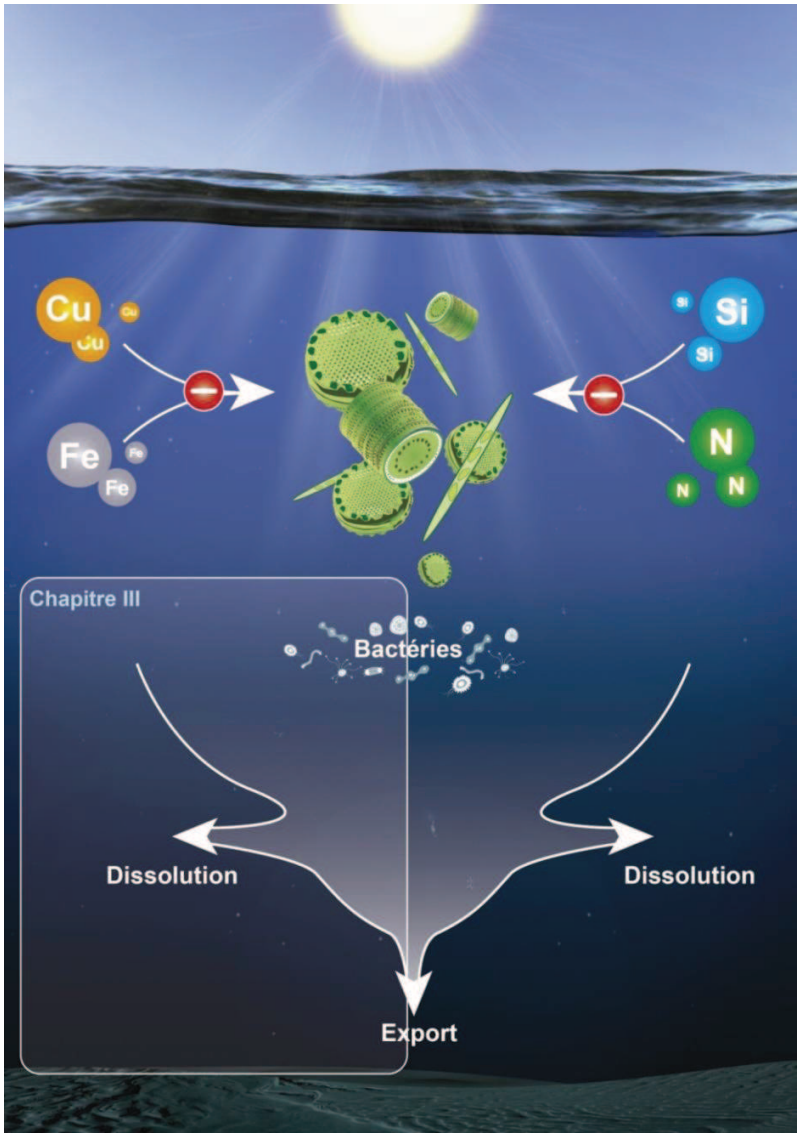

III. Chapitre III : Effet d'une carence stricte en Cu et d'une limitation en Fe sur la dissolution de la diatomée *Pseudo-nitzschia delicatissima*

1. Préambule

Dans le chapitre précédent, j'ai montré que la limitation en Fe entraîne, à un fort degré de limitation, une diminution du degré de silicification de *P. delicatissima*. Rappelons que dans son hypothèse, Boyle déduit qu'une diatomée limitée en Fe, puisqu'elle est plus silicifiée, se dissout moins rapidement. Les résultats du chapitre précédent vont donc à l'encontre de la théorie à la base de l'hypothèse de Boyle (1998). Dans ce chapitre, nous nous sommes directement intéressés aux effets des limitations en Fe et en Cu sur la dissolution du frustule de la diatomée *P. delicatissima*. Ces résultats sont réunis dans un article compagnon du celui présenté précédemment.

Nous avons également testé l'effet de la limitation en Fe et de la carence stricte en Cu sur la pompe à silicate, définie par Dugdale et collaborateurs (1995) comme l'export préférentiel de Si, de la zone euphotique vers les eaux profondes, comparé à l'export de N, lorsque la communauté phytoplanctonique est dominée par les diatomées. D'après les résultats obtenus par Takeda (1998), Boyle (1998) suggère que la limitation en Fe, en augmentant les rapports élémentaires Si : N des diatomées, engendrerait un export préférentiel de Si comparé à N. Nous avons voulu vérifier si l'augmentation du rapport élémentaire Si : N de la diatomée *P. delicatissima* avec une limitation en Fe induisait une augmentation de l'efficacité de la pompe à silicate. Pour cela, nous avons suivi l'évolution du rapport Si : N de P. *delicatissima,* préalablement limitée en Fe, durant sa dissolution. A l'inverse la carence stricte en Cu a engendré une diminution du rapport élémentaire Si : N de *P. delicatissima*. Nous avons donc étudié l'évolution de ce rapport durant la dissolution de cellules préalablement carencées strictement en Cu, afin de déterminer si la diminution du rapport élémentaire Si : N durant la croissance entraine une diminution de l'efficacité de la pompe à silicate.

En plus de la plasticité du frustule à l'échelle de la cellule, les résultats du chapitre précédent ont mis en évidence l'effet de l'environnement nutritionnel sur la plasticité du frustule à l'échelle moléculaire. Si l'effet des conditions abiotiques sur la dissolution du frustule a été assez largement exploré (Van Cappellen et al. 2002 et références incluses, Loucaides et al. 2012 et références incluses), l'effet de modification structurelle du frustule, induite par son environnement nutritionnel, n'a été que

peu étudié. Ainsi, dans cette étude, nous avons mis en parallèle les comportements de dissolution des diatomées et les propriétés intrinsèques des frustules, étudiés dans le chapitre précédent, afin de tenter de déterminer une relation entre les cinétiques de dissolution et la structure fine de frustule.

2. Copper and iron availability differently affect the morphology, the elemental composition, the frustule structure and the export ability of the diatom *Pseudo-nitzschia delicatissima*. Part II – Diatom dissolution

Boutorh Julia, Moriceau Brivaëla, Gallinari Morgane, Ragueneau Olivier, Bucciarelli Eva.

Université Européenne de Bretagne, France
Université de Brest, CNRS, IRD, UMR 6539 LEMAR, IUEM;
Technopôle Brest Iroise, Place Nicolas Copernic, 29280 Plouzané, France

To be submitted to Limnology and Oceanography

2.1. Résumé

Afin de mieux comprendre l'effet de la limitation en fer (Fe) et la carence stricte en cuivre (Cu) sur l'export de silicium (Si), nous avons examiné l'effet de ces stress en micronutriments sur la dissolution de la silice biogénique ($bSiO_2$) des diatomées. La dissolution des frustules de la diatomée *Pseudo-nitzschia delicatissima*, ayant poussé dans des conditions optimales, carencée strictement en Cu ou limitée en Fe, a été étudiée au cours d'expériences de dissolution d'une durée de vingt-deux jours. Les changements du rapport élémentaire Si : N au cours de la dissolution des frustules ont été suivis. Les concentrations en $bSiO_2$ et en acide silicique ont été mesurées afin de modéliser la dissolution des frustules de la diatomée en considérant deux phases de $bSiO_2$. Les frustules des diatomées limitées en micronutriments ont été plus résistants face à la dissolution que les frustules des diatomées non-limitées. Après environ un mois de dissolution, seuls 9 % de la $bSiO_2$ initiale des diatomées non limitées ont subsisté tandis que 25 % et 29 % de la $bSiO_2$ des cellules limitées ont été préservés. Quelles que soient les conditions de croissance, la dissolution de la $bSiO_2$ a eu lieu en deux étapes, la première vitesse de dissolution étant supérieure à la deuxième. Les différences entre la première et la deuxième vitesse de dissolution ont été plus prononcées pour les cellules ayant poussé en conditions optimales ou bien carencées strictement en Cu, que pour les cellules limitées en Fe. Les vitesses de dissolution les plus faibles, obtenues pour les diatomées limitées en Fe, ne peuvent pas être expliquées par le degré d'organisation plus faible et la réactivité plus importante de frustules limités en Fe comparés aux frustules carencés strictement en Cu, comme estimé par les spectres obtenus au moyen de la spectroscopie infrarouge à transformée de Fourier (IRTF). Cependant, les spectres IRTF suggèrent que les frustules limités en Fe soient associés à plus de matière organique que les frustules carencés strictement en Cu. Les cellules limitées peuvent exporter plus de Si que de N, puisque le rapport élémentaire Si : N de ces cellules a augmenté durant leur dissolution, alors qu'il est resté stable pour les cellules ayant poussé en conditions optimales.

2.2. Abstract

To better understand the effect of iron (Fe) limitation and copper (Cu) starvation on the silicon (Si) export, we examined the effect of these micronutrient stresses on diatom biogenic silica ($bSiO_2$) dissolution. The dissolution of *Pseudo-nitzschia delicatissima* frustule from diatoms grown under replete, Cu-starved and Fe-limited conditions was studied during a twenty-two days experiment. Changes of the cells elemental ratio Si : N has been monitored. $bSiO_2$ and silicic acid concentrations were measured to model the dissolution of diatom frustule considering two $bSiO_2$ phases. Frustules from the micronutrient-limited diatoms were more resistant to dissolution than replete ones. After almost one month of dissolution, only 9 % of the initial $bSiO_2$ from replete diatoms remained while 25 to 29 % of the $bSiO_2$ from limited-diatoms were preserved. Regardless the growth conditions, $bSiO_2$ dissolution occurred in two-steps, the first dissolution rate constant being higher than the second. Differences between first and second dissolution rate constants were more pronounced for cells grown under replete or Cu-starved conditions compared with those grown under Fe limitation. The lowest dissolution constants obtained for Fe-limited diatoms cannot be explained by the lower organization degree and the higher reactivity degree of Fe-limited frustules compared to Cu-starved frustules, as estimated from Fourier Transform InfraRed spectra (FTIR). However, FTIR spectra suggest that Fe-limited frustules may be associated to more organic matter than Cu-starved ones. Limited-cells may export more Si relative to N as their elemental ratio Si : N increased during dissolution, while it remained stable for cells grown in replete conditions.

2.3. Introduction

A mechanistic understanding of biogenic silica ($bSiO_2$) dissolution is necessary to quantify the fate of Si from the surface to the bottom of the ocean. To better understand the fate of diatom $bSiO_2$ in the water column, numerous laboratory experiments have already been realized, investigating for example the effect of the temperature (Kamatani 1982), the incorporation of aluminum within the frustule (Gehlen et al. 2002), the degree of under-saturation (Rickert et al. 2002), the existence of an organic coating surrounding diatoms (Bidle and Azam 1999), and the specific surface area (Dixit et al. 2001) on $bSiO_2$ dissolution. But while environmental conditions during growth greatly influence the frustule silicification (Claquin et al. 2002) and the cell stoichiometry (Geider and La Roche 2002), to our knowledge, very few studies have directly measured the effect of these changes in silicification due to nutrient availability during growth on $bSiO_2$ dissolution (Soler 2010).

Iron (Fe), metal present in the ocean surface water at very low concentrations, is essential for phytoplankton growth and its low availability may affect diatom silicification (Marchetti and Cassar and references therein). Iron low concentrations in surface water can limit phytoplankton growth in 50 % of the world ocean, including the Southern Ocean (Boyd and Ellwood 2010). Bottle incubations and *in situ* experiments pointed out that addition of Fe in these High Nutrient Low Chlorophyll (HNLC) zones, enhanced phytoplankton growth (de Baar et al. 2005). The scientific community is committed to understand effects of low Fe availability on the phytoplankton community and metabolism. Regarding diatoms, Fe limitations, as many nutrient stresses, decrease growth rates leading to a decoupling in macronutrient use (de Baar and La Roche 2003) and to an increase of Si : N and Si : C ratio in diatoms (Marchetti and Cassar 2009). Among the reasons cited for the increase in these ratios, an increase of the silica quotas of diatoms is often mentioned (Marchetti and Cassar 2009). These observations are the base of Boyle hypothesis (1998) who suggests that Fe-limited diatoms, having higher Si quotas would increase their density and sink faster, and consequently export more Si at the bottom of the ocean relative to cells grown in replete conditions. *Pseudo-nitzschia*, genus often dominating diatom fertilized bloom (Trick et al. 2010), is rarely found in southern ocean sediments (Marchetti and Harrison 2007). One may wonder if this poor representation of *Pseudo-nitzschia* frustules in the surface sediment is due to a genus specific susceptibility to dissolution or to the fact that they dominate bloom when Fe is not limiting.

Another trace metal, copper (Cu), may be found in ocean surface waters at nanomolar levels (Bruland and Lohan 2003). Two incubation experiments highlight that Cu concentrations are low enough

in some region of the world ocean to limit phytoplankton growth (Coale 1991; Peers et al. 2005). In the companion publication (Boutorh et al. this issue) we showed that a Cu starvation, while decreasing the growth rate of *Pseudo-nitzschia delicatissima,* did not affect the silicification degree of this diatom but decreased its Si : N elemental ratio.

On the contrary, this companion study pointed out that Fe limitation induced an increase in the Si : N ratio and led to a decrease in the Si content of *P. delicatissima* diatoms, which is opposite to the general assumption that Fe limitation induced an increase of the degree of silicification of diatoms (Boyle 1998). Moreover, Fourier Transform InfraRed spectroscopy (FTIR) analysis, undertook during this first experiment, indicates that Cu starvation and Fe limitation may affect *P. delicatissima* frustule chemical composition, which may possibly change its dissolution. In the present study, we focused on the effect of these different micronutrient growth conditions on the post-mortem dissolution of nutrient replete, Cu-starved and Fe-limited cells, by performing a twenty-two days dissolution experiment. Changes in Si : N elemental ratios of diatoms, followed all along their dissolution, allow to discuss the effect of these micronutrient limitations on the export of Si relative to N.

2.4. Materials and methods

2.4.1. Experimental design

Batch cultures of the marine pennate diatom *Pseudo-nitzschia delicatissima* (strain Pd08RB, solitary species isolated in 2008 by Beatriz Beker in the Bay of Brest, France, ca. 100 μm^3) were grown in duplicates in 10L- polycarbonate bottles in three different growth conditions: a replete medium (Control), an iron-limited medium (Fe limitation, inducing a 75 % decrease of the maximum growth rate) and a copper-starved medium (Cu starvation, inducing a 40 % decrease of the maximum growth rate) (for details on the culture experiment, see the companion paper Boutorh et al. this issue). When cells exhibited constant growth rates, cultures were filtered on 1 µm polycarbonate filters, re-suspended in a small volume of artificial seawater and then frozen at -20 °C, to kill the cells without disrupting the cell integrity. After slow thawing at room temperature, frozen cells were re-suspended in natural filtered seawater with low silicic acid (dSi) concentration (< 5 µmol L^{-1}) far below saturation level (~1200 µmol L^{-1}) in a 10 L-polycarbonate bottle for each growth conditions (i.e. control, Cu starvation and Fe limitation). The seawater, collected in the bay of Brest, was filtered on 0.7 µm Whatman GF/F filters to preserve the natural bacterial community and to remove phytoplankton and grazers. Cellular concentrations in each dissolution experiment were between 160000 cell mL^{-1} and 250000 cell mL^{-1} at T_0, first day of the

experiment. Diatoms were incubated during twenty-two days and each experiment was conducted in the dark at 17 °C. Incubated batches were equipped with a magnetic stirrer to homogenize the mixture and to limit the aggregate formation. pH and oxygen saturation level were measured daily to ensure that the conditions were not hypoxic (between 74 % and 98 % of O_2 during the experiment, and between 7.9 and 8.1 for the pH). During the whole dissolution experiments samples were taken regularly for $bSiO_2$, dSi concentration and Particulate Organic Nitrogen (PON) analysis.

2.4.2. Analytical method

2.4.2.1. Biogenic silica ($bSiO_2$)

$bSiO_2$ concentrations were determined using a variation of the Ragueneau and Tréguer method (1994) adapted to culture samples (Moriceau et al. 2007). Samples were filtered on 0.6 µm polycarbonate filters and rinsed with artificial seawater, desiccated during one night at 60 °C. Filters were digested in 20 mL NaOH (0.2 mol L^{-1}) for 3 hours at 95 °C and stirred regularly to ensure the complete dissolution of $bSiO_2$. The solutions were neutralized with 5 mL of HCl (1 mol L^{-1}), centrifuged and the supernatants were analyzed for dSi.

2.4.2.2. Silicic acid (dSi)

Silicic acid concentrations were determined on the 0.6 µm filtered seawater samples and on the digested $bSiO_2$ samples using the molybdate blue spectrophotometric method of Mullin and Riley (1965), as adapted by Tréguer and Le Corre (1975) and modified by Gordon et al. (1993) for use in segmented flow colorimetry with a Luebbe Technicon Autoanalyser (Precision, as relative standard deviation RSD, <1 %).

2.4.2.3. Particulate Organic Nitrogen (PON)

For PON content determination, samples were filtered on a pre-combusted Whatman GF/F filters (450 °C for 4 hours), and rinsed with artificial seawater containing no nutrient. The filters were desiccated at 60 °C overnight in pre-combusted glassware and stored until analysis using an elemental analyzer Thermo Fisher NA 2100 CN (Precision, as RSD, 1 %).

2.4.3. Modeling experiment

Most of the early studies that focused on $bSiO_2$ dissolution kinetics, used a one order equation to model the decrease in $bSiO_2$ concentration or the increase in dSi concentration over time (Truesdale et al. 2005). In some cases, the plot of ln $[(C_\infty - C_t) / C_\infty]$ against time (where C_∞ and C_t are the dissolved dSi concentration at times infinity and t, respectively) clearly indicate two distinct linear portions (e.g. Kamatani and Riley 1979, Kamatani 1982). This two-stage dissolution may suggest that the diatom frustule is composed of two fractions, or phases, that have different dissolution behaviors, as suggested in previous studies (Gallinari 2002; Moriceau et al. 2009; Soler 2010). Thereafter we subsequently name *phase* each part of the frustule that is characterized by different dissolution constant and solubility.

Modeling the dissolution of a multi-phase $bSiO_2$ requires more complex equations, i.e. more kinetics parameters. In order to determine if the frustule of *P. delicatissima* is made of one or two biogenic silica phases and to obtain the kinetics parameters, we follow the same reasoning than Moriceau et al. (2009): the $bSiO_2$ dissolution was modeled using equation with increasing complexity. To better constrain models, using the largest dataset possible, we used both $bSiO_2$ and dSi data measured independently to model frustule dissolution. Four mechanistic models corresponding to one or two phases of $bSiO_2$ were tested and compared.

2.4.3.1. Models

The first model represents one phase of biogenic silica (equation 1), using a simple first-order rate equation as described in Greenwood et al. (2001):

$$\hat{C}_{(t)} = C_0 . e^{-k.t} \qquad (1)$$

Where $\hat{C}_{(t)}$ is the concentration (µmol L^{-1}) calculated at time t (day), C_0 is the initial $bSiO_2$ concentration (µmol L^{-1}), and k is the dissolution constant (d^{-1}).

The following three models represent two phases of biogenic silica, but use different links between the two phases relative to the dissolution.

The second model assumes simultaneous dissolution of two different phases of biogenic silica as describes in Truesdale et al. (2005).

$$\hat{C}_{(t)} = C_1 . e^{-k_1.t} + C_2 . e^{-k_2.t} \qquad (2)$$

C_1 and C_2 are the concentrations (µmol L^{-1}) of the two $bSiO_2$ phases, and k_1 and k_2 (d^{-1}) are their respective dissolution constants.

In the third model (equation 3a and 3b) the frustule dissolves following two different dissolution constants succeeding each other. It can be considered that the frustule is made of two different phases of biogenic silica with one protecting the other one, or that changes in the environmental conditions lead to modification of the dissolution constant.

$$\hat{C}_{(t)} = C_0 . e^{-k_1 . t} \; ; 0 < t < t_s \qquad (3a)$$

$$\hat{C}_{(t)} = C_{t_s} . e^{-k_2 . (t - ts)} \; ; t > t_s \qquad (3b)$$

This model resembles the one from Kamatani (1982) and like model 2, estimates four parameters. C_0 is the initial $bSiO_2$ concentration (µmol L^{-1}), k_1 and k_2 (d^{-1}) are the dissolution constants. The substitution time t_s (day) is the time point at which the dissolution constant changes, and C_{t_s} is the concentration of $bSiO_2$ at the substitution time (µmol L^{-1}).

The fourth and last model considers that the first phase of $bSiO_2$ is not totally dissolved when the dissolution of the second phase begins (equation 4a and 4b)

$$\hat{C}_{(t)} = C_1 e^{-k_1 . t} + C_2 \qquad (4a)$$

$$\hat{C}_{(t)} = C_1 . e^{-k_1 . t} + C_2 . e^{-k_2 . (t - ts)} \qquad (4b)$$

Model 4 estimates five parameters. Until the time t_s (day) a single phase, with a concentration C_1 (µmol L^{-1}), dissolves at the dissolution constant k_1 (d^{-1}). After t_s this phase dissolves simultaneously with a second phase, which concentration is C_2 (µmol L^{-1}) and which dissolution constant is k_2 (d^{-1}).

2.4.3.2. Statistical analyses

To determine the model that best fits the data, statistical analyses were used to compare the quality of the fit and the robustness of the estimated parameters.

The goodness of the fit (Log(L), equation 5) takes into account the number of estimated parameters and the number of data available to constrain the model.

$$\log(L) = -\frac{N}{2} * \log\left(\left(\frac{\sum(\hat{C}_j - C_j)^2}{N}\right) + 1\right) \qquad (5)$$

N is the number of data points, C_j is a measured concentration for data point j, and the $\hat{C}_j$ is the corresponding model prediction.

As it uses two more parameters than the first model, model 2 and 3 always give a better fit than model 1. Hence, to justify an increase of the model complexity, which is done in this experiment by increasing the number of parameters, the model's goodness of the fit ($\log(L)$) should be at least 2 units higher per added parameter (Hilborn 1997). For example, the goodness of the fit with model 2 and model 3, Log(L_{M2}) and Log(L_{M3}), have to be 4 units higher than log(L_{M1}) because model 2 and 3 used two more parameters than model 1.

The robustness of the estimated parameters is calculated using the Jackknife, which gives the tendency of the sample correlation to over-estimate or under-estimate the true, unknown, correlation. The estimated bias is given under the form of a standard error (root mean square error, RMSE) (Davison 1997) and of a coefficient of variation (CV_{RMSE}) expressing the stability of the models (Elzein et al. 2011) by measuring the differences between experimental data and predicted values.

2.5. Results

2.5.1. $bSiO_2$ concentrations

The initial $bSiO_2$ concentrations measured in the three batches were 19.2 ± 8.6 µmol L^{-1}, n = 2, CI = 95 % for the control batch, 28.9 ± 3.8 µmol L^{-1}, n = 4, CI = 95 % for the Cu-starved batch and 12.5 ± 0.7 µmol L^{-1}, n = 5, CI = 95% for the Fe-limited batch. The standard deviation on the initial $bSiO_2$ concentration in the control and Cu-starved batches were quite high, probably attesting the difficulty to homogenize batches during sampling. The $bSiO_2$ concentration in the Cu-starved batch at T_1 (23.1 ± 1.3 µmol L^{-1}, n = 5, CI = 95 %) was higher than in the control batch (17.3 ± 1.8 µmol L^{-1}, n = 6, CI = 95 %). At T_1 the $bSiO_2$ concentration in the Fe-limited batch was 1.5-times lower than in the control batch (11.3 ± 0.2 µmol L^{-1}, n = 2, CI = 95 %). Due to lower standard errors on T_1 measurements than T_0 ones, and to insure that the cells were correctly homogenized after the freezing, we used $bSiO_2$ concentrations at T_1 as the starting point for the dissolution experiment. Reported to $bSiO_2$ concentration at T_1, ~ 30 % of the initial $bSiO_2$ remained at the end of the experiment in the Cu-starved and Fe-limited batches while ~ 20 % remained in control batch.

2.5.2. dSi concentrations

Initial dSi concentrations were the highest in the control and Cu-starved batches (17.34 µmol L^{-1} and 15.77 µmol L^{-1}, respectively) while it was about 3-times lower in the Fe-limited cells batch (5.44 ± 1.54 µmol L^{-1}, n = 3, CI = 95 %). dSi concentrations at T_1 were similar to those at T_0 (16.4 ± 1.5 µmol L^{-1}, n = 3, CI = 95 %, 16.6 ± 2.1 µmol L^{-1}, n = 3, CI = 95 % and 6.7 µmol L^{-1} for control, Cu-starved and Fe-limited batches, respectively). During the dissolution experiment, dSi concentrations remained far from $bSiO_2$ solubility (~ 1100 µmol L^{-1} at 16 °C, Dixit et al. 2001), with a maximum of 29.8 ± 3.5 µmol L^{-1} for replete batch, 32.3 ± 6.1 µmol L^{-1} for Cu-starved batch and 14.0 µmol L^{-1} for Fe-limited batch.

2.5.3. PON concentrations

We adopted the same strategy as for $bSiO_2$ and used PON concentrations at T_1 as the starting point for the degradation experiment. PON concentration in the control batch was lower than in the Cu-starved batch at T_1 (23.3 ± 0.8 µmol L^{-1}, n = 4, CI = 95 % and 43.7 ± 0.8 µmol L^{-1}, n = 3, CI = 95 %, respectively), and much lower in the Fe-limited batch (8.7 µmol L^{-1}). Reported to the PON concentration at T_1, few residual materials remained at the end of the experiment in the three batches (~ 7 %, ~ 10 % and ~ 14 % for control, Cu-starved and Fe-limited batch, respectively).

2.5.4. Si : N molar ratios

At T_1 the Si : N ratio in Fe-limited batch (1.3) was higher than in control and Cu-starved batches (0.7 ± 0.1 and 0.5 ± 0.04, respectively). Elemental ratios found at T_1 are similar to elemental ratio of cells during their growth (Boutorh et al. 2013, this issue). The Si :N ratio was overall constant in the control batch with an average of 1.0 ± 0.2, n = 16, CI = 95 % through the experiment (Table III-1). However, for batches containing the micronutrient-limited cells the trend is to an increase of the Si : N ratios. Indeed, in the Cu-starved batch the mean Si : N during the first fourteen days of experiment was 0.6 ± 0.2, n = 9, CI = 95 % with a 3-fold increase during the last seven days (2.0 ± 0.5, n = 6, CI = 95 %)(Table III-1). We observed a similar behavior for the Fe-limited batch, with an average Si : N ratio of 1.7 ± 0.8, n = 7, CI = 95 % during the six first days increasing to 5.8 ± 1.6, n = 9, CI = 95 % during the last fifteen days (Table III-1). Salter et al. (2007) had deployed sediment trap at 7 sites in the Southern Ocean with depth ranging between 86.9 and 248.2 meters. They found two groups of three sites with average Si : N molar ratios of 11.5 ± 1.2 and 1.3 ± 0.3 and one station that was not included in the two groups with a Si : N

molar ratio of 3.3. The residual Si : N molar ratios obtained after a 22-days dissolution experiments on cells grown under nutrient replete or micronutrient-limited conditions fit into the results of Si : N ratio measured in sediment trap deployed in the Southern Ocean where diatoms dominate export fluxes (Buesseler et al. 1998).

Table III-1 : Si : N molar ratios measured within the three batches throughout the dissolution experiment.

	Si : N first part of dissolution *	Si : N second part of dissolution **
Control batch	1.0 ± 0.2, n = 16, CI = 95 %	
Cu-starved batch	0.6 ± 0.2, n = 9, CI = 95 %	2.0 ± 0.5, n = 6, CI = 95 %
Fe-limited batch	1.7 ± 0.8, n = 7, CI = 95 %	5.8 ± 1.6, n = 9, CI = 95 %

* first part : from the beginning of the experiment to T_{14} for Cu starvation and T_6 for Fe limitation
** second part: from T_{15} for Cu starvation and T_7 for Fe limitation until the end of the dissolution experiment

2.5.5. Biogenic silica dissolution kinetics of *P. delicatissima*

The kinetics of the three treatments (replete, Cu-starved and Fe-limited) can be directly compared, as we measured specific dissolution rate constants (i.e. normalized from the initial $bSiO_2$ concentrations). For each dissolution experiment, the model reconstructs two datasets measured independently: the temporal evolution of dSi and of $bSiO_2$ concentrations. In the batch containing Fe-limited cells, the total Si concentration (the sum of $bSiO_2$ and dSi concentrations), which should be constant in this closed system, decreased significantly during the experiment. Total Si concentrations averaged 17.6 ± 0.7 µmol L^1, n = 7, CI = 95 % during the first seven days and 15.4 ± 0.6 µmol L^{-1}, n = 13, CI = 95 % during the last fifteen days of the experiment. Problems in sampling at the end of the experiment, probably due to aggregate formation in Fe-limited batch, are a potential explanation for this decrease. Therefore, in Fe-limited batch, both dSi and $bSiO_2$ concentrations were fitted by the model before day 7, and from day 7 to the end of the experiment only dSi concentrations had been modeled. We chose to fit dSi preferentially to $bSiO_2$ concentrations as dSi measurements are not so sensitive to particles heterogenic distribution in the batch.

The subsequent dataset obtained for the three experiments were fitted using the four mechanistic models. The goodness of the fit (Log(*L*)) was calculated as explained in the materials and methods section. For control and Fe-limited treatments, model 3 better fitted the data than models 1 and 2 (Table III-2).

Table III-2 : Goodness of the fit (Log(L)) calculated for the 4 models for $bSiO_2$ dissolution in control, Cu-starved and Fe-limited dissolution experiments.

	Control	Cu-starved	Fe-limited
Log (L_{M1})	90.6	80.8	99.8
Log (L_{M2})	95.8	96.9	108.0
Log (L_{M3})	96.8	96.9	109.1
Log (L_{M4})	96.3	96.8	109.6

For Cu-starved treatment Log(L_{M2}) and Log(L_{M3}) were similar. However, for the Cu-starved cells dissolution the standard deviation on k_2 obtained by model 2 (0.003 ± 0.002 d^{-1}, RMSE = 0.9) lead to a 66 % uncertainties on k_2 while the respective uncertainties on k_1 and k_2 values given by model 3 (Table III-3) are 4 % and 15 %. Thus, model 3 seems to give more realistic kinetic constants than model 2. For the three batches model 4 was disregarded, as Log(L_{M4}) was never two points higher than Log(L_{M2}) and Log(L_{M3}) (Table III-2). Thereby, for each treatments model 3 always gives the best fit.

Results presented in Table III-3 and Figure III-1 illustrate the differences in the dissolution pattern of cells grown in the three grown conditions. In each case, cells dissolved faster before the transition time t_s. The three t_s were comparable and ranged between 4.5 ± 0.3 and 7.5 ± 0.3 days (Table III-3). However, even if the dissolution pattern of cells grown in replete or micronutrient limiting conditions showed similarities, clear differences also exist between the three batches. At the beginning of the experiment, $bSiO_2$ dissolution behavior of control and Cu-starved frustules were similar as seen by model 3 results and fit (Figure III-1 and Table III-3). $bSiO_2$ started to dissolve quite fast with k_1 values of 0.22 ± 0.01 d^{-1} and 0.23 ± 0.01 d^{-1} in control and Cu-starved batches, respectively. Fe-limited diatoms underwent clear slower $bSiO_2$ dissolution since the beginning of the experiment, with k_1 value being ~3-times lower than for the two others treatments (k_1 = 0.072 ± 0.001 d^{-1}) (Table III-3). Second dissolution constants in control and Cu-starved batches (0.068 ± 0.003 d^{-1} and 0.021 ± 0.003 d^{-1}, respectively) were slower than the first ones. While the first dissolution constant of control and Cu-starved cells were similar, during the second part of the experiment the control cells dissolved 3.5-times faster than Cu-starved cells. Differences between the first and second dissolution constants in Fe-limited batch were less important than in the two other ones, the second dissolution constant decreasing only by 0.02 d^{-1} compared with the first one (Table III-3).

Table III-3 : Dissolution constants obtained using the model 3 in the three different dissolution experiments ± the root mean square deviation RMSD. The CV_{RMSE} are the coefficient of variation calculated from the Jackknif. % phase 1 and % phase 2 represent the percentage of the whole $bSiO_2$ concentration (C_0, µmol L^{-1}) which dissolved at the dissolution rate constant k_1 and k_2, respectively.

	C_0 (µM)	CV_{RMSE}	% phase 1	k_1 (d^{-1})	CV_{RMSE}
Control	1.07 ± 0.02	0.02	76	0.22 ± 0.01	0.04
Cu-starved	1.09 ± 0.01	0.01	63	0.23 ± 0.01	0.04
Fe-limited	0.97 ± 0.004	0.004	41	0.072 ± 0.001	0.01

	t_s (d)	CV_{RMSE}	% phase 2	k_2 (d^{-1})	CV_{RMSE}
Control	5.9 ± 0.2	0.04	24	0.068 ± 0.003	0.05
Cu-starved	4.5 ± 0.3	0.06	37	0.021 ± 0.003	0.13
Fe-limited	7.5 ± 0.3	0.04	59	0.045 ± 0.001	0.03

Dissolution constants obtained with the modeling experiment were in the same range as the one found in the literature, in studies that measured phytoplankton dissolution with bacteria on fresh or cleaned diatom frustule, with values ranging between 0.01 and 0.27 d^{-1} (e.g. Truesdale et al. 2005; Roubeix et al. 2008; Moriceau et al. 2009). Dissolution patterns in the three batches were consistent with other studies that found a two-step dissolution of the frustules (Kamatani 1982; Roubeix et al. 2008), i.e. with k_1 values > k_2 values. The first dissolution constant of control and Cu-starved cells were higher than most of the dissolution constants found in the literature, except for the dissolution of acid cleaned frustules of *Eucampia zodiacus* (k = 0.18 d^{-1}) (Kamatani 1982) and for the dissolution of fresh *Skeletonema marinoii* (k = 0.27 d^{-1}) modeled using a simultaneous dissolution of two phases of $bSiO_2$ (Moriceau et al. 2009).

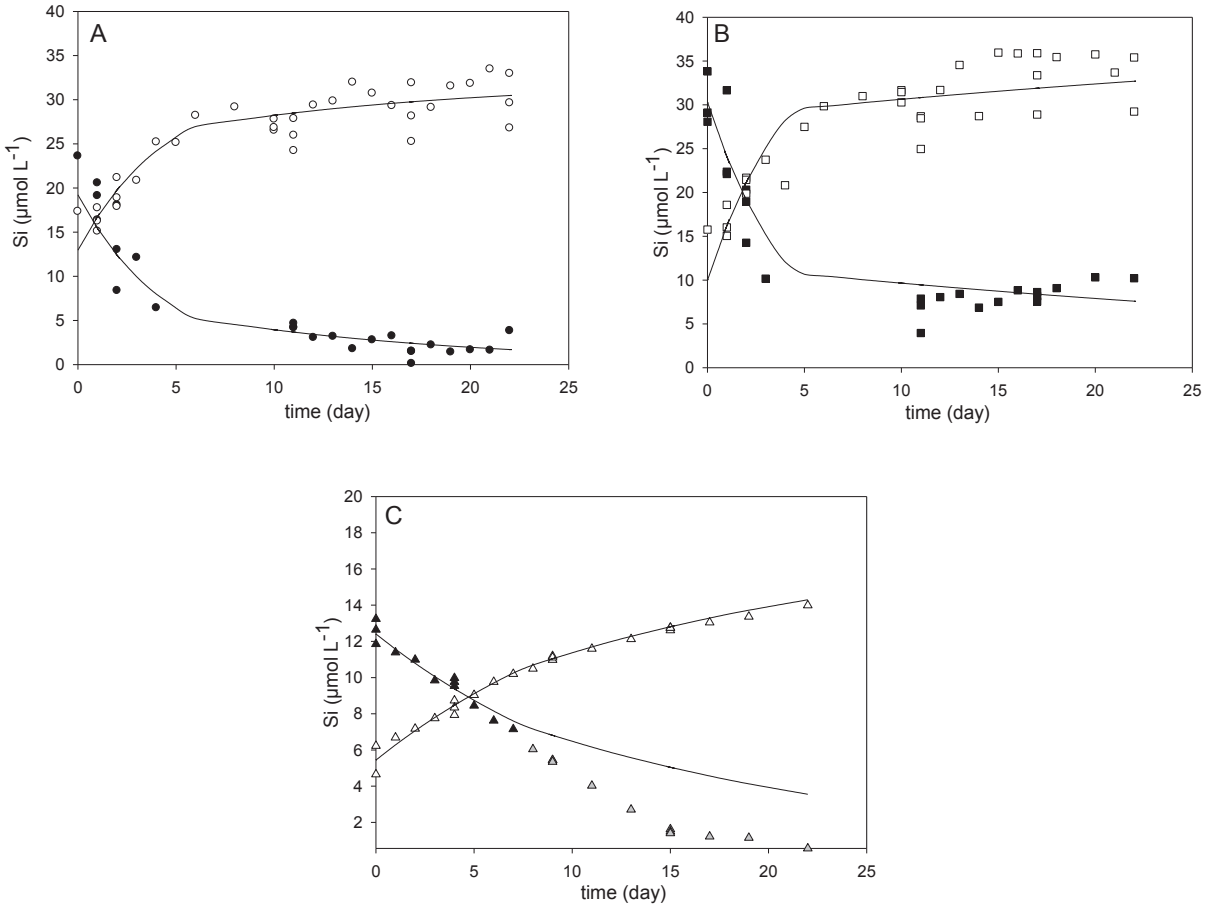

Figure III-1 : Temporal evolution of $bSiO_2$ concentrations (µmol L^{-1}, filled symbols) and dSi concentrations (µmol L^{-1}, open symbols) in control batch (A) the Cu-starved batch (B) and the Fe-limited batch (C). Symbols represent data obtained during experiments. Curves were obtained by modeling with model 3. For the Fe-limited experiment, the $bSiO_2$ dataset used for the modeling exclude values after 7 days of experiment (grey triangle).

2.6. Discussion

2.6.1. The effect of micronutrient availability on the dissolution of *P. delicatissima* frustule

A majority of experiments indicates a two-phase dissolution of diatom frustule (Truesdale et al. 2005, and references therein). The fractionated dissolution could represent the dissolution of different phases of $bSiO_2$, constituting the whole frustule, which have different chemical structure and could be more or less reactive, as previously suggested (Kamatani and Riley 1979; Gallinari 2002; Moriceau et al. 2009).

In the present study we proved that Cu starvation and Fe limitation during growth affect general $bSiO_2$ dissolution pattern. More precisely, these growth conditions modified the proportion of the $bSiO_2$ phases in the frustule of *P. delicatissima*, and their dissolution constants (Table III-3). The most easily dissolvable phase constitutes the greater part of *P. delicatissima* frustule when cells were grown under replete or Cu-starved conditions (73 % and 63 % of the whole $bSiO_2$, respectively). Contrariwise, the less soluble phase of Fe-limited frustule prevails, representing 59 % of the total $bSiO_2$ (Table III-3). Frustule of *P. delicatissima* cells grown under Cu starvation or Fe limitation has been analyzed by Fourier Transform InfraRed spectroscopy (FTIR) before the dissolution experiment (Boutorh et al. this issue). Results suggest that the variability in the dissolution constants of *P. delicatissima* frustule between the three treatments is the result of changes in the frustule chemical or physical structure due to different growth conditions. According to the FTIR results, three different structural changes have been evidenced that may explain the differences in dissolution observed in *P. delicatissima* cells grown under different micronutrients conditions.

The frustule of diatoms is made of amorphous and hydrated biogenic silica. Hydration of the silica surface, composed of siloxane bonds (Si-O-Si), results in the formation of silanol groups (Si-OH) (Van Cappellen et al. 2004). The negative charge of the silanol group at the seawater pH promotes water molecules dissociation and increase the water nucleophilic character, facilitating the hydrolysis of siloxane bonds (Dove 1994) and finally leading to the release of silicic acid ($Si(OH)_4$) in seawater. Thus, the quantity of silanol groups within the silica network could give an indication of the frustule reactivity. The reactivity degree was estimated (Boutorh et al. this issue) using the ratio between the integration of two bands of the FTIR spectra: the band at 950 cm^{-1} which is due to stretching vibration mode of Si-O from silanol groups Si-OH, and the band at 800 cm^{-1} corresponding to the bending vibration mode of bridging bond Si-O-Si. This ratio was 5-times higher for Fe-limited frustules than for Cu-starved frustules ($I_{950cm\text{-}1}/I_{800cm\text{-}1}$ = 10.2 and $I_{950cm\text{-}1}/I_{800cm\text{-}1}$ = 2.0, respectively), i.e. Fe-limited frustule reactivity degree seems to be much higher than the reactivity degree of Cu-starved cells. The value obtained for Cu-starved frustule was in the same range of variation than the one find by Loucaides et al. (2010) for organic matter-cleaned *Thalassiosira punctigera* frustules ($I_{950cm\text{-}1}/I_{800cm\text{-}1}$ = 0.98). Thus, FTIR results indicate that the growth conditions may indeed modify the silica lattice by changing the frustule reactivity degree. However, the higher reactivity degree of the Fe-limited frustule compared to Cu-starved frustule would rather support the assumption that *P. delicatissima* build a more easily dissolvable frustule in a Fe-restricted environment than during Cu starvation, which is contrasting with the dissolution constants obtained by modeling the dissolution experiment (Table III-3).

Another interesting ratio, defined by Gendron Badou et al. (2003), can be derived from FTIR spectra to investigate the mechanisms involved in $bSiO_2$ dissolution pattern. The parameter Ω, which represents the degree of organization of the silica network, is a ratio between the integrated band corresponding to the bending vibration mode of bridging bond Si-O-Si (800 cm^{-1}) and the integrated band attributed to the stretching vibration mode of non-bridging bond in SiO_4 tetrahedron (~1075 cm^{-1}). This estimated ratio was 3-times lower for the Fe-limited cells (Ω = 0.02) than for the Cu-starved cells (Ω = 0.06) indicating that cells grown under Cu starvation would build a more organized silica framework than cells grown under Fe limitation. Organization degree does not explain the trend obtained for frustules dissolution (Table III-3).

Consequently, FTIR results indicate that both reactivity degree and organization degree of *P. delicatissima* frustule are affected by growth conditions. However, the modifications observed cannot explain the lower dissolution efficiency of Fe-limited cells compared to Cu-starved cells (Table III-3 and Figure III-1). FTIR analyses done on Fe-limited and Cu-starved cells before their dissolution pointed out a striking higher quantity of organic matter associated with Fe-limited frustules compared to Cu-starved frustules (Boutorh et al. this issue). We suggest that the existence of these pools of organic matter associated to Fe-limited frustules may have an effect on their dissolution. A reinforcement of mechanical properties induced by the presence of organic compounds within a mineral structure had been previously found within the abalone shell (Hildebrand and Wetherbee 2003): the existence of a small amount of organic matter in the calcium carbonate structure increases its fracture resistance. The possible protective role of the organic matter associated with the diatom frustule has already been mentioned (Hecky et al. 1973). They suggested that diatoms species containing more amino acid within their frustule would be more resistant to dissolution. Following this reasoning, the higher quantity of organic matter associated to Fe-limited frustule compared to Cu-starved frustule may have induced a decrease of the global frustule dissolution.

2.6.2. Impact of Cu starvation and Fe limitation on Si export

A mechanistic understanding of diatom dissolution in seawater is important to simulate the recycling and the fate of $bSiO_2$ within the water column. The modeling exercise, done on data obtained during the dissolution of *P. delicatissima* grown under different limiting conditions, confirms that independently of the growth conditions the dissolution of *P. delicatissima* frustule always occurred in two steps, the first one being faster than the second one. Water column $bSiO_2$ dissolution constants, measured generally in surface water using Si isotope tracer, could be quite high, with values ranging from 0.027 d^{-1} to 0.27 d^{-1}

(10 yr^{-1} to 100 yr^{-1}, Nelson and Brzezinski, 1997 and references therein). These high dissolution constants lead to an efficient recycling of silica, with 10 to 100 % of the $bSiO_2$ produced being dissolved in the euphotic zone (Nelson et al. 1995; Treguer et al. 1995). Inversely, the $bSiO_2$ dissolution within sediment, assessed from flow-through experiments and from models applied on pore water dSi depth profiles, is quite low with values < 0.0014 d^{-1} (< 0.5 yr^{-1}, Van Cappellen et al. 2002 and references therein). This decrease in dissolution constants from ocean surface to deep sea sediments has been attributed to several processes, such as the presence of an organic coating surrounding cells, changes in temperature and dSi concentrations, differences in specific surface area and aluminum content of the frustule (Van Cappellen et al. 2002 and references therein), as well as the gradual elimination of reactive sites (named aging) and the precipitation of authigenic alumino-silicate minerals at the frustule surface during early diagenesis (Van Cappellen 1996, Dixit et al. 2001, Van Cappellen et al. 2002). Our results fit within the range of dissolution constant found at the surface of the ocean. Still, the second dissolution constant is very low, with, for example, the second dissolution constant of Cu-starved frustules being an order of magnitude lower than for the first one (Table III-3).

Even if almost all batch dissolution experiments indicate a two-step dissolution of $bSiO_2$ (Truesdale et al., 2005, and references therein), to our knowledge, none of the several ocean biogeochemical models have used two consecutive dissolution constants to simulate the post-mortem fate of diatoms in the water column. The dissolution constants used to parameterize biogenic silica dissolution generally range from 0.01 d^{-1} (Gehlen et al. 2006, Mongin et al. 2006) to 0.12 d^{-1} (Pondaven et al. 1998, Gnanadesikan 1999). As dissolution constants k_1 and k_2 fit within the range of dissolution constants found at the surface of the ocean, one may wonder what benefits provide the use of both k_1 and k_2. The *preservation capacity*, i.e. the percentage of $bSiO_2$ from *P. delicatissima* remaining at the end of the twenty-two days dissolution experiment, is quite different when considering either both or only one dissolution constant. The use of only the first dissolution constant k_1 leads to an under-estimated *preservation capacity* reaching less than 1 % for replete condition, whereas the use of only the second dissolution constant k_2 leads to an over-estimated *preservation capacity* reaching 21 % for replete cells. With the two dissolution constants, which is the pattern validated by the modeling experiment (Tables III-2 and III-3), the preservation capacity reached 9 % of the initial $bSiO_2$. Therefore, taking into account the two dissolution constants during diatoms settling to the sea floor is important to estimate (i) the amount of $bSiO_2$ dissolving within the euphotic zone, re-enriching water column in dSi and sustaining growth of new cells, and (ii) the amount of $bSiO_2$ reaching the sea floor. Regarding the effect of micronutrient limiting conditions, when using the two dissolution constants that succeed each, the *preservation capacity* of Cu-

starved and Fe-limited *P. delicatissima* increased by 25 % and 29 %, respectively. While cellular $bSiO_2$ measurements for this species indicate a decrease in the silicification degree at the Fe limitation degree studied (inducing a 75 % decrease of the maximum growth rate, Boutorh et al. this issue), our results confirm the part of the Boyle hypothesis (1998) claiming that Fe-limited cells dissolved slower than replete diatoms.

2.6.3. Effect of micronutrient availability on the silicate pump

The "silicate pump" defined by Dugdale et al. (1995) is the preferential export of Si from the euphotic zone compared to N. Numerous laboratories and field studies focused on the effect of Fe limitation on the elemental ratio of diatoms and demonstrated that low Fe availability leads to an increase in diatoms Si : C and Si : N ratios (Marchetti and Cassar, 2009, and references therein) and would consequently enhanced the silicate pump. Fe limitation during *P. delicatissima* growth had actually led to an increase in the diatoms Si : N ratio compared to replete cells (1.21 ± 0.37 and 0.63 ± 0.08, respectively) (Boutorh et al. this issue). During their dissolution, the present study highlights that the Si : N ratio of Fe-limited cells increased significantly to 5.8 ± 1.6 while the Si : N ratio of replete cells remained nearly constant (Table III-1). These results support the assumption that Fe-limited cells export more Si relative to N. Fe limitation may consequently increase the silicate pump. Moreover, biogenic silica is one of the ballast minerals with a density greater than organic matter increasing the settling velocity of particles (Armstrong et al. 2009 and references therein). Considering this ballast effect, the increase in the Si : N ratio of Fe-limited cells during their dissolution supports the idea of an increase in their density through the water column.

Opposite to the effect of Fe limitation, Cu starvation led to a significant decrease in the Si : N ratio of *P. delicatissima* during growth (0.50 ± 0.04) compare with control cells (0.63 ± 0.08) (Boutorh et al. this issue). Thus, elemental ratios measured on growing diatom would support the idea that Cu starvation would decrease the silicate pump. However, during the dissolution experiment, the Si : N ratio of Cu-starved cells progressively increased to 2.0 ± 0.5 (Table III-1), which was significantly higher than the one of replete cells. Like Fe limitation, Cu starvation favors the silicate pump. The contrasting results on Si : N ratios obtained during cell production and after their dissolution emphasize that elementary ratio of growing cells should be used with caution to estimate their fate. Indeed, as most of the remineralization occurs in the surface layer (Tréguer et De la Rocha 2013), the Si : N ratio of exported particles may be closer to those measured at the end of the dissolution experiments than those measured during production.

The decrease in Si quotas per cell surface with Fe limitation for *P. delicatissima* (0.81 ± 0.07 fmol μm^{-2}, n = 3, CI = 95 % for replete cells and 0.52 ± 0.14 fmol μm^{-2}, n = 4, CI = 95 % for Fe-limited cells) and for *Pseudo-nitzschia* in general at the highest degree of Fe limitation (Boutorh et al. this issue) is contrasting with the Boyle's assumption, i.e. a higher silica content of diatoms under Fe limitation. However, the increase in the Si : N ratios of Fe-limited cells, and thus, the increase of cells density, as well as their better preservation during cells dissolution compared to replete cells, are in accordance with Boyle hypothesis. Like Fe-limited cells, Cu-starved cells were more preserved from the dissolution than replete cells, and their density also increases during their dissolution as inferred by the increase in their Si : N ratios. Thus, it seems that micronutrient-limited *P. delicatissima* cells transport more efficiently $bSiO_2$ in the water column than nutrient replete *P. delicatissima* cells.

Chapitre IV.

Etude de l'effet des déficiences en Si ou en N sur la structure du frustule de *Thalassiosira weissflogii* et conséquences sur la dissolution de la silice biogénique

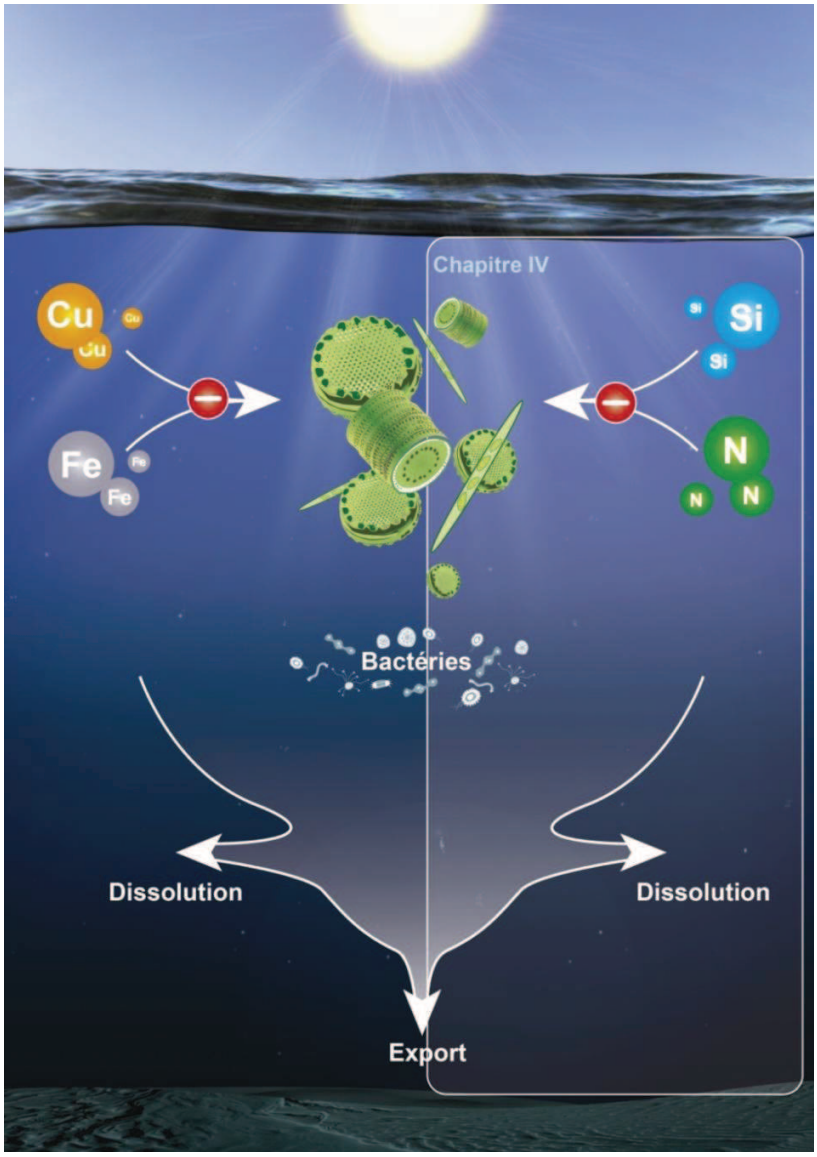

IV. Chapitre IV : Etude de l'effet des déficiences en Si ou en N sur la structure du frustule de *Thalassiosira weissflogii* et conséquences sur la dissolution de la silice biogénique

1. Préambule

Comme nous l'avons vu dans les chapitres précédents, la faible disponibilité en Fe, élément trace limitant la croissance des diatomées en période estivale dans environ 40 % de l'océan ouvert (Moore et al. 2002), va affecter non seulement le degré de silicification du frustule mais aussi sa structure fine. Ces modifications vont influencer la vitesse de recyclage de la $bSiO_2$ formée dans la couche de surface. L'acide silicique et les nitrates sont les deux macronutriments dont les faibles concentrations, durant la période estivale, limitent la croissance des diatomées dans environ 60 % de l'océan ouvert (Figure I-4) (Moore et al. 2002). Pendant cette thèse, j'ai cherché à comprendre et à quantifier l'impact des limitations en éléments nutritifs sur l'export de $bSiO_2$. Pour cela, il est nécessaire de quantifier la dissolution de la $bSiO_2$ dans l'océan global, en tenant compte des paramètres qui l'affectent selon les bassins océaniques. Avec l'étude de ces deux limitations supplémentaires (NO_3^- et dSi), nous obtenons donc une bonne cartographie de l'impact des limitations en éléments nutritifs sur la dissolution de la $bSiO_2$.

Dans un premier temps, j'ai voulu déterminer si la faible disponibilité de ces deux macronutriments durant le développement de la diatomée *T. weissflogii* affecte la structure globale et fine de son frustule, comme nous l'avons montré pour les limitations en micronutriments étudiées sur *P. delicatissima*. Ensuite, la dissolution des phases de $bSiO_2$ et leurs propriétés intrinsèques ont été suivies au cours de la dissolution de frustule de *T. weissflogii*, limitée ou non limitée, afin de déterminer si les comportements de dissolution peuvent s'expliquer par la structure fine de ces phases. Pour cela, nous avons reconstruit, à l'aide d'équations, l'évolution de la $bSiO_2$ et de la dSi au cours du temps et utilisé en parallèle l'outil IRTF (décrit plus précisément dans l'introduction du chapitre II) afin de suivre la structure des frustules au cours de la dissolution. Les spectres obtenus ont été étudiés en tenant compte de la cinétique de dissolution des différentes phases et de leur participation à la $bSiO_2$ totale.

Au cours de cette expérience, nous avons étudié l'impact des limitations en dSi et en NO_3^- sur le cycle du silicium, mais également l'impact sur l'export de carbone et le cycle du phosphore grâce aux collaborations mises en place avec Madeleine Goutx et Maxime Suroy, du Méditerranean Institut of Oceanography (MIO, Marseille), et avec Claire Labry et Daniel Delmas, du centre IFREMER de Brest.

L'objectif de Maxime Suroy et de Madeleine Goutx, pendant cette expérience, était, dans un premier temps, de définir un protocole permettant de mesurer la composition des acides gras associés au frustule, afin de mieux comprendre le degré d'association entre les pools de lipides et le frustule et leur impact sur la reminéralisation de la $bSiO_2$ et des acides gras. Cette première étude a fait l'objet d'une publication, présentée en annexe II, actuellement en révision dans Deep-Sea Research Part I et intitulée "Fatty acids associated with the frustule of diatoms and their fate during degradation – a case study in *Thalassiosira weissflogii*" (Suroy et al. in revision). Avec M. Suroy, nous nous sommes ensuite intéressés à l'impact des limitations en dSi et en NO_3^- sur la composition des pools de lipides et des glucides cellulaires, ainsi que leur devenir dans la colonne d'eau. Dans ce cadre, la dégradation du carbone et de l'azote organique particulaire, ainsi que celle des lipides et des monosaccharides, a été suivie et modélisée au cours du temps. Ce travail fait l'objet d'une publication intitulée « Degradation of diatom carbohydrates : a case study with N- and Si-stressed *Thalassiosira weissflogii* » qui est actuellement en cours d'écriture (Suroy et al. in prep).

Avec Claire Labry et Daniel Delmas nous nous sommes intéressés à la dynamique de régénération du phosphore particulaire, représentant l'une des principales composantes du phosphore dans les milieux oligotrophes et eutrophes peu profonds, grâce à la minéralisation bactérienne. C. Labry et D. Delmas ont cherché à identifier les formes de phosphore préférentiellement dégradées, ainsi que les facteurs contrôlant l'activité de minéralisation de ce phosphore particulaire. Pour ce faire, durant les expériences de dégradation, C. Labry et D. Delmas ont suivi l'évolution des différentes formes de phosphore (inorganique/organique, dissous/particulaire), les bactéries libres et attachées aux particules et l'activité des phosphatases alcalines associées (enzymes produites par les microorganismes responsables de la minéralisation du phosphore organique en phosphate). Les résultats de cette étude sont en cours d'analyse et feront également l'objet d'une publication.

Comme souligné précédemment, mon travail sur cette expérience a donc plus particulièrement concerné le cycle du silicium. L'étude de l'impact de l'environnement nutritionnel sur la structure et la dissolution de la $bSiO_2$ du frustule de la diatomée *Thalassiosira weissflogii* est présentée sous forme d'une publication qui sera soumise à Global Biogeochemical Cycles.

2. Effect of Si and N deficiencies on *Thalassiosira weissflogii* frustule structure and consequences on biogenic silica dissolution

Boutorh Julia[1], Moriceau Brivaëla[1], Gallinari Morgane[1], Suroy Maxime[2], Delmas Daniel[3], Amiel Caroline[4], Ragueneau Olivier[1]

[1] Université de Brest, Institut Universitaire Européen de la Mer (IUEM), CNRS, Laboratoire des Sciences de l'Environnement Marin, UMR 6539 CNRS/UBO/IFREMER/IRD, 29280 Plouzané, France.

[2] Aix-Marseille Université, Université du Sud Toulon-Var, CNRS/INSU, IRD, Mediterranean Institute of Oceanography (MIO), UM 110, 13288, Marseille, Cedex 09, France.

[3] IFREMER / Centre de Brest, Dept DYNECO (Dynamique de l'Environnement Côtier), Laboratoire Pélagos, BP 70, 29280 Plouzané, France.

[4] Plateau technique de Spectroscopie IRTF, Université de Caen Basse-Normandie, IUT de Génie Biologique, Campus 2, Bd du Maréchal Juin, 14032 CAEN cedex, France.

To be submitted to Global Biogeochemical Cycles

2.1. Résumé

Nous avons examiné l'effet de déficiences en acide silicique (dSi) et nitrate (NO_3^-) sur la structure du frustule de la diatomée marine *Thalassiosira weissflogii* et sur sa dissolution subséquente. Les concentrations en silice biogénique ($bSiO_2$) et en dSi ont été suivies au cours de la dissolution des cellules préalablement soumises à des déficiences en N ou en Si puis congelées, afin de modéliser la dissolution des frustules en considérant deux phases de $bSiO_2$. La spectroscopie infrarouge à transformée de Fourier (IRTF) a permis d'estimer les propriétés intrinsèques des frustules, tels que leur degré de réactivité, leur degré d'organisation, ainsi que la quantité relative de carbone associée aux frustules. L'IRTF a été utilisé tout au long de la dissolution des frustules, pour pouvoir comparer les propriétés intrinsèques des deux phases de $bSiO_2$. Les paramètres cinétiques obtenus indiquent que les diatomées ont suivi le même schéma global de dissolution: une période de dissolution lente, suivie par la dissolution de deux phases de $bSiO_2$, l'une se dissolvant plus rapidement que la seconde. Le première période de dissolution lente peut-être expliquée par la protection du frustule de la dissolution, par la présence de la membrane organique enveloppant le frustule, ainsi que celle d'exsudats organiques. Les limitations nutritives, en changeant les propriétés intrinsèques du frustule, diminue sa vitesse de dissolution globale. Plus particulièrement, les deux phases de $bSiO_2$ du frustule sont affectées par l'environnement nutritionnel. La vitesse de dissolution de la phase la plus soluble est similaire dans les trois expériences, mais sa part dans la composition du frustule est plus faible en cas de déficience nutritive que pour des conditions non limitantes. La vitesse de dissolution de la phase la plus lente n'est pas affectée par la déficience en N, mais est augmentée par la déficience en Si, ce qui peut être expliqué par la moins bonne organisation de cette phase lors d'une déficience en Si. La quantité relative de matière organique associée au frustule est plus particulièrement associée à la phase de $bSiO_2$ se dissolvant le plus lentement. Cette quantité est plus importante dans le cas d'une déficience en Si que lors d'une déficience en N, où elle reste inchangée. Ainsi, la phase de $bSiO_2$ dont la dissolution a été le plus accélérée par les conditions nutritionnelle possède une structure moins organisée et est associée à une plus grande quantité de matière organique. Les modifications dans la structure des frustules limités en nutriment entrainent leur meilleure préservation, avec 41 % et 51 % de la $bSiO_2$ initiale des cellules déficientes en Si et N restants au bout d'un mois de dissolution, contre 20 % pour les frustules des cellules non limitées.

2.2. Abstract

We examined the effect of silicic acid (dSi) or nitrate (NO_3^-) deficiencies on the frustule structure of the marine diatom *Thalassiosira weissflogii* and on its subsequent dissolution behavior. Biogenic silica ($bSiO_2$) and dSi concentrations were measured during the dissolution of cells previously submitted to Si or N deficiency, to model their frustules dissolution considering two $bSiO_2$ phases. Fourier Transform InfraRed spectroscopy (FTIR) gave an estimation of the intrinsic frustule properties, such as their reactivity degree, their organization degree and the relative amount of carbon associated with their frustule. FTIR was used all along frustule dissolution to compare the intrinsic properties of the two $bSiO_2$ phases. The kinetic parameters obtained indicate that diatoms have followed the same overall dissolution pattern: a period of slow dissolution, followed by the dissolution of the two $bSiO_2$ phases. The first period of slow dissolution may be explained by the protection of the frustule from the dissolution by the organic coating as well as the presence of organic exudates. The nutritional environment, by changing the intrinsic properties of the frustule, decreases its overall dissolution rate. More particularly, the two $bSiO_2$ phases were affected by the nutritional environment. The dissolution constant of the fast dissolving phase was similar in all three experiments, but the proportion of this phase in the whole frustule was lower in case of nutrient deficiency than for non-limiting conditions. The dissolution constant of the slow dissolving phase was not affected by N deficiency, but was increased by the Si deficiency. This can be explained by the lower organization degree of this phase under Si deficiency. The relative amount of organic material associated with frustule was more particularly associated with the slow dissolving $bSiO_2$ phase, and was more important under Si deficiency than under N deficiency, where it was unchanged. Thus the $bSiO_2$ phase whose dissolution was the most accelerated by the nutritional conditions had the less organized structure and was associated with a larger amount of organic matter. Changes in the structure of nutrient-limited frustules led to their better preservation, with 41 % and 51 % of the initial $bSiO_2$ from Si- and N-deficient cells remaining after one month of dissolution, against 20 % from frustules of non-limited cells.

2.3. Introduction

Diatoms are estimated to account for a large majority of the total primary production (Nelson et al. 1995). These micro-algae, which have the particularity of being encased in a siliceous shell, the frustule, can integrate bigger particles such as aggregates (Thornton 2002) and fecal pellets (Schrader 1971). The fast sinking rates of those big particles makes them major actors of the sedimentary flux (Turner 2002). In particular, diatoms have been estimated to represent 40 % of the export flux of particulate organic carbon (POC) (Jin et al. 2006). Considering the importance of diatoms in sedimentation flux, and because they need silicic acid (dSi) to build their frustule composed of biogenic silica ($bSiO_2$), they are key organisms for both carbon and silicon cycles (Smetacek 1999). Nutrient limiting conditions have been confirmed as promoting the excretion of extracellular polymeric substances (EPS) by diatoms, those extracellular carbohydrates increasing cells stickiness and leading to aggregates formation (Thornton 2002; Turner 2002). Consequently, nutrient limitations may have significant effect on the export of diatoms $bSiO_2$ to the seafloor by increasing the sedimentation flux. However, the export efficiency of $bSiO_2$ from diatom also depends on remineralization rates.

Several experiments have focused on processes affecting diatom $bSiO_2$ dissolution, such as the presence of the organic coating surrounding the frustule (Bidle and Azam 1999), changes in temperatures and dSi concentrations in diatom environment (Kamatani 1982; Rickert et al. 2002), the association between aluminum and Si atoms (Gehlen et al. 2002), or the frustule surface characteristics like the specific surface area (Dixit and Van Cappellen 2002) and the amount of reactive sites at the frustule surface (Van Cappellen 1996). On the other hand, effects of chemical and physical characteristics of the frustule structure on $bSiO_2$ dissolution have rarely been investigated. Diatom frustule structure is complex, and involves associations between the silica lattice and organic matter pools (Abramson et al. 2009; Suroy et al. in revision), some of the latter supposed to be involved in diatom cell wall biogenesis (Kröger and Poulsen 2008; Tesson and Hildebrand 2013). The silica metabolism and the resulting silicification degree have already been showed to be affected by nutrient availability (Martin-Jezequel et al. 2000; Claquin et al. 2002). It may be suggested that frustule fine structure is also affected by nutrient limitation, and that it may significantly affect its subsequent dissolution.

Using a global marine ecosystem mixed-layer model, Moore et al. (2002) have estimated that, during summer, nitrate (NO_3^-) and dSi concentrations limit diatom production in 50 % and 11 % of total ocean area, respectively. In the present study, we examined the effect of dSi and NO_3^- deficiencies on the post-mortem $bSiO_2$ dissolution behavior of the marine diatom *Thalassiosira weissflogii*. Diatoms dissolution was followed during thirty days dissolution experiments, and was

subsequently modeled. Using Fourier Transform InfraRed spectroscopy (FTIR) analysis, changes in $bSiO_2$ structure and global composition was assessed throughout diatoms dissolution. This strategy aims to confirm structural differences between the two dissolving phases, already evidenced by Kamatani and Riley (1979) and Truesdale et al. (2005), and to investigate if frustule dissolution is partially or totally affected by nutrient availability during growth.

2.4. Materials and methods

2.4.1. Culture

The centric diatom *Thalassiosira weissflogii* (strain CCMP 1049) was grown in Conway medium (Walne 1966) at 20 °C under continuous illumination at 241 ± 74 photons m^{-2} s^{-1} at the IFREMER station in Argenton. When the diatom concentration reached 400 000 cell mL^{-1}, 10 L of culture were sampled, centrifuged at 2000 tr min^{-1}, and diatoms were killed by freezing the remaining pellet at -20 °C. These cells represent our control; they experienced no limitation during growth and had a good photosynthesis efficiency at their photosystem II, as estimated by measurement of the Quantum Yield (QY) using the AquaPen-C AP-C 100 fluorometer high physiological status. Indeed, those cells had a QY of 0.58 which is similar to the one obtained by Soler (2010) on the same species under replete conditions (QY = 0.61).

Another 20 L of *T. weissflogii* culture from Argenton were split in two aliquots. Each 10 L of culture was centrifuged and rinsed before being re-suspended in two 10 L-polycarbonate bottles. In the first batch, diatoms were re-suspended in modified f/2 medium (Guillard 1975) containing no silicic acid while the second batch was filled with modified f/2 medium containing no nitrate. Limitation experiments were undertaken during 6 days at 18 °C under fluorescent light at an irradiance of 158 ± 39 µmol photons m^{-2} s^{-1} and a 12 h: 12 h light:dark cycle. Thereafter, diatoms from the first batch are named Si-deficient and diatoms from the second batch are named N-deficient. Samples to monitor nutrient concentration of the medium, cell dimensions and concentrations, cellular carbon, nitrogen and $bSiO_2$, QY measurements and concentration of extracellular polymeric substances were taken on a daily basis. Diatom cells were then centrifuged, rinsed with artificial seawater and killed by freezing at – 20 °C.

2.4.2. Dissolution experiments

Experimental design: The three pellets of frozen diatom cells were slowly thawed at room temperature, and then re-suspended in three polycarbonate batches containing 10 L of natural seawater previously filtered on 0.7 µm Whatman GF/F filters, to keep only the natural procaryotic

community while removing most phytoplankton and zooplankton. Physical and chemical characteristics of the seawater sampled on October 23, 2012, at the SOMLIT-Portzic station are detailed in the website http://somlit-db.epoc.u-bordeaux1.fr/bdd.php?serie=ST&sm=3. Briefly, the natural seawater used for the dissolution experiments had, at the day of sampling, a pH of 7.9, NO_3^-, PO_4^{3-} and dSi concentrations of 3.38 µmol L^{-1}, 0.30 µmol L^{-1} and 4.88 µmol L^{-1}, respectively, and a bacterial concentration of 679 533 cell mL^{-1}. The thirty days dissolution experiments were conducted in the dark at 16.3 ± 0.2 °C, on an orbital shaker table to homogenize the mixture.

Sampling strategy: pH and oxygen saturation level were monitored on a daily basis to evaluate if hypoxic or anoxic conditions were reached in batches. During fifteen days, daily samples were taken to measure biogenic silica ($bSiO_2$) and silicic acid (dSi) concentrations. Samples were taken on larger interval after day 15. To evaluate changes in diatom frustule structure and composition, samples for Fourier Transform Infrared Spectroscopy analysis were taken at T_0, T_1, T_6, T_9, T_{22} and T_{30} in each batch. Control and Si-deficient batch were also sampled at T_{15} and T_3, respectively. Prokaryotic concentrations were measured daily the first four days of experiments and then at T_7, T_{11}, T_{15}, T_{18}, T_{25} and T_{30}. After thirty days of sampling, about 60 % of the initial volume remained in the bottles, to minimize the artifact due to the batch.

2.4.3. Analytical methods

2.4.3.1. Cell abundance

Flow cytometry was used to count cells in batches. Mortality of T. *weissflogii* was assessed by staining cultures with 0.1 µmol L^{-1} of SYTOX Green (Molecular probes, Invitrogen, Eugene, Oregon, USA) for 30 minutes and quantifying FL1 fluorescence (stained cells were considered as dead cells). Measurements were made with a FACScalibur flow cytometer (BD Biosciences, San Jose, CA USA) using an argon blue laser (488 nm).

2.4.3.2. Free and attached prokaryotes concentrations

Free and total prokaryotes were counted under microscope on 0.2 µm black polycarbonate filters after staining with DAPI (4',6-diamidino-2-phenylindole). Filtration of the whole sample allowed the measurement of the total prokaryote concentrations and filtration of a 3 µm pre-filtered sample allowed the measurement of free prokaryote concentrations. Attached prokaryote concentration was calculated by subtracting free to total prokaryote cell number.

2.4.3.3. Biogenic silica ($bSiO_2$)

$bSiO_2$ concentrations were determined using a variation of the Ragueneau and Tréguer (1994) method adapted to culture samples (Moriceau et al. 2007). Samples were filtered on 0.6 µm polycarbonate filters and rinsed with artificial seawater. The filters were desiccated during one night at 60 °C. Filters were then digested in 20 mL of NaOH (0.2 mol L^{-1}) for 3 hours at 95 °C. The digestate was then cooled and neutralized with 5 mL of HCl (1 mol L^{-1}). Remaining particles in digestates were removed using centrifugation and the supernatant was later analyzed for silicic acid (dSi).

2.4.3.4. Silicic acid (dSi)

Silicic acid concentrations of the surrounding seawater and for $bSiO_2$ analysis were determined on 0.6 µm filtered samples from the three batches and on digestates from $bSiO_2$ samples using the molybdate blue spectrophotometric method of Mullin and Riley (1965), as adapted by Tréguer and Le Corre (1975) and modified by Gordon et al. (1993) for use in segmented flow colorimetry. We used a Bran and Luebbe Technicon Autoanalyser (Precision, as Relative Standard Deviation RSD, < 1 %).

2.4.3.5. Bound Extracellular Polymeric Subtances (EPSb) and intern carbohydrates

Ten mL-samples were centrifuged 20 minutes at 4000 rpm. Pellets containing bound EPS (EPSb) (Thorton 2002 and references therein) and intern carbohydrates were divided in two fractions, High Weight (HW) and Low Weight (LW) EPSb, using the method of Takahashi et al. (2009). After re-suspension of the pellet in 2mL of distilled water, 6mL of absolute ethanol was added, and the EPSb was allowed to precipitate overnight at –20°C. After centrifugation during 20 min at 4000 rpm, supernatant contained the LW fraction and the pellet contained the HW fraction of the EPSb + intern carbohydrate. Fractions were separated and dried at 50 °C. EPSb + intern carbohydrate were then dosed in each fraction using the colorimetric method of Dubois et al. (1956). After re-suspension of dried samples in 1 mL of distilled water, 1 mL of phenol (5 %) and 5mL H_2SO_4 (96 %) were added. After 30 minutes of reaction, the coloration was measured at 485 nm using a Secomam PRIM Light spectrophotometer. Concentrations are expressed as glucose equivalents (mg equiv. glucose L^{-1}) (Precision, as RSD, 2 %).

2.4.3.6. Transparent ExoPolymeric particles (TEP)

TEP concentrations were measured following the method described in detail in Passow (1995). Between 3 and 10 mL of mixture from the three batches were filtered on 0.4 µm

polycarbonate filters. Filtration volumes were adjusted each day to avoid filters clogging. Filtration was carried out under low and constant vacuum (150 mm of Hg). TEP were colored with 500 µL of a solution of alcian blue (0.02 % alcian blue in 0.06 % acetic acid at pH 2.5) during less than 2 second. Excess of alcian blue was rinsed using milli-Q water and filters were stored at – 20°C. Before analysis, filters were digested in 6 mL of 80 % H_2SO_4 during 2 hours, with constant shaking. Samples absorption was measured at 787 nm against milli-Q water as a reference, using a Secomam PRIM Light spectrometer. Results are expressed in absorbance of the samples per milliliters filtered (Abs mL^{-1}) (Precision, as RSD, 4 %).

2.4.3.7. Fourier Transform Infra Red (FTIR) spectroscopy

Samples (100 mL) were centrifuged 20 minutes at 4000 rpm. Pellets were rinsed using distilled water and frozen at -20°C for at least 24h before being freeze-dried. Samples for frustule analysis were exposed to low-temperature ashing (LTA) during 9 hours, using a Plasma – ACE_5 plasma oven (Gala Instrument) equipped with an oxygen gas bottle to obtain oxygen plasma, so as to remove diatom intracellular and exposed organic matter (Vanbennekom et al. 1989; Koning et al. 2007; Loucaides 2009). For FTIR analysis, dried samples were re-suspended in milli-Q water and concentrated by centrifugation. A 20 µL aliquot per sample was deposited in triplicate on a silicon microplate, which was desiccated overnight at 40°C before FTIR spectra collection using a HTS-XT high-throughput microplate extension (Bruker) on a FTIR spectrometer (Tensor 27 Bruker). Spectra were collected between 4000 and 700 cm^{-1} at a spectral resolution of 8 cm^{-1} with 64 scans added and averaged. Triplicate indicated a 97 % repeatability of FTIR measurement. The baseline was corrected and each spectrum was decomposed, in triplicate, between 1300 and 700cm^{-1} into Gauss curves, using the Origin 8.5 software.

2.4.4. Kinetic parameters for $bSiO_2$ dissolution

Until recently, a simple exponential equation, and thus one dissolution constant, was used to approximate $bSiO_2$ dissolution (Hurd and Birdwhistell 1983; Tréguer et al. 1989; Truesdale et al. 2005). However, (i) this equation is not kinetically correct as it considers that all molecules are available for dissolution at any time, which is not the case for a solid like the frustule (Truesdale et al. 2005) and (ii) numerous $bSiO_2$ dissolution kinetics evidenced a two-stage dissolution (e.g. Kamatani and Riley 1979, Truesdale et al. 2005, and references therein, Moriceau et al. 2009) that would be best modeled by more complex equations. This fractionated dissolution could be the result of a frustule made of two fractions of $bSiO_2$, or phases, which have different dissolution constants and solubilities (Gallinari 2002; Moriceau et al. 2009). Consequently, in the present study, we tested and

compared four different dissolution models (Moriceau et al. 2009) to reconstruct the temporal evolution of both $bSiO_2$ and dSi concentrations.

2.4.4.1. Biogenic silica dissolution kinetics: equations

The first dissolution model uses a simple first-order rate equation for each parameter:

$$\widehat{[bSiO_2]}_{(t)} = [bSi0_2]_0 . e^{-k.t} \quad (1)$$

$$\widehat{[dSi]}_{(t)} = [dSi]_0 + [bSiO_2]_0 . (1 - e^{-k.t}) \quad (2)$$

Where $\widehat{[bSiO_2]}_{(t)}$ and $\widehat{[dSi]}_{(t)}$ are the model estimation for$bSiO_2$ and dSi concentrations (µmol L^{-1}) calculated at time t (day), $[bSiO_2]_0$ and $[dSi]_0$ are the initial concentrations in batch (µmol L^{-1}), k is the dissolution constant (d^{-1}).

The following three models reconstruct dissolution over time considering two $bSiO_2$ phases having their own dissolution parameters. For clarity, only equations that aimed to reconstruct $bSiO_2$ data are presented below. Equations for dSi measurements reconstruction are deduced from the following equations like equation 2 is derived from equation 1.

The second model is a sum of exponentials, as described in Truesdale et al. (2005):

$$\hat{C}_{(t)} = C_1 . e^{-k_1.t} + C_2 . e^{-k_2.t} \quad (3)$$

C_1 and C_2 are the $bSiO_2$ concentrations (µmol L^{-1}) of the two phases and k_1 and k_2 (d^{-1}) are their respective dissolution constants.

The third dissolution model considers that $bSiO_2$ dissolution parameters changed after a certain time, as suggested by Kamatani and Riley (1979) (equation 4a and 4b).

$$\hat{C}_{(t)} = C_0 . e^{-k_1.t} \; ; 0 < t < t_s \quad (4a)$$

$$\hat{C}_{(t)} = C_{t_s} . e^{-k_2.(t-ts)} \; ; t > t_s \quad (4b)$$

Like model 2, this model estimates four parameters. C_0 is the initial concentration (µmol L^{-1}), k_1 and k_2 (d^{-1}) are the dissolution constants. The substitution time t_s (d) is the point at which the dissolution constant changes, and C_{t_s} is the concentration at the substitution time (µmol L^{-1}).

The fourth and last model considers that the first phase of $bSiO_2$ is not totally dissolved when the dissolution of the second phase begins (equation 5a and 5b):

$$\hat{C}_{(t)} = C_1 e^{-k_1.t} + C_2 \quad (5a)$$

$$\hat{C}_{(t)} = C_1.e^{-k_1.t} + C_2.e^{-k_2.(t-ts)} \quad (5b)$$

Model 4 estimates five parameters. Until the time t_s a single phase, with a concentration C_1 (µmol L^{-1}), dissolves with the dissolution constant k_1 (d^{-1}). After t_s this phase dissolves simultaneously with a second phase, which concentration is C_2 (µmol L^{-1}) and which dissolution constant is k_2 (d^{-1}).

2.4.4.2. Biogenic silica dissolution kinetics: statistics

To determine the model that best fit the data, statistical analyses were used to compare the quality of the fit and the robustness of the estimated parameters.

The goodness of the fit (Log(*L*) equation 6) considers the number of estimated parameters and the number of data available to constrain the model.

$$\log(L) = -\frac{N}{2} * \log\left(\left(\frac{\sum(\hat{C}_j - C_j)^2}{N}\right) + 1\right) \quad (6)$$

N is the number of data points, C_j is a measured concentration for data point j, and the $\hat{C}_j$ is the corresponding model prediction.

As it uses 2 more parameters than the first model, model 2 and 3 always give a better fit than model 1. Hence, to justify an increase of the model complexity, which is done in this experiment by increasing the number of parameters, model goodness of the fit ($\log(L)$) should be at least 2 units higher per added parameter (Hilborn 1997). For example, model 2 best fit the data than model 1 if the goodness of the fit with model 2 (Log(*L*M2)) is at least 4 points higher than Log(*L*M1).

The robustness of the estimated parameters is calculated using the Jackknife which gives the tendency of the sample correlation to over-estimate or under-estimate the true, unknown, correlation. The estimated bias is given under the form of a standard error (root mean square error, RMSE) (Davison 1997) and of a coefficient of variation (CV_{RMSE}) expressing the stability of the models (Elzein et al. 2011) by measuring the differences between experimental data and predicted values.

2.5. Results

2.5.1. Diatom culture conditions during limitation experiments

Two distinct concepts referred to nutrient limitation: stress and deficiency (Moore et al. 2013). The former is a physiological response to a nutrient shortage while the latter is defined as the stoichiometric lack of one element relative to another. All nutrients concentrations were monitored during the six days of the limitation experiments. Nutrient Si : N : P ratios in each batch were compared to Redfield (1934) and Brzezinski (1985) ratios (Figure IV-1). This diagram indicates that cells in the f/2 medium containing no dSi were Si-deficient, while cells in the f/2 medium containing no nitrate were mostly N-deficient. During the last day of the limitation experiment in N-deficient batch, the dSi concentration (3.0 ± 0.3 µmol L^{-1}) appears to be more deficient than NO_3^- (Figure IV-1). However, as this deficiency occurred on the ultimate day of experiment, it is likely that N-deficient cells were primarily affected by NO_3^- deficiency.

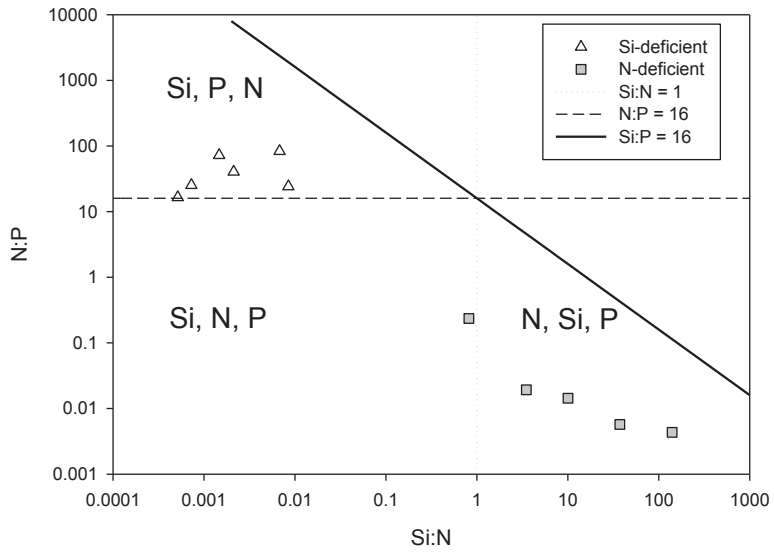

Figure IV-1 : Si:N:P ratios measured during the limitation experiment in the N-deficient and Si-deficient batches. The axes are expressed in common logarithm scale. Areas were delimited using Redfield (1934) and Brzezinski (1985) ratios, the potential limiting nutrients are reported in order of priority.

In the Si-deficient batch, dSi concentrations stayed close to zero from the beginning (0.3 ± 0.4 µmol L^{-1}) to the end of the limitation experiment (1.7 ± 1.8 µmol L^{-1}), and were lower than the half-saturation constants for dSi (Ks (Si) = 3.9 ± 5.0, n = 25, Sarthou et al. 2005). pH value in the Si-deficient batch was quite high after six days of limitation (pH = 9.3). Literature compiled by Hinga (2002) indicated that *T.pseudonana* can maintain a constant growth rate at pH ranging between 6.8

and 8.9. Consequently, it is likely that *T. weissflogii* cells in this batch were also carbon-limited. In Si-deficient batch, at the end of the limitation experiment, phosphate and nitrate concentrations (2.92 ± 1.25 µmol L^{-1} and 243.7 ± 6.2 µmol L^{-1}) were above Ks (P) and Ks (N) (0.24 ± 0.29 µmol L^{-1}, n = 14 and 1.6 ± 1.9 µmol L^{-1}, n = 35, respectively, Sarthou et al. 2005): therefore Si-deficient cells did not undergo P or N limitation. Concentration of living diatom in this batch gently declined over the limitation experience, from 599 742 ± 2737 cell mL^{-1} to 443 634 ± 11995 cell mL^{-1}. At the end of the experiment, $bSiO_2$ concentration was 11.7 ± 0.3 µmol L^{-1}. The QY of Si-deficient cells decreased the last day of the limitation experiment (0.21), which was the indication to stop the limitation experiment.

In the N-deficient batch, NO_3^- concentration stayed closed to zero during all the limitation experiment (0.1 ± 0.2 µmol L^{-1} at T_0 and 0.0 ± 0.02 µmol L^{-1} at T_6) and was lower than Ks (N). pH value reached 8.6 the last day of experiment, so it is unlikely that N-deficient cells underwent carbon limitation. The phosphate concentration in N-deficient batch measured the last day of experiment (11.9 ± 0.7 µmol L^{-1}) was above Ks (P) indicating that these cells were not P-limited. The second day of the limitation experiment, dSi concentration (2.9 µmol L^{-1} at T_2) was below Ks (Si). Consequently, N-deficient cells were also Si-limited. Concentration of living diatom in this batch gently declined over the limitation experiment, from 630855 ± 5915 cell mL^{-1} to 586090 ± 11959 cell mL^{-1}. $bSiO_2$ concentration at the end of the limitation experiment in N-deficient batch reached 15.6 ± 0.4 µmol L^{-1}. Like for Si-deficient cells, the QY of N-deficient cells decreased the last day of the limitation experiment (0.34).

Table IV-1 summarizes the elemental composition, dimensions, and the physiological status of control, Si-deficient and N-deficient cells, the last day of the limitation experiment and constitutes the initial conditions of the $bSiO_2$ dissolution experiments.

2.5.2. Dissolution experiment: general parameters

The oxygen values were low during the first day of the dissolution experiment in each batch (1 %, 26 % and 66 % for control, Si-deficient and N-deficient, respectively) but it increases sharply the second day (91 %, 59% and 56 % for control; Si-deficient and N-deficient respectively) and remained up to 80 % from the fourth day until the end of the experiments.

Table IV-1 : Elemental compositions, elemental ratios, cell dimensions, concentrations in extracellular polymeric substances and quantum yield of control, Si-deficient and N-deficient cells. The carbon and nitrogen quotas are normalized per cell volume and the biogenic silica quotas are normalized per cell surface. Results are presented as the means ± confidence interval (CI = 95%). The quantum yield (QY) gives an estimation of the efficiency of the photosynthesis at the Photosystem II.

	Control	Si-deficient	N-deficient
C (mol $Lcell^{-1}$)	5.9 ± 0.1 (n = 3)	13.5 ± 0.8 (n = 3)	11.4 ± 0.0 (n = 3)
N (mol $Lcell^{-1}$)	0.98 ± 0.09 (n = 3)	1.63 ± 0.14 (n = 3)	0.93 ± 0.02 (n = 3)
$bSiO_2$ (fmol μm^{-2})	10.3 ± 0.1 (n = 3)	6.0 ± 0.2 (n = 3)	6.0 ± 0.1 (n = 3)
C:N	6.1± 0.6 (n = 3)	8.2 ± 0.3 (n = 3)	6.9 ± 0.3 (n = 3)
Si:C	0.12 ± 0.003 (n = 3)	0.03 ± 0.002 (n =3)	0.04 ± 0.001 (n = 3)
Si:N	0.7 ± 0.07 (n = 3)	0.3 ± 0.03 (n = 3)	0.6 ± 0.02 (n = 3)
Cell volume (μm^3)	1488.4 ± 116.8 (n = 50)	1364.2 ± 149.7 (n = 50)	1140.0 ± 139.4 (n = 37)
Cell surface (μm^2)	100.4 ± 8.6 (n = 50)	94.5 ± 7.9 (n = 50)	87.9 ± 9.3 (n= 37)
TEP (Abs $mL^{-1)}$	0.38 ± 0.02 (n = 3)	0.58 ± 0.01 (n = 3)	0.62 ± 0.02 (n = 3)
EPSb HW (mg equiv. glucose L^{-1})	80.0 ± 10.4 (n = 3)	138.6 ± 21.2 (n = 3)	619.3 ± 90.3 (n = 3)
QY	0.58	0.21	0.34

2.5.3. Prokaryotic concentration during dissolution experiments

In the three batches the prokaryotic concentration strongly increased at the beginning of the experiment (Figure IV-2). The maximum increase occurred in the Si-deficient batch where it reached 348 10^6 cell mL^{-1} the 3rd day of experiment, i.e. 500-times higher than the initial concentration in the natural seawater collected. In the control batch the maximum prokaryotic concentration was also reached the third day (248 10^6 cell mL^{-1}) while it was reached the fourth day in the Si-deficient batch (187 10^6 cell mL^{-1}).

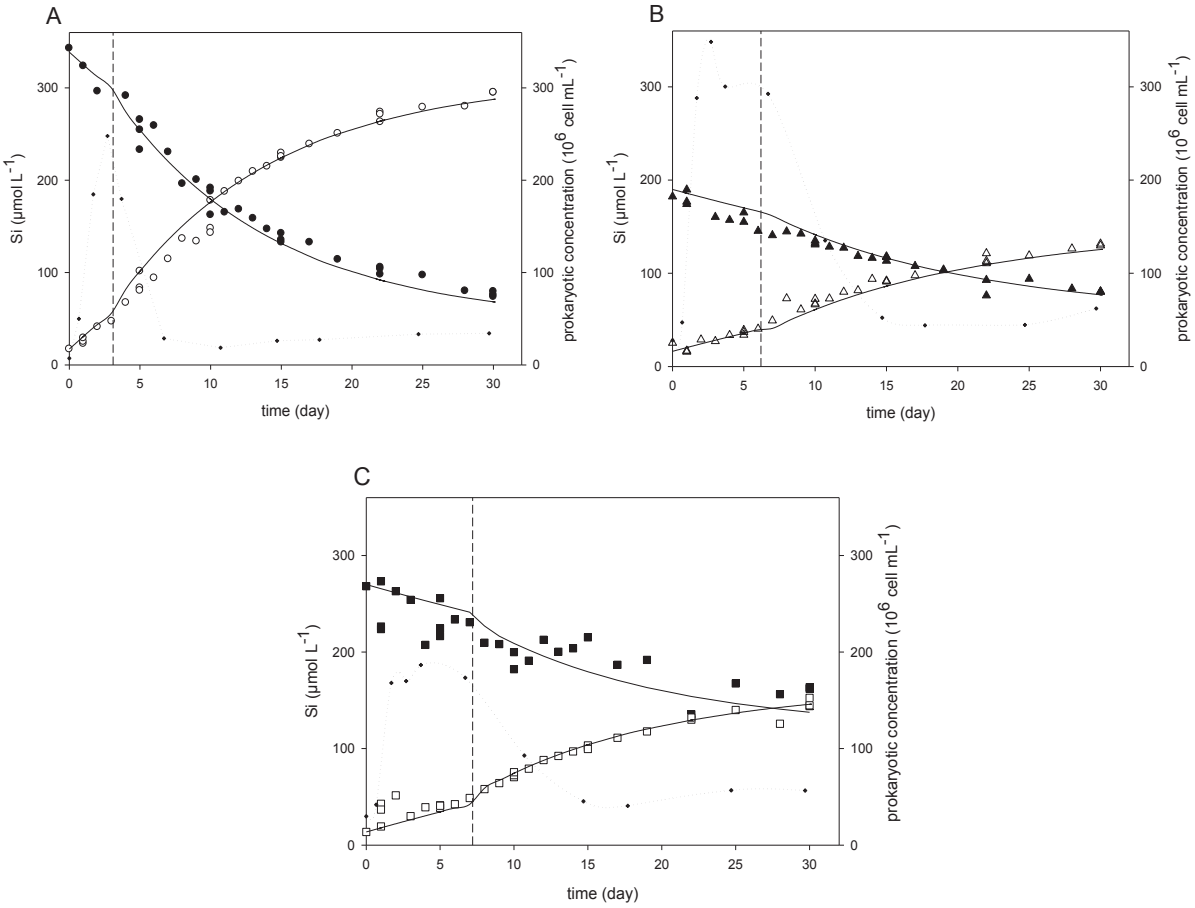

Figure IV-2 : Temporal evolution of $bSiO_2$ concentration in µmol L^{-1} (filled symbols), dSi concentration in µmol L^{-1} (open symbols) and prokaryotic concentration in 10^6 cell mL^{-1} (cross and dotted curves) in the batch containing control cells (A) Si-deficient cells (B) and N-deficient cells (C). Symbols represent the data obtained during the experiment. Solid curves were obtained by modeling the variation of Si with model 1 from T_0 to the transition time T_S and with model 2 after T_s. The transition time in each experiment is represented by a vertical dash line. For the control experiment both dSi and $bSiO_2$ dataset were modeled while only dSi dataset was modeled in Si-deficient and N-deficient experiments.

In the control batch, from the third day of experiment the prokaryotic concentration decreased sharply to attain 29 10^6 cell mL^{-1} the seventh day of experiment and then remained relatively steady until the end of the experiment (34 10^6 cell mL^{-1} at T_{30}). The decreased in prokaryotic concentration in deficient-batches lasted longer to reach after fifteen days 52 10^6 cell mL^{-1} for the Si-deficient batch and 45 10^6 cell mL^{-1} for the N-deficient batch. Then, like for the control batch, the prokaryotic concentration remained almost constant in batches containing deficient-cells until the end of the experiment (62 10^6 cell mL^{-1} in Si-deficient batch and 57 10^6 cell mL^{-1} in the N-deficient batch). These high concentrations can be explained by the high diatom concentrations in the batches, an experimental choice made in this study to be able to follow numerous parameters. However, even higher bacterial concentrations can be encountered in natural environments as in diatom detritus,

where diatoms are concentrated and where bacteria concentrations could reach value up to 10^{11} cell mL^{-1} (Ragueneau et al. 2006, and references therein).

2.5.4. $bSiO_2$ and dSi concentrations during dissolution experiments

When diatoms have been re-suspended and homogenized at the beginning of the dissolution experiment, the dSi concentrations were 17.2 µmol L^{-1}, 25.3 µmol L^{-1} and 13.6 µmol L^{-1} in control, Si-deficient and N-deficient batches, respectively. During the dissolution experiment, dSi concentrations remained far from $bSiO_2$ solubility (~ 1000 µmol L^{-1} at 16 °C, Dixit et al. 2001), with a maximum of 295.0 ± 0.04 µmol L^{-1} for control, 130.7 ± 1.4 µmol L^{-1} for Si-deficient and 148.7 ± 5.5 µmol L^{-1} for N-deficient.

Initial $bSiO_2$ concentration was higher in control batch (342.9 µmol L-1) than in N-deficient and Si-deficient batches (268.2 µmol L^{-1} and 182.3 µmol L^{-1}, respectively). $bSiO_2$ concentrations progressively decreased overtime (Figure IV-2). At the end of the dissolution experiment, 20 % of the initial $bSiO_2$ concentration remained in the control batch (76.4 ± 2.9 µmol L^{-1} at T_{30}) while higher percentage of the deficient-diatoms $bSiO_2$ remained: 44 % in the Si-deficient batch (80.3 ± 0.2 µmol L^{-1} at T_{30}) and 60 % in N-deficient batch (156.5 ± 10.8 µmol L^{-1} at T_{30}).

2.5.5. $bSiO_2$ dissolution kinetics

$bSiO_2$ dissolution rate depends on the initial $bSiO_2$ concentrations. The dissolution constants were calculated in this study from concentrations normalized to the initial concentration, and were consequently not influenced by the differences in the initial $bSiO_2$ concentrations between the three batches. For each dissolution experiment, the four models described in the Materials and methods Section were tested to reconstruct dSi and $bSiO_2$ concentrations over time. Comparison of the estimated dSi and $bSiO_2$ values to the two dataset measured independently during the dissolution experiment allows to estimate the goodness of the fit. From the latter and from the Jackknife we chose which dissolution model best describe the dissolution pattern. While particles heterogenic distribution does not affect dSi measurements it could strongly affect $bSiO_2$ sampling. Triplicate $bSiO_2$ measurements in control batch pointed out a weak standard error on the determination of the $bSiO_2$ concentration. Consequently, both $bSiO_2$ and dSi temporal evolutions in control batch were fitted using the four models. However, in both Si-deficient and N-deficient batches, $bSiO_2$ measurements exhibited a quite strong heterogeneity. As the determination of the model that best fit the data could be bias by a poor $bSiO_2$ sampling, only the dSi increase in those batches were modeled.

In the three dissolution experiment Log(*L*M4) was more than 6 points higher than Log(*L*M1) and more than 2 points higher than Log(*L*M2) and Log(*L*M3) (Table IV-2). At first sight, model 4 best

represent the dissolution pattern of *T. weissflogii.* Model 4 calculated a transition time, Ts, which corresponded to strong changes in the prokaryotic concentrations in the three batches (Figure IV-2 and Table IV-3). It is likely that this apparent best modeling with Model 4 represented a modification in the intensity of the dissolution due to modification in the prokaryotic concentrations, rather than the chemical dissolution kinetics of $bSiO_2$. Model 1 was run from T_0 to the transition time Ts obtained with model 4, to obtain the dissolution constant k_0 for the period of slow dissolution at the beginning of each experiment (Table IV-3). The four mechanistic models were once again run from Ts to the end of the experiment, to assess the chemical dissolution kinetics of $bSiO_2$. After Ts, the dissolution of $bSiO_2$ from deficient-cells was best described by Model 2 (Table IV-2). Both Model 2 and 3 could describe the dissolution pattern of control cells (Table IV-2), but to compare control to deficient-cells, Model 2 was chosen.

Table IV-2: Likelihood (Log(*L*)) calculated by the 4 models for $bSiO_2$ dissolution in control, Si-deficient and N-deficient batch, first from data collected during the entire duration of the experiment (from T_0 to T_{30}) and secondly from T_s estimated by Model 4 (3.1 ± 0.2, 6.2 ± 0.2 and 7.2 ± 0.1 days for control, Si-deficient and N-deficient, respectively) until the end of the dissolution experiment (from T_s to T_{30}).

	From T_0 to T_{30}				From T_s (M4) to T_{30}			
	Log (L_{M1})	Log (L_{M2})	Log (L_{M3})	Log (L_{M4})	Log (L_{M1})	Log (L_{M2})	Log (L_{M3})	Log (L_{M4})
Control	182.6	185.7	188.4	191.2	158.3	168.1	168.4	168.6
Si-deficient	103.4	104.7	108.2	114.8	71.5	81.9	81.4	81.9
N-deficient	102.5	105.0	109.9	119.9	67.7	76.6	75.8	76.7

Independently of growth conditions, the frustule dissolution of *Thalassiosira weissflogii* followed the same global pattern: (i) a period during which $bSiO_2$ dissolved slowly, and (ii) a two-phase dissolution. Depending on growth conditions, differences existed in the proportion of the $bSiO_2$ phases and their dissolution constants. During the period of slow dissolution, at the beginning of the experiment, the dissolution constant k_0 was higher in control batch than in deficient batches. This period lasted twice as long in deficient-batch as in control batch (Figure IV-2 and Table IV-3). After Ts, the dissolution constant of the fast dissolving phase was quite similar in the three experiments (between 0.081 ± 0.003 d^{-1} and 0.091 ± 0.002 d^{-1}, Table IV-3), but the part of this phase on the whole frustule vary greatly. Indeed, this phase dominated the composition of control cells (86 % of the $bSiO_2$), while it represented slightly less than half of the $bSiO_2$ from deficient cells (65 % and 59 % for Si-deficient and N-deficient cells, respectively). The slow dissolving phase represented 14%, 35% and 41% of the whole replete cells, Si-deficient cells and N-deficient cells, respectively. This phase was dissolving faster for Si-deficient cells (0.0079 ± 0.0008 d^{-1}) than for control cells (0.0031 ± 0.0019 d^{-1}) and N-deficient cells (0.0022 ± 0.0018 d^{-1}) (Table IV-3).

Table IV-3: Dissolution constants obtained using the model 1 from the beginning of each experiment to the transition time T_S, expressed in day, followed by constants obtained by Model 2 from Ts to the end of the experiment. The transition time Ts corresponds to a modification in the intensity of the dissolution due to modification in the prokaryotic concentrations, highlight by Model 4. Phase 1 and Phase 2 represent the two phases of $bSiO_2$, expressed in percentage of $bSiO_2$, dissolving at the dissolution constant k_1 and k_2 from T_s to the end of the experiment, respectively. Dissolution constants are expressed per day ± the root mean square deviation RMSD. The CV_{RMSE} are the coefficient of variation of the previous parameter, calculated from the Jackknife. Both $bSiO_2$ and dSi data were fit for the dissolution of the control cells. For the dissolution of Si-deficient cells and N-deficient cells, only the increase in dSi concentration was fitted.

	Model 1				Model 2					
	k_0	CV_{RMSE}	T_s	CV_{RMSE}	Phase 1	Phase 2	k_1	CV_{RMSE}	k_2	CV_{RMSE}
Control	0.041±0.005	0.11	3.1±0.2	0.06	86 %	14 %	0.091 ± 0.002	0.02	0.0031 ± 0.0019	0.6
Si-deficient	0.022±0.002	0.08	6.2±0.2	0.04	65 %	35 %	0.081±0.003	0.03	0.0079±0.0008	0.1
N-deficient	0.016±0.001	0.08	7.2±0.1	0.02	59 %	41 %	0.086±0.009	0.1	0.0022±0.0018	0.8

2.5.6. FTIR analysis

Some bands overlap on FTIR spectra between 1300 cm^{-1} and 700 cm^{-1} and we used spectrum decomposition to assign the bands in this wavenumber region. Decomposition was done in triplicate on each spectrum to ensure that it was reproducible and reliable.

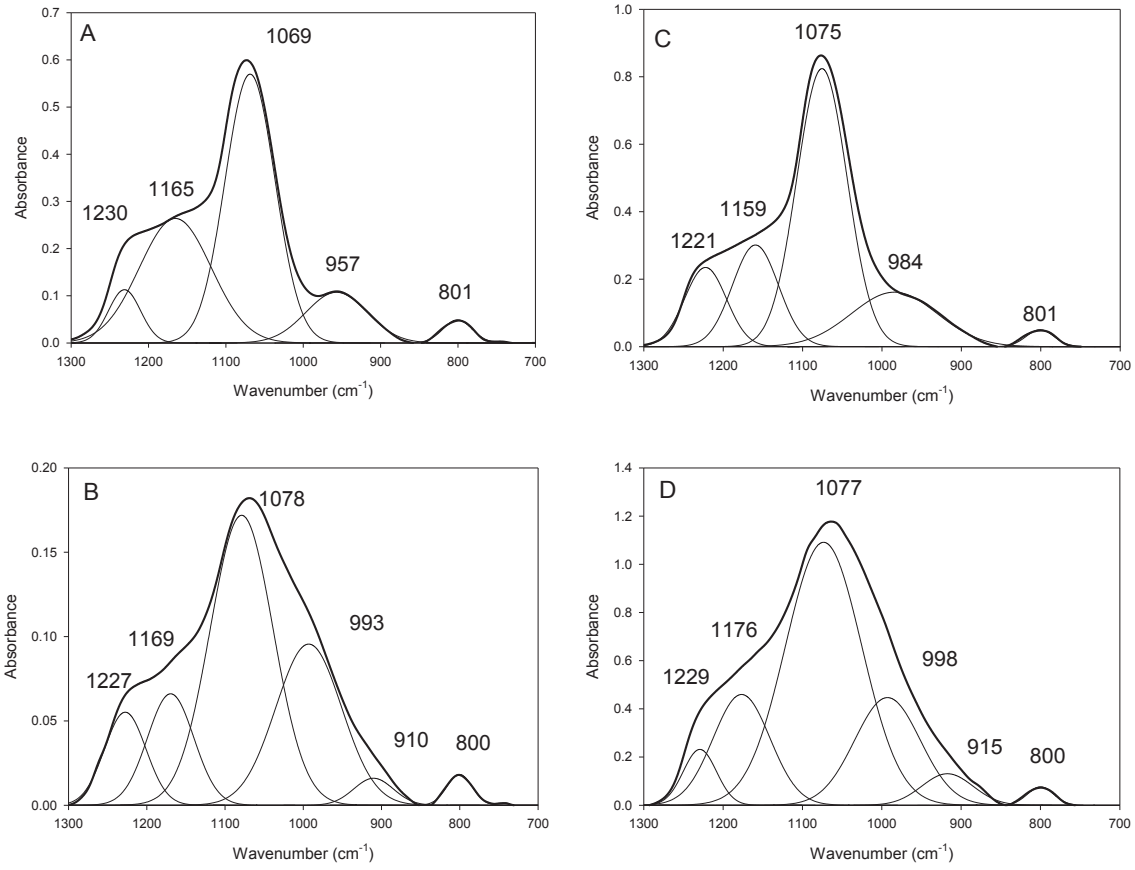

Figure IV-3 : Decomposition of Fourier Transform InfraRed (FTIR) spectra between 1300 and 700 cm^{-1} for control cells at T_0 (A) and T_{22} (B) and for control cells exposed to low temperature ashing harvested at T_0 (C) and T_{25} (D). Large curves represent the FTIR spectra obtained using FTIR analysis. Fine curves represent the decomposition obtained using OriginPro 9 Software, with the wavenumber associated to the maximum absorbance.

The FTIR spectra from control cells from T_0 to T_9, were decomposed, and peaks obtained in the silica vibration region at 1069, 957 and 801 cm^{-1} (Figure IV-3A) were attributed to Si-O stretching from SiO_4, Si-O stretching and Si-O-Si bending, respectively (Table IV-4).

Table IV-4: Band assignment for FTIR spectroscopy used in this study.

Functional Groups	Region (cm^{-1})	Comments	Reference
Si-O	~1075	Si-O stretching of SiO_4	Gendron Badou et al. 2003
Si-OC	990-945	symmetric Si-OC stretching	Socrates 2001
Si-OH	955-830	Si-O stretching from Si-OH	Socrates 2001
Si-O	800	bending Si-O-Si	Gendron Badou et al. 2003
$Si-CH_3$	~765	Si-C stretching	Socrates 2001

To validate decomposition and attribution of silica peak, the spectra of control cells harvested at T_0 and exposed to low temperature ashing, LTA (see Materials and Methods Section), was also collected and decomposed (Figure IV-3C). The decomposition for control cleaned frustules at T_0 was similar to those from control whole cells (Figure IV-3A), except that the peak at 957 cm^{-1} switches to 984 cm^{-1}. The peak at 984 cm^{-1} is in the range of vibration attributed to symmetric Si-OC stretching (Table IV-4) and could represent a fraction of C which was not ionized by LTA. From T_{15} to T_{30}, the spectra decomposition showed the peak positioned around 990 cm^{-1} also observed in the decomposition of cleaned frustule from T_0 sample and another peak at 910 cm^{-1} attributed to Si-O stretching from Si-OH (Figure IV-3B). FTIR analyses done on cleaned frustules at T_{25} validate this decomposition (Figure IV-3D). The band obtained around 950 cm^{-1} in the spectra of control whole cell at T_0 may be the result of the superposition of two bands: Si-O stretching from Si-OH (910 cm^{-1}) and asymmetric Si-O stretching from Si-OC (~ 990 cm^{-1}). This interpretation is suggested by the switch of the peak from 957 cm^{-1} to 984 cm^{-1} in the cleaned frustule at T_0 and the presence of two peaks, one around 990 cm^{-1} and one around 910 cm^{-1} in the spectra decomposition of the partially dissolved frustule.

Decompositions of both Si-deficient and N-deficient cells spectra (Figure IV-4) lead to the same peak attribution than the one used for the control cells during the second part of the experiment.

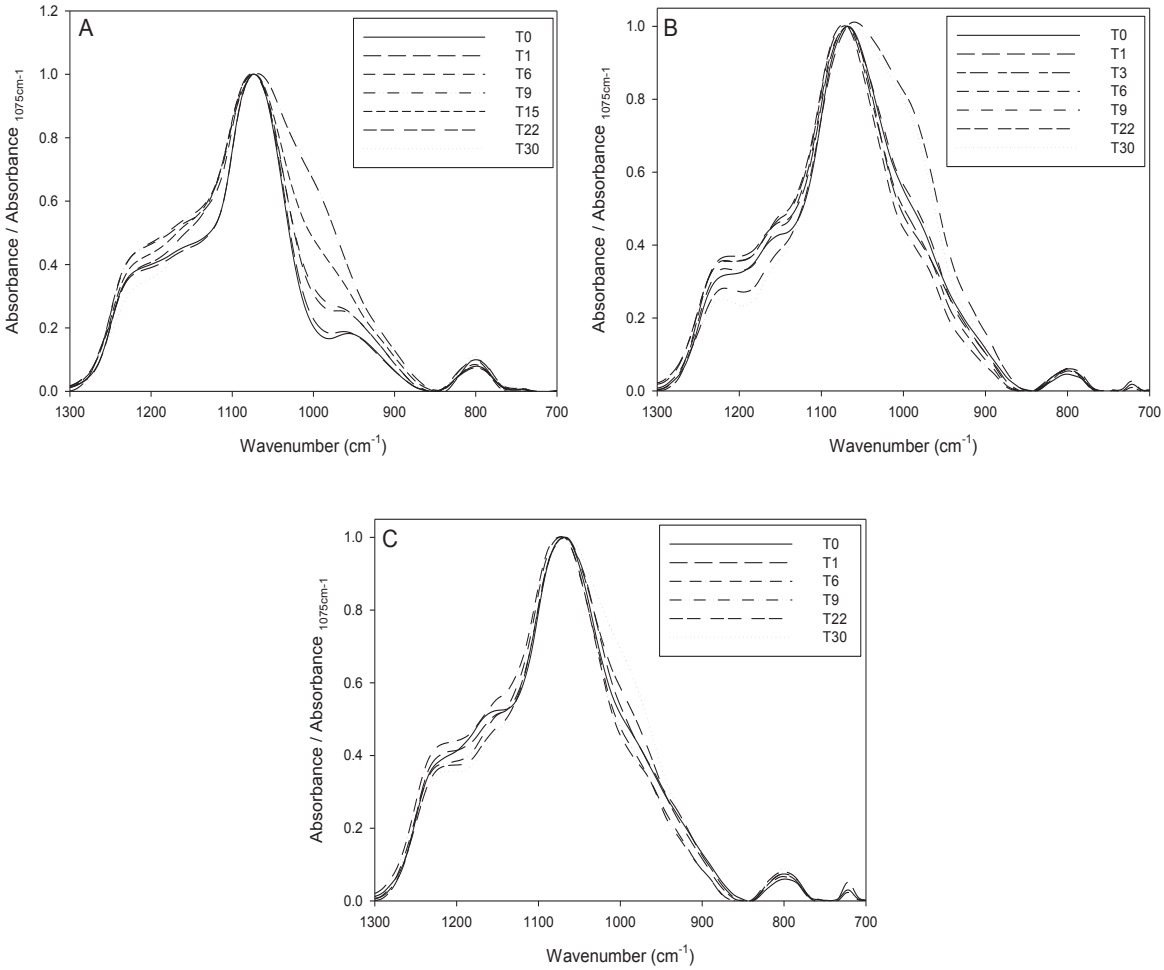

Figure IV-4: Evolution of the FTIR spectra in the region of 1300-700 cm^{-1} for control cells (A), Si-deficient cells (B), N-deficient cells (C) throughout cells dissolution. Spectra were normalized to the maximum absorbance attained at 1075 cm^{-1}.

The reactivity of the biogenic silica can be estimated from FTIR spectra using a reactivity degree calculated as the ratio of the relative area of the peak assigned to Si-O stretching from Si-OH to the one attributed to Si-O stretching from SiO_4 (1075 cm^{-1}, Figure IV-5A) (Schmidt et al. 2001). To represent Si-OH function (silanol) in control cells spectra from T_0 to T_9 we used the peak at 955 cm^{-1} despite the fact that this peak must result of both Si-OH and Si-OC. Consequently the estimated reactivity degree is overestimated for control cell between T_0 and T_9. After T_9 and for deficient cells the peak at 910 cm^{-1} was used. The reactivity degree sharply increased in control cells from T_0 to T_1 (5.2 ± 0.2), remained high to T_9 (5.8 ± 0.3) before decreasing by an order of magnitude from T_9 to T_{15} (0.6 ± 0.1) and increased slightly until the end of the experiment (1.04 ± 0.17)(Figure IV-5A). The reactivity degree decreased from T_0 (1.8

± 0.1) to T_6 (0.7 ± 0.1) for Si-deficient cell frustules and increased to T_{22} (2.7 ± 0.1) to finally decrease slightly at T_{30} (2.2 ± 0.1). Reactivity degree of N-deficient cells also decreased from T_0 (1.6 ± 0.1) to T_6 (0.6 ± 0.1) and then increased to T_{30} (1.1 ± 0.03). The reactivity degree during the first day of experiment was 1.8-fold higher in control cells (3.0 ± 0.1) than in deficient cells (1.8 ± 0.1 and 1.6 ± 0.1 for Si-deficient and N-deficient cells, respectively). And at the end the reactivity degree was higher for Si-deficient cell compared to N-deficient and control cells (2.2 ± 0.1, 1.1 ± 0.03 and 1.04 ± 0.17 for Si-deficient, N-deficient and control cells, respectively).

The second ratio is the parameter Ω, as defined by Gendron Badou et al. (2003), which represents the degree of organization of the silica network. Ω is the ratio between the estimated areas of the peak assigned to Si-O-Si binding (800 cm^{-1}) and the peak attributed to Si-O stretching from SiO_4 (1075 cm^{-1})(Figure IV-5B). This ratio was nearly constant throughout the cells dissolution in each experiment (0.050 ± 0.008, n = 7, for control cells; 0.034 ± 0.004, n = 6, for N-deficient cells; 0.025 ± 0.002, n = 7 for Si-deficient cells). Values obtained were in the range of those found by Loucaides et al. (2010) for organic matter cleaned samples of diatom culture and sediments or synthetic amorphous silica (0.03 - 0.05). Ω was higher for controls cells than for N-deficient cells, which was itself higher than for Si-deficient cells.

The third ratio was defined in the present study to assess the relative importance of C atoms associated to the silica lattice. This ratio was calculated using the estimated area of the symmetric Si-OC stretching peak (995 cm^{-1}) over the peak attributed to Si-O-Si bending (800 cm^{-1}) (Figure IV-5C). As previously mention the Si-OC attributed peak was likely present within spectra of control cells at T_0, T_1, T_6 and T_9, but at a non-measurable area. This ratio was measured from T_{15} in control batch (12.2 ± 0.7). It increased until T_{22} and then remained constant until T_{30} (15.5 ± 1.6 and 15.2 ± 1.7 respectively). In Si-deficient batch, this ratio decreased from T_0 (25.2 ± 0.7) to T_1 (11.1 ± 0.7), remained nearly constant until T_6 (10.5 ± 1.0), increased by almost 3-fold from T_6 to T_{22} (27.2 ± 0.10) and remained constant until T_{30} (27.0 ± 0.1). In N-deficient batch, this ratio decreased from T_0 (15.3 ± 0.8) to T_6 (7.2 ± 1.5), then increased until T_{22} (16.8 ± 1.4) and remained constant until the end of the experiment (16.8 ± 0.2 at T_{30}). The first day of the dissolution experiment, this ratio was higher in Si-deficient batch than in N-deficient batch. At the end of the experiment this ratio was also higher for Si-deficient cells than for N-deficient and control cells, which were similar.

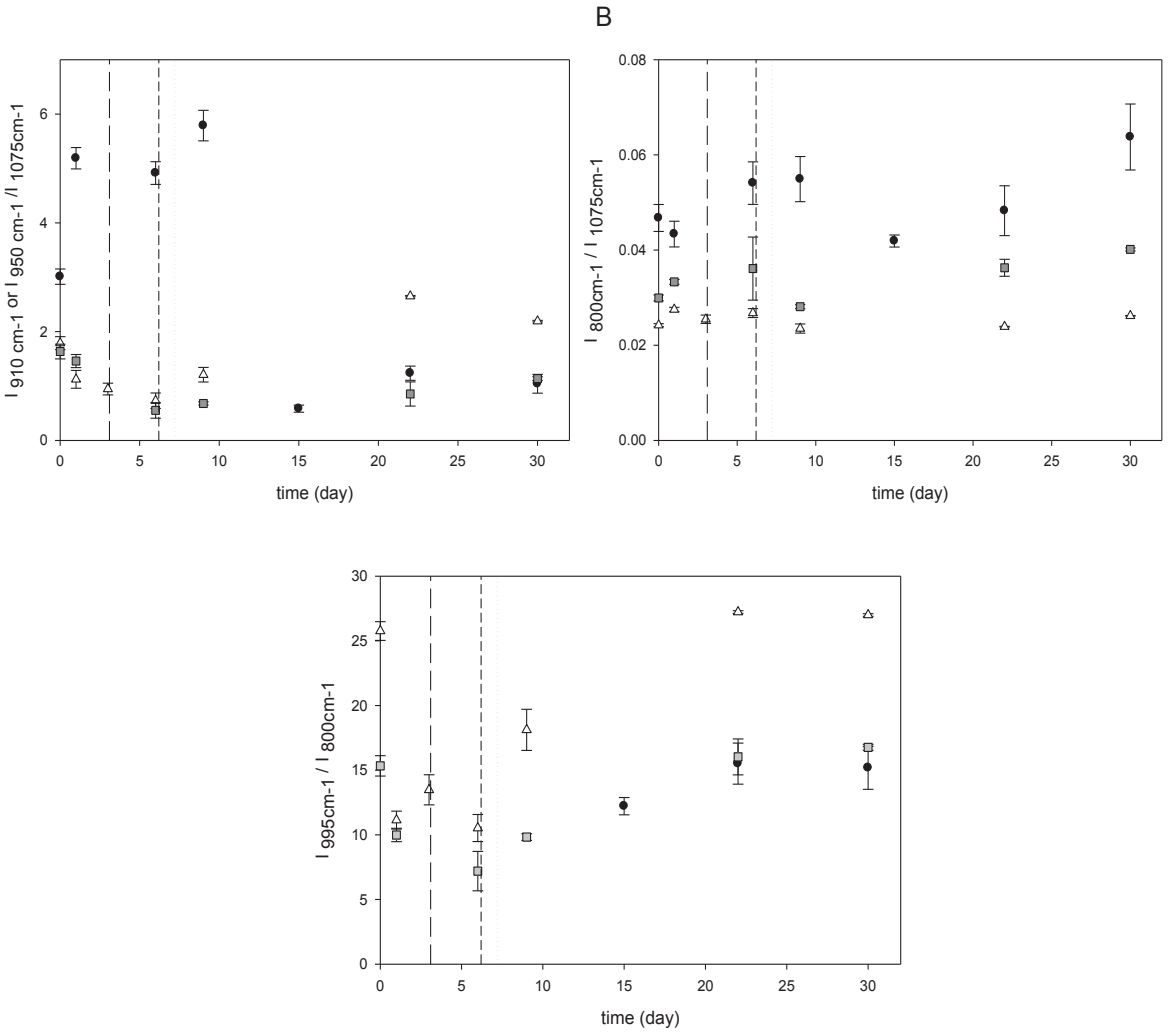

Figure IV-5: Temporal evolution of the estimated ratios $I_{910\ cm\text{-}1}$ or $I_{950cm\text{-}1}$ / $I_{800cm\text{-}1}$ (A), $I_{800cm\text{-}1}$ / $I_{1075cm\text{-}1}$ (B) and $I_{995cm\text{-}1}$ / $I_{800cm\text{-}1}$ (C). The first ratio was estimated from the peak found at 955 cm^{-1} for control cells at T_0, T_1, T_3, T_9, and 910 cm^{-1} for all the other spectra. The evolution is presented for control cells (black dot), Si-deficient cells (open triangle) and N-deficient cells (grey square). The values represent the average ratio obtained after multiple decomposition of each spectra between 1300 cm^{-1} and 700 cm^{-1} (n = 3). Standard errors represent the variability of the estimated ratio using decomposition. Vertical lines represent the transition time obtained using model 4 in control batch (long dash), Si-deficient batch (short dash) and N-deficient batch (dotted).

2.6. Discussion :

2.6.1. $bSiO_2$ dissolution

The dissolution of the biogenic silica, which consists of chemical depolymerisation of SiO_4, occurred when the silica is in contact with the seawater, which is under saturated relative to silicic acid. In 1961, Lewin suggested the existence of an organic protective coating surrounding the frustule whose presence has been hypothesized to retard the dissolution (Lewin 1961; Kamatani 1971; Kamatani and Riley 1979). This hypothesis was confirmed later, with clear evidence that the removing of this organic coating by bacteria is a limiting factor of $bSiO_2$ dissolution (Patrick and Holding 1985; Bidle and Azam 1999). Cells in good metabolic health are able to maintain their organic coating, and dissolution rates of living diatom are closed to zero (Nelson et al. 1976): thus the viability of diatom cells will affect their depolymerization. In the present experiment, diatoms were killed by freezing. Nevertheless, the dissolution pattern of $bSiO_2$ showed a period during which dissolution was reduced, corresponding in all experiments to the length of the prokaryotic peak (Figure IV-2). This period lasted between 3.1 ± 0.2 days and 7.2 ± 0.1 days (Table IV-3).

Induction of cell wall proteins has been evidenced for *T. pseudonana* under nutrient limitation and in particular under silicon limitation (Kröger and Poulsen 2008, and references therein) while it was not observed for nitrate limitation. Both Si-deficient and N-deficient cells underwent Si limitation, and they may have produced these proteins.

Regarding the organic exudates, as TEP and EPSb HW concentrations, they were higher in nutrient deficient batch than in control batch before collecting and freezing diatoms (Table IV-1). Indeed, these molecules are secreted by cells when subjected to nutrient limitation (Thornton 2002). TEP (Moriceau et al. 2007) and EPS (Welch and Vandevivere 1994) have been showed to affect $bSiO_2$ dissolution. Consequently, another explanation to the more efficient protection of frustules from deficient-cells than control cells (as seen by the lower k_0 of deficient cells than control cells) and the longer duration of the period of slow dissolution for deficient cells (as seen by the higher Ts in deficient batches compare to control batch) could be the higher concentration of weakly degradable organic exudates in deficient batches. We suggest that the low dissolution of the $bSiO_2$ at the beginning of the experiment was due to both the organic coating and the presence of other organic components excreted by cells before their death.

Once the organic matter protection has been removed by bacteria, $bSiO_2$ started to dissolve more efficiently, since the silica lattice was exposed to the external environment. Most of the early study focusing on $bSiO_2$ dissolution used a simple mathematical equation to model the dissolution, i.e. a simple exponential (equation 1). However, as mention by Truesdale et al. (2005), this approach is not necessarily valid as it is based on the assumption that all the molecules of the solid are available for dissolution at any time, which is the case in homogeneous solution but not in heterogeneous system where molecules can be left on the thickness of a solid. Therefore a large majority of batch dissolution experiment is best modeled by a sum of exponential (Truesdale et al. 2005). Indeed, in the present study, the dissolution kinetics was best reconstructed considering two phase of $bSiO_2$ which represented different proportions of the whole frustule, and which had their own dissolution constant.

2.6.2. Toward a better characterization of the $bSiO_2$ phases

Using FTIR spectroscopy during dissolution, we followed frustules organization and reactivity, as well as the relative abundance of carbon associated with the frustule, to try to identify different structures which could illustrate that frustules are composed of these two different $bSiO_2$ phases. FTIR allows calculating a Ω ratio between the integrated band at 800 cm^{-1} (Si-O-Si) and the band at 1075 cm^{-1} (Si-O of SiO_4), and which can be used as an indicator of the degree of organization of the silica lattice. In each of the three experiments, this ratio was nearly constant throughout cells dissolution (Figure IV-5B), while the most soluble phase progressively became minority, and the least soluble phase became majority. Applied to the water column, it means that the degree of organization of the frustule changes a little or does not change when settling from the surface to the bottom of the ocean. This is in accordance with Loucaides et al. (2010) results, who obtained the same range of Ω values for organic matter cleaned cultured *Thalassiosira punctigera* diatoms, whether for fresh frustule (Ω = 0.03) or artificially aged frustule (Ω = 0.04), as well as for biosiliceous lake sediment sediments (Ω = 0.03). As changes in the dominance of the two $bSiO_2$ phases are not accompanied by changes in the degree of organization of the silica lattice, the two $bSiO_2$ phases cannot be attributed to two types of crystalline organization.

The reactivity of diatom frustule was estimated using the ratio between the integrated peak attributed to Si-OH stretching (915 – 955 cm^{-1}) and the one attributed to Si-O stretching of SiO_4 (1075 cm^{-1}) (Schmidt et al. 2001) (Figure IV-5A). The estimated reactivity degree of control cells was high until T_9 (Figure IV-5). As mention in the Results section, this ratio may have been over-estimated as the integrated peak at 955 cm^{-1} may be a superposition of the Si-OC stretching vibration peak (990-945 cm^{-1}) and Si-OH stretching vibration peak (955-830 cm^{-1}) (Table IV-4). Considering only control experiment, the

higher reactivity that represents a higher amount of silanol groups (Si-OH) seems to be explained by the predominance of the fast dissolving phase at the beginning of the dissolution. However, when looking at the reactivity pattern of the two other dissolution experiments (Si- and N-deficient cells), the predominance of the fast dissolving phase is not concomitant to a highest reactivity. This suggests that the reactivity degree (i.e. the relative amount of silanol groups within the silica lattice) measured using FTIR, is not that representative of the surface reactivity, which drives $bSiO_2$ dissolution. This is confirmed by the strong increase of the reactivity degree observed at the end of the control dissolution while it has been shown that surface silanol groups decreased with aging (Van Cappellen 1996; Dixit and Van Cappellen 2002).

As mention above, the diatom frustule is not only constituted by a mineral network. Some organic matter pools are involved in the morphogenesis of the silica nanopatterns and got closely associated to the silica lattice (Abramson et al. 2009). The organic components associated with $bSiO_2$ are diverse, as determined by many studies (polysaccharides, Kröger and Poulsen 2008, and references therein, Tesson and Hildebrand 2013; proteins, Kröger and Poulsen 2008, and references therein, Sumper and Brunner 2008; and lipids, Kates and Volcani 1968, Suroy et al. in revision). In *Thalassiosira weissflogii*, the existence of a peak at 980 cm^{-1}, assigned to Si-OC stretching, only identifiable during the second part of the dissolution of control cells and throughout all the dissolution of deficient cells, could be attributable to the existence of these pools of organic matter associated to the silica lattice. In the three batches, throughout the two $bSiO_2$ phases dissolution, this ratio increased to reach a plateau after twenty-two days of experiment (Figure IV-5C). The increase of this ratio in each batch, when the slow-dissolving phase became predominant, suggested that these organic matter pools are preferentially associated to this silica phase. This conclusion is also emphasized by another study on the same species that showed that most fatty acid associated with the frustule of *T. weissflogii* are in fact associated with the slowly dissolving phase (Suroy et al. in revision).

2.6.3. Effect of nutrient availability during growth on frustule dissolution

We have seen that the overall dissolution patterns were similar in the three dissolution experiments underwent on *Thalassiosira weissflogii* cells, i.e. a period of slow dissolution due to the protection by organic matter (organic coating, organic exudates) and then the dissolution of two $bSiO_2$ phases. However, the comparison of the three experiments highlights that nutrient deficiency affects $bSiO_2$ dissolution.

Firstly, the frustule of deficient cells seems to be longer and more efficiently protected from dissolution than replete cells, maybe because of a more pronounced excretion of organic exudates and to a more protective action of these organic matter pools. Secondly, nutritional environment changes both dissolution constants and proportions of the $bSiO_2$ phases. As seen above, while the fast dissolving phase is majority in the control frustule, the slow dissolving phase constituted about half of the frustule in deficient-cells. The dissolution constants k_1 were almost the same in the three dissolution experiments. The low dissolution constants k_2 was higher for Si-deficient cells than for control and N-deficient cells (Table IV-3). Changes in the frustule chemical or physical structure due to the environmental conditions may explain the variability obtained in the dissolution constants of *T. weissflogii*. When comparing FTIR ratios measured at the end of the three dissolution experiments, which give indications on the intrinsic properties of the slow dissolving phase, the strongest reactivity degree was measured for Si-deficient cells. These cells also exhibit the lowest organization degree and the highest proportion of Si-OC bonds. This observation suggests that Si deficiency, by increasing the relative amount of silanol groups and of Si-OC bonds, tend to disorganize the silica lattice, which would enhanced the dissolution rate of the slow dissolving phase of *T. weissflogii*.

These differences in proportions and dissolution constants of the $bSiO_2$ phases induced a greater susceptibility to dissolution of the frustules from non-limited cells compared with those of limited cells. In one month, almost 80 % of the total $bSiO_2$ produced by *T. weissflogii* when growing in optimal nutritional conditions was dissolved. In contrast, when exposed to Si and N deficiencies, only slightly more than half of the initial $bSiO_2$ was dissolved after one month. As a mean of comparison, Van Cappellen et al. (2002) estimated that the residence time of detritus in the surface waters to be on the order of weeks.

2.6.4. Relevance for the oceanic silicon cycle

Van Cappellen et al. (2002) pointed out a strong difference between the predicted specific dissolution rates for world average surface ocean, estimated at 84 yr^{-1}, and the world average observed values, 16 yr^{-1}, calculated from observed values on the upper 150 m of the ocean. They suggest that this 5-fold difference may be explained by the inhibitory effect of organic coating. The dissolution constant obtained here during the first slow dissolution period, i.e. when cells were probably protected from dissolution by the organic coating as well as organic exudates, ranged between 5.8 yr^{-1} for N-deficient cells and 15.0 yr^{-1} for replete cells (Table IV-3), which in is the range of order of the world average observed value and support the assumption of Van Cappellen et al. (2002).

Then, when the silica lattice comes into contact with the seawater, the dissolution of two $bSiO_2$ phases occurs. Taking into account the existence of the two $bSiO_2$ phases, which constitute the whole frustule and which have dissimilar dissolution constants, is important when one would represent the Si cycle within the water column. The use of only the dissolution rate constant k_1 or the dissolution rate constant k_2 to model the decrease in $bSiO_2$ concentrations through the water column will lead to over-estimation or under-estimation of the dissolution. This could therefore result in bad estimation of the amount of $bSiO_2$ recycled in the upper ocean or exported to the seafloor. Considering the two $bSiO_2$ phases of control cells and their respective proportions and dissolution constants, 20 % of the initial $bSiO_2$ concentration remained at the end of the dissolution experiment. The use of only the higher dissolution constant k_1, generally measured on short dissolution experiment, leads to estimate that 7 % of the initial $bSiO_2$ concentration of control cells remained at the end of the experiment. Reversely the use of only the lower dissolution constant k_2 leads to estimate that almost 90 % of the initial $bSiO_2$ concentration remained. Usually, in ocean biochemical models, only a single dissolution constant is used to parameterize the dissolution of silica within the water column, with values ranging between 0.01 and 0.25 d^{-1} (Pondaven et al. 1998; Gnanadesikan 1999; Mongin et al. 2006). These values are higher but in the same range of variations than the highest dissolution constant k_1 obtained in the present study, and are order of magnitudes higher than the lower dissolution constant k_2. When estimating the residence time of the fast dissolving phase, which is in the order of 10 days, the fast dissolving phase never leaves the euphotic zone. When considering that the slow dissolving phase may represent up to 40 % of the whole frustule (Table IV-3), and has a residence time in the order of months, the slow dissolving phase constitutes most of the $bSiO_2$ stock below the euphotic zone. The present study suggests that a better parameterization of the biogenic silica dissolution in global model could be done using one fast dissolution constant in the surface layer and one slow dissolution constant in the rest of the water column. The fast dissolution constant may consider the protection by organic pools, which can still be efficient on dead diatoms.

Moreover, nutrient deficiencies affect frustule dissolution and preservation. Using dissolution constants obtained by modeling, we had estimated the preservation capacity, i.e. the percentage of $bSiO_2$ remaining after one month of dissolution in each batch. The preservation capacity of control cells is 20 %, while it was 41 % for Si-deficient cells and 51 % for N-deficient cells. Therefore, deficient-cells are far more preserved from dissolution that replete cells. The preservation is even better after N-deficiency than after Si-deficiency.

Chapitre V.

Conclusions et perspectives

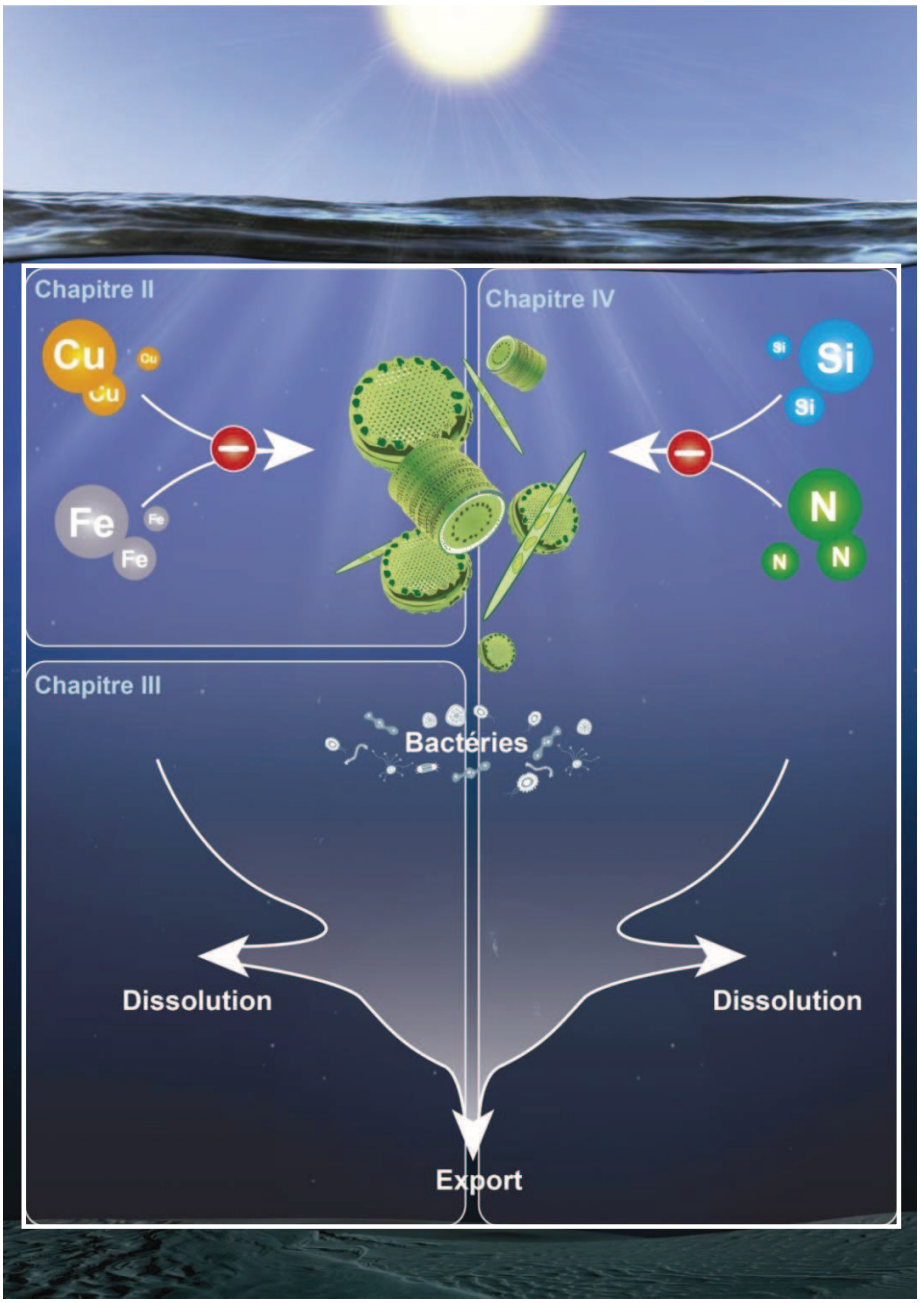

V. Chapitre V : Conclusions et perspectives

1. Conclusions

La zone mésopélagique est la couche de l'océan se situant sous la zone euphotique et allant jusqu'à 1000 m de profondeur (Buesseler et Boyd 2009). Cette couche de l'océan, aussi définie comme la « twilight zone », est difficile à échantillonner, entraînant une faible caractérisation du devenir de la matière dans cette zone. Une approche empirique a été utilisée pour estimer les flux dans cette zone, en utilisant une décroissance exponentielle de l'export avec la profondeur. Les modèles utilisés ne permettent cependant pas de contraindre correctement la zone de courbure liant la production primaire de surface au flux mesuré à 1000 m, comme l'illustre, pour le carbone, la figure d'Antia et collaborateurs (2001) (Figure V-1). De plus, l'estimation de l'efficacité de l'export va être fortement dépendante du modèle utilisé (Antia et al. 2001). Une meilleure compréhension des mécanismes qui régissent la variabilité du flux d'export dans cette couche de l'océan est donc importante pour l'étude des cycles biogéochimiques majeurs, tels que les cycles du carbone ou silicium.

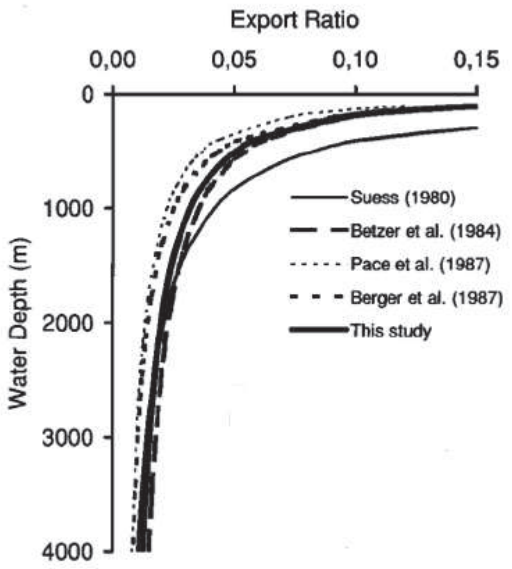

Figure V-1 : Tirée de Antia et al. (2001). Relation entre le taux d'export (flux de carbone organique particulaire / production primaire) et la profondeur, en utilisant des algorithmes de la littérature et de l'étude d'Antia et al. (2001).

Si les facteurs abiotiques influençant la dissolution des diatomées (température, concentration en dSi, association Si-aluminium) ont été assez largement étudiés (Van Cappellen et al. 2002 et

références incluses), les facteurs biotiques ont été moins explorés. Le rôle des bactéries dans la biodégradation de la membrane organique protégeant le frustule après la mort de la cellule est le facteur biotique le plus connu pour affecter la dissolution du frustule des diatomées (Bidle et Azam 1999). L'effet de l'environnement nutritionnel lors de la croissance des diatomées sur la dissolution de la $bSiO_2$ composant leur frustule n'a été que peu examiné (Soler 2010). Pourtant, les limitations en nutriments sont connues pour affecter le degré de silicification des cellules, c'est-à-dire le contenu en Si rapporté à la surface cellulaire (Martin-Jezequel et al. 2000; Claquin et al. 2002). Il est donc logique de se demander comment ces limitations peuvent affecter la structure fine du frustule (composition et degré d'organisation) et ainsi ses propriétés de dissolution. Pendant ma thèse je me suis donc intéressée à l'effet de certaines conditions nutritionnelles, connues pour être les limitations majoritaires de l'océan global (Figure V-2), sur la structure et le devenir des frustules de deux diatomées modèles, une pennée, *Pseudo-nitzschia delicatissima*, et une centrique, *Thalassiosira weissflogii*.

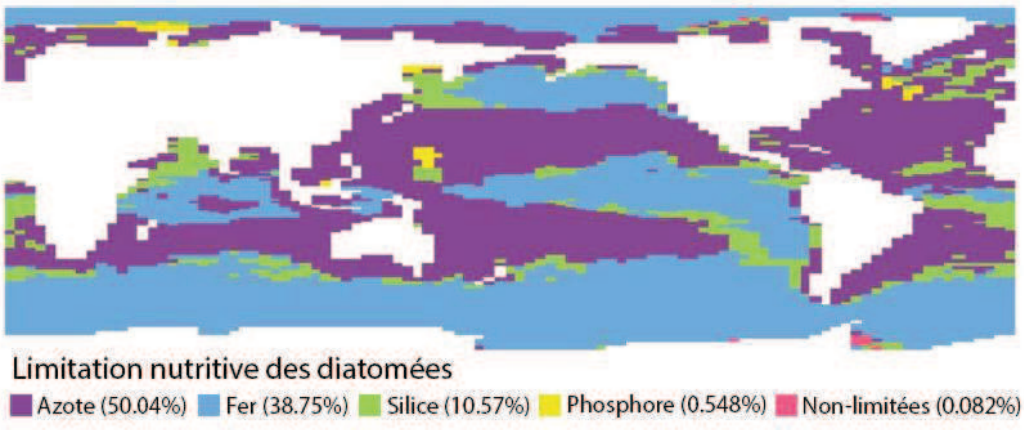

Figure V-2 : Répartition des limitations en sels nutritifs et éléments traces subies par les diatomées en période estivale d'après Moore et collaborateurs (2002). Le pourcentage de la surface totale de l'Océan où chaque élément nutritif limite la croissance des diatomées est indiqué.

La première étape a consisté en l'exploration de la plasticité structurelle du frustule des diatomées soumises à des conditions nutritives limitantes (micro et macronutriments). Cette plasticité a été étudiée sur deux échelles (1) celle de la cellule et (2) celle de la structure moléculaire du frustule. Dans une deuxième étape, l'impact de cette plasticité sur la dissolution de la $bSiO_2$ du frustule des diatomées a été étudié.

Cette stratégie en deux étapes visait à répondre aux questions posées en introduction. Tout d'abord, les réponses apportées vont être décrites, puis les perspectives ouvertes par ce travail vont être exposées.

i) Quel est l'effet de l'environnement nutritif sur la structure du frustule des diatomées ?

Je me suis tout d'abord intéressée aux effets (1) de la limitation en Cu, susceptible de limiter la croissance phytoplanctonique dans certaines régions de l'Océan mondial (Coale 1991, Peers et al. 2005) et dont les effets sur la composition élémentaire des diatomées ont été peu étudiés (Annett et al. 2008), et (2) à la limitation en Fe, limitant la production des diatomées en période estivale dans 39 % de l'océan ouvert (Moore et al. 2002).

L'effet d'une carence stricte en Cu sur le degré de silicification de la diatomée *Pseudo-nitzschia delicatissima* fait l'objet d'un article qui sera soumis à Limnology and Oceanography : « Copper and iron availability affects differently the elemental composition and the export ability of the diatom *Pseudo-nitzschia delicatissima*. Part I – Elemental composition and frustule structure » (Chapitre II). **La carence stricte en Cu, qui entraine une diminution de 40 % du taux de croissance maximal de *P. delicatissima*, n'a pas induit de modification du contenu en silice biogénique ($bSiO_2$) par surface cellulaire (Figure V-3). La carence stricte en Cu a tout de même engendré un découplage dans l'utilisation des nutriments, avec une diminution du rapport Si : N.**

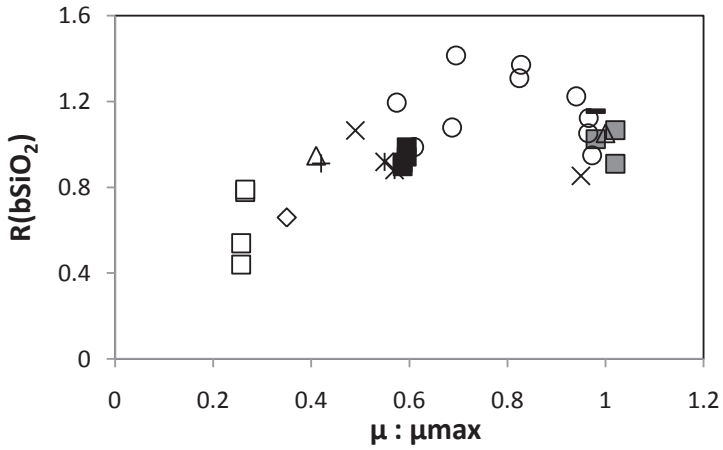

Figure V-3: Variation relative du contenu en $bSiO_2$ par surface cellulaire ($R(bSiO_2)$) en fonction de la variation relative du taux de croissance spécifique (µ : µmax) pour *P. delicatissima* (non limitée : ■ ; carencée strictement en cuivre : ■; limitée en fer : □), *P. heimii* type 1 (×, Marchetti et Harrison 2007), *P.* cf. *heimii* type 2 (*, Marchetti et Harrison 2007), *P. dolorosa* (−, Marchetti et Harrison 2007), *P.* cf. *turgidula* (+, Marchetti et Harrison 2007), *P. multiseries* (◊, Marchetti and Harrison 2007), *P*. cf. *calliantha* (Δ, Marchetti et Harrison 2007) and *P. pseudodelicatissima* (○, Sugie et Yoshimura 2013). Les valeurs pour *P. pseudodelicatissima* ont été recalculées à partir des quotas cellulaires en C, N et $bSiO_2$ (Sugie et Yoshimura 2013) et des volumes et surfaces cellulaires correspondants (aimablement communiqué par le Dr K. Sugie).

Dans cette même étude, les résultats obtenus lorsque *P. delicatissima* était soumise à une très forte limitation en Fe ont été comparés à ceux présentés dans deux articles récents (Marchetti et Harrison 2007 ; Sugie et Yoshimura 2013). **La compilation des données obtenues sur 8 espèces du genre *Pseudo-nitzschia* indique clairement une tendance entre le degré de silicification et le degré de limitation en Fe, avec en particulier une diminution du degré de silicification aux plus forts degrés de limitation en Fe** (Figure V-3). Ainsi, si aucune tendance générale n'existe quant à l'effet de la limitation en Fe sur le degré de silicification des diatomées en général (Marchetti et Cassar 2009 ; Bucciarelli et al. 2010), une tendance nette existe pour le genre *Pseudo-nitzschia*.

L'effet des conditions limitantes en micronutriment a également été étudié à l'échelle du frustule, au moyen de la spectroscopie IRTF (voir en introduction du chapitre II). Les spectres obtenus donnent des indications sur les propriétés intrinsèques du frustule (structure et composition) en fonction des conditions de croissance. J'ai comparé le degré d'organisation (défini par Gendron-Badou et collaborateurs (2003)), le degré de réactivité (défini par Schmidt et collaborateurs (2001)), ainsi que les bandes caractéristiques de certaines liaisons de molécules organiques, sur les spectres IRTF des frustules de *P. delicatissima* ayant subi des limitations en Fe et Cu. **Les résultats indiquent que le frustule de *P. delicatissima* ne possède pas le même degré d'organisation, la même réactivité ni la même quantité de matière organique associée au réseau siliceux, selon que la cellule se soit développée en conditions de carence stricte en Cu ou de limitation en Fe**. **Ainsi, à la plasticité du contenu global du frustule en $bSiO_2$, s'ajoute la plasticité du frustule à l'échelle moléculaire (Boutorh et al. en préparation, Chapitre II).**

Dans un deuxième temps, je me suis intéressée aux limitations en acide silicique et en nitrate, macronutriments dont les faibles concentrations en période estivale limitent la production des diatomées dans 60 % de l'océan ouvert, d'après le modèle de Moore et al. (2002) (Figure V-2).

L'étude de l'effet de la faible disponibilité de Si ou N sur la structure du frustule de la diatomée centrique *T. weissflogii* est présentée dans l'article «Effect of Si and N deficiencies on *Thalassiosira weissflogii* frustule structure and consequences on biogenic silica dissolution» qui sera soumis à « Global Biogeochemical Cycles.» (Chapitre IV). Cette diatomée a été exposée à deux environnements stressants différents, l'un majoritairement limité en N, avec une co-limitation N-Si, et le second majoritairement limité en Si, avec une co-limitation Si-C. Dans les deux cas, le degré de silicification a diminué d'un facteur 1,7, rappelant que le contenu en $bSiO_2$ du frustule dépend majoritairement de la disponibilité en dSi.

Les propriétés intrinsèques des frustules de la diatomée *T. weissflogii* soumise à ces conditions nutritives différentes a également été étudiée au moyen de la spectroscopie IRTF et comparée à celle de cellule ayant poussé en condition non limitantes. Il apparait qu'**en conditions de croissance limitées, le frustule de *T. weissflogii* possède une réactivité et un degré d'organisation plus faible, ainsi qu'une quantité de matière organique associée au frustule plus importante**. De plus, les deux environnements nutritifs limitants n'ont pas eu les mêmes effets sur les propriétés intrinsèques des frustules. En effet, les frustules plus déficitaires en Si présentaient une quantité de matière organique associée à leur frustule plus importante que les frustules plus déficitaires en N, et un degré d'organisation plus faible. **Ainsi, si les co-limitations Si-C et N-Si ont affecté de façon similaire le degré de silicification du frustule de *T. weissflogii*, l'étude par spectroscopie IRTF indique clairement des différences dans les structures fines des frustules (Boutorh et al. en préparation, Chapitre IV).**

Toutes les limitations en éléments nutritifs étudiées modifient le rapport élémentaire des diatomées modèles. De même, le degré de silicification des cellules, excepté celui des cellules carencées strictement en Cu, est diminué. Ces changements s'accompagnent de modifications de la structure fine du frustule, visibles à l'échelle moléculaire.

ii) L'environnement nutritif des diatomées affecte-il la dissolution post-mortem des frustules ?

Six expériences de dissolution ont été réalisées, sur les cellules de *T. weissflogii* limitées et non limitées en macronutriments (Si, N), et les cellules de *P. delicatissima* limitées et non limitées en micronutriments (Fe, Cu). L'évolution des concentrations en $bSiO_2$ et en dSi au cours de la dissolution des frustules a été reconstruite à l'aide d'équations. Cette reconstruction a mis en évidence l'existence de deux phases de $bSiO_2$ constituant les frustules, chaque phase ayant une vitesse de dissolution qui lui est propre, comme précédemment suggéré par plusieurs études (e.g. Gallinari et al. 2002, Moriceau et al. 2009).

Une période de protection du frustule a été montrée lors de la dissolution des diatomées *T. weissflogii* limitées ou non, non visible sur la cinétique de dissolution des frustules de *P. delicatissima*. Cette protection a été attribuée à la présence de matière organique, que ce soit sous la forme de l'enveloppe organique entourant le frustule ou de substances polymériques extracellulaires excrétées

par les cellules avant leur mort. Les cellules de *T. weissflogii* limitées en macronutriments étaient mieux protégées de la dissolution, i.e. la constante de dissolution mesurée pendant cette période était plus faible et cette période a duré plus longtemps. Cette protection plus efficace des cellules limitées est associée à la présence d'une plus grande quantité de substances polymériques extracellulaires.

La modélisation de la cinétique de la dissolution indique une modification dans la participation relative de chaque phase de $bSiO_2$ dans la constitution du frustule, attribuée aux différents environnements nutritionnels (Table V-1). Dans le cas d'un environnement nutritif non limitant, la phase la plus soluble de $bSiO_2$ représente la part majoritaire du frustule des diatomées *P. delicatissima* (73 % de la $bSiO_2$ totale) et *T. weissflogii* (80 % de la $bSiO_2$ totale). La phase la plus soluble représente respectivement 63 % et 41 % de la $bSiO_2$ de *P. delicatissima* carencée strictement en Cu ou limitée en Fe, et 52 et 44 % de *T. weissflogii* déficiente en Si ou en N. (Boutorh et al. en préparation, Chapitre III et IV).

Table V-1 : Tableau récapitulatif de l'effet des limitations en éléments nutritifs sur les proportions et les vitesses de dissolution des deux phases de $bSiO_2$ composant les frustules de *P. delicatissima* et de *T. weissflogii*. % Phase 1 et 2 indiquent l'importance relative de chaque phase de $bSiO_2$ dans la constitution du frustule. k_1 représente la vitesse de dissolution de la phase de $bSiO_2$ la plus soluble, la phase 1. k_2 représente la vitesse de dissolution de la phase de $bSiO_2$ la moins soluble, la phase 2. Les changements de proportion ou de vitesse de dissolution allant dans le sens d'une plus faible dissolution des frustules limités en nutriments sont indiqués en vert. Les changements de proportion ou de vitesse de dissolution indiqués en rouge vont dans le sens d'une plus forte dissolution des frustules limités en nutriments.

	P. delicatissima		
	Contrôle	Carencée en Cu	Limitée en Fe
% Phase 1	76	63	41
k_1 (d^{-1})	0.22 ± 0.01	0.23 ± 0.01	0.072 ± 0.001
% Phase 2	24	37	59
k_2 (d^{-1})	0.068 ± 0.003	0.021 ± 0.003	0.045 ± 0.001

	T. weissflogii		
	Contrôle	Déficiente en Si	Déficiente en N
% Phase 1	86	65	59
k_1 (d^{-1})	0.091±0.002	0.081±0.003	0.086±0.009
% Phase 2	14	35	41
k_2 (d^{-1})	0.003±0.002	0.0079±0.0008	0.002±0.002

L'environnement nutritif au cours de la croissance des diatomées a également un impact sur les vitesses de dissolution des différentes phases de $bSiO_2$ (Table V-1). **Aucune des limitations étudiées ne changent la vitesse de dissolution de la phase la plus soluble (Phase 1), à l'exception de la limitation en Fe qui la diminue d'un facteur 3. A l'inverse toutes les limitations, excepté la déficience en N, affectent la vitesse de dissolution de la phase la moins soluble (Phase 2) (Table V-I).** La phase la moins soluble du frustule de *P. delicatissima* s'est dissout moins rapidement lorsque les cellules se sont développées dans les conditions limitantes en micronutriments. Dans le cas de *T. weissflogii*, la vitesse de dissolution de la phase la moins soluble est augmentée par la déficience en Si (Table V-1). Les changements dans les constantes de dissolution semblent indiquer que la structure fine de chaque phase pourrait elle aussi être modifiée. Ces modifications surviennent même lorsque la croissance cellulaire nette (production plus dissolution) est négative, comme pour *T. weissflogii*.

La structure du frustule a été suivie tout au long de la dissolution des cellules de la diatomée *T. weissflogii* ayant subi les différentes conditions nutritives. La structure fine globale des frustules est décrite par les spectres IRTF obtenus en début d'expérience, elle ne permet pas de différencier les propriétés intrinsèques de chaque phase. Par contre, puisque la phase la moins soluble devient majoritaire en fin de dissolution, sa structure fine apparait sur les spectres des frustules prélevés en fin d'expérience. Pour comprendre l'impact des conditions nutritionnelles sur les propriétés intrinsèques de la phase de $bSiO_2$ la moins soluble, j'ai utilisé les degrés de réactivité et d'organisation, calculés d'après les études respectives de Schmidt et collaborateurs (2001) et Gendron Badou et collaborateurs (2003). De plus, **j'ai établi un nouvel indicateur permettant d'estimer la quantité relative de liaisons Si-OC associées à cette phase (Boutorh et al. en préparation, Chapitre IV)**.

Entre T_{22} et T_{30}, période pendant laquelle la phase de $bSiO_2$ la moins soluble était majoritaire, ces paramètres sont restés globalement constants, confirmant qu'ils sont représentatifs de cette phase (Figure V-4). La déficience en Si a augmenté le degré de réactivité de la phase de $bSiO_2$ la moins soluble tandis que la déficience en N ne semble pas l'avoir affecté. Les deux environnements nutritifs limitants ont entrainé une diminution du degré d'organisation de la phase la moins soluble, et ceci de façon plus importante pour les diatomées plus déficientes en Si. La déficience en Si a également entrainé une augmentation de la quantité relative de liaisons Si-OC associées au frustule de *T. weissflogii* ce qui n'a pas été le cas pour les cellules déficientes en N. Ainsi, s'il avait déjà été montré que les conditions environnementales, comme des changements de salinité ou de concentrations en aluminium, influent sur l'architecture des diatomées (Vrieling et al. 1999, 2000), **les travaux présentés dans cette thèse**

montrent que l'environnement nutritif des diatomées peut modifier la structure multiphasique du frustule, en affectant au moins les propriétés intrinsèques de la phase de $bSiO_2$ la moins soluble.

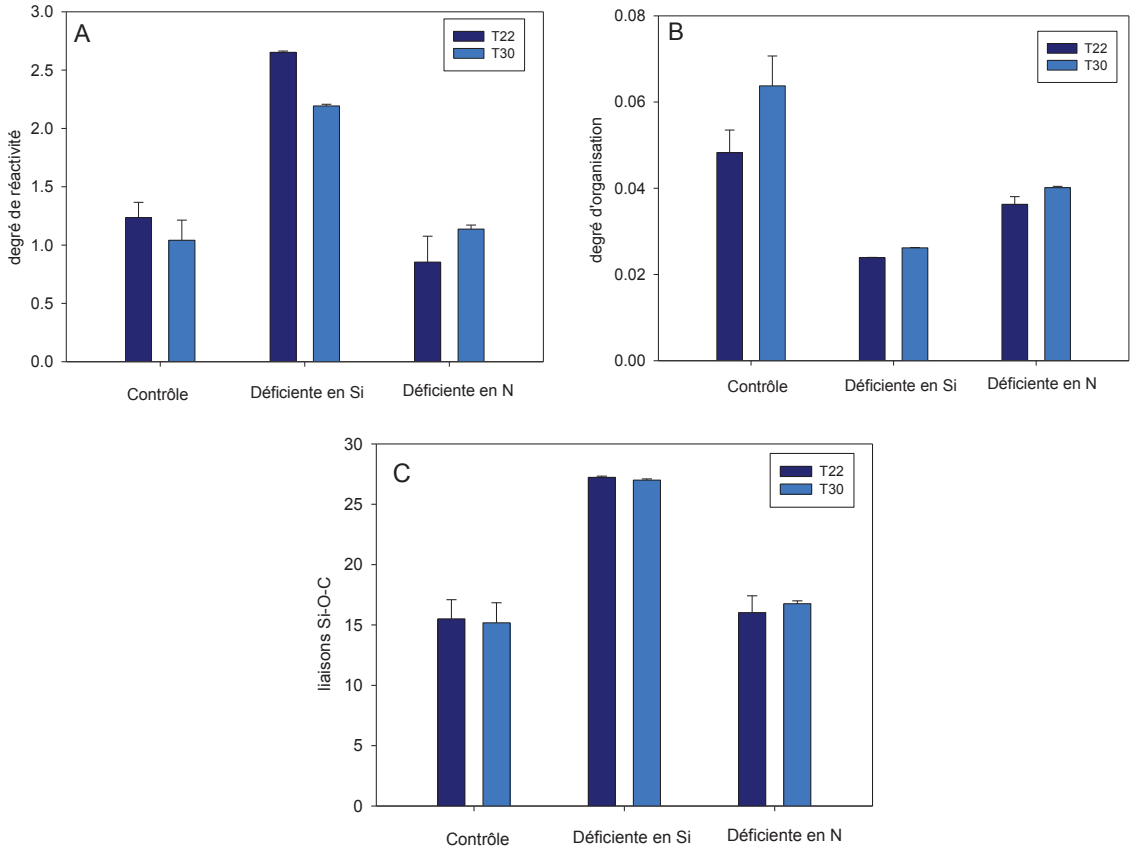

Figure V-4: Degré de réactivité (A), d'organisation (B) et quantité relative de liaisons Si-OC (C) de la phase la moins soluble du frustule de *T. weissflogii*, estimées par IRTF, après 22 et 30 jours de dissolution. Les cellules s'étaient préalablement développées dans des conditions optimales (contrôle) ou dans des conditions de déficiences majoritaires en Si et en N.

Nous avons ensuite cherché à savoir si nous pouvions établir un parallèle entre les changements de vitesse de dissolution et les propriétés intrinsèques des phases de $bSiO_2$ composant le frustule.

Dans le cas des cellules déficientes en Si, l'augmentation du degré de réactivité entre le début de l'expérience de dissolution, où la phase la plus soluble est majoritaire, et la fin de l'expérience de dissolution, où la phase la moins soluble est majoritaire, suggère que cet indice ne permet pas d'estimer la réactivité de surface du frustule, qui est connue pour diminuer avec la dissolution ou le vieillissement des frustules (Van Cappellen 1996). Cependant, la vitesse de dissolution la plus élevée de la phase la moins soluble, obtenue pour les cellules déficientes en Si, est associée à une plus grande quantité de groupements silanols comparée aux phases moins solubles des deux autres conditions. Les groupements

silanols semblent fragiliser le réseau siliceux, comme le suggère le plus faible degré d'organisation de la phase la moins soluble des cellules déficientes en Si (Figure V-4).

Dans le chapitre III, nous avons suggéré que la grande quantité de matière organique associée au réseau siliceux du frustule de *P. delicatissima* limitée en Fe renforce le frustule face à la dissolution. Dans le chapitre IV, nous avons montré que la quantité relative de liaisons Si-OC associée au frustule de *T. weissflogii* augmente tandis que la phase la moins soluble devient majoritaire, ce qui indique que la matière organique est davantage associée à la phase de $bSiO_2$ la moins soluble. Cette hypothèse est renforcée par les récents travaux de Suroy et collaborateurs (en révision) qui montrent que la plupart des acides gras associés au frustule de *T. weissflogii* sont associés à la phase de $bSiO_2$ se dissolvant lentement. La phase de $bSiO_2$ la moins soluble du frustule de *T. weissflogii* a une constante de dissolution plus élevée et une quantité de matière organique associée au frustule plus importante lorsque les cellules ont été exposées à une déficience en Si (Table V-I et Figure V-4). Cette observation suggère que plus la quantité de matière organique associée au réseau siliceux de la phase la moins soluble est importante, plus la dissolution de cette phase est favorisée. Comme les groupements silanols, les liaisons Si-OC pourraient désorganiser le réseau siliceux.

Pour résumer, nous suggérons que la déficience en Si, en augmentant la quantité relative de groupements silanols et de liaisons Si-OC de la phase de $bSiO_2$ la moins soluble du frustule de *T. weissflogii*, tend à diminuer le degré d'organisation de cette phase et à favoriser sa dissolution. Cette hypothèse ne peut être vérifiée pour la diatomée *P. delicatissima*, car la faible quantité de matériel restant à la fin de l'expérience de dissolution n'a pas permis d'estimer les propriétés intrinsèques de la phase de $bSiO_2$ la moins soluble. Par contre, si la matière organique du frustule de *P. delicatissima* est plus particulièrement associée à la phase la moins soluble, cela expliquerait que la phase la moins soluble de *P. delicatissima* limitée en Fe ait une vitesse de dissolution plus rapide que celle de *P. delicatissima* carencée en Cu.

Ainsi, les résultats de six expériences de dissolution indiquent clairement que, lorsque les diatomées ont subi des limitations en macro ou micronutriments durant leur croissance, leurs frustules auront une propension à la dissolution moins importante que ceux des cellules s'étant développées dans des conditions non limitantes. Ces différences s'expliquent plus particulièrement par les modifications des proportions entre phases de $bSiO_2$ du frustule et de leurs vitesses de dissolution. Ces différentes vitesses s'expliquent quant à elles par des modifications de la structure fine des phases du frustule.

iii) Quel est l'effet des l'environnement nutritif des diatomées sur l'export de $bSiO_2$?

Les six expériences de dissolution réalisées sur les diatomées *P. delicatissima* et *T. weissflogii* ont permis d'estimer leur préservation au bout de 22 et 30 jours de dissolution. Les résultats indiquent qu'au bout de 22 jours de dissolution de *P. delicatissima*, seuls 9 % de la $bSiO_2$ initiale des cellules non limitées étaient toujours présents, tandis que 25 % restaient dans le cas d'une croissance en condition de carence stricte en Cu, et 29 % restaient dans le cas d'une limitation en Fe. L'étude sur la diatomée *T. weissfloggi* indique qu'après 30 jours de dissolution, 20 % de la $bSiO_2$ initiale des cellules non limitées étaient toujours présents, tandis que 41 % et 51 % restaient dans les expériences où les diatomées avaient été préalablement exposées à une déficience en Si ou N, respectivement. **Les diatomées ayant subi une limitation nutritive durant leur croissance sont donc mieux préservées.**

La reminéralisation et l'export de $bSiO_2$ au sein de la colonne d'eau peuvent ainsi être estimés. Si l'on considère une vitesse de sédimentation de 1,5 m j^{-1} pour les cellules libres (Smayda 1970, 1971; Bienfang 1981, les expériences de dissolution permettent d'estimer le recyclage de la $bSiO_2$ au sein de la zone euphotique, estimée ici à 100 m de profondeur (Figure V-5A). Les cellules non limitées étant plus solubles que les cellules limitées, elles fourniront plus de dSi pour soutenir la production régénérée.

Les grosses particules, tels que les agrégats et les pelotes fécales, sont les contributeurs majeurs du flux de sédimentation, en raison de leurs vitesses de sédimentation élevées (Turner 2002). La probabilité que les cellules limitées soient intégrées dans ces grosses particules est importante, puisqu'à la fin d'un bloom de diatomées, c'est-à-dire lorsque les éléments nutritifs deviennent limitants, la formation d'agrégats est favorisée (Turner 2002 et références incluses). Si l'on considère une vitesse de sédimentation moyenne de 100 m j^{-1} pour les agrégats et les pelotes fécales (Alldredge et Gotschalk 1988, Wassmann et al. 1999) on peut estimer l'export de $bSiO_2$ sous la couche de mélange, comprise entre 50 m et 500 m, et jusqu'aux sédiments, estimés ici à 4000 m de profondeur (Figure V-5B).

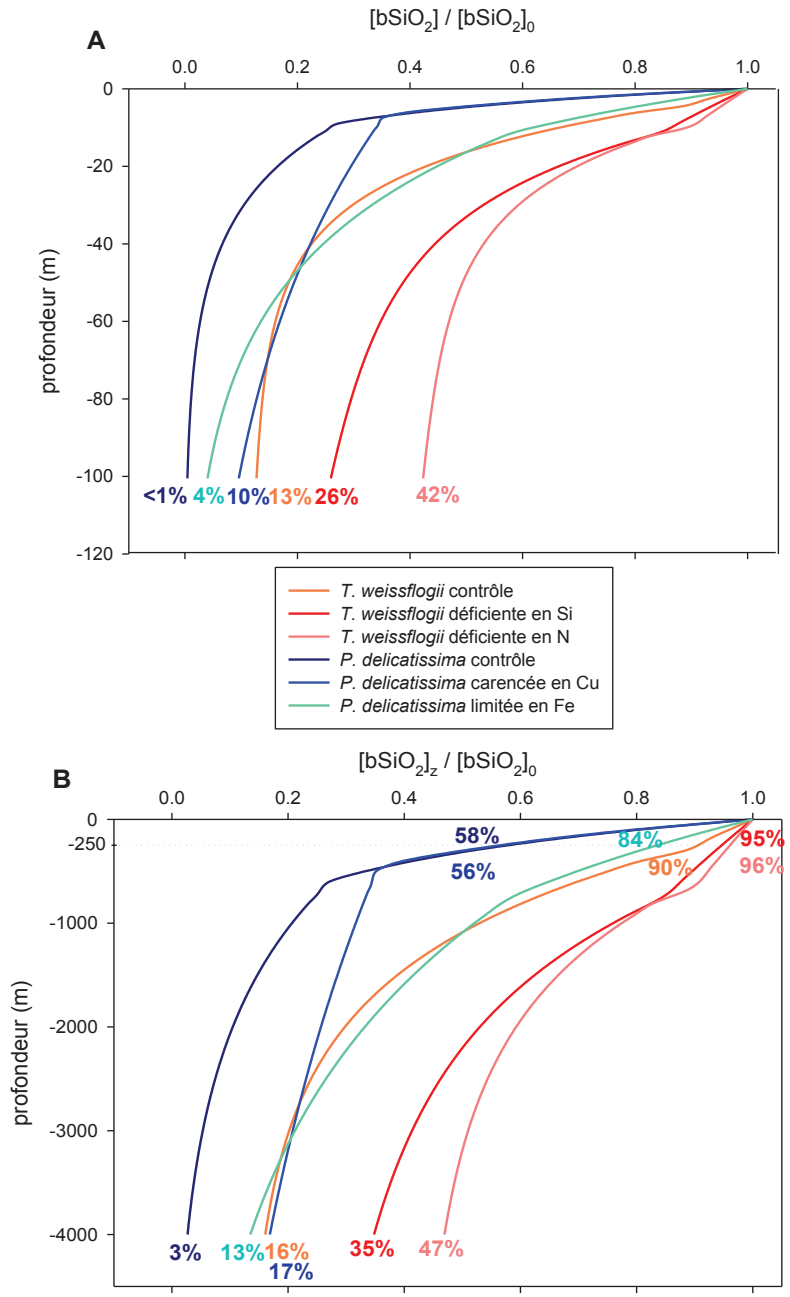

Figure V-5 : Evolution de la $bSiO_2$ normalisée par le concentration initiale en $bSiO_2$, dans les 6 expériences de dissolutions, en fonction de la profondeur, en considérant une vitesse de sédimentation de 1.5 m j^{-1} pour les cellules libres (A) (Smayda 1970) et 100 m j^{-1} pour les agrégats (B) (Alldredge et Gotschalk 1988). Les courbes ont été tracées à partir des paramètres cinétiques obtenus après reconstruction des données de $bSiO_2$ et de dSi au moyen de modèles de cinétique, validés dans le chapitre III pour *P. delicatissima*, et dans le chapitre IV pour *T. weissflogii*. Les chiffres indiquent le pourcentage de la concentration initiale de $bSiO_2$ restant à - 100 m (A), - 250 m et - 4000 m (B) de profondeur.

En estimant une profondeur moyenne de la zone de mélange de 250 m, l'efficacité d'export de la $bSiO_2$ sous cette couche sera supérieure pour les cellules limitées en nutriments, excepté pour les diatomées carencées strictement en Cu pour lesquelles l'efficacité d'export est similaire aux cellules non limitées. Au niveau des sédiments, les cellules limitées en nutriments semblent mieux préservées (Figure V-5B). **Ainsi, l'export de $bSiO_2$, qu'il soit considéré sous la couche de mélange ou jusqu'aux sédiments, est favorisé lorsque les diatomées ont été soumises à un environnement nutritif limitant.** La vitesse à laquelle se dissout la $bSiO_2$ lorsqu'elle est intégrée à des agrégats ou pelotes fécales est plus faible que celle des cellules libres (Moriceau et al. 2007; Schultes et al. 2010). Ainsi, grâce à l'intégration de diatomées limitées en nutriments durant leur croissance dans les agrégats et / ou pelotes fécales de zooplancton, l'export de $bSiO_2$ pourrait être doublement favorisé, d'une part par le fait même d'être intégré dans ces grosses particules, et d'autre part, par la meilleure préservation des frustules limitées en nutriments, même si elles sont moins silicifiées.

Les résultats de ces travaux de thèse montrent que les limitations en éléments nutritifs entraînent des changements dans les propriétés intrinsèques des frustules des diatomées ainsi que dans les proportions et les vitesses de dissolution des phases de $bSiO_2$ constituant les frustules. Les frustules des diatomées limitées en nutriments sont ainsi protégés de la dissolution, et l'export de $bSiO_2$ des cellules limitées est par conséquent favorisé (Figure V-6).

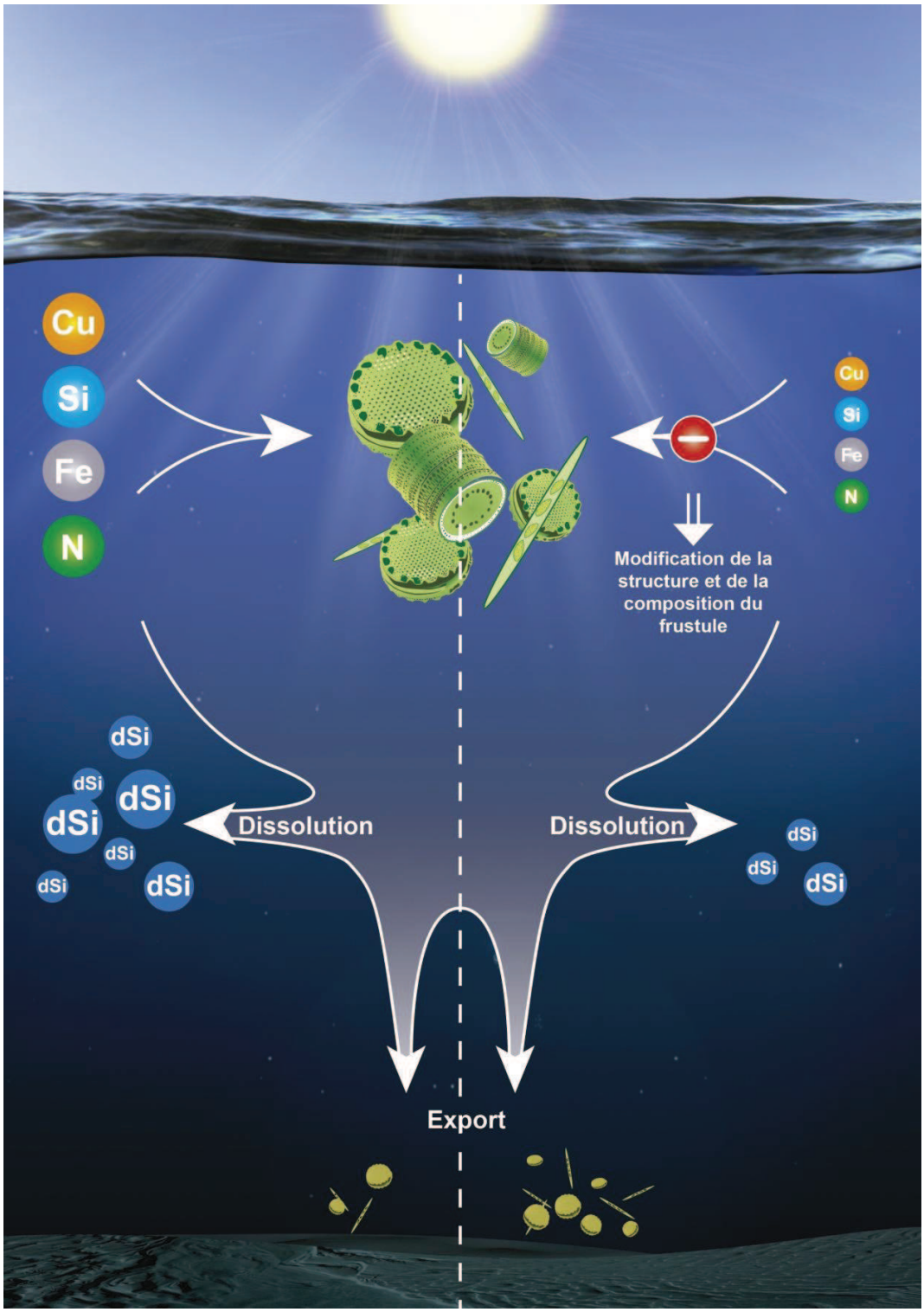

Figure V-6 : Schéma récapitulatif de l'effet des conditions nutritionnelles sur la dissolution et l'export de la silice biogénique des diatomées, mise en évidence dans le cadre de ces travaux de thèse. Réalisation Sébastien Hervé.

2. Perspectives

A la lumière des conclusions de ces travaux, de nouvelles pistes de recherche sont envisageables afin de mieux comprendre la structure fine du frustule ainsi que l'effet de modifications de cette structure sur la dissolution et l'export des diatomées. Plusieurs propositions vont être listées ci-après, de la plus fine échelle, celle du frustule, à l'amélioration des modèles biogéochimique globaux.

1) **Une étude de la structure et de la composition du frustule de différentes espèces de diatomées (pennées et centriques), dans des conditions très contrôlées de carence stricte ou de limitation en macronutriments.**

La stratégie développée au chapitre IV consistait à limiter fortement des diatomées en macronutriments, dans le but de déterminer si la disponibilité des nutriments dans le milieu de croissance induit des modifications dans l'architecture et la composition du frustule, et affectent sa dissolution. Les résultats indiquent que les limitations affectent à la fois la réactivité et le degré d'organisation du réseau siliceux, ainsi que la quantité relative de matière organique associée au frustule. Pour compléter cette étude, il serait intéressant de réaliser des expériences de limitation et de carence stricte en macronutriments dans des conditions de croissance extrêmement contrôlées, en chémostats. Ce dispositif permet une culture en continue, par l'apport constant de milieu dans la culture et le retrait constant de culture à un débit similaire, dans le but de maitriser les concentrations en sels nutritifs auxquelles les cellules sont exposées. L'analyse structurelle des diatomées limitées par la spectroscopie IRTF pourrait, au cours de ces expériences, être appuyée par une analyse structurelle complémentaire au moyen, par exemple, de la spectroscopie ^{29}Si RMN. Cette technique permet d'étudier la coordination des atomes de silicium dans le frustule des diatomées ainsi que les modifications structurelle de la $bSiO_2$ (La Vars et al. 2013).

2) **Comment la limitation en Fe affecte la structure et la composition du frustule d'une espèce de diatomée très abondante dans les sédiments de l'Océan Austral, *Fragilariopsis kerguelensis*? Est-ce que ces modifications peuvent expliquer sa bonne préservation dans les sédiments ?**

Les chapitres II et III se sont focalisés sur un genre de diatomées qui domine parfois les blooms phytoplanctoniques après une fertilisation en fer, *Pseudo-nitzschia*. Une autre diatomée pennée répond à ces fertilisations en Fe, *Fragilariopsis kerguelensis* (e.g. Hoffmann et al. 2006). Cette diatomée à la

particularité d'avoir un frustule très silicifié, ce qui pourrait expliquer l'abondance de cette espèce dans les sédiments de l'Océan Austral (e.g. Zielinski et Gersonde 1997). Les travaux de cette thèse indiquent que la structure et la composition du réseau siliceux vont grandement influencer son recyclage et son export au sein de la colonne d'eau. Il serait donc intéressant de développer la même stratégie d'étude que celle adoptée dans ce présent travail sur *Pseudo-nitzschia* à la diatomée *Fragilariopsis kerguelensis*, à savoir une étude de l'effet de différents degrés de limitation en Fe sur (i) la composition élémentaire de la diatomée, (ii) la structure et la composition fine du frustule et (iii) l'évolution de la structure et la composition fine du frustule au cours de sa dissolution. Comprendre les mécanismes qui gouvernent la composition élémentaire et la dissolution de deux diatomées qui dominent les blooms après fertilisation en Fe dans les régions HNLC, *Pseudo-nitzschia* et *Fragilariopsis kerguelensis*, pourrait permettent une meilleure compréhension des mécanismes qui régissent l'export de $bSiO_2$ dans ces régions de l'Océan mondial à fort dépôt d'opale (DeMaster 1981).

3) De l'étude de processus, en laboratoire, vers de nouvelles études plus fidèles aux conditions en milieu naturel

Cette thèse repose essentiellement sur des études de processus en laboratoire, nécessaires à une meilleure compréhension de la variabilité spatiale et temporelle de la dissolution de la $bSiO_2$ dans la colonne. Ces études sont indispensables car elles permettent de travailler, en conditions contrôlées, sur les processus biotiques et abiotiques qui influencent la cinétique de dissolution de la silice biogénique. Il apparaît toutefois que ces études, si elles s'avèrent nécessaires pour une compréhension mécanistique, ne reproduisent pas les conditions environnementales rencontrées par les particules *in-situ*. Une confrontation des résultats de laboratoire aux lois obtenues empiriquement à partir de données *in-situ* permet de définir les limites de telles expériences.

En 2002, Ragueneau et collaborateurs ont établi une équation empirique permettant de prédire dans n'importe quelle zone de l'océan, les valeurs Si : C des particules sédimentant dans la colonne d'eau ($(Si : C)_z$) à partir de leur rapports Si : C à la surface ($(Si : C)_0$) et de la profondeur (z) :

$$(Si : C)_z = (Si : C)_0 \times z^{0,41}$$

Cette équation a été appliquée aux valeurs des rapports Si : C obtenues durant les expériences de dissolution / dégradation de *Thalassiosira weissflogii* (chapitre III pour l'expérience de dissolution et thèse de Maxime Suroy, 2013, pour l'expérience de dégradation), en utilisant une vitesse de chute réaliste pour des cellules libres, de 1.5 m $jour^{-1}$ (Miklasz et Denny 2010) (Figure V-7).

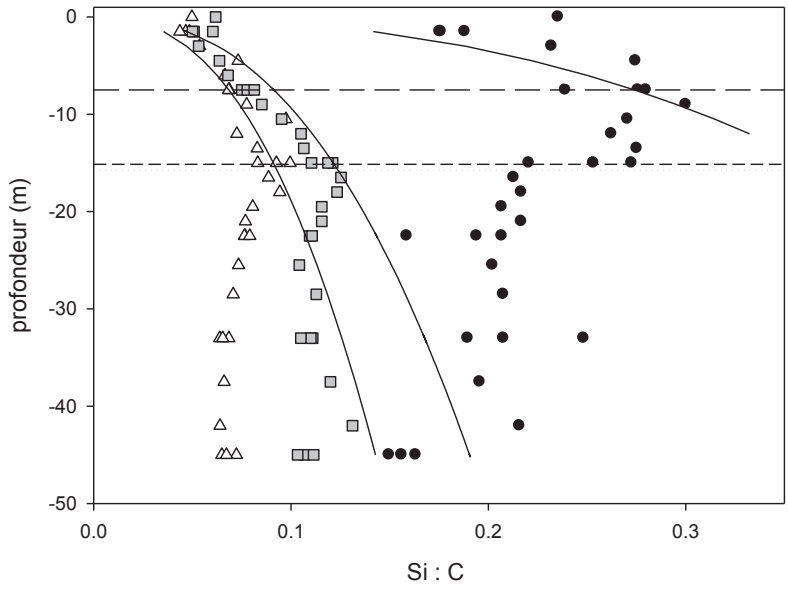

Figure V-7: Evolution du rapport Si : C (µmol L^{-1} : µmol L^{-1}) avec la profondeur. Les symboles représentent les valeurs obtenues durant les 30 jours d'expériences de dissolution/dégradation (●: contrôle, ▲ : Si-déficientes, ■: N-déficientes). Les profondeurs associées ont été calculées en considérant une vitesse de chute de 1.5 m j^{-1}. Les courbes correspondent à l'évolution des rapports Si : C avec la profondeur, estimées en utilisant l'équation de Ragueneau et al. (2002) : $(Si : C)_z = (Si : C)_0 \times z^{0,41}$. Les rapports $(Si : C)_0$ utilisés dans les trois expériences correspondent aux rapport mesurés avant de procéder aux expériences de dissolution / dégradation (Table IV-1). Les droites horizontales correspondent aux profondeurs de transition estimées, à partir desquelles la vitesse de dégradation des diatomées change et diminue, d'après les cinétiques de dégradation de carbone organique particulaire (Suroy 2013). Les profondeurs de transition estimées sont représentées par les longs tirets pour le contrôle, par les tirets courts pour les cellules Si-déficientes et par les pointillés pour les cellules N-déficientes.

Ce graphique indique clairement que, pour les trois expériences, les rapports Si : C suivent la loi empirique décrite par Ragueneau et al. (2002) jusqu'aux profondeurs de transition estimées, à partir desquelles les vitesses de dégradation du carbone organique particulaire des diatomées diminuent (Suroy 2013) : les rapports Si : C n'augmentent alors plus avec la profondeur. A ce moment, la prise en compte d'un maillon trophique supérieur, le zooplancton, paraît nécessaire. En effet, l'ingestion des diatomées par le zooplancton entraine la production de pelotes fécales, avec une augmentation théorique du Si : C de 2 à 10 entre le matériel ingéré et le matériel des pelotes fécales (Ragueneau et al. 2006 et références incluses). Il est donc sans doute nécessaire de poursuivre les études sur l'export des particules à la fois par des études de processus en laboratoire mais également à la fois dans des conditions plus proches du milieu naturel, soit en faisant intervenir la présence du zooplancton dans des

expériences en laboratoire, soit en réalisant des études en mésocosmes, dispositif expérimental plus fidèle à la réalité du milieu marin.

4) **Réalisation d'un modèle mécanistique reflétant la variabilité de la dissolution de la $bSiO_2$ des diatomées au sein de la colonne d'eau, pouvant ensuite être intégré dans les modèles des écosystèmes**

Dans la plupart des modèles biogéochimiques globaux, la dissolution de la silice est paramétrée au moyen d'une seule vitesse de dissolution. Pourtant, il apparait que l'intensité de la dissolution de la silice varie grandement au sein de la colonne d'eau. Tout d'abord, la présence de l'enveloppe organique autour du frustule limite les zones de contact entre la $bSiO_2$ et l'eau de mer environnante, engendrant une dissolution faible dans les zones de surface de l'océan. Ensuite, lorsque cette couche de surface est dégradée, le frustule est alors en contact avec l'eau de mer, et sa dissolution fait intervenir deux phases de $bSiO_2$ dont les proportions et les vitesses de dissolution diffèrent (chapitres III et IV). La réalisation d'une loi empirique intégrant la complexité de la dissolution de la silice biogénique au sein de la colonne d'eau pourrait permettre de mieux paramétrer le flux de silice dans les modèles biogéochimiques globaux.

VI. Bibliographie

Abramson, L., Wirick, S., Lee, C., Jacobsen, C. and Brandes, J. A. (2009). "The use of soft X-ray spectromicroscopy to investigate the distribution and composition of organic matter in a diatom frustule and a biomimetic analog." Deep-Sea Research Part II:Topical Studies in Oceanography 56(18): 1369-1380.

Aizawa, K. and Miyachi, S. (1986). "Carbonic anhydrase and CO_2 concentrating mechanisms in microalgae and cyanobacteria." FEMS Microbiology Letters 39(3): 215-233.

Alldredge, A. L. and Gotschalk, C. (1988). In situ settling behavior of marine snow, DTIC Document.

Alverson, A. J. (2007). "Strong purifying selection in the silicon transporters of marine and freshwater diatoms." Limnology and Oceanography 52(4): 1420-1429.

Annett, A. L., Lapi, S., Ruth, T. J. and Maldonado, M. T. (2008). "The effects of Cu and Fe availability on the growth and Cu : C ratios of marine diatoms." Limnology and Oceanography 53(6): 2451-2461.

Antia, A. N., Koeve, W., Fischer, G., Blanz, T., Schulz-Bull, D., Scholten, J., Neuer, S., Kremling, K., Kuss, J., Peinert, R., Hebbeln, D., Bathmann, U., Conte, M., Fehner, U. and Zeitzschel, B. (2001). "Basin-wide particulate carbon flux in the Atlantic Ocean: Regional export patterns and potential for atmospheric CO_2 sequestration." Global Biogeochemical Cycles 15(4): 845-862.

Armstrong, R. A. P., Michael L. Lee, Cindy. Wakeham, Stuart G. (2009). "Settling velocity spectra and the ballast ratio hypothesis." Deep Sea Research Part II: Topical Studies in Oceanography 56(18): 1470-1478.

Bidle, K. D. and Azam, F. (1999). "Accelerated dissolution of diatom silica by marine bacterial assemblages." Nature 397(6719): 508-512.

Bidle, K. D. and Azam, F. (2001). "Bacterial control of silicon regeneration from diatom detritus: Significance of bacterial ectohydrolases and species identity." Limnology and Oceanography 46(7): 1606-1623.

Bidle, K. D., Manganelli, M. and Azam, F. (2002). "Regulation of oceanic silicon and carbon preservation by temperature control on bacteria." Science 298(5600): 1980-1984.

Bienfang, P. K. (1981). "Sinking rates of heterogeneous, temperate phytoplankton populations." Journal of Plankton Research 3(2): 235-253.

Boutorh, J., Bucciarelli, E., Boukerma, K., Rinnert, E., Ragueneau, O. and Moriceau, B. (this issue). "Copper and iron availability affects differently the elemental composition and the export ability of the diatom *Pseudo-nitzschia delicatissima*. Part I – Elemental composition and frustule structure." To be submitted to Limnology and Oceanography.

Boutorh, J., Moriceau, B., Gallinari, M., Ragueneau, O. and Bucciarelli, E. (this issue). "Copper and iron availability affects differently the elemental composition and the export ability of the diatom *Pseudo-nitzschia delicatissima*. Part II – Diatom dissolution." To be submitted to Limnology and Oceanography.

Boutorh, J., Moriceau, B., Gallinari, M., Suroy, M., Delmas, D., Amiel, C. and Ragueneau, O. (in prep). "Effect of Si and N deficiencies on *Thalassiosira weissflogii* frustule structure and consequences on biogenic silica dissolution." To be submitted to Global Biogeochemical Cycles

Boyd, P. and Ellwood, M. (2010). "The biogeochemical cycle of iron in the ocean." Nature Geoscience 3(10): 675-682.

Boyd, P. W., Watson, A. J., Law, C. S., Abraham, E. R., Trull, T., Murdoch, R., Bakker, D. C. E., Bowie, A. R., Buesseler, K. O., Chang, H., Charette, M., Croot, P., Downing, K., Frew, R., Gall, M., Hadfield, M., Hall, J., Harvey, M., Jameson, G., LaRoche, J., Liddicoat, M., Ling, R., Maldonado, M. T., McKay, R. M., Nodder, S., Pickmere, S., Pridmore, R., Rintoul, S., Safi, K., Sutton, P., Strzepek, R., Tanneberger, K., Turner, S., Waite, A. and Zeldis, J. (2000). "A mesoscale phytoplankton bloom in the polar Southern Ocean stimulated by iron fertilization." Nature 407(6805): 695-702.

Boyle, E. (1998). "Oceanography - Pumping iron makes thinner diatoms." Nature 393(6687): 733-734.

Broecker, W. S. (1991). "The great ocean conveyor." Oceanography 4(2): 79-89.

Broecker, W. S., Peng, T.-H. and Beng, Z. (1982). "Tracers in the Sea" Lamont-Doherty Geological Observatory, Columbia University.

Bruland, K. W. and Lohan, M. C. 2003. "Controls of Trace Metals in Seawater", p. 23-47. *In* H. Elderfield [ed.], Treatise on Geochemistry. Elsevier Ltd.

Brzezinski, M. A. (1985). "The Si: C: N ratio of marine diatoms: interspecific variability and the effect of some environmental variables." Journal of Phycology 21(3): 347-357.

Brzezinski, M. A., Krause, J. W., Church, M. J., Karl, D. M., Li, B., Jones, J. L. and Updyke, B. (2011). "The annual silica cycle of the North Pacific subtropical gyre." Deep Sea Research Part I: Oceanographic Research Papers 58(10): 988-1001.

Bucciarelli, E., Pondaven, P. and Sarthou, G. (2010). "Effects of an iron-light co-limitation on the elemental composition (Si, C, N) of the marine diatoms *Thalassiosira oceanica* and *Ditylum brightwellii*." Biogeosciences 7(2): 657-669.

Buesseler, K., Ball, L., Andrews, J., Benitez-Nelson, C., Belastock, R., Chai, F. and Chao, Y. (1998). "Upper ocean export of particulate organic carbon in the Arabian Sea derived from thorium-234." Deep-Sea Research Part II 45(10-11): 2461-2487.

Buesseler, K. O. and Boyd, P. W. (2009). "Shedding light on processes that control particle export and flux attenuation in the twilight zone of the open ocean." Limnology and Oceanography 54(4): 1210.

Canadell, J. G., Le Quere, C., Raupach, M. R., Field, C. B., Buitenhuis, E. T., Ciais, P., Conway, T. J., Gillett, N. P., Houghton, R. A. and Marland, G. (2007). "Contributions to accelerating atmospheric CO_2 growth from economic activity, carbon intensity, and efficiency of natural sinks." Proceedings of the National Academy of Sciences of the United States of America 104(47): 18866-18870.

Chadd, H. E., Newman, J., Mann, N. H. and Carr, N. G. (1996). "Identification of iron superoxide dismutase and a copper/zinc superoxide dismutase enzyme activity within the marine cyanobacterium Synechococcus sp. WH 7803." FEMS microbiology letters 138(2-3): 161-165.

Chiovitti, A., Harper, R. E., Willis, A., Bacic, A., Mulvaney, P. and Wetherbee, R. (2005). "Variations in the substituted 3-linked mannans closely associated with the silicifed wall of diatoms." Journal of Phycology 41(6): 1154-1161.

Claquin, P., Martin-Jezequel, V., Kromkamp, J. C., Veldhuis, M. J. W. and Kraay, G. W. (2002). "Uncoupling of silicon compared with carbon and nitrogen metabolisms and the role of

the cell cycle in continuous cultures of *Thalassiosira pseudonana* (Bacillariophyceae) under light, nitrogen, and phosphorus control." Journal of Phycology 38(5): 922-930.

Coale, K. H. (1991). "Effects of iron, manganese, copper, and zinc enrichments on productivity and biomass in the sub-arctic Pacific." Limnology and Oceanography 36(8): 1851-1864.

Coates, J. 2006. "Interpretation of Infrared Spectra, A Practical Approach". Encyclopedia of Analytical Chemistry. John Wiley & Sons, Ltd.

Coradin, T. and Lopez, P. J. (2003). "Biogenic silica patterning: Simple chemistry or subtle biology?" Chembiochem 4(4): 251-259.

Cowie, G. L. and Hedges, J. I. (1996). "Digestion and alteration of the biochemical constituents of a diatom *Thalassiosira weissflogii* ingested by an herbivorous zooplankton (Calanus pacificus)." Limnol. Oceanogr. 41(4).

Davison, A. C. (1997). "Bootstrap methods and their application" Cambridge university press.

de Baar, H. J. W., Boyd, P. W., Coale, K. H., Landry, M. R., Tsuda, A., Assmy, P., Bakker, D. C. E., Bozec, Y., Barber, R. T., Brzezinski, M. A., Buesseler, K. O., Boye, M., Croot, P. L., Gervais, F., Gorbunov, M. Y., Harrison, P. J., Hiscock, W. T., Laan, P., Lancelot, C., Law, C. S., Levasseur, M., Marchetti, A., Millero, F. J., Nishioka, J., Nojiri, Y., van Oijen, T., Riebesell, U., Rijkenberg, M. J. A., Saito, H., Takeda, S., Timmermans, K. R., Veldhuis, M. J. W., Waite, A. M. and Wong, C. S. (2005). "Synthesis of iron fertilization experiments: From the iron age in the age of enlightenment." Journal of Geophysical Research-Oceans 110(C9).

de Baar, H. J. W. and La Roche, J. (2003). "Trace metals in the oceans: Evolution, biology and global change". G. Wefer, F. Lamy and F. Mantoura, Berlin, 79-105 Springer-Verlag Berlin.

De Stefano, L., Rendina, I., De Stefano, M., Bismuto, A. and Maddalena, P. (2005). "Marine diatoms as optical chemical sensors." Applied Physics Letters 87(23): 233902-233902-233903.

DeMaster, D. J. (1981). "The supply and accumulation of silica in the marine environment." Geochimica et Cosmochimica Acta 45(10): 1715-1732.

Dixit, S. and Van Cappellen, P. (2002). "Surface chemistry and reactivity of biogenic silica." Geochimica Et Cosmochimica Acta 66(14): 2559-2568.

Dixit, S., Van Cappellen, P. and van Bennekom, A. J. (2001). "Processes controlling solubility of biogenic silica and pore water build-up of silicic acid in marine sediments." Marine Chemistry 73(3–4): 333-352.

Dove, P. M. (1994). "The dissolution kinetics of quartz in sodium-chloride solutions at 25-degrees-C to 300-degrees-C." American Journal of Science 294(6): 665-712.

Dubois, M., Gilles, K. A., Hamilton, J. K., Rebers, P. A. and Smith, F. (1956). "Colorimetric method for determination of sugars and related substances." Analytical Chemistry 28(3): 350-356.

Dugdale, R. C., Wilkerson, F. P. and Minas, H. J. (1995). "The role of a silicate pump in driving new production." Deep Sea Research Part I: Oceanographic Research Papers 42(5): 697-719.

Durkin, C. A., Marchetti, A., Bender, S. J., Truong, T., Morales, R., Mock, T. and Armbrust, E. V. (2012). "Frustule-related gene transcription and the influence of diatom community

composition on silica precipitation in an iron-limited environment." Limnology and Oceanography 57(6): 1619-1633.

Elzein, T., Blarquez, O., Gauthier, O. and Carcaillet, C. (2011). "Allometric equations for biomass assessment of subalpine dwarf shrubs." Alpine Botany 121(2): 129-134.

Fowler, S. W. and Knauer, G. A. (1986). "Role of large particles in the transport of elements and organic compounds through the oceanic water column." Progress in Oceanography 16(3): 147-194.

Foyer, C. H., Harbinson, J. and Mullineaux, P. (1994). "Oxygen metabolism and the regulation of photosynthetic electron transport." Causes of photooxidative stress and amelioration of defense systems in plants.: 1-42.

Fröhlich, F. and Gendron-Badou, A. (2002). "La spectroscopie infrarouge, un outil polyvalent." Géologie de la Préhistoire, AEEGP, éditeur. Paris: 662-677.

Gallinari, M. (2002). Dissolution et préservation de la silice biogénique dans les sédiments marins, Université de Bretagne Occidentale.

Gallinari, M., Ragueneau, O., Corrin, L., DeMaster, D. J. and Treguer, P. (2002). "The importance of water column processes on the dissolution properties of biogenic silica in deep-sea sediments I. Solubility." Geochimica Et Cosmochimica Acta 66(15): 2701-2717.

Gehlen, M., Beck, L., Calas, G., Flank, A.-M., Van Bennekom, A. and Van Beusekom, J. (2002). "Unraveling the atomic structure of biogenic silica: evidence of the structural association of Al and Si in diatom frustules." Geochimica et Cosmochimica Acta 66(9): 1601-1609.

Gehlen, M., Bopp, L., Ernprin, N., Aumont, O., Heinze, C. and Raguencau, O. (2006). "Reconciling surface ocean productivity, export fluxes and sediment composition in a global biogeochemical ocean model." Biogeosciences 3(4): 521-537.

Geider, R. J. and La Roche, J. (2002). "Redfield revisited: variability of C : N : P in marine microalgae and its biochemical basis." European Journal of Phycology 37(1): 1-17.

Gendron-Badou, A. c., Coradin, T., Maquet, J., Fröhlich, F. and Livage, J. (2003). "Spectroscopic characterization of biogenic silica." Journal of Non-Crystalline Solids 316(2–3): 331-337.

Gensemer, R. W. (1990). "Role of aluminum and growth rate on changes in cell size and silica content of silica-limited populations of *Asterionella ralfsii* var. *Americana* (Baccilariophyceae) " Journal of Phycology 26(2): 250-258.

GIEC. 2007. "Résumé à l'intention des décideurs". *In* S. Solomon, D. Qin, M. Manning, Z. Chen, M. Marquis, K.B. Averyt, M.Tignor et H.L. Miller [ed.], Changements climatiques 2007 : Les éléments scientifiques. Contribution du Groupe de travail I au quatrième Rapport d'évaluation du Groupe d'experts intergouvernemental sur l'évolution du climat. Cambridge University Press, Cambridge, UK et New York, NY, USA.

Giordano, M., Kansiz, M., Heraud, P., Beardall, J., Wood, B. and McNaughton, D. (2001). "Fourier transform infrared spectroscopy as a novel tool to investigate changes in intracellular macromolecular pools in the marine microalga *Chaetoceros muellerii* (Bacillariophyceae)." Journal of Phycology 37(2): 271-279.

Gnanadesikan, A. (1999). "A global model of silicon cycling: Sensitivity to eddy parameterization and dissolution." Global Biogeochemical Cycles 13(1): 199-220.

Gómez, F., Claustre, H., Raimbault, P. and Souissi, S. (2007). "Two high-nutrient low-chlorophyll phytoplankton assemblages: the tropical central Pacific and the offshore Perú-Chile Current." Biogeosciences 4(6): 1101-1113.

Gordon, L. I., Jennings Jr, J. C., Ross, A. A. and Krest, J. M. (1993). "A suggested protocol for continuous flow automated analysis of seawater nutrients (phosphate, nitrate, nitrite and silicic acid) in the WOCE Hydrographic Program and the Joint Global Ocean Fluxes Study." WOCE Operations Manual, Part 3(3): 91-91.

Greenwood, J. E., Truesdale, V. W. and Rendell, A. R. (2001). "Biogenic silica dissolution in seawater — in vitro chemical kinetics." Progress in Oceanography 48(1): 1-23.

Guillard, R. (1975). "Culture of phytoplankton for feeding marine invertebrates." Culture of Marine Invertebrate Animals: 29 - 60.

Hamm, C. E., Merkel, R., Springer, O., Jurkojc, P., Maier, C., Prechtel, K. and Smetacek, V. (2003). "Architecture and material properties of diatom shells provide effective mechanical protection." Nature 421(6925): 841-843.

Hecky, R. E., Mopper, K., Kilham, P. and Degens, E. T. (1973). "The amino acid and sugar composition of diatom cell-walls." Marine Biology 19(4): 323-331.

Helmecke, O., Behrens, P. and Menzel, H. (2007). "Bio-inspired construction of silica surface patterns." Handbook of Biomineralization:. Biomimetic and bioinspired chemistry 2.

Hilborn, R. (1997). "The ecological detective: confronting models with data" Princeton University Press.

Hildebrand, M. (2008). "Diatoms, biomineralization processes, and genomics." Chemical reviews 108(11): 4855-4874.

Hildebrand, M. and Wetherbee, R. 2003. "Components and Control of Silicification in Diatoms", p. 11-57. *In* WernerE G. Müller [ed.], Silicon Biomineralization. Progress in Molecular and Subcellular Biology. Springer Berlin Heidelberg.

Hinga, K. R. (2002). "Effects of pH on coastal marine phytoplankton." Marine Ecology Progress Series 238(28): 300.

Hoagland, K. D., Rosowski, J. R., Gretz, M. R. and Roemer, S. C. (1993). "Diatom extracellular polymeric substances - function, fine-structure, chemistry, and physiology." Journal of Phycology 29(5): 537-566.

Hoffmann, L. J., Peeken, I. and Lochte, K. (2007). "Effects of iron on the elemental stoichiometry during EIFEX and in the diatoms *Fragilariopsis kerguelensis* and *Chaetoceros dichaeta*." Biogeosciences 4(4): 569-579.

Hoffmann, L. J., Peeken, I., Lochte, K., Assmy, P. and Veldhuis, M. (2006). "Different reactions of Southern Ocean phytoplankton size classes to iron fertilization." Limnology and Oceanography 51(3): 1217-1229.

Hurd, D. C. and Birdwhistell, S. (1983). "On producing a more general model for biogenic silica dissolution." American Journal of Science 283(1): 1-28.

Hutchins, D. A. and Bruland, K. W. (1998). "Iron-limited diatom growth and Si : N uptake ratios in a coastal upwelling regime." Nature 393(6685): 561-564.

Ingalls, A. E., Whitehead, K. and Bridoux, M. C. (2010). "Tinted windows: the presence of the UV absorbing compounds called mycosporine-like amino acids embedded in the frustules of marine diatoms." Geochimica et Cosmochimica Acta 74(1): 104-115.

Jin, X., Gruber, N., Dunne, J., Sarmiento, J. and Armstrong, R. (2006). "Diagnosing the contribution of phytoplankton functional groups to the production and export of particulate organic carbon, $CaCO_3$, and opal from global nutrient and alkalinity distributions." Global Biogeochemical Cycles 20(2).

Kamatani, A. (1971). "Physical and chemical characteristics of biogenous silica." Marine Biology 8(2): 89-95.

Kamatani, A. (1982). "Dissolution rates of silica from diatoms decomposing at various temperatures." Marine Biology 68(1): 91-96.

Kamatani, A. and Riley, J. P. (1979). "Rate of Dissolution of Diatom Silica Walls in Seawater." Marine Biology 55(1): 29-35.

Kates, M. and Volcani, B. (1968). "Studies on the biochemistry and fine structure of silica shell formation in diatoms. Lipid components of the cell walls." Z. Pflanzenphysiol 60: 19-29.

Koning, E., Gehlen, M., Flank, A. M., Calas, G. and Epping, E. (2007). "Rapid post-mortem incorporation of aluminum in diatom frustules: Evidence from chemical and structural analyses." Marine Chemistry 106(1-2): 208-222.

Kröger, N. and Poulsen, N. 2008. "Diatoms-From Cell Wall Biogenesis to Nanotechnology", p. 83-107. Annual Review of Genetics. Annual Review of Genetics. Annual Reviews.

La Vars, S. M., Johnston, M. R., Hayles, J., Gascooke, J. R., Brown, M. H., Leterme, S. C. and Ellis, A. V. (2013). "29Si {1H} CP-MAS NMR comparison and ATR-FTIR spectroscopic analysis of the diatoms *Chaetoceros muelleri* and *Thalassiosira pseudonana* grown at different salinities." Analytical and bioanalytical chemistry: 1-7.

Lelong, A., Bucciarelli, E., Hégaret, H. and Soudant, P. (2013). "Iron and copper limitations differently affect growth rates and photosynthetic and physiological parameters of the marine diatom *Pseudo-nitzschia delicatissima*." Limnology and Oceanography 58(2): 613-623.

Lewin, J. C. (1961). "The Dissolution of Silica from Diatom Walls." Geochimica Et Cosmochimica Acta 21(3-4): 182-198.

Lobel, K., West, J. and Hench, L. (1996). "Computational model for protein-mediated biomineralization of the diatom frustule." Marine Biology 126(3): 353-360.

Loir, M. (2004). "Guide des diatomées: plus de 200 micro-algues siliceuses photographiées" Delachaux et Niestlé.

Lorenzen, C. J. (1966). "A method for the continuous measurement of in vivo chlorophyll concentration." Deep Sea Research and Oceanographic Abstracts 13(2): 223-227.

Loucaides, S. (2009). Dissolution of biogenic silica: Roles of pH, salinity, pressure, electrical charging and reverse weathering. Netherlands Institute of Ecology. Utrecht, Utrecht University.

Loucaides, S., Behrends, T. and Van Cappellen, P. (2010). "Reactivity of biogenic silica: Surface versus bulk charge density." Geochimica Et Cosmochimica Acta 74(2): 517-530.

Loucaides, S., Koning, E. and Van Cappellen, P. (2012). "Effect of pressure on silica solubility of diatom frustules in the oceans: Results from long-term laboratory and field incubations." Marine Chemistry 136: 1-6.

Loucaides, S., Van Cappellen, P. and Behrends, T. (2008). "Dissolution of biogenic silica from land to ocean: Role of salinity and pH." Limnology and Oceanography 53(4): 1614-1621.

Loucaides, S., Van Cappellen, P., Roubeix, V., Moriceau, B. and Ragueneau, O. (2012). "Controls on the recycling and preservation of biogenic silica from biomineralization to burial." Silicon 4(1): 7-22.

Maldonado, M. T., Allen, A. E., Chong, J. S., Lin, K., Leus, D., Karpenko, N. and Harris, S. L. (2006). "Copper-dependent iron transport in coastal and oceanic diatoms." Limnology and Oceanography 51(4): 1729-1743.

Marchetti, A. and Cassar, N. (2009). "Diatom elemental and morphological changes in response to iron limitation: a brief review with potential paleoceanographic applications." Geobiology 7(4): 419-431.

Marchetti, A. and Harrison, P. J. (2007). "Coupled changes in the cell morphology and the elemental (C, N, and Si) composition of the pennate diatom *Pseudo-nitzschia* due to iron deficiency." Limnology and Oceanography 52(5): 2270-2284.

Martin-Jezequel, V., Hildebrand, M. and Brzezinski, M. A. (2000). "Silicon metabolism in diatoms: Implications for growth." Journal of Phycology 36(5): 821-840.

Martin, J. H. (1990). "Glacial-interglacial CO_2 change: The Iron Hypothesis." Paleoceanography 5(1): 1-13.

Memery, L. 2011. "Le climat à découvert", p. 67/285. *In* CNRS [ed.].

Merchant, S. S., Allen, M. D., Kropat, J., Moseley, J. L., Long, J. C., Tottey, S. and Terauchi, A. M. (2006). "Between a rock and a hard place: Trace element nutrition in *Chlamydomonas*." Biochimica et Biophysica Acta (BBA) - Molecular Cell Research 1763(7): 578-594.

Miklasz, K. A. and Denny, M. W. (2010). "Diatom sinking speeds: Improved predictions and insight from a modified Stokes' law." Limnology and Oceanography 55(6): 2513-2525.

Milligan, A. J. and Morel, F. M. M. (2002). "A proton buffering role for silica in diatoms." Science 297(5588): 1848-1850.

Mock, T., Samanta, M. P., Iverson, V., Berthiaume, C., Robison, M., Holtermann, K., Durkin, C., BonDurant, S. S., Richmond, K., Rodesch, M., Kallas, T., Huttlin, E. L., Cerrina, F., Sussmann, M. R. and Armbrust, E. V. (2008). "Whole-genome expression profiling of the marine diatom *Thalassiosira pseudonana* identifies genes involved in silicon bioprocesses." Proceedings of the National Academy of Sciences of the United States of America 105(5): 1579-1584.

Mongin, M., Nelson, D. M., Pondaven, P. and Tréguer, P. (2006). "Simulation of upper-ocean biogeochemistry with a flexible-composition phytoplankton model: C, N and Si cycling and Fe limitation in the Southern Ocean." Deep Sea Research Part II: Topical Studies in Oceanography 53(5): 601-619.

Moore, C. M., Mills, M. M., Arrigo, K. R., Berman-Frank, I., Bopp, L., Boyd, P. W., Galbraith, E. D., Geider, R. J., Guieu, C., Jaccard, S. L., Jickells, T. D., La Roche, J., Lenton, T. M., Mahowald, N. M., Maranon, E., Marinov, I., Moore, J. K., Nakatsuka, T., Oschlies, A., Saito, M. A., Thingstad, T. F., Tsuda, A. and Ulloa, O. (2013). "Processes and patterns of oceanic nutrient limitation." Nature Geoscience 6(9): 701-710.

Moore, J. K., Doney, S. C., Glover, D. M. and Fung, I. Y. (2002). "Iron cycling and nutrient-limitation patterns in surface waters of the World Ocean." Deep Sea Research Part II: Topical Studies in Oceanography 49(1): 463-507.

Moriceau, B., Garvey, M., Passow, U. and Ragueneau, O. (2007). "Evidence for reduced biogenic silica dissolution rates in diatom aggregates." Marine Ecology Progress Series 333: 129-142.

Moriceau, B., Goutx, M., Guigue, C., Lee, C., Armstrong, R., Duflos, M., Tamburini, C., Charrière, B. and Ragueneau, O. (2009). "Si–C interactions during degradation of the diatom

Skeletonema marinoi." Deep Sea Research Part II: Topical Studies in Oceanography 56(18): 1381-1395.

Mullin, J. and Riley, J. (1965). "The spectrophotometric determination of silicate-silicon in natural waters with special reference to sea water." Analytica Chimica Acta 46: 491:501.

Naumann, D., Helm, D. and Labischinski, H. (1991). "Microbiological characterizations by FT-IR spectroscopy." Nature 351(6321): 81-82.

Nelson, D. M. and Brzezinski, M. A. (1997). "Diatom growth and productivity in an oligotrophic midocean gyre: A 3-yr record from the Sargasso Sea near Bermuda." Limnology and Oceanography 42(3): 473-486.

Nelson, D. M., Goering, J. J., Kilham, S. S. and Guillard, R. R. (1976). "Kinetics of silicic acid uptake and rates of silica dissolution in the marine diatom *Thalassiosira pseudonana*." Journal of Phycology 12(2): 246-252.

Nelson, D. M., Treguer, P., Brzezinski, M. A., Leynaert, A. and Queguiner, B. (1995). "Production and dissolution of biogenic silica in the ocean - Revised global estimates, comparison with regional date and relationship to biogenic sedimentation." Global Biogeochemical Cycles 9(3): 359-372.

Nimer, N. A., Ling, M. X., Brownlee, C. and Merrett, M. J. (1999). "Inorganic carbon limitation, exofacial carbonic anhydrase activity, and plasma membrane redox activity in marine phytoplankton species." Journal of Phycology 35(6): 1200-1205.

Passow, U. and Alldredge, A. L. (1995). "A dye-binding assay for the spectrophotometric measurement of transparent exopolymer particles (TEP)." Limnology and Oceanography 40(7): 1326-1335.

Passow, U., French, M. A. and Robert, M. (2011). "Biological controls on dissolution of diatom frustules during their descent to the deep ocean: Lessons learned from controlled laboratory experiments." Deep-Sea Research Part I-Oceanographic Research Papers 58(12): 1147-1157.

Passow, U., Shipe, R. F., Murray, A., Pak, D. K., Brzezinski, M. A. and Alldredge, A. L. (2001). "The origin of transparent exopolymer particles (TEP) and their role in the sedimentation of particulate matter." Continental Shelf Research 21(4): 327-346.

Patrick, S. and Holding, A. J. (1985). "The effect of bacteria on the solubilization of silica in diatom frustules." Journal of Applied Bacteriology 59(1): 7-16.

Peers, G. and Price, N. M. (2006). "Copper-containing plastocyanin used for electron transport by an oceanic diatom." Nature 441(7091): 341-344.

Peers, G., Quesnel, S. A. and Price, N. M. (2005). "Copper requirements for iron acquisition and growth of coastal and oceanic diatoms." Limnology and Oceanography 50(4): 1149-1158.

Pondaven, P., Fravalo, C., Ruiz-Pino, D., Treguer, P., Queguiner, B. and Jeandel, C. (1998). "Modelling the silica pump in the Permanently Open Ocean Zone of the Southern Ocean." Journal of Marine Systems 17(1-4): 587-619.

Pondaven, P., Gallinari, M., Chollet, S., Bucciarelli, E., Sarthou, G., Schultes, S. and Jean, F. (2007). "Grazing-induced changes in cell wall silicification in a marine diatom." Protist 158(1): 21-28.

Price, N. M., Harrison, G. I., Hering, J. G., Hudson, R. J., Nirel, P. M. V., Palenik, B. and Morel, F. M. M. (1988-1989). "Preparation and chemistry of the artificial algal culture medium Aquil." Biological Oceanography 6: 443–461.

Ragueneau, O., Dittert, N., Pondaven, P., Treguer, P. and Corrin, L. (2002). "Si/C decoupling in the world ocean: is the Southern Ocean different?" Deep-Sea Research Part II:Topical Studies in Oceanography 49(16): 3127-3154.

Ragueneau, O., Schultes, S., Bidle, K., Claquin, P. and La Moriceau, B. (2006). "Si and C interactions in the world ocean: Importance of ecological processes and implications for the role of diatoms in the biological pump." Global Biogeochemical Cycles 20(4).

Ragueneau, O. and Tréguer, P. (1994). "Determination of biogenic silica in coastal waters: applicability and limits of the alkaline digestion method." Marine Chemistry 45(1–2): 43-51.

Raven, J. and Waite, A. (2004). "The evolution of silicification in diatoms: inescapable sinking and sinking as escape?" New Phytologist 162(1): 45-61.

Redfield, A. C. (1934). "On the proportions of organic derivatives in sea water and their relation to the composition of plankton" University Press of Liverpool.

Reimann, B. E. F., Leivin, J. C. and Volcani, B. E. (1966). "Studies on the biochemistry and fine structure of silica shell formation in diatoms. II. The structure of the cell wall of *Navicula Pelliculosa* (Bréb.) Hilse." Journal of Phycology 2(2): 74-84.

Reimann, B. E. F., Lewin, J. C. and Volcani, B. E. (1965). "Studies on the biochemistry and fine structure of silica shell formation in diatoms: I. The structure of the Cell Wall of *Cylindrotheca fusiformis* Reimann and Lewin." The Journal of Cell Biology 24(1): 39-55.

Rickert, D., Schluter, M. and Wallmann, K. (2002). "Dissolution kinetics of biogenic silica from the water column to the sediments." Geochimica Et Cosmochimica Acta 66(3): 439-455.

Roubeix, V., Becquevort, S. and Lancelot, C. (2008). "Influence of bacteria and salinity on diatom biogenic silica dissolution in estuarine systems." Biogeochemistry 88(1): 47-62.

Round, F. E., Crawford, R. M. and Mann, D. G. (1990). "The diatoms: the biology and morphology of the genera" Cambridge University Press.

Salter, I., Lampitt, R. S., Sanders, R., Poulton, A., Kemp, A. E. S., Boorman, B., Saw, K. and Pearce, R. (2007). "Estimating carbon, silica and diatom export from a naturally fertilised phytoplankton bloom in the Southern Ocean using PELAGRA: A novel drifting sediment trap." Deep-Sea Research Part II-Topical Studies in Oceanography 54(18-20): 2233-2259.

Sarmiento, J. and Toggweiler, J. (1984). "A new model for the role of the oceans in determining atmospheric pCO_2." Nature 308(5960): 621-624.

Sarthou, G., Timmermans, K. R., Blain, S. and Tréguer, P. (2005). "Growth physiology and fate of diatoms in the ocean: a review." Journal of Sea Research 53(1–2): 25-42.

Scheffel, A., Poulsen, N., Shian, S. and Kröger, N. (2011). "Nanopatterned protein microrings from a diatom that direct silica morphogenesis." Proceedings of the National Academy of Sciences 108(8): 3175-3180.

Schmidt, M., Botz, R., Rickert, D., Bohrmann, G., Hall, S. R. and Mann, S. (2001). "Oxygen isotopes of marine diatoms and relations to opal-A maturation." Geochimica Et Cosmochimica Acta 65(2): 201-211.

Schrader, H.-J. (1971). "Fecal pellets: role in sedimentation of pelagic diatoms." Science 174(4004): 55-57.

Schultes, S., Lambert, C., Pondaven, P., Corvaisier, R., Jansen, S. and Ragueneau, O. (2010). "Recycling and Uptake of $Si(OH)_4$ when Protozoan Grazers Feed on Diatoms." Protist 161(2): 288-303.

Smayda, T. J. (1970). "The suspension and sinking of phytoplankton in the sea." Oceanography and Marine Biology: an annual review 8.

Smayda, T. J. (1971). "Normal and accelerated sinking of phytoplankton in the sea." Marine Geology 11(2): 105-122.

Smetacek, V. (1999). "Diatoms and the ocean carbon cycle." Protist 150(1): 25-32.

Socrates, G. (2001). "Infrared and Raman characteristic group frequencies: tables and charts" Wiley Chichester.

Soler, C. (2010). Impact des conditions de croissance sur le métabolisme et les interactions Si-OC des diatomées. Conséquences sur la vitesse de reminéralisation de la silice biogène et de la matière organique, Université de Bretagne Occidentale.

Stuart, B. H. (2004). "Infrared spectroscopy: fundamentals and applications" Wiley. com.

Sugie, K. and Yoshimura, T. (2013). "Effects of pCO_2 and iron on the elemental composition and cell geometry of the marine diatom *Pseudo-nitzschia pseudodelicatissima* (Bacillariophyceae)." Journal of Phycology 49(3): 475-488.

Sumper, M. and Brunner, E. (2008). "Silica biomineralisation in diatoms: the model organism *Thalassiosira pseudonana*." ChemBioChem 9(8): 1187-1194.

Sunda, W. G. and Huntsman, S. A. (1995). "Iron uptake and growth limitation in oceanic and coastal phytoplankton." Marine Chemistry 50(1): 189-206.

Sunda, W. G., Price, N. M. and Morel, F. M. (2005). "Trace metal ion buffers and their use in culture studies." Algal culturing techniques: 35-63.

Suroy, M. (2013). Rôles du frustule des diatomées et des conditions nutritives de leur croissance sur l'export de carbone dans les océans, Université d'Aix-Marseille

Suroy, M., Boutorh, J., Panagiotopoulos, C., Goutx, M. and Moriceau, B. (in prep). "Degradation of diatom carbohydrates : a case study with N- and Si-stressed *Thalassiosira weissflogii*."

Suroy, M., Moriceau, B., Boutorh, J. and Goutx, M. (in revision). "Fatty acids associated with the frustule of diatoms and their fate during degradation – a case study in *Thalassiosira weissflogii*." Deep-Sea Research Part I.

Sverjensky, D. A. and Sahai, N. (1996). "Theoretical prediction of single-site surface-protonation equilibrium constants for oxides and silicates in water." Geochimica Et Cosmochimica Acta 60(20): 3773-3797.

Takahashi, E., Ledauphin, J., Goux, D. and Orvain, F. (2009). "Optimising extraction of extracellular polymeric substances (EPS) from benthic diatoms: comparison of the efficiency of six EPS extraction methods." Marine and Freshwater Research 60(12): 1201-1210.

Takeda, S. (1998). "Influence of iron availability on nutrient consumption ratio of diatoms in oceanic waters." Nature 393(6687): 774-777.

Tamburini, C., Garcin, J., Gregori, G., Leblanc, K., Rimmelin, P. and Kirchman, D. L. (2006). "Pressure effects on surface Mediterranean prokaryotes and biogenic silica dissolution during a diatom sinking experiment." Aquatic Microbial Ecology 43(3): 267-276.

Tande, K. S. and Slagstad, D. (1985). "Assimilation efficiency in herbivorous aquatic organisms-The potential of the ratio method using ^{14}C and biogenic silica as markers." Limnology and Oceanography: 1093-1099.

Tesson, B., Genet, M. J., Fernandez, V., Degand, S., Rouxhet, P. G. and Martin-Jézéquel, V. (2009). "Surface Chemical Composition of Diatoms." Chembiochem 10(12): 2011-2024.

Tesson, B. and Hildebrand, M. (2013). "Characterization and Localization of Insoluble Organic Matrices Associated with Diatom Cell Walls: Insight into Their Roles during Cell Wall Formation." Plos One 8(4).

Tesson, B., Masse, S., Laurent, G., Maquet, J., Livage, J., Martin-Jézéquel, V. and Coradin, T. (2008). "Contribution of multi-nuclear solid state NMR to the characterization of the *Thalassiosira pseudonana* diatom cell wall." Analytical and Bioanalytical Chemistry 390(7): 1889-1898.

Thamatrakoln, K. and Hildebrand, M. (2007). "Analysis of *Thalassiosira pseudonana* silicon transporters indicates distinct regulatory levels and transport activity through the cell cycle." Eukaryotic Cell 6(2): 271-279.

Thornton, D. C. O. (2002). "Diatom aggregation in the sea: mechanisms and ecological implications." European Journal of Phycology 37(2): 149-161.

Timmermans, K. R., van der Wagt, B. and de Baar, H. J. W. (2004). "Growth rates, half-saturation constants, and silicate, nitrate, and phosphate depletion in relation to iron availability of four large, open-ocean diatoms from the Southern Ocean." Limnology and Oceanography 49(6): 2141-2151.

Tréguer, P., Kamatani, A., Gueneley, S. and Quéguiner, B. (1989). "Kinetics of dissolution of Antarctic diatom frustules and the biogeochemical cycle of silicon in the Southern Ocean." Polar Biology 9(6): 397-403.

Tréguer, P. and Le Corre, P. (1975). "Manuel d'analyse des sels nutritifs dans l'eau de mer (utilisation de l'autoanalyseur II Technicon), 2eme Edition." Université de Bretagne Occidentale, Brest, France.

Treguer, P., Nelson, D. M., Vanbennekom, A. J., Demaster, D. J., Leynaert, A. and Queguiner, B. (1995). "The silica balance in the world ocean - A reestimate." Science 268(5209): 375-379.

Tréguer, P. J. and De La Rocha, C. L. (2013). "The world ocean silica cycle." Annual Review of Marine Science 5: 477-501.

Trick, C. G., Bill, B. D., Cochlan, W. P., Wells, M. L., Trainer, V. L. and Pickell, L. D. (2010). "Iron enrichment stimulates toxic diatom production in high-nitrate, low-chlorophyll areas." Proceedings of the National Academy of Sciences 107(13): 5887-5892.

Tripp, B. C., Smith, K. and Ferry, J. G. (2001). "Carbonic anhydrase: new insights for an ancient enzyme." Journal of Biological Chemistry 276(52): 48615-48618.

Truesdale, V. W., Greenwood, J. E. and Rendell, A. R. (2005). "In vitro, batch-dissolution of biogenic silica in seawater–the application of recent modelling to real data." Progress in Oceanography 66(1): 1-24.

Turner, J. T. (2002). "Zooplankton fecal pellets, marine snow and sinking phytoplankton blooms." Aquatic Microbial Ecology 27(1): 57-102.

Twining, B. S. and Baines, S. B. 2013. "The Trace Metal Composition of Marine Phytoplankton", p. 191-215. *In* C. A. Carlson and S. J. Giovannoni [eds.], Annual Review of Marine Science, Vol 5. Annual Review of Marine Science.

Van Bennekom, A., Buma, A. and Nolting, R. (1991). "Dissolved aluminium in the Weddell-Scotia Confluence and effect of Al on the dissolution kinetics of biogenic silica." Marine Chemistry 35(1): 423-434.

Van Beusekom, J. and Weber, A. (1992). Decreasing diatom abundance in the North Sea: the possible significance of aluminium. International Symposium Series.

Van Cappellen, P. (1996). "Reactive surface area control of the dissolution kinetics of biogenic silica in deep-sea sediments." Chemical Geology 132(1-4): 125-130.

Van Cappellen, P., Dixit, S., Gallinari, M. and Institut, O. 2004. "Biogenic silica dissolution and the marine Si cycle: kinetics, surface chemistry and preservation", p. 417-454. Biogeochemical Silicium Cycle: Elemental to Global Scale. Oceanis : Serie De Documents Oceanographiques. Inst Oceanographique.

Van Cappellen, P., Dixit, S. and van Beusekom, J. (2002). "Biogenic silica dissolution in the oceans: Reconciling experimental and field-based dissolution rates." Global Biogeochemical Cycles 16(4): 23-21-23-10.

Vanbennekom, A. J., Jansen, J. H. F., Vandergaast, S. J., Vaniperen, J. M. and Pieters, J. (1989). "Aluminum-Rich Opal - an Intermediate in the Preservation of Biogenic Silica in the Zaire (Congo) Deep-Sea Fan." Deep-Sea Research Part a-Oceanographic Research Papers 36(2): 173-190.

Volk, T. and Hoffert, M. I. (1985). "Ocean carbon pumps: Analysis of relative strengths and efficiencies in ocean-driven atmospheric CO_2 changes." The Carbon Cycle and Atmospheric CO_2: Natural Variations Archean to Present: 99-110.

Vrieling, E. G., Beelen, T. P. M., van Santen, R. A. and Gieskes, W. W. C. (2000). "Nanoscale uniformity of pore architecture in diatomaceous silica: A combined small and wide angle X-ray scattering study." Journal of Phycology 36(1): 146-159.

Vrieling, E. G., Poort, L., Beelen, T. P. M. and Gieskes, W. W. C. (1999). "Growth and silica content of the diatoms *Thalassiosira weissflogii* and *Navicula salinarum* at different salinities and enrichments with aluminium." European Journal of Phycology 34(3): 307-316.

Walne, P. R. (1966). "Experiments in the large-scale culture of the larvae of Ostrea edulis L." Fishery Investigations. Series II 25(4).

Wassmann, P., Hansen, L., Andreassen, I. J., Riser, C. W., Urban-Rich, J. and Båmstedt, U. (1999). "Distribution and sedimentation of faecal on the Nordvestbanken shelf, northern Norway, in 1994." Sarsia 84(3-4): 239-253.

Welch, S. A. and Vandevivere, P. (1994). "Effect of microbial and other naturally occurring polymers on mineral dissolution." Geomicrobiology journal 12(4): 227-238.

Zeroual, W., Choisy, C., Doglia, S. M., Bobichon, H., Angiboust, J.-F. and Manfait, M. (1994). "Monitoring of bacterial growth and structural analysis as probed by FT-IR spectroscopy." Biochimica et Biophysica Acta (BBA)-Molecular Cell Research 1222(2): 171-178.

Zielinski, U. and Gersonde, R. (1997). "Diatom distribution in Southern Ocean surface sediments (Atlantic sector): Implications for paleoenvironmental reconstructions." Palaeogeography, Palaeoclimatology, Palaeoecology 129(3–4): 213-250.

VII. Liste des Figures

VIII. Liste des Tables

Annexes

IX. Annexes

1. Annexe I: Etude de l'évolution de l'architecture de la diatomée *Coscinodiscus granii* durant sa dissolution

Les analyses effectuées mettent en évidence les phases de $bSiO_2$ composant le frustule des diatomées via leurs propriétés de dissolution et de solubilité, ainsi que par leurs compositions biochimiques. Jusqu'à présent, aucune étude n'a établi si ces phases sont identifiables visuellement et si elles correspondent à des zones particulières de l'architecture du frustule. Ce travail est actuellement en cours, en collaboration avec Philippe Elies, ingénieur d'Etude à la Plateforme d'imagerie et de mesures en microscopie de l'UBO, avec Sébastien Hervé, infographiste à l'IUEM, et avec Marie-Sol Richard Hernandez, étudiante à l'UBO. Cette étudie est réalisée au moyen d'un suivi en 3 dimensions de la dissolution de la diatomée de grande taille *Coscinodiscus granii*, par Microscopie Electronique à Balayage (MEB) et Microscopie à Force Atomique (AFM).

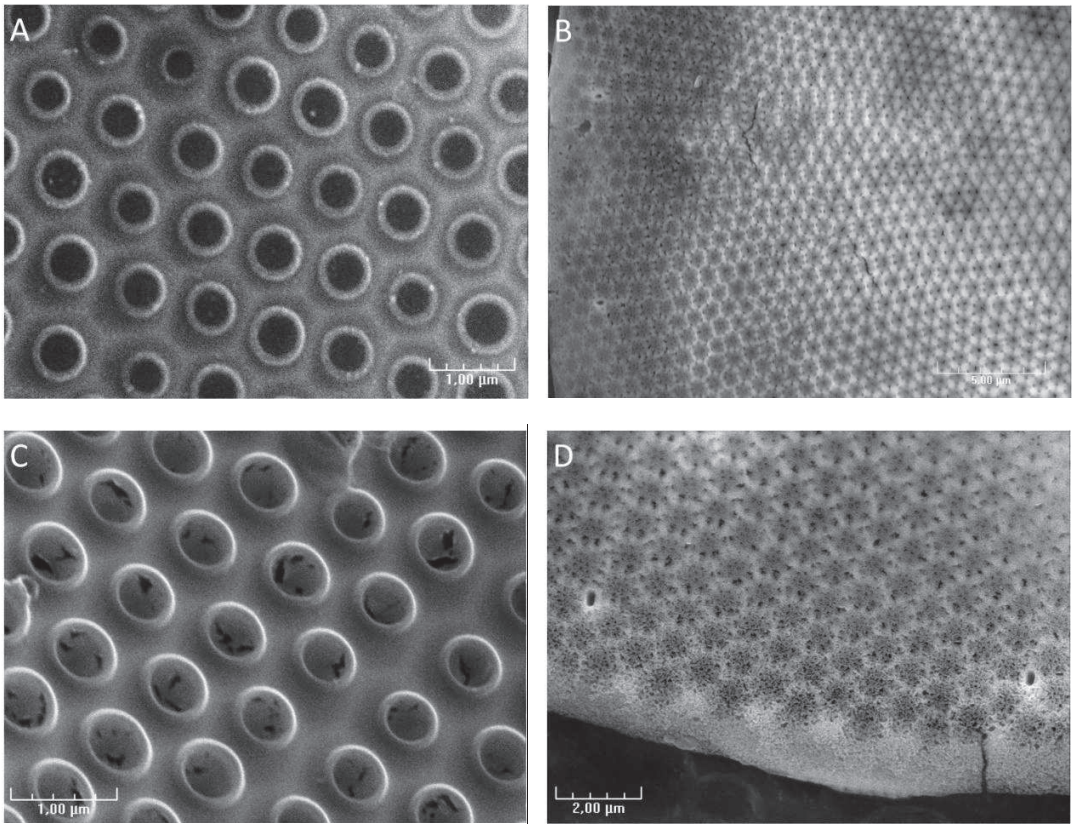

Figure 1: Images réalisée au microscope électronique à balayage (MEB) de la diatomée C*oscinodiscus granii*, avant une expérience de dissolution (A,B) et après 30 jours de dissolution (C,D).

Les résultats préliminaires présentés ici (figure 1) montrent que, plus qu'un élargissement des pores des valves, la dissolution du frustule entraine une porosité du frustule sur toute sa surface. Plusieurs modèles de mécanismes moléculaires pour la formation de la silice biogénique ont été suggérés. Notamment, le modèle de Sumper (2002), pouvant prédire l'architecture complexe des valves du genre *Coscinodicus*, postule que les SDVs produisent des émulsions de micro- et nano-gouttes organiques et que le contact entre ces gouttes et milieu aqueux, contenant la dSi, entrainerait la polymérisation de la dSi et la perte d'une fraction des gouttes organiques par co-précipitation. Il est possible qu'une forte association $bSiO_2$-matière organique soit ainsi créee autour des pores du frustule. Le chapitre 4 suggère que la phase la moins soluble du frustule des diatomées soit liée à des pools de matière organique. Ainsi, la $bSiO_2$ située autour des pores du frustule de *Coscinodiscus granii* pourrait représenter la phase du frustule peu soluble, ce qui expliquerait pourquoi, après 30 jours de dissolution et 65 % de la $bSiO_2$ initiale dissoute, les pores du frustule ne se sont pas élargis.

2. Annexe 2: Fatty acids associated with the frustule of diatoms and their fate during degradation – a case study in *Thalassiosira weissflogii*.

L'impact des limitations en dSi et en NO_3^- a été étudié sur le cycle du silicium, à travers une expérience de dissolution de la diatomée *Thalassiosira weissflogii*, présentée dans le chapitre IV de cette thèse. Durant cette expérience, l'effet de ces limitations sur l'export de carbone à également été étudié, en collaboration avec Madeleine Goutx et Maxime Suroy, du Méditerranean Institut of Oceanography (MIO, Marseille). L'objectif de Maxime Suroy et de Madeleine Goutx, pendant cette expérience, était en partie de définir un protocole permettant de mesurer la composition des acides gras associés au frustule, afin de mieux comprendre le degré d'association entre les pools de lipides et le frustule et leur impact sur la reminéralisation de la $bSiO_2$ et des acides gras. Cette première étude a fait l'objet d'une publication, actuellement en révision dans Deep-Sea Research Part I, et présentée ici.

Fatty acids associated with the frustule of diatoms and their fate during degradation – a case study in *Thalassiosira weissflogii*.

Maxime Suroy[1], Brivaëla Moriceau[2], Boutorh Julia[2], Madeleine Goutx[1].

[1]Aix-Marseille Université, Université de Toulon, CNRS/INSU, IRD, Mediterranean Institute of Oceanography (MIO), UM 110, 13288, Marseille, Cedex 09, France.

[2]Université de Brest, Institut Universitaire Européen de la Mer (IUEM), CNRS, Laboratoire des Sciences de l'Environnement Marin, UMR 6539 CNRS/UBO/IFREMER/IRD, 29280 Plouzané, France.

Corresponding author: Suroy, Maxime:Maxime.suroy@univ-amu.fr. Tel. +0033 491829050

Abstract:

Diatoms are major actors in the export of organic carbon out of the euphotic zone. Yet, the processes linking biogenic silica and carbon sedimentation fluxes to deep oceanic layers remain unclear. Analysing organic fractions in biominerals is challenging because efficient cleaning often led to structural alteration of organic molecules. Hence, although lipids are widely used as biogeochemical markers in ocean flux study, few studies have dealt with the lipids that are associated with frustules. In the present study, a protocol was set up to extract and quantify the fatty acids associated to the frustule of the diatom species *Thalassiosira weissflogii*. The protocol involves solvent extraction of diatom external lipids, followed by clean frustule dissolution by 4% NaOH during 1h at 95°C and subsequent solvent re-extraction of frustule-associated lipids. Results confirmed that this protocol was efficient first, to isolate the frustule from the rest of the cellular organic carbon and second to extract and quantify fatty acids (FA) associated to frustules of this species. FA composition of the frustules was significantly different from that of the whole cells consisting primarily of 14:0, 16:0 and 18:0 FA, as well as a smaller portion of 16:1 and 18:1 unsaturated FA. Frustule-associated FA constituted 7 % of the total FA and 1.8 % of the total POC. The 30 days *T. weissflogii* degradation/dissolution experiment suggested that frustule FA 14:0 and 16:0 were mainly associated with the $bSiO_2$ phase dissolving slowly as no degradation of this pool was measured despite 78 % frustule dissolution. At the end of the degradation experiment, this pool constituted 5.8 % of the remaining total POC suggesting an effective protection by the frustule through strong interaction with the organic matrix which is consistent with the correlation observed at depth between Si and POC sedimentation fluxes.

Keywords: Frustule, Diatoms, Organic Carbon, Lipids, Carbon Export

I. Introduction

Diatoms are characterised by a silicified cell wall, commonly known as the frustule. This frustule partially consists of amorphous silica that forms mineral structures by precipitation of orthosilicic acid (Martin-Jézéquel et al., 2000). Such a structure presents great evolutionary advantages to cells, such as turgor resistance and protection against predation (Raven and Waite, 2004 and reference therein), or optical properties (Kucki, 2009), partially explaining the success of diatoms and the presumed number of diatom species (more than 200 000, Mann and Droop, 1996). This success is illustrated by diatom's predominant role in primary production in the ocean (Falkowski et al., 1998) but also in the export of organic matter (OM) to the ocean depths (Nelson et al., 1995; Volk and Hoffert, 1985). Diatom frustule-bound organic compounds are diverse. The formation of the frustule starts within silicon deposition vesicles and requires a peculiar association between organic compounds and silicon (Hildebrand, 2008). Many studies have demonstrated the role of proteins and polyamines during the precipitation of silica in diatoms (Brunner et al., 2009). The presence of sugars closely associated with frustule is also confirmed in recent studies, but their role in the biomineralisation process remains unclear (Chiovitti et al., 2005; Tesson and Hildebrand, 2013). In contrast, because they are not assumed to be functionally critical to the formation of the biogenic silica, little is known about the potential association of lipids in frustules.

Diatoms (Fileman et al., 1998) and frustule-bound organic compounds (Bridoux and Ingalls, 2010; Bridoux et al., 2012; Hedges et al., 2001; Ingalls et al., 2010) provide organic matter to the sediment. Compilation of deep sedimentation fluxes of POC and minerals (Armstrong et al., 2002; Buesseler, 1998; De La Rocha and Passow, 2007) show correlations between those fluxes. More specifically, deep sedimentation fluxes of particulate organic carbon (POC) and biogenic silica ($bSiO_2$) are also correlated when expressed basin by basin (Ragueneau et al., 2006). Using an independent data base, Ragueneau and co-workers (2002) showed that the evolution of the Si/C in all areas of the ocean can be predicted using an empirical relationship. In other words, the sinking of $bSiO_2$ and POC are linked in such a manner that knowing Si/C in the surface layer, one can theoretically extrapolate the flux of POC from the flux of $bSiO_2$. But what processes could explain such a link between the preserved fraction of organic matter and the $bSiO_2$?

The preservation of a fraction of organic matter during the sedimentation through the water column to the sediment depends on the balance between sinking and degradation processes. Biominerals in general and $bSiO_2$ in particular could impact both processes. As suggested by the ballast ratio hypothesis (Armstrong et al., 2009, 2002; Klaas and Archer, 2002), the sinking of organic matter ballasted by dense biominerals be it as shells or once incorporated to the same large particles

like aggregates or fecal pellets (Thornton, 2002; Turner, 2002) should be faster than the sinking of non-ballasted organic matter. Moreover $bSiO_2$ may also slow down the degradation as some studies hypothesized that the diatom frustule surrounding the cellular organic matter could protect the internal pool against bacterial degradation (Goutx et al., 2007; Moriceau et al., 2009). But these studies were undertaken on living diatoms and this hypothesis is not confirmed by degradation studies made on dead diatoms (Soler et al., 2010).

Other studies have evidenced the presence of another organic pool intimately linked to the frustule that could potentially explain the correlation between organic carbon and $bSiO_2$. This fraction of organic matter preserved at great depths is proportional to the flux of biominerals (Armstrong et al., 2009, 2002; François et al., 2002; Klaas and Archer, 2002; Ragueneau et al., 2006, 2002). In our study, we hypothesized that the preserved organic matter can be partially formed by the pool of lipids associated to or embedded in the silica matrix.

The presence of an organic coating has been so far mainly deduced from $bSiO_2$ dissolution experiments on whole versus cleaned frustule (Bidle and Azam, 1999; Kamatani and Riley, 1979; Patrick and Holding, 1985). From the experimental results described in the study by Bidle and Azam (1999), it seems that this pool is removed by bacteria within hours or few days after the death of diatoms. Only few diatoms can reach the sediment with an intact organic coating as shown by a minimum of 50 % dissolution of the $bSiO_2$ observed in most oceanic sites. The frustule-embedded OM is more difficult to assess as the chemical reagents known to dissolve the silica (NaOH, Na_2CO_3 and HF) generally react with the targeted polymer organic compounds. The inclusion of proteins in the silica matrix and their implication in silicification have been well-investigated (Hildebrand, 2003; Hildebrand et al., 2009; Kröger et al., 2002, 1999, 1997, 1994). The presence of other molecules less directly involved on silicification processes, such as lipids or sugars, has been much less studied.

Kates and Volcani (1968) described the lipid composition of the cell wall for the first time after breaking and washing the cells. To our knowledge, this study remains the only one dealing at the molecular level with lipids associated to diatom frustules. Recent works studied this organosilicon structure and noted the importance of lipid-like compounds embedded in the frustule of diatoms using spectroscopic methods (Soler et al., 2010; Tesson et al., 2008). These global methods that avoid dissolution procedures and the potential denaturation of most organic molecules, confirm the presence of OM associated with the frustule but did not reveal details about the structure and amounts of the classes of compounds detected.

In the present work, our approach combined the procedures of Ragueneau and Tréguer (1994) and Chiovitti et al. (2005) and enabled the complete dissolution of the frustules and the study

of released FA. The protocol was developed on the diatom *Thalassiosira weissflogii* and a 30-day dissolution/degradation experiment was carried out first to validate our protocol and second to understand the fate of frustule-associated lipids during biodegradation.

II. Material and Methods

1. Culture conditions and sampling

The strain *Thalassiosira weissflogii* (CCMP n°1049) was provided by the National Centre for Marine Algae and Microbiota. Three cultures (A, B and C cultures) were grown in f/2 medium under a 14/10 h light/dark cycle at 18 °C in 2 l glass flasks (Guillard and Ryther, 1962) in sterile conditions. Culture C was grown in another growth chamber under similar growth conditions (temperature, light intensity and cycles). Differences in the carbon content of cultured cells were observed (15.6 ± 0.2, 15.6 ± 0.1 and 10.9 ± 0.1 pmol.cell^{-1} in cultures A, B and C, respectively). The cell concentration was determined by flow cytometry (FACS Calibur, BD biosciences®).

Samples were collected as soon as cultures reached the stationary phase (~10^5 cell.ml^{-1} and 15 days of growth). Triplicate of 10 ml of culture were sampled in cultures B and C for the 'whole cells' analysis and filtered on pre-combusted GF/F filters (0.7-µm mesh size) as generally done in other studies (Table 1). Lipids from whole cells were extracted according to the Bligh and Dyer protocol (1959) and thus do not include the frustule-associated fraction. Culture A was not sampled for lipid composition analysis in whole cells. The carbon content of cells in batch A was similar to that of cells in batch B, suggesting composition similarity between A and B cultures. Except the 20:5(n-3) FA (see Fig. 4 below), this latter assumption was supported by the low SD of average percentages of individual FA in total FA, derived from the analysis of FA in triplicate samples from both B and C cultures. To obtain the 'pellet' samples, triplicates of 50 ml of the three cultures were centrifuged at 5400 *g* (20 min).

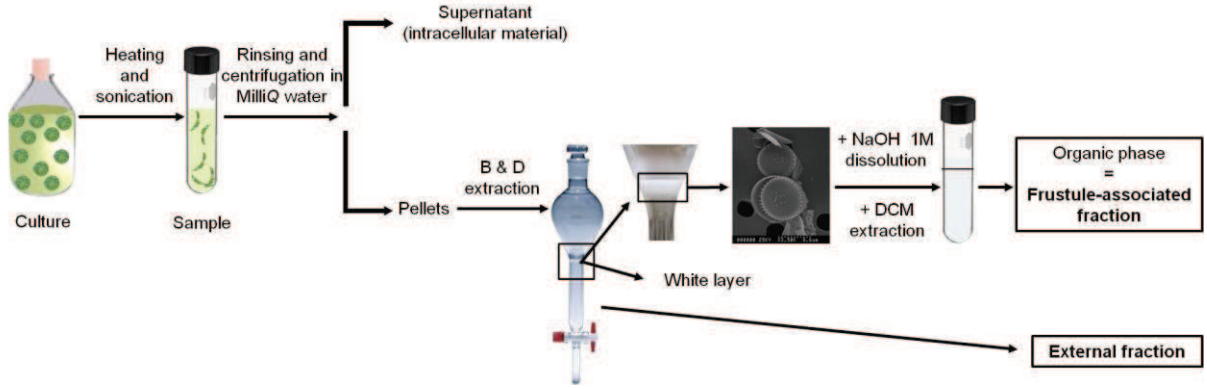

Figure 1. Schematic representation showing the different steps of the protocol. Cells are broken using hot sonication and centrifuged three times with milli*Q* water to remove intracellular material. Pellets of fragmented frustules are then extracted using organic solvents following the Bligh and Dyer protocol (B&D). The organic phase contains the external fraction. Frustules accumulated at the interface form a "white layer" composed of washed frustules (see photo of scanning electron microscopy). Frustules are dissolved with NaOH 1M at 95 °C to release frustule-associated fraction that is further extracted with CH_2Cl_2 at pH<2.

2. Frustule isolation

Pellet samples were resuspended in 40 ml milli*Q* water and were hot-sonicated at 70 °C for 5 min to fragment the cells (Fig. 1). Tubes were subsequently centrifuged at 5400 *g* for 40 min at 4 °C. The supernatants were removed, and this step was repeated once at lower centrifugation speed (3800 *g* for 20 min) to eliminate any non-frustule material. After removing the supernatant, the pellets were again resuspended in 40 ml milli*Q* water and centrifuged at 3200 *g* for 20 min. This treatment cleared the frustules from most cell content. However, fluorescence of chlorophyll molecules was noticeable on flow cytometer analysis of the washed pellets indicating external organic material still present on frustule fragments (Fig.2).

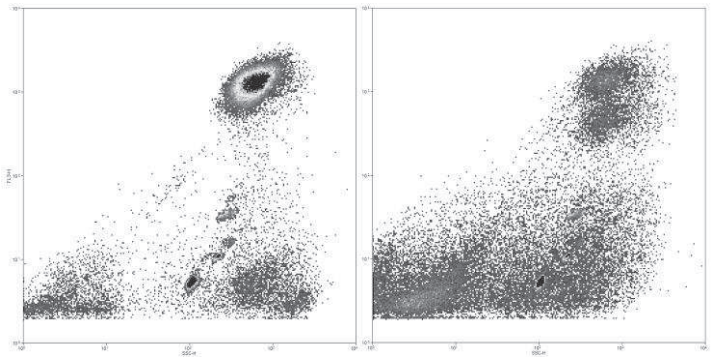

Figure 2. Cytograms of whole cells (A) and isolated frustules after three centrifugations with 40 ml of Milli*Q* water (B). Cytograms represent the chlorophyll fluorescence of particles function of their granularity (side scatter). Some frustules still show fluorescence of chlorophyll molecules indicating presence of external material.

In a second step, this external organic material probably more intimately linked to the frustules than the previous cell content, was separated from fragmented frustules using a modified protocol of Bligh and Dyer. Briefly, the washed pellets were transferred to glass tubes. A monophasic mixture of dichloromethane/methanol/1M salt water (1/2/0.8, v/v/v) (9.5 ml) was added for the lipid extraction. After the addition of an internal standard (nonadecanoic acid methyl ester, Me19:0, Sigma Aldrich®) and sonication (10 min), tube contents were transferred to separatory funnels. Tubes were rinsed with 9.5 ml of the monophasic mixture. The separatory funnel contents were made biphasic by adding 5 ml dichloromethane (DCM) and 5 ml milli*Q* water. After vigorous shaking and settling, the organic phases were collected, and the aqueous phases were re-extracted with 10 ml DCM. The organic phases were combined and concentrated under a gentle flux of nitrogen. The lipid extracts such obtained from the pellets of isolated frustules constituted our lipid 'external' fractions.

3. Extraction of frustule-associated lipids

Frustules cleaned from their 'external' fraction were visualised by scanning electronic microscopy during the cleaning procedure to check for their integrity and the absence of 'external' organic matter at the end of this step. Frustule fragments formed a white layer at the basis of the aqueous phase (methanol/water mixture) remaining in the separatory funnel after the Bligh and Dyer extraction (Fig. 1). Scanning electron microscopy analysis of this white layer samples showed an amalgam of clean silica frustules (Fig. 3). Hydrophilic compounds that may be present in the aqueous phase were not analysed further. The white layer and the top aqueous phase were transferred into glass bottle in which sodium hydroxide (1 $mol.l^{-1}$ final concentration) was added. These bottles were later transferred to a water bath at 95 °C for 1 h to promote the entire dissolution of frustules. The basic reactant not only dissolves the silica matrix but can cleave covalent associations between FA and polymers. After a rapid cooling on ice, the bottle contents were acidified using HCl and re-extracted in a liquid-liquid phase using 50 ml DCM (the aqueous phase was approximately 70 ml). This last extraction step was repeated three times to ensure the complete extraction of the remaining lipids in the aqueous phase. Extracts thus obtained were called the 'frustule-associated' fractions. The internal standard (Me19:0) was not added before dissolved frustule extraction in order to control the absence of contamination in the 'frustule-associated' extract from the 'external' fraction. Consequently, the same extraction recovery was used for the quantification of both 'external' and 'frustule-associated' lipids.

4. Biodegradation experiment

For the degradation experiment, the *T. weissflogii* strain was supplied and grown in a large volume culture by the Experimental Station of Argenton (Ifremer, France). Cells were pelleted and

killed by freezing at -20 °C for 4 days. Pellets were resuspended in a Nalgene® flask filled with 10 l of 0.7-µm filtered seawater from Brest Bay (France). The 0.7-µm filtered water contained the natural prokaryotic community required to degrade and utilize the algal material as growth substrate. The flask was incubated on an orbital shaker table at 70 rpm in the dark at 18 °C. The degradation experiment lasted 30 days. Samples (50 ml) were collected from the flask every 6 days, in duplicate or triplicate, and subjected to centrifugation for frustule isolation and lipid extraction as described in the previous section. Briefly, cells were sonicated, pelleted to remove medium and extracted according to Bligh and Dyer for analysis of external FA composition. Cleaned frustules were submitted to NaOH dissolution and re-extracted for analysis of frustule-associated FA fraction.

5. Bulk parameters: $bSiO_2$, POC and prokaryotic concentrations

$bSiO_2$ and POC concentrations were followed during the whole degradation experiment by filtering 10 ml of the batch content on polycarbonate (0.4-µm mesh size) and GF/F (0.7-µm mesh size) filters, respectively.

$bSiO_2$ concentrations were measured using a variation of the method of Ragueneau and Tréguer (1994) described in Moriceau et al. (2009). Filters were digested in 20 mL of 0.2 M NaOH for 3 hours at 95°C and stirred regularly to ensure the dissolution of all $bSiO_2$. As no lithogenic silica was present in the diatom culture, only one longer digestion step was done. The solution was then acidified with 5mL of HCl 1M, centrifuged to remove solids and analysed for silicic acid concentrations (dSi). dSi was measured using the molybdate blue spectrophotometric method of Mullin and Riley (1955), as adapted by Tréguer and Le Corre, (1975) and modified by Gordon et al. (1993) for use in segmented flow colorimetry. We used a Bran and Luebbe Technicon Autoanalyser (<1% precision).POC filters were desiccated overnight in an oven at 50 °C, and POC was quantified by using a Carlo Erba NA 2100 CN analyser coupled to a Finnigan Delta S mass spectrometer.

Prokaryotes were counted over time in 10 ml samples to assess their growth. Free and attached prokaryotes were separated by filtration (3-µm mesh size) and counted on black 0.2-µm filters after staining with DAPI (4',6-diamidino-2-phenylindole).

Prokaryotic carbon in degradation flask samples was calculated by using conversion factors (20 and 50 x 10^{-15} molC.cell^{-1} for free and attached prokaryotes, respectively) according to Turley and Mackie (1994) for the north-eastern Atlantic Ocean.

6. Lipid analysis

a. Derivatisation and purification.

Lipid extracts were trans-esterified using BF_3-Methanol and toluene for 1 h at 70 °C. Fatty acid methyl esters (FAME) were extracted from the mixture with 3 x 2 ml of Hexane/Ethyl Ether (98/2, v/v) and evaporated to dryness under nitrogen. FAME were purified onto a bond elute microcolumn with a mix of Hexane-Ethylacetate (99/1, v/v). Columns were conditioned with 9 ml Hexane-Ethyl Acetate (99/1, v/v) followed by 3 ml Hexane. Columns were rinsed with 1.4 ml Hexane (to remove hydrocarbons), and FAMEs were eluted by 1.6 ml Hexane-Ethyl Acetate (99/1, v/v).

Extracts from the degradation experiment were first saponified (KOH 1 $mol.l^{-1}$ for 1 h at 70 °C) and were silylated using a N,O-bis(trimethysilyl)trifluoroacetamide (BSTFA)-pyridine mixture according to Rontani et al. (2011). Briefly, after saponification, BSTFA and pyridine were added to the dried lipid extract (1/2, v/v). Tubes were placed at 50 °C for 1 h, and then their contents were dried under a gentle stream of nitrogen and resuspended in ethyl acetate and BSTFA. This reaction transforms OH-containing molecules to their trimethylsilyl (TMS) derivatives. Injections of trimethylsilyl ether (TMSE) were made in the 12 hrs following derivatisation due to their unstable nature. This method allowed us to analyse FA, sterols and phytol simultaneously in their TMS ether forms. Indeed, the phytil side chain of chlorophyll is released during saponification (phytol) and transformed to its TMS derivative. Sterols are also present in diatoms, primarily in a free form (*i.e.*, non-esterified, Volkman and Hallegraeff, 1988). Four sterols (Volkman and Hallegraeff, 1988) were identified, but we combined them in this study. Sterols were quantified by reference to a calibration curve of a cholesterol standard. The quantification of phytol was semi-quantitative using a calibration curve of TMS20:0.

The impact on PUFA of the step involving heating the silica/organic matter complex was tested. The percentage recoveries of arachidonic acid (20:4(n-6)) after incubation for one hour both at 40 °C and 70 °C were in the range of the RSD. Other authors also reported saponification of lipid extracts at 100 °C without noticeable effect on poly-unsaturated FA quantification (Chen et al., 2011; Goutx et al., 2007).

b. GC/MS analysis.

FAME and TMSE were analysed by gas chromatography/mass spectrometer (GC/MS) (TraceISQ, ThermoElectron) at an ionization energy of 70 eV for *m/z* range of 50-400 for FAME and 50-600 for TMSE, using hydrogen as carrier gas at a flow rate of 1.2 $ml.min^{-1}$. The injector (used in splitless mode) and detector temperatures were 250 and 320 °C respectively. For FAME analysis, the initial column temperature was held for 2 min at 70 °C then ramped at 12 $°C.min^{-1}$ (ramp 1) to 140 °C, and then at 5 $°C.min^{-1}$ (ramp 2) to 200 °C, which was held for 5 min, then finally ramped at 12 $°C.min^{-1}$ (ramp 3) to 275 °C and held for 10 min. FA, sterols and phytol from the degradation

experiment were analysed in their TMS forms using the same conditions as FAME analysis on the same GC/MS. The ramp temperature only was modified as follow: the initial temperature was set at 70 °C and successively increased to 130 °C at 20 °C.min^{-1}, then to 250 °C at 5 °C.min^{-1} and finally at 3 °C.min^{-1} to 300 °C, held for 40 min. The source temperature was set at 200 °C. FAME and TMSE were identified by comparison with retention time and mass spectra of commercial standards (provided by Sigma Aldrich®) and quantified by reference to calibration curves. The positions of the double bounds were all identified with the exception of that of 16:1, 16:2 and 24:1 for which we did not run standards. All determination coefficients were up to 0.99. Tricosanoic acid methyl ester standard (Me23:0) was introduced prior to injection to check analytical variability. The mean analytical recovery, taking into account all preparative steps except dissolution, was in the range of the Relative Standard Deviation (4 to 9 % for peak areas and from 0.04 to 0.11 % for the retention time) and was approximately 83 %. As we did not add any standard to the frustule-bound fraction, internal standard (19:0 in its trimethylsilyl or methyl form) was used to check whether any cellular material (that contained the internal standard) may have contaminated the 'frustule-bound' fraction. All concentration values were blank and recovery corrected.

7. Flow cytometry.

Samples were analysed using the FACSCalibur (BD Biosciences®) of the PRECYM flow cytometry platform (http://precym.com.univ-mrs.fr) equipped with a blue (488 nm) air-cooled argon laser and a red (634 nm) diode laser. Data were collected using the CellQuest software (BD Biosciences®). The analysis was performed *a posteriori* using SUMMIT v4.3 software (Beckman Coulter). *T. weissflogii* cells were optically resolved based on their intensities in light scatter and red fluorescence (chlorophyll *a* related). TruCount beads (BD Biosciences®) and 2-µm beads (Fluoresbrite YG, Polyscience®) were added to the samples as an internal standard to monitor the instrument stability and to determine the volume analysed by the instrument. Flow cytometry analysis was used to test frustule isolation and to measure prokaryotic presence in samples without additional prokaryotic counting.

8. Statistical analysis.

All analyses were performed with R (R Core Team, 2012), a freeware for statistical analysis available at http://cran.r-project.org/. A Mann-Whitney *U* test was also used to test the hypothesis H_0 that there is no difference between FA concentration averages during the degradation experiment. We fixed the significance level at 5 %.

To compare the FA profiles of ‘whole cells’, ‘extrenal’ and ‘frustule-associated’ fractions, a classical multidimensional scaling (MDS) was used on an Euclidean distance matrix of FA standardised concentrations. Using k-means clustering, we partitioned our samples into three groups. The number of clusters in this analysis must be defined by the analyst. We choose three clusters because we have three sample types and also because it was the result of the estimation by optimum average silhouette width using the fpc package in the R software (Christian, 2010). Confident ellipses at 50 and 95 % were added to the plot to represent results from cluster analysis and to comfort MDS observations.

Table 1. Fatty Acid (FA) compositions (mol %) of diatoms from the *Thalassiosira* genus.

	T.pseudonana[1]	*T.pseudonana*[2*]	*T.pseudonana*[2§]	*T.oceanica*[2*]	*T.oceanica*[2§]	*T.weissflogii*[3α]	*T.weissflogii*[3β]	*T.weissflogii*[4]
Saturates								
12:0	Tr	-	-	-	-	-	-	-
14:0	14.3	3.5	6.1	18.4	10.0	9.1	8.5	6.2
15:0	0.8	0.6	1.0	1.6	1.1	1.3	1.3	0.9
16:0	11.2	18.4	26.9	23.0	23.7	28.3	26.4	26.4
17:0	0.1	-	-	-	-	-	-	-
18:0	0.7	1.6	1.4	0.3	1.0	1.1	0.2	0.9
20:0	0.1	1.1	0.3	-	-	-	-	0.2
22:0	Tr	-	-	-	-	-	-	0.1
24:0	Tr	-	-	-	-	0.1	0.1	0.1
Sum %	27.2	25.2	35.7	43.3	35.8	39.9	36.5	34.8
Mono-UNS								
16:1(n-13)t	0.4	Tr	-	0.5	-	0.4[Ω]	0.3[Ω]	-
16:1(n-7)	18.0	21.0	32.0	30.0	25.8	40.5	40.8	18.3
16:1(n-5)	0.3	1.6	Tr	Tr	0.2	0.6[Ω]	0.7[Ω]	0.8[ϕ]
18:1(n-9)	0.5	2.0	1.5	0.5	5.0	0.5	0.5	0.5
18:1(n-7)	0.1	0.1	0.2	4.0	Tr	0.2	0.1	0.6
20:1(n-9)	0.2	-	-	-	-	-	-	Tr
24:1	-	-	-	-	-	0.3	0.1	0.1[ϕ]
Sum %	19.5	24.7	33.7	35.0	31.0	41.2	41.4	20.3
Poly-UNS								
16:2(n-7)	2.7	1.1	1.8	0.7	-	-	-	-
16:2(n-4)	4.5	0.7	1.4	1.4	-	-	-	6.6[ϕ]
16:3(n-4)	12.7	7.1	4.8	3.5	6.4	5.8[Ω]	6.6[Ω]	12.3
16:4(n-1)	2.3	2.3	0.8	0.8	3.9	-	-	-
18:2(n-9)	Tr	-	-	-	-	-	-	-
18:2(n-6)	0.4	1.8	1.3	1.0	1.1	0.7	0.6	0.2

18:3(n-6)	0.2	-	-	-	-	-	-	-
18:3(n-3)	0.1	0.8	0.7	1.1	0.9	-	-	-
18:4(n-3)	5.3	5.8	4.0	1.8	5.2	2.6	3.1	1.4
20:4(n-6)	0.3	1.1	0.9	Tr	Tr	θ	θ	Tr
20:4(n-3)	0.3	-	-	-	-	-	-	-
20:5(n-3)	19.3	23.9	12.1	11.0	13.4	7.4	9.6	22.5
22:6(n-3)	3.9	3.5	1.5	1.4	0.8	0.9	0.1	1.9
Sum %	52.0	48.1	29.3	22.7	31.7	11.9	13.5	44.9
other	1.3	2.0	1.3	0.4	1.5	0.3	0.1	-
Total	100.0	100.0	100.0	101.4	100.0	100.1	99.1	100.0

[1]From Volkman et al. (1989). Culture was made in G/2 medium and with a 12hr/12hr light/dark cycle at 20 °C.

[2]From Volkman and Hallegraeff (1988)**.** FA were analyzed in free fatty acids[*] and triacylglycerols[§] separately in two different species grown in f/2 medium (enriched with Na-EDTA for T. oceanica) and with a 12hr/12hr light/dark cycle at 17.5 °C.

[3]From Klein Breteler et al. (2005). Their results are presented from two separated continuous cultures of *T. weissflogii* ([3α] and [3β]) grown on f/2 medium and with a 16hr/8hr light dark cycle at 15 °C. [Ω]Double bond position is not indicated for three FA: 16:1, 16:1 and 16:3. For a convenient presentation, we assume their identity according to their contribution. [θ]Two FA, 20:4(n-6) and 20:5(n-3), are pooled in their study.

[4]From this study (average of two independent cultures). [Φ]In our study, the position of some double bonds are not localized.

Tr = Trace<0.05% as we assume in Volkman and Hallegraeff (1988). For non detected FA, a – is indicated. UNS = unsaturated.

III. Results

1. FA composition of *Thalassiosira weissflogii*

Whole cells (WC) fractions from two different cultures (B and C) had similar FA compositions. The average composition (n = 6) was also similar to literature data on the same genus (Table 1) and did not show obvious differences despite various methodologies used in previous studies (Table 1). The composition of WC was dominated by palmitic acid 16:0 (26.4 ± 3.4 %, n = 6) (Table 1). The other dominant FA were those classically found in diatoms: palmitoleic acid (16:1(n-7)) and eicosapentaenoic acid (20:5(n-3) or EPA) (18.3 ± 4.3 % and 22.5 ± 9.6 %, respectively). A characteristic feature was the dominance of 16-carbon atom unsaturated FA compared to 18-carbon atom unsaturated FA (38.0 % versus 2.7 %, respectively) (Table 1). Also, 20:0 and 22:0 saturated FA were found in notably low amounts (their sum was < 0.5 %), but their presence was confirmed by the analysis of their mass spectra. Traces of heptadecanoic acid (17:0) and pentadecenoic acid (15:1) represented less than 0.1 % of the total FA in WC. Those FA are generally attributed to prokaryotes (Kaneda, 1991). Considering their low contribution to the total composition, the share of these FA most likely reflected the presence of few bacteria. This scarcity was confirmed by flow cytometry, which showed notably few microorganisms other than diatoms in the cultures (Fig. 2). Therefore, we did not take these bacterial markers into account in the FA profile of *T. weissflogii*.

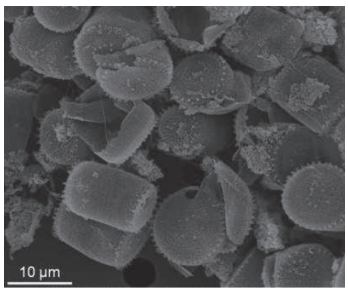

Figure 3. Frustules fragments of *Thalassiosira weissflogii* freed from their “external fraction” observed in scanning electron microscopy.

The ‘external’ fractions showed of the three cultures (A, B, and C), as for whole cells, a dominance of 16:0, 16:1(n-7) and 20:5(n-3) FA (18.0 ± 4.4 %, 18.2 ± 3.2 % and 28.6 ± 6.8 %, respectively, n = 9) (Fig. 4). Taking into account the 16:2 and 16:3(n-4) FA, these FA represented more than 85.9 % of the total FA for both WC and ‘external’ fractions.

The 'frustule-associated' fraction was dominated by saturated 14:0 and 16:0 FA (17.3 ± 5.9 % and 57.0 ± 4.9 %, respectively) (Fig. 4). This predominance of saturated FA led to a lower contribution of other FA. Contrarily to the WC and 'external' fraction, unsaturated FA with 16-carbon atoms were much less abundant in frustule-associated fraction (38.0 %, 41 % and 10.8 % in WC, 'external' and 'frustule-associated' fractions, respectively) (Fig. 4). Moreover, no branched nor 17:0 FA prokaryote markers were found in these fractions emphasizing the non-contamination of 'frustule-associated' fraction. The major difference with FA composition of the whole cell was the low degree of unsaturation of the FA from the frustule.

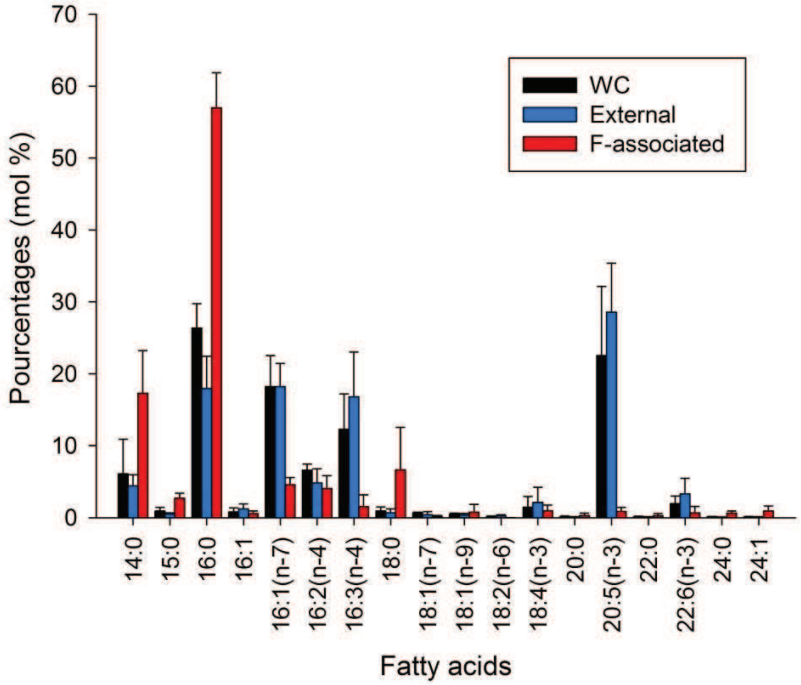

Figure 4. Relative FA compositions of whole cells, external and frustule-associated fractions. All samples are gathered under each bar by averaging the FA contribution in each culture. n = 6 for whole cells (culture B and C) and n = 9 for the two other fractions (cultures A, B and C). Error bars represent the standard deviation.

Using k-means clustering method and MDS, comparison of FA profiles enabled to identify three "groups": WC and 'external' fractions from culture A and B on the one hand, WC and 'external' fractions from culture C on the other hand, and a third group composed of 'frustule-associated' fractions from all cultures (Fig. 5). The fact that A, B and C 'frustule-associated' fractions were gathered together emphasized the specificity of frustule FA profiles regardless of the culture conditions. The difference between culture C and the two other cultures may be explained by a higher contribution and variability

of 20:5(n-3) FA in culture C in both 'external' and whole cells samples (Fig. 4), which were most probably related to the different growth chamber (see section 2.1) or to a lag time for the sampling regarding the growth curve.

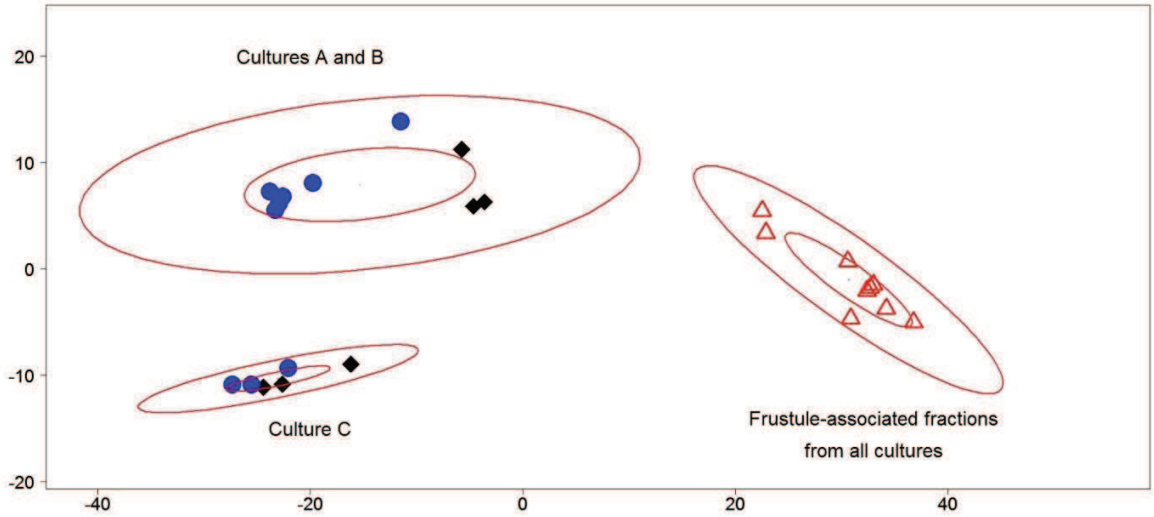

Figure 5. Graphical representation of the classical multidimensional scaling analysis of whole cells samples (black diamonds), external fractions (grey dots) and frustule-associated fractions (white triangles). Confident ellipses containing 50 and 95% of the data used to build clusters obtained from *k*-means analysis are represented.

2. Biotic degradation of diatom cells

Diatom material for the degradation experiment was obtained from the continuous reactor culture from Argenton. The overall degradation of the diatom material was reflected in the decrease of both POC and $bSiO_2$ concentrations over the 30-day incubation period (from 1480.2 to 496.6 ± 14.5 $\mu mol.l^{-1}$ and from 342.9 $\mu mol.l^{-1}$ to 76.4 ± 2.4 $\mu mol.l^{-1}$ for POC and $bSiO_2$, respectively) (Fig. 6). As expected, prokaryotes largely contributed to diatom decomposition, as shown by the increase in prokaryotic carbon during the first 4 days (Fig. 6). A total of 22 % of the initial $bSiO_2$ still remained in the batch at the end of the incubation experiment.

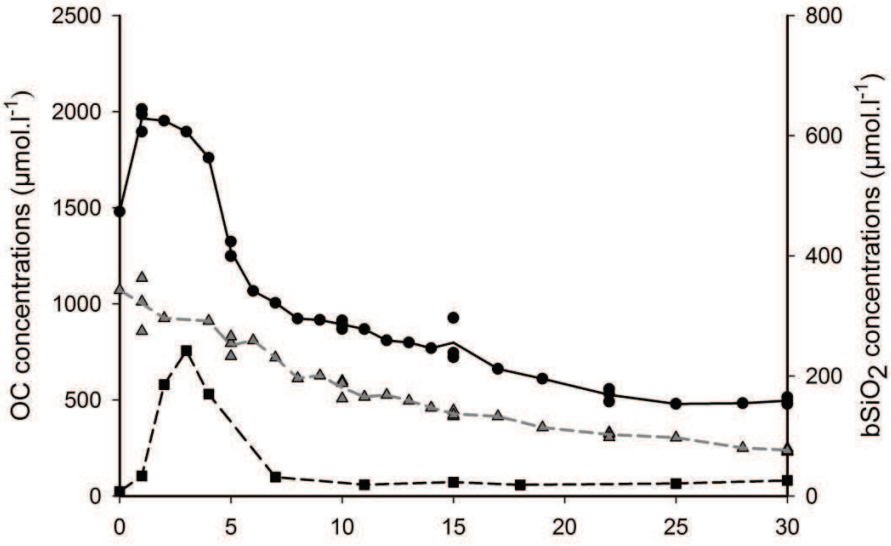

Figure 6. Evolution of concentrations of total POC (black dots), bacterial OC (black squares), and biogenic silica ($bSiO_2$, grey triangles) during the course of the degradation experiment. Solid and dashed lines represent averaged value for each parameter. OC (particulate and bacterial) and $bSiO_2$ concentrations are expressed as $\mu mol.l^{-1}$. For a convenient representation, the y axis for $bSiO_2$ concentration is on the right of the graph.

During the course of the degradation experiment, we focused on the kinetics of 'frustule-associated' FA and compared them with the kinetics of external lipids to highlight differences in degradation trends of the two fractions. External phytol and sterols represented 10.5 ± 3.2 % of the total external lipid pool (FA + Sterols + Phytol) at day 0. Their decrease over time from 17.7 ± 5.9 µmol $C.l^{-1}$ to below the detection limit at day 18 for phytol and from 18.0 ± 6.3 µmol $C.l^{-1}$ to 5.6 ± 0.8 µmol$C.l^{-1}$ for sterols, well reflected the degradation of external algal material (Fig. 7). Four main sterols were found and quantified over the course of the degradation experiment (data not shown). Total sterol concentrations exhibited an increase at day 6, mainly because of the analytical variability that was quite high between replicates. In particular at day 6, one sample over the 3 replicates was different and more concentrated than the 2 others resulting in the high standard deviation particularly noticeable at day 6 on Figure 7. This increase was due to the 24-methylene cholesterol. We do not believe that this increase had significance in term of a specific process occurring at day 6. More interesting was the fact that from day 6 to the end of the degradation/dissolution experiment, phytoplankton sterols decreased over time, and were never observed in the frustule-associated fractions indicating a good separation between external lipids and frustule-associated' lipids. This observation and the fact that the internal standard

(19:0) added to the pellet extraction medium has never been found in the 'frustule-associated' fraction confirmed that our protocol accurately separated these two fractions.

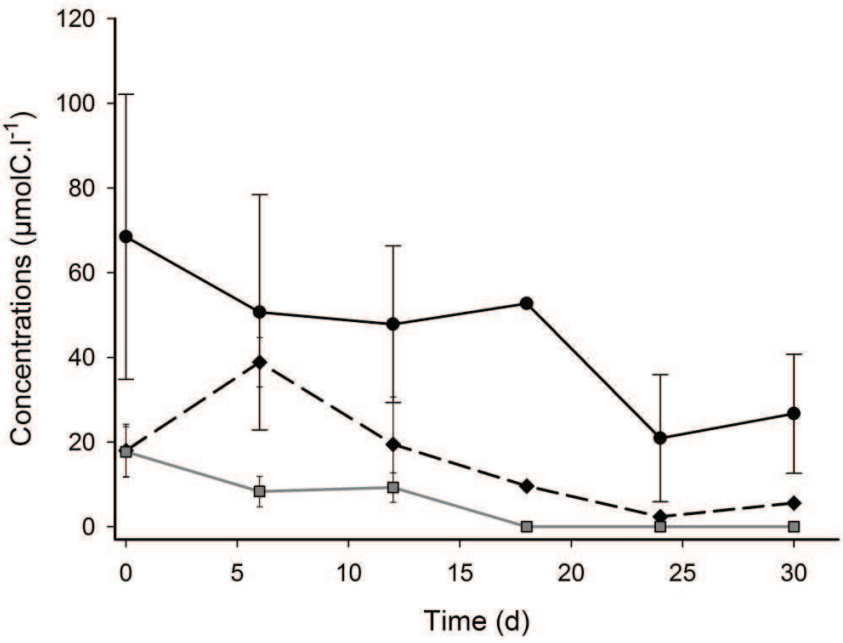

Figure 7. Concentrations (µmolC.l^{-1}) of total unsaturated FA (black dots and solid line), total sterols (black diamonds and dashed line) and phytol (grey squares and line) in external fractions at each sampling day during the course of the degradation experiment. Error bars represent standard deviation (n = 3). After day 12, phytol concentrations were under detection limit. At day 18, n=1.

The saturated FA proportion (especially 18:0) of the 'external' fraction during degradation was higher than in cultures used to set up the protocol. Several factors may increase saturated FA in pellets. The culture used for degradation was more mature than culture used to set up the protocol and proportions of unsaturated FA more susceptible to oxidative attack than saturated ones, decrease in mature cells. Moreover, prokaryotes enriched in saturated FA, were present in the culture medium at initial time of the degradation. In addition to this, centrifugation used to sample the pellet for the degradation experiment concentrates OM in general and not only diatoms. Thus, there was no possible interpretation of the kinetics of degradation of external saturated FA. On the opposite, unsaturated FA that dominated the FA in the diatom *Thalassiosira weissflogii* (50.7±6.5 % of Total FA) (Table 1) may be taken as markers of fresh diatom material (Balzano et al., 2011; Najdek et al., 2002). They were proportionally less concentrated in the "degradation culture" (Table 2). However, their decay over time (from 68.5 ± 27.5 µmol C.l^{-1} to 26.7 ± 10.2 µmol C.l^{-1} between days 0 and 30) (Fig. 7) reflected the

prokaryotic degradation of the algal lipids. Unsaturated FA individual components (Fig. 8), that characterized the algae in both the WC and external fractions (namely C16:1n7, C16:2n4, C16:3n4, C18:1n7, C18:1n9, C20:5n3 and C22:6n3) (Fig. 4), also showed a similar decrease over time at various degree depending on the component. Polyunsaturated FA almost disappeared after 12 days incubation (a little later for C16:3n4) whereas C16:1n7, C18:1n7 showed their stronger decrease at days 24. The slowest decrease was observed for the C18:1n9 at days 30.

Table 2. FA compositions (mol %) of *Thalassiosira weissflogii* in this study.

	T.weissflogii[a]	*T.weissflogii* for degradation[b]
Saturates		
14:0	6.2	4.2
15:0	0.9	2.1
16:0	26.4	37.3*
18:0	0.9	32.5*
20:0	0.2	0.9
22:0	0.1	-
24:0	0.1	0.4
Sum %	34.8	77.4
Mono-UNS		
16:1(n-7)	18.3	4.0
16:1	0.8	1.0
16:1$^{\phi}$	-	0.3$^{\phi}$
18:1(n-9)	0.5	2.6
18:1(n-7)	0.6	2.3
20:1(n-9)	Tr	-
24:1	0.1	-
Sum %	20.3	10.2
Poly-UNS		
16:2	6.6	1.4
16:3(n-4)	12.3	1.6
18:2(n-6)	0.2	0.7
18:4(n-3)	1.4	-
20:3	-	0.3
20:4(n-6)	Tr	0.4
20:5(n-3)	22.5	5.9
22:6(n-3)	1.9	2.1

Sum %	44.9	12.4
Total	100.0	100.0

[a]FA composition at the end of the growth phase (average of the two cultures, n = 6).

[b]FA composition at the beginning of the degradation experiment (n = 3).

[*]Some FA bacterial markers were found in lipid extracts from degradation experiment samples (15:0iso, 15:0anteiso and 17:0). We choose to not take them into account and keep the composition found during growth of *T. weissflogii*. However, it is clear that other FA such as palmitic and stearic acids are shared by diatoms and bacteria.

[Φ]Another 16:1 FA was found in FA profiles but the position of its double bond was not localized.

At the beginning of the degradation experiment, saturated FA, 14:0, 16:0 and 18:0, constituted the major part of the 'frustule-associated' FA (92.5 % of the total FA), as seen in the diatom cultures (Fig. 3). The concentration of the frustule-associated saturated FA 14:0 and 16:0 did not exhibit significant differences over time (Fig. 9), whereas the concentration of 18:0 decreased significantly after day 12 (Mann-Whitney *U* test, $p < 0.05$). This finding suggested a different association with silica phases of the 18:0 compared to the 14:0 and 16:0. Possibly, 18:0 was associated with a more soluble silica phase, the dissolution of this phase being then necessary for 18:0 to be bioavailable. Unsaturated FA such as hexadecenoic acid 16:1 and oleic acid (18:1(n-9)) were still present in the frustule of *T. weissflogii* at the end of incubation. More generally, these results were in line with a protective effect of the frustule on its associated lipid fraction.

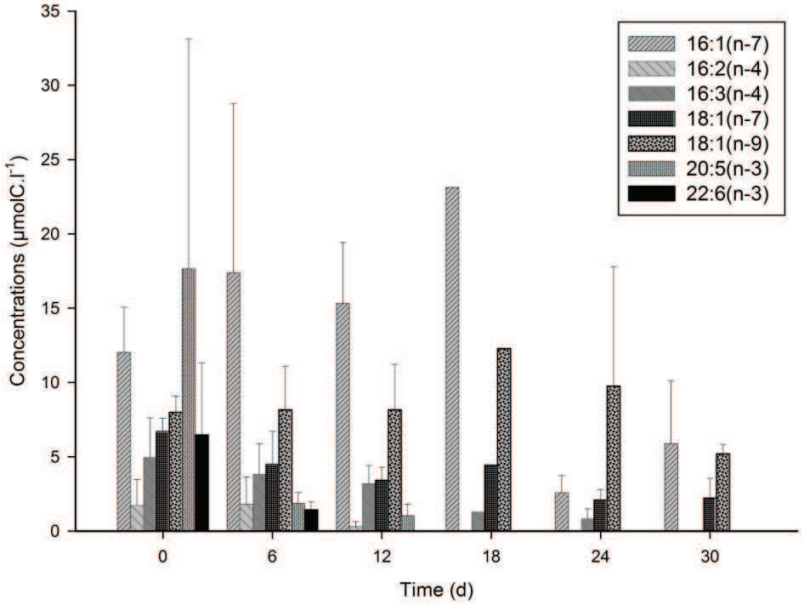

Figure 8. Concentrations (µmolC.l^{-1}) of individual unsaturated FA characteristic of external fractions at each sampling day during the course of the degradation experiment. Error bars represent standard deviation (n = 3). At day 18 and 30, n = 1.

IV. Discussion

1. Evidence for frustule-associated fatty acids in *Thalassiosira weissflogii*

The FA composition of *Thalassiosira weissflogii* was similar to that reported in the literature for diatoms, with a predominance of 16:0, 16:1(n-7) and 20:5(n-3), which are often used as diatom markers (Dalsgaard et al., 2003) (Table 1). The proportions of saturated FA (approximately 35 %) were comparable to those found in the same species. Only few composition differences existed compared to results on the same species from Klein Breteler et al. (2005), with respect to unsaturated FA, especially the proportions of 16:1(n-7) and 20:5(n-3). This may come from differences in growth conditions (detailed in Table 1) known to impact physiological status and biochemical pools (Coombs et al., 1967; Vrieling et al., 1999).

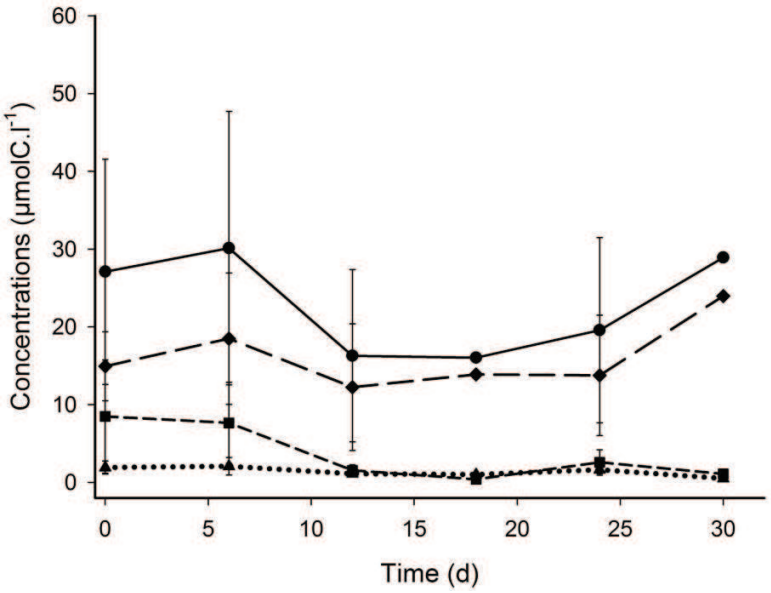

Figure 9. Mean concentrations (µmolC.l^{-1}) of total FA (dots and solid line), saturated 14:0 (triangles and dotted line), 16:0 (diamonds and long-dashed line) and 18:0 (squares and short-dashed line) in frustule-associated material during the degradation. Error bars represent standard deviation (n = 3). At day 18 and day 30, n = 1. Note that the pattern of concentration increase at day 18 may be due to this unique sample.

In addition to these cellular lipids, our study showed that a significant pool of FA inaccessible to conventional lipid extraction technics was associated to the frustule of the diatom *Thalassiosira weissflogii*. It is now well established that existing interactions between the silica frustule and the organic

matter depends on the diatom freshness or at the opposite of their burial period up to their fossilization in sediments. Breaking these interactions requires the use of either strong acids or oxidizing agents, either solvent. Depending on objectives, some protocols are adapted to the study of the silica content of the frustule and aim at denaturing and removing all organic material that it contains (Kamatani, 1971; Loucaides et al., 2008), others require the removal of silica to release organic matter (Bridoux and Ingalls, 2010; Ingalls et al 2003; Kröger et al 1994). In the latter case, the difficulty lies in preserving the integrity of the molecular structures after treatment of the sample. Recently, Morales et al. (2013) proposed a successful protocol to clean fresh diatoms for isotopic analysis of diatom frustule-bound nitrogen. However, the harsh oxidative treatment transformed all organic nitrogen into nitrates preventing analysis of biochemical groups and molecular structures.

To our knowledge the first characterisation of a lipid pool embedded into the frustules of *T. weissflogii* was done by using nuclear magnetic resonance on SDS/EDTA/H_2O_2 extracted frustules of *T. pseudonana* by Tesson et al. (2008). Their results indicated the presence of C=C from double bonds, -(CH_n)- from aliphatic chains and C=O from carbonyl groups of FA. Previously, Kates and Volcani (1968) were the first to strongly demonstrate a lipid/frustule association in seven marine diatom species and to analyse FA. These authors washed frustules using distilled water and they added, after a Bligh and Dyer lipid extraction, a methanolic-HCl step to cleave bound-lipids. As such, the cell wall lipid composition was likely dominated by cellular material together with externally bound-lipids as no silica dissolution step was included in the protocol, as shown by our experiment in which fatty acid composition of external fraction was mainly identical to the fatty acid composition of the whole cell.

In our study, we pushed a step further the protocol of Kate and Volcani by adding an hot NaOH silica dissolution step after the first B&D extraction of washed fragmented diatom pellets. Briefly, in our protocol, frustule pellets were isolated from the cellular material by sequential washings and centrifugation of fragmented diatoms in pure water followed by a B&D extraction of external lipids. Then, silica frustules were dissolved with NaOH (1mol. l^{-1}) and re-extracted at acidic pH by dichloromethane solvent to obtain the frustule-associated lipids. Long chain carboxylic acids are major constituents of diatom lipids. They are free or esterified to glycerol, to other alcohols, or to more complex glycosidic and phosphatidic moieties. After sonication and water washing treatments, a fraction of the cellular lipids remained attached to the silica frustule through either hydrogen bonding, or electrostatic and hydrophobic interactions with other molecules constitutive of the cell wall. This was

confirmed by the flow cytometry analysis of frustule pellets showing chla after cells fragmentation and washings.

The B&D protocol was particularly suitable to remove the lipid external fraction with preservation of intact molecular structures. The monophasic solvent extraction mixture (chloroform/methanol/0.1M NaCl in water) is a powerful extracting agent for both disruption of these bonding's and lipid dissolution (Kates, 1986), while the second step through addition of proper amounts of chloroform and water, achieves an efficient separation of hydrophobic and hydrophilic compounds by changing the monophasic mixture into biphasic. The NaOH treatment of frustules free from the external organic material gives access to the organic matter associated to the silica matrix. Not only NaOH increases silica dissolution but it is widely use to cleave hydrogen and covalent bonds, which favour separation of FA from the silica phase and most probably from the organic matrix that may be present. We did not use oxidizing agent such as perchloric acid suitable for the extraction of aqueous metabolites (Ingalls et al. 2009) as it has a deleterious effect on lipid components. We tested the use of HF to dissolve silica but precautions required for its use (plastic or polypropylene containers) makes its use incompatible with the analysis of lipids.

The efficiency of our protocol for isolating and extracting frustule-associated lipids was demonstrated first by the absence of cellular compounds (i. e. phytol and sterols) in frustule-associated lipids, secondly by the fact that the internal standard (19:0) added to the cellular fraction was not recovered with the frustule-associated lipid fraction (see section 2.4) and finally, because FA markers of prokaryotes that contributed for a few percent of the pellets total carbon were also absent from the frustule-associated lipids. In addition, we used our isolation/extraction protocol at different stages of dissolution of the silica phases during a bacterial degradation experiment of these diatoms. Frustule-associated FA thus extracted were found similar to that of frustule-associated FA in fresh *Thalassiosira weissflogii* diatom culture validating our protocole and showing little accessibility of these FA to degradation.

External FA were identified as cellular lipids because of their composition similar to that of FA in whole cells. While results did not show any specific FA marker of the frustule, frustule-associated FA were characterised by a very low degree of unsaturation with predominance of 14:0, 16:0 and 18:0 FA. Although high pH (NaOH 1 $mol.l^{-1}$) and the absence of chlorophyll favour neither autoxidation nor photooxidation (Petit et al., 2013; Rontani, 2001), the reactivity of unsaturated FA to oxidation could have led to a decrease of unsaturation degree due to experimental conditions and extraction process.

However, tests to determine the effect of temperature (70 °C) on polyunsaturated FA (20:4(n-6)), and previous observations that report unsaturated FA conservation during hot saponification (> 100 °C, see section 2.7.1), suggest that our protocol had little effect on FA unsaturation. Oleic acid (18:1(n-9)) and the unidentified 16:1 FA were present in the 'frustule-associated' fraction isolated from *T. weissflogii* cultures, even after 30 days of degradation. Thus, 16:1 and 18:1 FA may likely be associated to a resistant to degradation/dissolution phase of organic or silica matrices.

The very strong similarity between FA profiles of frustules of the different cultures (Fig. 5), although clear differences appeared for others fractions, indicated that 'frustule-associated' FA were less sensitive to growth conditions than cellular FA. Nevertheless, the study of Soler et al. (2010) shows an effect of nutrient starvations, especially phosphorus starvation, on the FTIR- analysed biochemical composition of *T. weissflogii* frustule. These authors suggested that biochemical changes lead to frustule structure changes leading *in fine* to changes in $bSiO_2$ dissolution. Therefore, although frustule-associated FA in sediments may not be used as markers of nutrient regime during paleoproduction, changes in other biochemical fractions should be considered when studying frustules in deep sediments.

Kates and Volcani (1968) suggested that lipids could be distributed according to their unsaturation level in the frustule. The degradation of the 18:0 and some unsaturated FA (16:1(n-7), 18:2(n-6), 20:4(n-6) and 20:5(n-3)) of the frustule while 14:0 and 16:0 were almost not degraded at all is in agreement with a non-homogenous association of FA with the frustule. These results also confirm the existence of different organic pools in the silica matrix of the frustules (Abramson et al., 2009; Tesson et al. 2008, 2013) and of different silica phases associated with different pool of organic matter (Moriceau et al., 2009). Using a spectroscopic method, Abramson et al. (2009) concluded that the OM encased within the structure of the frustule, which is resistant to different chemical attacks, may be protected from decomposition until the release of this matter into the surrounding environment occurs. This last method advantageously allowed locating the organic pools in *Cylindrotheca fusiformis* because of its thin frustule. However it is not valid to accurately quantify organic pools and it can hardly be adapted to other species as thicker frustules absorb X-rays too strongly. In contrast, our methodology may be used to quantify the pool of FA embedded in the frustule of a large choice of diatom species.

2. Implications for the export of organic matter

In some cases, huge numbers of fresh diatom cells can sink out of the euphotic layer (Martin et al., 2011), carrying with them different pool of organic matter; extra-, intra-cellular and intra-frustule. On

the contrary to what was previously thought, the fraction of organic matter embedded or associated to the frustule could be an important fraction of the total POC (1.8 % of the diatom POC in surface water and up to 5.8 % of the diatom POC after 30 days of degradation).

To better understand the implication of this result in term of export, we compared our experimental data to the *in situ* data compiled by Ragueneau et al. (2002). More precisely, data from the Northern Antarctic Circumpolar Current site (NACC) were used for comparison because $bSiO_2$ dissolution at this site (82 % of $bSiO_2$ dissolution at 4224 m depth) was comparable to the final dissolution measured in our degradation/dissolution experiment (78 % of our initial $bSiO_2$ after 30 days incubation). The 'frustule-associated' FA represented 5.8 % of the total POC at the end of our experiment. The amount of these 'frustule-associated' FA for each mol of $bSiO_2$ after 78 % of dissolution was 0.23 molC FA.mol $bSiO_2^{-1}$. Assuming that 14:0 and 16:0 FA are associated to the less soluble phase of the frustule without excluding possible association with the organic matrix, the flux of the 'frustule-associated' FA at 4224 m may be estimated from the $bSiO_2$ flux (0.14 $mol.m^{-2}.yr^{-1}$) found at this site. This calculated 'frustule-associated' FA flux amounted to 0.0322 $molC.m^{-2}.yr^{-1}$ which represents 64 % of the POC flux at 4224 m at NACC site. When N in frustules is on the order of 15 µmol N/g opal and the C associated with amino acids is also reported in units of µmol C/g (Ingalls et al., 2010), this calculation suggests that our protocol extracts frustule-bound fatty acids and another FA fraction not embedded but strongly associated to the frustule and the organic matrix.

Keeping in mind the limitation of this comparison, especially in terms of the species studied (low latitude widespread species) and experimental conditions that did not consider *in situ* conditions (temperature, pressure, grazing), our study still raises the possible importance of the contribution of 'frustule-associated' FA to the organic carbon flux. According to our simple calculation, these 'frustule-associated' FA could represent an important part of the POC reaching the sediment. Interestingly, this assessment is in line with the correlation observed at depth between the sedimentation flux of POC and the sedimentation flux of $bSiO_2$ as revealed by the study of Armstrong et al. (2009, 2002), Francois et al. (2002), Klaas and Archer (2002) and Ragueneau et al. (2006).

In further studies of sinking particles and sediments, a more systematic hydrolysis/dissolution of deep samples should be used to consider this intra-frustule organic matter and to correctly estimate the sedimentation of the different organic pools. Until now, the different protocol used showed that this fraction is taken into account when measuring total POC but not when characterizing the different

organic pools. As such, this fraction could be part of the large uncharacterized organic matter pool at depths (Wakeham, 1995).

As shown by our degradation/dissolution results, the 'frustule-associated' organic matter is not available to prokaryotes before the complete frustule dissolution. As a result and because of the saturation in dissolved silicon in interstitial water in bottom sediments (Van Cappellen, 2002), its release in sediments should be slower than previously thought and could not be a valuable source of energy for the organisms feeding on the seafloor. Another point of interest is the better preservation of lipids in sediments and their usefulness as biomarkers in paleoceanographic studies (Wakeham, 1995). The fact that sterols are not found embedded in the frustule of *T. weissflogii*, although many deep sediment analysis reveal their presence (Wakeham et al., 1997), could be used to estimate the proportion of intracellular versus 'frustule-associated' organic carbon in opal dominated sediments.

Conclusion

Our study suggests an interesting and effective protocol to approach the FA composition of the organic matter embedded in or strongly associated to the frustule. Clear differences exist between the FA composition of the whole cell and the FA composition of the OM embedded and associated to the frustule which are characterised by a very low degree of unsaturation. Moreover, FA composition of the whole cell seem a lot more sensitive to small differences in the growth conditions than FA associated to the frustule. When *T. weissflogii* underwent a 30 days degradation, the FA associated to the frustule represented 5.8 % of the remaining POC suggesting the importance of their role in carbon export. With our study we infer that organic matter associated to the frustule or embedded in the frustule may be consider when investigating carbon export. This pool could partially explain the correlation observed at depth between Si and C sedimentation fluxes despite the decoupling between $bSiO_2$ dissolution and POC degradation processes.

Acknowledgments

We thank Daniel Delmas from Ifremer-Brest for prokaryote counting during the degradation experiment. We also thank Chantal Bezac for SEM micrography. The authors are grateful to two anonymous reviewers who greatly help improving the manuscript. Flow cytometry analyses were performed with the PRECYM platform (http://www.com.univ-mrs.fr/PRECYM/) with the help of Aude Barani. This work was supported by the UTIL project of the LEFE/CYBER program of CNRS/INSU. MS was supported by a Ph.D grant from Aix-Marseille University.

References

Abramson, L., Wirick, S., Lee, C., Jacobsen, C.J., Brandes, J.A., 2009. The use of soft X-ray spectromicroscopy to investigate the distribution and composition of organic matter in a diatom frustule and a biomimetic analog. Deep Sea Research Part II - Topical Studies in Oceanography 56, 1369–1380.

Armstrong, R.A., Lee, C., Hedges, J.I., Honjo, S., Wakeham, S.G., 2002. A new, mechanistic model for organic carbon fluxes in the ocean based on the quantitative association of POC with ballast minerals. Deep Sea Research Part II - Topical Studies in Oceanography 49, 219–236.

Armstrong, R.A., Peterson, M.L., Lee, C., Wakeham, S.G., 2009. Settling velocity spectra and the ballast ratio hypothesis. Deep Sea Research Part II: Topical Studies in Oceanography 56, 1470–1478.

Balzano, S., Pancost, R.D., Lloyd, J.R., Statham, P.J., 2011. Changes in fatty acid composition in degrading algal aggregates. Marine Chemistry 124, 2–13.

Bidle, K.D., Azam, F., 1999. Accelerated dissolution of diatom silica by marine bacterial assemblages. Nature 397, 508–512.

Bridoux, M.C., Annenkov, V. V, Keil, R.G., Ingalls, A.E., 2012. Widespread distribution and molecular diversity of diatom frustule bound aliphatic long chain polyamines (LCPAs) in marine sediments. Organic Geochemistry 48, 9–20.

Bridoux, M.C., Ingalls, A.E., 2010. Structural identification of long-chain polyamines associated with diatom biosilica in a Southern Ocean sediment core. Geochimica et Cosmochimica Acta 74, 4044–4057.

Brunner, E., Gröger, C., Lutz, K., Richthammer, P., Spinde, K., Sumper, M., 2009. Analytical studies of silica biomineralization: towards an understanding of silica processing by diatoms. Applied Microbiology and Biotechnology 84, 607–16.

Buesseler, K.O., 1998. The decoupling of production and particulate export in the surface ocean. Global Biogeochemical Cycles 12, 297–310.

Chen, X., Wakeham, S.G., Fisher, N.S., 2011. Influence of iron on fatty acid and sterol composition of marine phytoplankton and copepod consumers. Limnology and Oceanography 56, 716–724.

Chiovitti, A., Harper, R.E., Willis, A., Bacic, A., Mulvaney, P., Wetherbee, R., 2005. Variations in the substituted 3-linked mannans closely associated with the silicified walls of diatoms. Journal of Phycology 41, 1154–1161.

Christian, H., 2010. fpc: Flexible procedures for clustering. R package version 2.0-2. http://CRAN.R-project.org/package=fpc.

Coombs, J., Darley, W.M., Holm-Hansen, O., Volcani, B.E., 1967. Studies on the biochemistry and fine structure of silica shell formation in diatoms. Chemical composition of Navicula pelliculosa during silicon-starvation synchrony. Plant Physiology 42, 1601–6.

Dalsgaard, J., St John, M.A., Kattner, G., Müller-Navarra, D., Hagen, W., 2003. Fatty acid trophic markers in the pelagic marine environment. Advances in Marine Biology 46, 225–340.

De La Rocha, C.L., Passow, U., 2007. Factors influencing the sinking of POC and the efficiency of the biological carbon pump. Deep Sea Research Part II - Topical Studies in Oceanography 54, 639–658.

Falkowski, P.G., Barber, R.T., Smetacek, V., 1998. Biogeochemical controls and feedbacks on ocean primary production. Science 281, 200–206.

Fileman, T.W., Pond, D.W., Barlow, R.G., Mantoura, R.F.C., 1998. Vertical profiles of pigments, fatty acids and amino acids: Evidence for undegraded diatomaceous material sedimenting to the deep ocean in the Bellingshausen Sea, Antarctica. Deep Sea Research Part I - Oceanographic Research Papers 45, 333–346.

François, R., Honjo, S., Krishfield, R., Manganini, S., 2002. Factors controlling the flux of organic carbon to the bathypelagic zone of the ocean. Global Biogeochemical Cycles 16, 1087.

Gordon, L.I., Jennings, J.C., Ross, A.A., Krest, J.M., 1993. A suggested protocol for continuous flow automated analysis of seawater nutrients (phosphate, nitrate, nitrite and silicic acid) in the WOCE Hydrographic Program and the Joint Global Ocean Fluxes Study. WHP Operations and Methods. WOCE Hydrographic Program Office. Methods manual 19–1.

Goutx, M., Wakeham, S.G., Lee, C., Duflos, M., Guigue, C., Liu, Z., Moriceau, B., Sempéré, R., Tedetti, M., Xue, J., 2007. Composition and degradation of marine particles with different settling velocities in the northwestern Mediterranean Sea. Limnology and Oceanography 52, 1645–1664.

Guillard, R.R.L., Ryther, J.H., 1962. Studies of marine planktonic diatoms : I. Cyclotella nana Hustedt, and Detonula confervacea (Cleve) Gran. Canadian Journal of Microbiology 8, 229–239.

Hedges, J.I., Baldock, J.A., Gélinas, Y., Lee, C., Peterson, M.L., Wakeham, S.G., 2001. Evidence for non-selective preservation of organic matter in sinking marine particles. Nature 409, 801–804.

Hildebrand, M., 2003. Biological processing of nanostructured silica in diatoms. Progress in Organic Coatings 47, 256–266.

Hildebrand, M., 2008. Diatoms, biomineralization processes, and genomics. Chemical reviews 108, 4855–74.

Hildebrand, M., Holton, G., Joy, D.C., Doktycz, M.J., Allison, D.P., 2009. Diverse and conserved nano- and mesoscale structures of diatom silica revealed by atomic force microscopy. Journal of Microscopy 235, 172–87.

Ingalls, A.E., Whitehead, K., Bridoux, M.C., 2010. Tinted windows: The presence of the UV absorbing compounds called mycosporine-like amino acids embedded in the frustules of marine diatoms. Geochimica et Cosmochimica Acta 74, 104–115.

Kamatani, A., 1971. Physical and chemical characteristics of biogenous silica. Marine Biology 95.

Kamatani, A., Riley, J.P., 1979. Rate of dissolution of diatom silica walls in seawater. Marine Biology 55, 29–35.

Kates, M., Volcani, B.E., 1968. Studies on the biochemistry and fine structure of silica shell formation in diatoms. Lipid components of the cell walls. Z. Pflanzenphysiol 19–29.

Klaas, C., Archer, D.E., 2002. Association of sinking organic matter with various types of mineral ballast in the deep sea: Implications for the rain ratio. Global Biogeochemical Cycles 16.

Klein Breteler, W.C.M., Schogt, N., Rampen, S.W., 2005. Effect of diatom nutrient limitation on copepod development: the role of essential lipids. Marine Ecology Progress Series 291, 125–133.

Kröger, N., Bergsdorf, C., Sumper, M., 1994. A new calcium binding glycoprotein family constitutes a major diatom cell wall component. The EMBO journal 13, 4676–4683.

Kröger, N., Deutzmann, R., Sumper, M., 1999. Polycationic peptides from diatom biosilica that direct silica nanosphere F formation. Science 286, 1129–1132.

Kröger, N., Lehmann, G., Rachel, R., Sumper, M., 1997. Characterization of a 200-kDa diatom protein that is specifically associated with a silica-based substructure of the cell wall. European Journal of Biochemistry 250, 99–105.

Kröger, N., Lorenz, S., Brunner, E., Sumper, M., 2002. Self-assembly of highly phosphorylated silaffins and their function in biosilica morphogenesis. Science 298, 584–6.

Kucki, M., 2009. Biological Photonic Crystals: Diatoms. PhD Thesis. University of Kassel. Department of Natural Science pp 166.

Loucaides, S., Van Cappellen, P., Behrends, T., 2008. Dissolution of biogenic silica from land to ocean: Role of salinity and pH. Limnology and Oceanography 53, 1614–1621.

Mann, D.G., Droop, S.J.M., 1996. 3. Biodiversity, biogeography and conservation of diatoms. Hydrobiologia 336, 19–32.

Martin, P., Lampitt, R.S., Jane Perry, M., Sanders, R., Lee, C., D'Asaro, E., 2011. Export and mesopelagic particle flux during a North Atlantic spring diatom bloom. Deep Sea Research Part I - Oceanographic Research Papers 58, 338–349.

Martin-Jézéquel, V., Hildebrand, M., Brzezinski, M.A., 2000. Silicon metabolism in diatoms : implications for growth. Journal of Phycology 36, 821–840.

Moriceau, B., Goutx, M., Guigue, C., Lee, C., Armstrong, R.A., Duflos, M., Tamburini, C., Charrière, B., Ragueneau, O., 2009. Si–C interactions during degradation of the diatom Skeletonema marinoi. Deep Sea Research Part II - Topical Studies in Oceanography 56, 1381–1395.

Mullin, J.B., Riley, J.P., 1955. The colorimetric determination of silicate with special reference to sea and natural waters. Analytica Chimica Acta 12.

Najdek, M., Debobbis, D., Miokovic, D., Ivancic, I., 2002. Fatty acid and phytoplankton compositions of different types of mucilaginous aggregates in thenorthern Adriatic. Journal of Plankton Research 24, 429–441.

Nelson, D.M., Tréguer, P., Brzezinski, M.A., Leynaert, A., Quéguiner, B., 1995. Production and dissolution of biogenic silica in the ocean : Revised global estimates , comparison with regional data and relationship to biogenic sedimentation. Global Biogeochemical Cycles 9, 359–372.

Patrick, S., Holding, A.J., 1985. The effect of bacteria on the solubilization of silica in diatom frustules. Journal of Applied Microbiology 7–16.

Petit, M., Sempéré, R., Vaultier, F., Rontani, J.-F., 2013. Photochemical production and behavior of hydroperoxyacids in heterotrophic bacteria attached to senescent phytoplanktonic cells. International Journal of Molecular Sciences 14, 11795–11815.

R Core Team, 2012. R: A language and environment for statistical computing. R Foundation for Statistical Computing, Vienna, Austria.

Ragueneau, O., Dittert, N., Pondaven, P., Tréguer, P., Corrin, L., 2002. Si/C decoupling in the world ocean: is the Southern Ocean different? Deep Sea Research Part II - Topical Studies in Oceanography 49, 3127–3154.

Ragueneau, O., Schultes, S., Bidle, K.D., Claquin, P., Moriceau, B., 2006. Si and C interactions in the world ocean: Importance of ecological processes and implications for the role of diatoms in the biological pump. Global Biogeochemical Cycles 20, 1–15.

Ragueneau, O., Tréguer, P., 1994. Determination of biogenic silica in coastal waters: applicability and limits of the alkaline digestion method. Marine Chemistry 45, 43–51.

Raven, J.A., Waite, A.M., 2004. The evolution of silicification in diatoms: inescapable sinking and sinking as escape? New Phytologist 162, 45–61.

Rontani, J.-F., 2001. Visible light-dependent degradation of lipidic phytoplanktonic components during senescence: a review. Phytochemistry 58, 187–202.

Rontani, J.-F., Zabetti, N., Wakeham, S.G., 2011. Degradation of particulate organic matter in the equatorial Pacific Ocean: Biotic or abiotic? Limnology and Oceanography 56, 333–349.

Soler, C., Claquin, P., Goutx, M., Ragueneau, O., Moriceau, B., 2010. Impact of nutrient starvation on the biochemical composition of the marine diatom Thalassiosira weissflogii: from the whole cell to the frustule fraction. Biogeosciences Discussions 7, 5953–5995.

Tesson, B., Hildebrand, M., 2013. Characterization and localization of insoluble organic matrices associated with diatom cell walls: Insight into their roles during cell wall formation. PloS one 8, e61675.

Tesson, B., Masse, S., Laurent, G., Maquet, J., Livage, J., Martin-Jézéquel, V., Coradin, T., 2008. Contribution of multi-nuclear solid state NMR to the characterization of the Thalassiosira pseudonana diatom cell wall. Analytical and Bioanalytical Chemistry 390, 1889–1898.

Thornton, D.C.O., 2002. Diatom aggregation in the sea: mechanisms and ecological implications. European Journal of Phycology 37, 149–161.

Tréguer, P., Le Corre, P., 1975. Manuel d'analyse des sels nutritifs dans l'eau de mer. Utilisation de l'autoanalyseur II Technicon. Université de Bretagne Occidentale, Brest.

Turner, J.T., 2002. Zooplankton fecal pellets, marine snow and sinking phytoplankton blooms. Aquatic Microbial Ecology 27, 57–102.

Van Cappellen, P., 2002. Biogenic silica dissolution in the oceans: Reconciling experimental and field-based dissolution rates. Global Biogeochemical Cycles 16.

Volk, T., Hoffert, M.I., 1985. Ocean carbon pumps: Analysis of relative strengths and efficiencies in ocean-driven atmospheric CO2 changes, in: Sunquist, E.T., Broecker, W.S. (Eds.), The Carbon Cycle and Atmospheric CO2: Natural Variations Archean to Present. American Geophysical Union, Washington, DC, pp. 99–110.

Volkman, J.K., Hallegraeff, G.M., 1988. Lipids in marine diatoms of the genus Thalassiosira : Predominance of 24-methylenecholesterol. Phytochemistry 27, 1389–1394.

Vrieling, E., Poort, L., Beelen, T., 1999. Growth and silica content of the diatoms Thalassiosira weissflogii and Navicula salinarum at different salinities and enrichments with aluminium. European Journal of Phycology 307–316.

Wakeham, S.G., 1995. Lipid biomarkers for heterotrophic alteration of suspended particulate organic matter in oxygenated and anoxic water columns of the ocean. Deep Sea Research Part I - Oceanographic Research Papers 42, 1749–1771.

Wakeham, S.G., Lee, C., Hedges, J.I., Hernes, P.J., Peterson, M.L., 1997. Molecular indicators of diagenetic status in marine organic matter. Geochimica et Cosmochimica Acta 61, 5363–5369.

Abstract

Diatoms are microalgae that contribute up to 75% of oceanic primary production and are major players in the oceanic biogeochemical silicon (Si) cycle. Understanding the mechanisms affecting the biogenic silica ($bSiO_2$), constituting the diatom frustule, is necessary to improve the understanding of oceanic Si cycling. In summer, most of the open ocean is limited by low nutrient availability. Thus, the main objective of this thesis is to study the effect of diatom nutritional environment on biogenic silica ($bSiO_2$) dissolution and export. This study focused on iron (Fe), Si and nitrogen (N) limitations, i.e. nutrients whose low concentrations during summer limit diatom production in the majority of the world ocean. One originality of this thesis is to study the copper (Cu) limitation, whose impact on the elemental composition and dissolution of diatoms has rarely been studied. The effects of micronutrient limiting conditions were studied on the pennate diatom *Pseudo-nitzschia delicatissima* while macronutrient limiting conditions were studied on the centric diatom *Thalassiosira weissflogii*.

The first stage of this work was to study the effect of nutrient limiting conditions at two different scales of diatoms frustule: the cell scale, with the study of the silicification degree of diatoms, and the frustule scale, with the study of its structure and composition using Fourier Transform InfraRed spectroscopy (FTIR). The second stage of this work consisted of the study of the diatom post-mortem fate through the study of the dissolution kinetics of $bSiO_2$ from diatom frustule.

The FTIR results clearly indicate that, in addition to the plasticity of global $bSiO_2$ content, diatom frustule also has plasticity at the molecular scale, depending on growth conditions. The organization degree and the reactivity degree of the silica lattice are both affected by diatom nutritional environment. The relative amount of organic matter associated with frustule is also affected by nutrient availability. Through these changes, the nutritional environment affects the dissolution of diatom frustules, which showed a two-stage dissolution in all six dissolution experiments, illustrating the biphasic composition of the frustule. The results indicate that the growth conditions affect both the proportion and the dissolution rates of these $bSiO_2$ phases.

By changing the intrinsic properties of the $bSiO_2$ phases, nutrient limited-frustules will be dissolving less than non-limited diatom frustule. Therefore, the diatom nutrient environment affects $bSiO_2$ export. In *P. delicatissima*, only 9 % of the initial $bSiO_2$ remained from replete cells at the end of the twenty-two days dissolution experiment, while about 25 % remained from Cu-starved and Fe-limited cells. Macronutrient-limited *T. weissflogii* were also more preserved after one month of dissolution with 41 % and 51 % of the initial $bSiO_2$ remaining for cells predominantly Si- or N-limited, respectively, whereas 20% of the initial $bSiO_2$ was preserved in replete cells. These results suggest that the biogenic silica dissolution in global ocean models could be better parameterized taking into account (i) the dissolution kinetics of the two $bSiO_2$ phases and (ii) an enhanced $bSiO_2$ preservation of nutrient-limited cells.

Key words: Diatoms – Biogenic silica – Frustule – Nutrients – Dissolution – Export

Résumé

Les diatomées sont des micro-algues qui participent à hauteur de 35 à 75 % à la production primaire océanique et qui sont les acteurs majeurs du cycle biogéochimique du silicium (Si) dans l'océan. Comprendre les mécanismes qui affectent la dissolution de la silice biogénique ($bSiO_2$) constituant le frustule des diatomées est nécessaire afin d'améliorer la compréhension du cycle océanique du Si. En période estivale, la majorité de l'océan ouvert est limitée par de faibles disponibilités en éléments nutritifs. Les travaux réalisés dans cette thèse ont donc pour objectif majeur d'étudier l'effet de l'environnement nutritionnel des diatomées sur la dissolution et l'export de silice biogénique ($bSiO_2$). Cette étude s'est focalisée sur les limitations en fer (Fe), en Si et en azote (N), c'est-à-dire sur les éléments nutritifs dont les faibles concentrations en période estivale limitent la production de diatomées dans une grande majorité de l'océan mondial. Une des originalités de cette thèse consiste en l'étude de la limitation en cuivre (Cu), dont les impacts sur la composition élémentaire et la dissolution des diatomées ont été peu étudiés. Les effets des conditions limitantes en micronutriments ont été étudiés sur la diatomée pennée *Pseudo-nitzschia delicatissima* tandis que les limitations en macronutriments ont été étudiées sur la diatomée centrique *Thalassiosira weissflogii*.

La première étape de ce travail a consisté en l'étude de l'effet de conditions nutritives limitantes sur deux échelles du frustule des diatomées : celle de la cellule, avec l'étude du degré de silicification des diatomées, et celle du frustule, avec l'étude de sa structure et sa composition fine, au moyen de la spectroscopie InfraRouge à Transformée de Fourier (IRTF). La seconde étape de ce travail a consisté en l'étude du devenir post-mortem de ces cellules à travers l'étude de la cinétique de dissolution de la $bSiO_2$ constituant leur frustule.

Les résultats obtenus par IRTF indiquent clairement qu'à la plasticité du contenu global en $bSiO_2$ du frustule des diatomées, s'ajoute la plasticité du frustule à l'échelle moléculaire, en fonction des conditions de croissance. Le degré d'organisation et le degré de réactivité du réseau siliceux sont tous deux affectés par l'environnement nutritif des diatomées. La quantité relative de matière organique associée au frustule varie également avec la disponibilité des éléments nutritifs. A travers ces changements, l'environnement nutritionnel affecte la dissolution du frustule des diatomées qui, dans les six expériences de dissolution, se déroulent en deux étapes, illustrant la composition biphasique du frustule. Les résultats indiquent que les conditions de croissance vont affecter la proportion et les vitesses de dissolution de la $bSiO_2$ de ces phases. Par la modification des propriétés intrinsèques des phases de $bSiO_2$, le frustule des diatomées limitées en nutriments auront une propension à la dissolution moins importante que celle des diatomées non-limitées. De ce fait, l'environnement nutritif des diatomées affecte l'export de $bSiO_2$. Pour *P. delicatissima*, seuls 9 % de la $bSiO_2$ initiale des cellules non limitées sont préservés après 22 jours de dissolution, tandis qu'environ 25 % sont préservés en cas de carence stricte en Cu ou de limitation en Fe durant la croissance. Les frustules de *T. weissflogii* limitées en macronutriment sont également mieux préservés après un mois de dissolution, avec 41 % et 51 % de la $bSiO_2$ initiale restante pour les cellules majoritairement limitées en Si ou en N, respectivement, comparés au 20 % de préservation pour les cellules non-limitées. Ces résultats suggèrent que la dissolution de la silice dans les modèles globaux de l'océan pourrait être mieux paramétrée en tenant compte (i) de la cinétique de dissolution des deux phases de silice biogénique et (ii) de la meilleure préservation de la $bSiO_2$ des cellules limitées en nutriments.

Mots clés: Diatomées – Silice biogénique – Frustule – Nutriments – Dissolution – Export